Cellular Interactions and Phenotypic Characteristics of GMP-Grade Tregs in Kidney Transplantation: Trafficking, Function, and Tissue Context



Nora Salah Atallah

St Catherine College
Nuffield Department of Surgical Sciences
University of Oxford

Supervisors: Professor Fadi Issa and Dr Joanna Hester

Thesis submitted for DPhil in Surgical Sciences in Hilary Term 2026

Abstract

Cellular Interactions and Phenotypic Characteristics of GMP-Grade Tregs in Kidney Transplantation: Trafficking, Function, and Tissue Context

Nora Atallah, St Catherine's College and Nuffield Department of Surgical Sciences, University of Oxford, DPhil in Surgical Sciences

Regulatory T cells (Tregs) are central mediators of immune tolerance, maintaining immune homeostasis and preventing excessive immune activation. In transplantation, adoptive Treg therapy has emerged as a promising strategy to promote graft tolerance and reduce reliance on long-term pharmacological immunosuppression. However, the therapeutic efficacy of Tregs depends on their ability to maintain a stable regulatory phenotype, migrate to sites of inflammation, and interact effectively with other immune cell populations. I hypothesised that clinically expanded Tregs exhibit distinct molecular and homing characteristics, that their suppressive function is modulated by interactions with monocytes, and that these properties collectively shape immune responses following transplantation.

This thesis utilised samples from a Treg cell therapy clinical trial to investigate the phenotype, mechanisms of action, and tissue-specific properties of Treg-mediated immune modulation. Three aims were addressed: first, to characterise the molecular profile, homing receptor expression, and chemokine secretion of Good Manufacturing Practice (GMP)-expanded human polyclonal Tregs. Second, to assess their suppressive function and determine the contribution of monocytes. Third, to evaluate systemic and intragraft effects of Treg therapy, including spatial profiling of kidney biopsies.

In the first experimental chapter, transcript profiling and multiparameter flow cytometry demonstrated that expanded GMP-grade Tregs preserved lineage identity, with sustained FOXP3 and CD25 expression. Their trafficking profile was consistent with localisation to peripheral inflamed tissues, characterised by increased expression of CCR4 and CCR8. Upon stimulation, Tregs also secreted a distinct chemokine profile, including CXCL8 and CCL24.

In the second experimental chapter, the role of monocytes in Treg-mediated suppression was examined using *in vitro* suppression assays. $CD14^+$ monocytes were selectively depleted and reintroduced to assess their contribution. Expanded Tregs exhibited potent suppression of effector T cell proliferation, which was significantly enhanced in the presence of monocytes.

In the third experimental chapter, longitudinal immune monitoring following autologous Treg infusion was complemented with spatial transcriptomic analysis of protocol kidney biopsies. Post-therapy biopsies showed regulatory-type immune infiltrates, with increased spatial proximity between monocytes, B cells, and dendritic cells, alongside chemokine patterns consistent with coordinated immune cell recruitment.

Collectively, these findings demonstrate the functional capability of clinically expanded Tregs, highlight a key role for monocytes in optimising their suppressive activity, and provide tissue-level evidence that Treg therapy reshapes the graft microenvironment towards controlled immune regulation. These insights inform the rational design of Treg-based therapies and strategies for immunosuppression minimisation in transplantation.

Acknowledgement

Throughout my DPhil journey, I have been extremely fortunate to be surrounded by generous mentors, supportive colleagues, and an unwavering network of family and friends. First and foremost, I would like to express my deepest gratitude to my supervisors, Professor Joanna Hester and Professor Fadi Issa. Joanna's mentorship has been fundamental to my development as a researcher; her patience, scientific rigour, and commitment to high-quality research have shaped the way I think, work, and approach experimental challenges. Fadi's insight, encouragement, and broad scientific perspective consistently pushed me to think more critically and expansively about my work. Their combined guidance, trust, and support were central to the successful completion of this DPhil, and I am sincerely grateful for the opportunity to work under their supervision.

I am profoundly thankful for the generous financial support provided by the Saudi Arabian Cultural Bureau in London, the King Abdullah International Medical Research Center (KAIMRC), and the Ministry of National Guard in Saudi Arabia. Their continued support enabled me to focus fully on my research and training throughout my doctoral studies.

My sincere thanks extend to the TWO Study team, whose collaborative efforts were integral to this work. I am grateful to Dr Paul Harden, Dr Matthew Brook, Dr Matthew Bottomley, Dr Hisashi Hashimoto, Dr Oliver McCallion, Dr Quan Yao Ho, Ms Merve Bilici, and Ms Emina Voss for their assistance, expertise, and support throughout the conduct of the TWO Study trial.

I would also like to thank the wider members of the Translational Research and Immunology Group (TRIG), all of whom contributed in different ways to this project. In particular, I am deeply grateful to Dr Hisashi Hashimoto, the first colleague with whom I began my laboratory work, for his guidance, patience, and generosity in teaching me experimental techniques. I would like to thank Dr Sarah Short for her outstanding organisation of the laboratory rota, for being a wonderful friend, and for the many valuable scientific discussions I shared. I am also very grateful to Dr Guido Lewik for being a great friend and for his help with thoughtful discussions throughout my studies. I am thankful to Dr Amy Cross for her guidance and thoughtful advice. I am especially appreciative of Dr Marie Sion for her lovely presence and kindness within the group, to Dr Megan Bradbury for her positive spirit, and to Mr. Joseph Beckett for his support and contributions within the group.

A special thank you goes to my colleague Dr Ahmed Alkhateeb, whose support with data analysis, calm reassurance, and steady encouragement added confidence during some of the most challenging periods of my DPhil. I am also grateful to Dr Alaa Alzahrani for her continued help and encouragement throughout my studies.

I would like to thank Monica Dolton and Eleanor Wilson, who during my early years in the group provided invaluable support with administrative matters, and Jessica Doondeea, whose excellent management contributed greatly to the smooth running of our work within the department at the John Radcliffe Hospital (JR). I am also thankful to the Institute of Developmental & Regenerative Medicine (IDRM); although we moved to this building toward the end of my studies, it provided an inspiring environment with outstanding facilities and a welcoming community.

Outside of TRIG, I would like to thank Dr Paul Harden, Professor Chris Pugh, Dr Matthew Brook, and Dr Henk Giele, my examiners for Transfer of Status and Confirmation of Status, for their constructive discussions and valuable feedback.

Finally, and most importantly, I would like to express my deepest gratitude to my family. To my daughter Reem, who was an integral part of my Oxford journey, thank you for your unwavering belief in me, your constant encouragement, and the countless conversations we shared; you have always been my closest companion and best friend. To my son Rayan, who also shared this journey with me through its highs and lows, thank you for your patience, strength, and steadfast support. I am deeply grateful to my father for always believing in me, encouraging me, and taking pride in my achievements.

To my mother, whose courage and resilience during her battle with cancer were a constant source of strength and inspiration, thank you for your unconditional love, unwavering support, and enduring faith in me throughout this journey. I would also like to thank my siblings, Sara, Mansour, and Ahmad, for their love and support, with special gratitude to my sister Sara and my brother-in-law Amro for their care and guidance throughout this time. Finally, I extend my heartfelt thanks to my dear friends Maha Bokhamseen and Suha Arab for their kindness, compassion, and support during difficult moments.

Dedication

This thesis is dedicated to the soul of my dear mother, Faten Green, who endured her suffering with strength, patience, and grace, whose love and presence remain with me always.

It is also dedicated to my beloved father, the greatest father I could ever ask for. Thank you for your unconditional love, constant support, wisdom, and for always believing in me. Your guidance, kindness, and strength have shaped who I am today.

It is also dedicated to my beloved children, Reem and Rayan. You were part of this journey through its challenges and quiet victories, and your love, belief, and strength carried me every step of the way.

You are my source of inspiration, my pride, and my greatest achievement.

Everything I do is, and will always be, for you.

With all my love



Abbreviations

aGVHD	acute graft-versus-host disease
AMR	Antibody-mediated rejection
APCs	Antigen-presenting cells
Bregs	Regulatory B cells
CAR	Chimeric Antigen Receptor
CCR	C-C motif chemokine receptor
CXCR	C-X-C motif chemokine receptor
CCR4	C-C motif chemokine receptor 4
CCR7	C-C motif chemokine receptor 7
CCR8	C-C motif chemokine receptor 8
CXCR4	C-X-C motif chemokine receptor 4
CXCR6	C-X-C motif chemokine receptor 6
CCL19	C-C motif chemokine ligand 19
CCL24	C-C motif chemokine ligand 24
CXCL8	C-X-C motif chemokine ligand 8
cGVHD	chronic graft-versus-host disease
CKD	Chronic Kidney Disease
CEACAM1	Carcinoembryonic antigen-related cell adhesion molecule 1
CLA	Cutaneous lymphocyte-associated antigen
CMV	Cytomegalovirus
CNIs	Calcineurin Inhibitors
CNS2	Conserved Noncoding Sequence 2
cRF	Calculated reaction frequency
CTLA-4	cytotoxic T-lymphocyte-associated protein 4
CTLs	Cytotoxic T lymphocytes
COVID	Coronavirus Disease 2019, SARS-CoV-2 virus
DAMPs	damage-associated molecular patterns
DCs	Dendritic Cells
cDC1	Conventional dendritic cells type 1
cDC2	Conventional dendritic cells type 2
DC-SIGN	Dendritic-cell-specific intercellular adhesion molecule-3-grabbing non-integrin
DEGs	Differentially expressed genes
DSAs	donor-specific antibodies
EBV	Epstein-Barr virus
eGFR	Estimated glomerular filtration rate
ESRD	End-Stage Renal Disease
FFPE	Formalin-fixed paraffin-embedded
FOXP3	Forkhead box P3
GALT	gut-associated lymphoid tissue
GITR	Glucocorticoid-induced TNFR-related protein
GMP	Good Manufacturing Practice
GPA33	Glycoprotein A33
GPCRs	G protein-coupled receptors

GVHD	Graft-versus-Host Disease
h	Human, Homo sapiens
HSCT	Hematopoietic Stem Cell Transplantation
ICIs	Immune checkpoint inhibitors
IDO	indoleamine 2,3-dioxygenase
IFN-γ	Interferon-gamma
IL	Interleukin
IL-2R	IL-2 receptor
iTr35	IL-35-producing regulatory T cells
iTregs	*in vitro*-induced Tregs
ITGAX	Integrin alpha X
ITGAM	Integrin alpha M
LAG3	Lymphocyte activation gene 3
LP	Liposomal prednisolone
Ig	Immunoglobulin
mAbs	Monoclonal antibodies
MDSCs	Myeloid-derived suppressor cells
MELD	Model for End-Stage Liver Disease
MHC	Major Histocompatibility Complex
MMF	Mycophenolate Mofetil
Mregs	Regulatory macrophages
MSCs	Mesenchymal Stem Cells
mRNA	Messenger RNA
NK	Natural Killer Cells
Nrp-1	Neuropilin-1
PBMCs	Peripheral blood mononuclear cells
pDCs	Plasmacytoid DCs
pTregs	peripheral Tregs
RCTs	Randomised Controlled Trials
REML	Restricted maximum likelihood
ROS	Reactive Oxygen Species
scRNA-seq	Single-cell RNA sequencing
STAT	Signal Transducer and Activator of Transcription
TCM	Central memory T cells
TEM	Effector memory T cells
TCR	T cell receptor
Teffs	Effector T Cells
TEM	Transendothelial migration
TGF-β	Transforming Growth Factor-Beta
Th cells	Helper T cells
Th17	T helper 17
thyTregs	thymic-derived regulatory T cells
TNF-α	Tumour Necrosis Factor-alpha
tol-DC	Tolerogenic Dendritic Cells
Tregs	Regulatory T Cells
TSDR	Treg-specific demethylated region
tTregs	thymic Tregs

TWO Study	Transplantation Without Overimmunosuppression Study
Tx	Transplantation
UMAP	Uniform manifold approximation and projection
γc	γ chain
7-AAD	7-Aminoactinomycin D

Table of Content

Abstract I
Acknowledgement III
Dedication V
Abbreviations VI
Table of Content IX
1 Chapter 1: General Introduction 1
1.1 Background of organ transplantation 1
1.1.1 Milestones in the development of organ transplantation 1
1.1.2 Prevalence of organ failure and the need for transplantation 2
1.1.3 Advances and challenges in pharmacological immunosuppression for transplantation 4
1.1.4 Limitations and risks of current immunosuppressive therapies 6
1.1.5 Immune regulation approaches to minimise immunosuppression 7
1.2 Key immune cell subsets involved in transplant rejection 8
1.2.1 Macrophages & Monocytes 8
1.2.2 Natural Killer Cells 8
1.2.3 B Cells 9
1.2.4 T Cells 9
1.2.5 Regulatory T Cells (Tregs) 10
1.2.5.1 Development 10
1.2.5.2 Phenotype 11
1.2.5.3 Plasticity and stability 11
1.2.5.4 Treg suppressive function 13
1.3 Immune cell crosstalk in transplantation 14
1.3.1 Antigen-presenting cells (APCs) 14
1.3.2 Direct cell-to-cell communication 15
1.3.3 Soluble mediators: cytokines and chemokines 15
1.3.3.1 Cytokine networks in transplantation 15
1.3.3.2 Chemokine networks in transplantation 17
1.4 Homing and chemokine receptor expression 20
1.4.1 Leukocyte homing 20
1.4.2 T cell homing 21
1.4.3 Treg homing 22
1.5 Cellular therapy in transplantation 23
1.5.1 Types of cellular therapies used in transplantation 23

1.5.2 Treg therapy in transplantation 24
1.6 The Transplantation Without Overimmunosuppression (TWO) study trial 25
1.6.1 Initial study protocol: Alemtuzumab induction with delayed Treg infusion 26
1.6.2 Modified study protocol: Basiliximab induction with early Treg infusion 26
1.6.3 Manufacturing and Treg Therapy 27
1.6.4 Summary and implications for future research 28
1.7 Thesis aims & objectives 28
1.8 Thesis hypotheses 29
2 Chapter 2: Materials and Methods 30
2.1 Human material 30
2.1.1 TWO Study clinical trial protocol 30
2.1.2 Healthy blood donors 30
2.2 General laboratory methods 30
2.2.1 Isolation of PBMC by density gradient centrifugation 30
2.2.2 Cryopreservation and thawing of human leukocytes 31
2.3 Cell isolation and sorting 31
2.3.1 Isolation and expansion of human Tregs 31
2.3.2 Isolation of human myeloid cells and monocytes 31
2.4 *In vitro* suppression assays 32
2.4.1 Treg *in vitro* suppression assay 32
2.4.2 Treg-monocyte suppression assay 32
2.5 *In vitro* stimulation assays 33
2.5.1 Cell source and preparation 33
2.5.2 Assessment of chemokine and cytokine production 34
2.5.2.1 Clinical Tregs and conventional T cells chemokine production 34
2.5.2.2 Cytokine production in Treg and monocyte co-culture 35
2.6 Flow cytometry analysis 35
2.6.1 Staining with cell proliferation dye 35
2.6.2 Clinical Treg staining 35
2.6.3 *Ex vivo* Treg staining 36
2.6.4 Chemokine receptor staining 36
2.7 TWO Study peripheral blood immunomonitoring 36
2.7.1 Peripheral blood sampling for immune monitoring 36
2.7.2 Staining whole blood with DuraClone Antibody Cocktail Panels 37
2.8 Gene expression analysis using the nCounter Nanostring technology 38
2.8.1 Overview of nCounter technology 38

2.8.2 RNA isolation 38
2.8.3 nCounter gene expression analysis 38
2.9 Spatial transcriptomics analysis of kidney biopsies using 10X Xenium 39
2.9.1 Platform overview 39
2.9.2 Sample preparation 39
2.9.3 Spatial analysis using the Xenium in situ platform 39
2.10 Statistical analysis 41
3 Chapter 3: Homing Potential and Molecular Phenotype of Clinically Expanded Tregs 42
3.1 Introduction 42
3.1.1 Chapter aims 43
3.2 Results 43
3.2.1 Clinically expanded Tregs are transcriptionally similar to non-expanded Tregs but differ significantly from conventional T cells 43
3.2.1.1 Comparison to conventional CD4+ T cells 44
3.2.1.2 Differences in gene expression between clinical Tregs & $CD8^+$ T cells 46
3.2.1.3 Assessment of transcriptional changes in *ex vivo* and clinical Tregs 48
3.2.2 Expression of homing receptors 49
3.2.2.1 Basic characteristics of clinical Tregs 50
3.2.2.2 Differences in homing markers on Tregs and T cells 50
3.2.2.3 Similarities in homing markers on *ex vivo* and clinical Tregs 54
3.2.3 Production of chemokines 56
3.2.3.1 Effect of IL-2 on chemokine production by Tregs 56
3.2.3.2 Comparison of chemokine secretion by Tregs and conventional T cells 57
3.2.3.3 Impact of allogeneic stimulation on chemokines produced by conventional T cells and Tregs 58
3.3 Discussion 59
4 Chapter 4: *In vitro* Interactions Between Tregs and Monocytes 65
4.1 Introduction 65
4.1.1 Chapter aims 66
4.2 Results 66
4.2.1 Treg *in vitro* expansion and testing 66
4.2.1.1 Tregs sorting & expansion 66
4.2.1.2 Treg fold expansion and FOXP3 expression analysis 67
4.2.1.3 Assessment of Treg suppressive capacity using *in vitro* suppression assays 67
4.2.2 Role of monocytes in Treg-mediated suppression 69
4.2.2.1 *In vitro* suppression by Tregs in the presence and absence of monocytes 70
4.2.2.2 Investigation of cytokine production within suppression assays 73

4.3 Discussion....77
5 Chapter 5: Investigation into Impact of Treg Therapy on Circulating and Graft-Resident Leukocytes in Renal Transplant Recipients....81
5.1 Introduction....81
5.1.1 Chapter aims....82
5.2 Results....82
5.2.1 Study design....82
5.2.2 Phenotypical analysis of peripheral leukocytes in TWO study participants....83
5.2.2.1 Analysis of main immune populations post transplantation....84
5.2.3 Analysis of graft infiltrating cells in TWO study biopsies using spatial transcriptomics....92
5.2.3.1 Experimental design....92
5.2.3.2 Integration of spatial transcriptomics to define cellular composition in kidney allografts 93
5.2.3.3 Immune profiling and transcriptional signatures in kidney transplant biopsies....94
5.2.3.4 Chemokine expression changes following Treg therapy....96
5.2.3.5 Spatial organisation and immune cell neighbourhood remodelling....98
5.2.3.6 Differential gene expression and cluster transcriptomic shifts....101
5.3 Discussion....104
6 Chapter 6: General Discussion....108
6.1 Summary of findings....108
6.2 General discussion....109
6.3 Limitations....113
6.4 Future directions....114
6.5 Conclusion....115
References....116
Appendix....124

Table of Figures

Figure 1.1.2 Global distribution of total kidney transplantation rates (deceased + living donors). 3
Figure 1.4.1 Leukocyte migration across endothelium. 21
Figure 1.6.4 Schematic representation of Treg therapy in the TWO Study. 27
Figure 3.2.1 Workflow for gene expression profiling of clinical Tregs, ex vivo Tregs, and conventional T cells ($CD4^+$ and $CD8^+$) using the NanoString nCounter platform. 44
Figure 3.2.2 Volcano plot showing differential gene expression between clinical (GMP-grade) Tregs and $CD4^+$ T cells. 46
Figure 3.2.3 Volcano plot showing differential gene expression between clinical (GMP-grade) Tregs and $CD8^+$ T cells. 47
Figure 3.2.4 Volcano plot showing differential gene expression between clinical (GMP-grade) Tregs and Ex vivo Tregs. 49
Figure 3.2.5 Frequency of $CD25^{hi}$ $FOXP3^+$ and $Helios^+$ cells within the clinical (GMP-grade) Treg population. 50
Figure 3.2.6 Experimental workflow for assessment of chemokine receptor expression on T cell subsets. .51
Figure 3.2.7 Paired comparison of homing receptor expression in clinical Tregs under unstimulated (green) and anti-CD3/CD28-stimulated (blue) conditions. 52
Figure 3.2.8 Surface expression of homing receptors on clinical Tregs (green), $CD4^+$ T cells (blue), and $CD8^+$ T cells (orange) without stimulation. 53
Figure 3.2.9 Surface expression of homing receptors on clinical Tregs (green), $CD4^+$ T cells (blue), and $CD8^+$ T cells (orange) after 72-hour anti-CD3/CD28 stimulation. 54
Figure 3.2.10 Quantitative analysis of homing receptor expression in ex vivo Tregs before and after stimulation. 55
Figure 3.2.11 Comparison of homing receptor expression in clinical (GMP-grade) versus ex vivo (freshly isolated) Tregs before (green) and after (blue) anti-CD3/CD28 stimulation. 56
Figure 3.2.12 Effect of IL-2 on chemokine production by clinical Tregs. 57
Figure 3.2.13 Chemokine secretion by Tregs, $CD4^+$, and $CD8^+$ T cells following CD3/CD28 stimulation. 58
Figure 3.2.14 Chemokine secretion by Tregs, $CD4^+$, and $CD8^+$ T cells following allogeneic stimulation. 59
Figure 4.2.1 Human Treg Isolation and Expansion Protocol. 66
Figure 4.2.2 Expansion and FOXP3 Expression of Polyclonal Tregs. 67
Figure 4.2.3 Flow Cytometry Gating Strategy and Suppressive Function of Polyclonal Expanded Tregs. 68
Figure 4.2.4 Experimental Design to Assess the Role of Monocytes in Treg-Mediated Suppression. 69
Figure 4.2.5 Effect of Monocytes on Treg-Mediated Suppression of T Cell Proliferation. 72
Figure 4.2.6 HU Th Cytokine Panel: Cytokine Profiling in Suppression Assays Across Experimental Conditions. 76
Figure 5.2.1 Diagrammatic representation of the immunosuppressive regimen used in the TWO Study. 83
Figure 5.2.2 Absolute counts of circulating leukocytes and lymphocytes in peripheral blood following kidney transplantation. 86
Figure 5.2.3 Longitudinal analysis of $CD4^+$ and $CD8^+$ T cell dynamics in peripheral blood following Treg therapy. 87
Figure 5.2.4 Longitudinal analysis of peripheral Treg and $Helios^+$ Treg dynamics following Treg therapy in kidney transplant recipients. 89
Figure 5.2.5 Longitudinal dynamics of circulating monocytes and their subsets in Treg therapy versus control groups. 91
Figure 5.2.6 Workflow overview of 10x Xenium in situ spatial transcriptomics applied to kidney transplant biopsies from the TWO study. 93

Figure 5.2.7 Spatial transcriptomic profiling and cell type annotation of kidney transplant biopsies using 10x Xenium platform. 94
Figure 5.2.8 Characterisation of immune cell populations in kidney transplant biopsies using spatial transcriptomics. 95
Figure 5.2.9 Differential chemokine expression patterns across experimental conditions and immune cell types. 97
Figure 5.2.10 Spatial plots and neighbourhood enrichment analyses reveal tissue architecture and immune cell interactions in the kidney microenvironment. 101
Figure 5.2.11 Transcriptional reprogramming of $CD14^+$ monocytes, $CD16^+$ monocytes, regulatory T cells (Tregs), and B cells following clinical-grade Treg therapy. 103
Figure 6.2.1 Summary of the main findings across experimental chapters. 112

Table of Tables

Table 1.2.1. Chemokines and their roles in immune cell migration. 19
Table 2.5.1. Antibodies used for flow cytometric analysis. 34
Table 2.8.1. DURAClone panels used for immune phenotyping in the TWO Study clinical trial. 37
Table 2.10.1. Demographics of patients included in the trial. 40
Table 5.2.1 Schedule of assessments and interventions for participants included in the immunomonitoring sub study. 84

1 Chapter 1: General Introduction

1.1 Background of organ transplantation

Organ transplantation is a life-saving treatment for patients with end-stage organ failure, significantly improving survival rates and quality of life. Advances in surgical techniques, immunosuppressive therapies, and immunomodulatory strategies have contributed to the increasing success of transplantation. However, challenges remain, including organ shortages, immune rejection, and long-term complications of immunosuppressive therapy. This section provides an overview of the history of transplantation, the prevalence of organ failure, the development of immunosuppressive strategies, and the role of immune regulation in transplantation.

1.1.1 Milestones in the development of organ transplantation

The history of organ transplantation is marked by a series of groundbreaking milestones that have progressively shaped the field. The first successful human organ transplant was performed in 1954 by Dr. Joseph Murray, who transplanted a kidney between identical twins, thereby eliminating the risk of immune rejection and demonstrating the feasibility of organ transplantation due to genetic identity[1, 2]. This achievement laid the foundation for future advances in transplantation immunology and clinical practice.

A pivotal breakthrough followed with the discovery of the major histocompatibility complex (MHC) and its role in graft rejection, which emphasised the importance of human leukocyte antigen (HLA) typing and donor-recipient compatibility[3]. As understanding of the immune mechanisms underlying rejection expanded, so did the development of strategies to overcome them. The introduction of immunosuppressive agents in the 1960s marked a transformative era, significantly improving graft survival rates and establishing a cornerstone for modern transplant medicine[4].

Beyond pharmacological advancements, the exploration of xenotransplantation has emerged as a promising solution to the chronic shortage of donor organs. A landmark case occurred recently, involving the transplantation of a genetically modified pig heart into a human patient, which represented a significant leap forward in the field. Despite the graft's eventual failure due to diastolic dysfunction, the case demonstrated the clinical feasibility of xenotransplantation[5]. In parallel, advances in ex situ machine perfusion have transformed organ preservation and assessment, with centres such as Oxford pioneering normothermic

perfusion technologies that maintain donor organs in near-physiological conditions. These innovations allow prolonged preservation, objective functional assessment prior to implantation, and the potential rehabilitation of marginal grafts, thereby improving organ utilisation and supporting clinical translation in transplantation[6].

The ongoing evolution of transplantation has been influenced by a deeper understanding of immune signalling pathways. Activation of both adaptive and innate immune response, triggered by the recognition of alloantigens and damage-associated molecular patterns (DAMPs), plays a pivotal role in graft rejection. These insights have informed the development of targeted immunomodulatory strategies aimed at prolonging graft survival and improving long-term outcomes[2].

Overall, the integration of advancements in surgical techniques, immunosuppressive therapies, and immunomodulatory strategies has significantly improved the outcomes of organ transplantation, transforming it into a viable treatment for patients with end-stage organ failure.

1.1.2 Prevalence of organ failure and the need for transplantation

The rising prevalence of chronic diseases worldwide has significantly increased the incidence of organ failure, leading to an ever-growing demand for transplantation. Chronic kidney disease (CKD), for example, affects approximately 9.1% of the global population, with nearly 700 million individuals experiencing various stages of the disease[7]. Among them, many progress to end-stage renal disease (ESRD), necessitating dialysis or kidney transplantation as the only viable treatment options. In 2017 alone, CKD was directly responsible for approximately 1.2 million deaths globally, underscoring the urgent need for effective renal replacement therapies[7].

Similarly, heart failure remains a leading cause of morbidity and mortality worldwide. For patients with advanced-stage disease, heart transplantation offers the most effective treatment, significantly improving both survival and quality of life[8]. However, the demand for donor organs far exceeds the supply, resulting in prolonged waiting times and high mortality rates among those on transplant lists[9]. In the United States alone, over 100,000 individuals are currently on the waiting list for organ transplants, with kidneys being the most sought-after, followed by livers, hearts, and lungs[10]. Despite efforts to expand the donor pool, including the use of marginal donors and living donations, the gap between organ availability and demand continues to widen[10].

Global disparities in access to transplantation are significant, with high-income countries achieving much higher transplant rates compared to low- and middle-income regions, where financial, infrastructural, and regulatory challenges severely limit access. Data from the Global Observatory on Donation and Transplantation reveals a substantial gap in kidney transplantation rates between low-income countries in Africa and South America compared to developed nations, highlighting stark inequities in access to transplantation services, as shown in Figure 1.1.2[11].

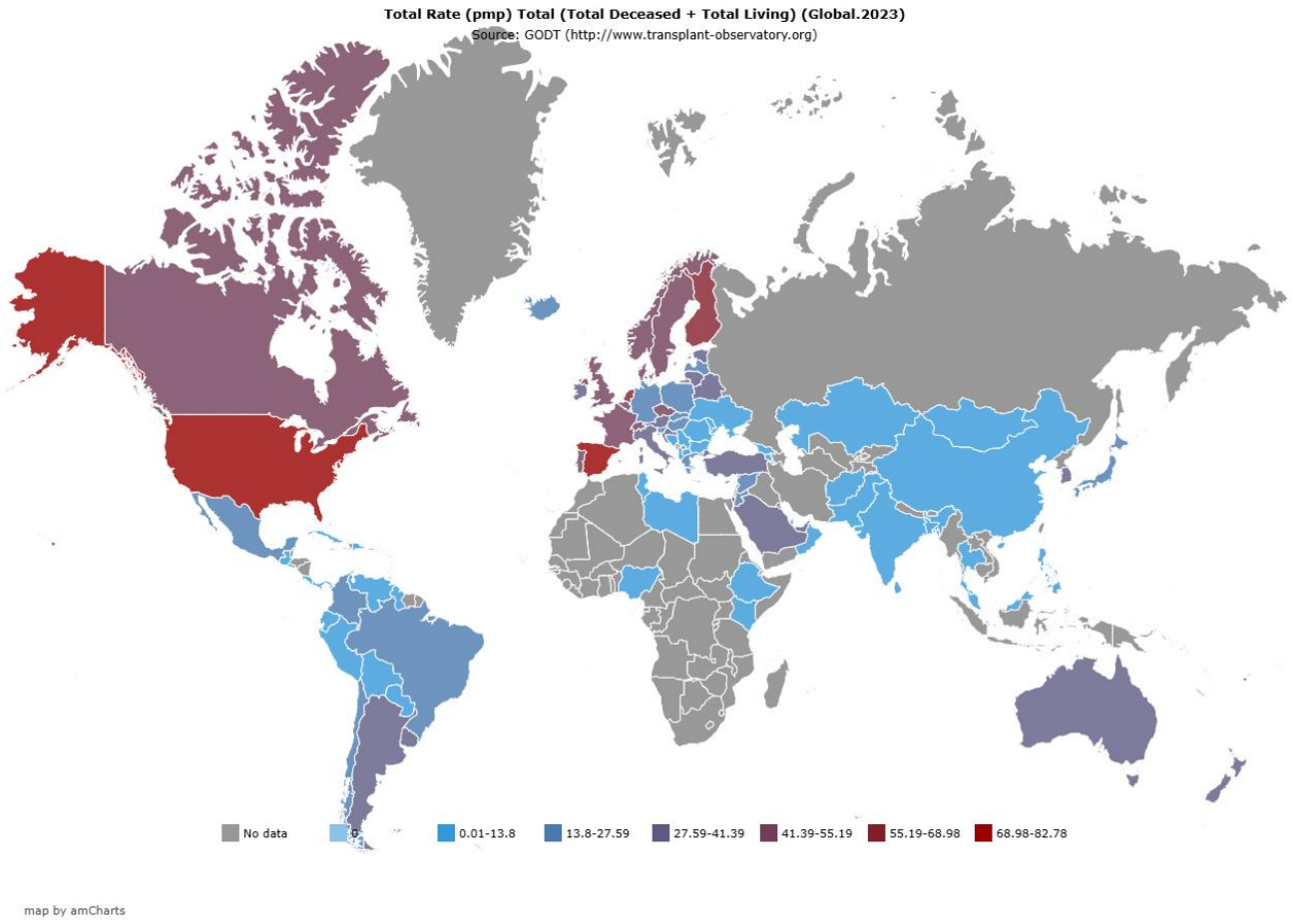


Figure 1.1.2 Global distribution of total kidney transplantation rates (deceased + living donors).

*World map illustrating the total rate of kidney transplants per million population (PMP), combining both deceased and living donors, as reported by the Global Observatory on Donation and Transplantation. Regions with no available data are indicated in grey. A colour gradient is used to represent transplantation rates, with sky blue indicating low transplantation rates, Purple indicating moderate rates, and red indicating high transplantation rates. This visualisation highlights the significant geographical disparities in access to kidney transplantation services worldwide. * Data of the WHO-ONT Global Observatory on Donation and Transplantation. (Adapted from https://www.transplant-observatory.org/data-charts-and-tables/chart/) [11].*

The gap in kidney transplantation rates is particularly evident in regions like sub-Saharan Africa and Southeast Asia, where transplant rates per million population are critically lower compared to those in Western Europe and North America. Furthermore, socioeconomic disparities within countries, such as in the

United States, result in higher mortality rates among African Americans and low-income populations on transplant waiting lists due to limited access to healthcare resources[1].

The scarcity of donor organs has urged significant research into alternative solutions, such as xenotransplantation, bioengineered organs, and the utilisation of marginal donors[12, 13]. Recent advancements in xenotransplantation, including the genetic modification of porcine donors to reduce immunogenicity, have shown promising results in non-human primate models and early human trials[12]. Additionally, bioengineering approaches, such as the development of tissue-engineered organs and the use of stem cells to regenerate damaged tissues, are being explored to alleviate the organ shortage crisis[13]. However, these approaches remain in experimental stages and face substantial regulatory and ethical challenges before they can be widely implemented.

The increasing burden of organ failure, coupled with the persistent shortage of donor organs and disparities in access to transplantation, underscores the need for innovative strategies to expand the donor pool and improve transplant outcomes. Addressing these challenges requires a multifaceted approach, including optimising organ utilisation, enhancing immunosuppressive regimens, and advancing research in regenerative medicine and xenotransplantation.

1.1.3 Advances and challenges in pharmacological immunosuppression for transplantation

The success of organ transplantation relies on effective control of the recipient immune response to prevent graft rejection. This is primarily achieved through pharmacological immunosuppression, using combinations of drugs that target different aspects of immune activation.

A. Calcineurin Inhibitors (CNIs) - Core of immunosuppression

CNIs, such as cyclosporine and tacrolimus, form the cornerstone of immunosuppressive regimens by inhibiting T-cell activation through the calcineurin-NFAT (Nuclear Factor of Activated T cells) pathway, thereby reducing interlukin-2 (IL-2) production and limiting acute rejection[4]. However, their long-term use is associated with nephrotoxicity and reduced efficacy against memory T-cell responses. In addition, CNIs can impair the proliferation, stability, and suppressive function of Tregs, thereby limiting immune regulation. Beyond immunological effects, CNIs are associated with metabolic complications, including diabetes, dyslipidaemia, and bone loss, highlighting the need for careful long-term monitoring[14].

B. Antiproliferative agents - Supporting role

Antiproliferative agents, particularly mycophenolate mofetil (MMF), play a critical role in inhibiting T-cell proliferation and complementing the effects of CNIs[15]. Clinical studies have demonstrated that MMF-based regimens are effective in reducing acute rejection and maintaining graft function, particularly when combined with tacrolimus. These regimens are also associated with improved renal function and favourable long-term outcomes[15].

C. Corticosteroids - Broad anti-inflammatory effects

Corticosteroids exert broad anti-inflammatory effects by suppressing cytokine production and immune cell infiltration[16]. Although widely used, their long-term application is limited by systemic side effects. Liposomal delivery systems for corticosteroids, such as liposomal prednisolone (LP), can enhance local delivery to the graft, reduce systemic side effects, and improve therapeutic efficacy. Strategies to improve targeted delivery, including LP, are being explored to enhance efficacy while reducing toxicity[16].

D. mTOR Inhibitors - Selective immunomodulation

mTOR inhibitors, such as sirolimus (rapamycin), suppress T-cell proliferation by targeting cellular growth and metabolic pathways and are associated with a reduced risk of post-transplant malignancies[17]. In addition to their role in maintenance immunosuppression, mTOR inhibition is of particular interest in Treg-based therapies, as rapamycin preferentially limits conventional T-cell expansion while supporting Treg stability and enrichment during *ex vivo* culture. Sirolimus has been shown to selectively suppress the expansion of naïve T cells, which initiate new immune responses, while enhancing the function of cytomegalovirus (CMV)-specific effector memory T cells by modulating the IL-2 receptor (IL-2R)-driven Signal Transducer and Activator of Transcription 5 (STAT5) signalling pathway. This selective immunomodulatory effect makes sirolimus a valuable agent both for long-term immunosuppression and for the development of Treg cell therapy approaches in transplantation[17].

E. Co-stimulation Blockade - Improved renal outcomes

Co-stimulation blockade, particularly with belatacept (a CTLA4-Ig fusion protein that blocks T-cell costimulation), has emerged as an effective alternative to CNIs, offering significant benefits in long-

term renal function and reduced nephrotoxicity[18]. Belatacept blocks the CD28-CD80/86 pathway, preventing T-cell activation without the nephrotoxic effects associated with CNIs. Long-term results from a phase 3 study demonstrated that belatacept-based regimens were associated with significantly improved renal function, as evidenced by higher eGFR, and a 43% reduction in the risk of death or graft loss compared to cyclosporine-based regimens[18]. Additionally, belatacept-based therapies showed comparable patient and graft survival rates to cyclosporine, highlighting its potential as a safer and more effective alternative in maintaining graft function post-transplantation[18].

F. Biological Agents - Targeted immunosuppression

Monoclonal antibodies (mAbs) are an important component of targeted immunosuppression in kidney transplantation, enabling selective modulation of immune pathways involved in rejection[19]. Two key agents are basiliximab, a non-depleting anti-CD25 antibody, and alemtuzumab, a lymphocyte-depleting anti-CD52 antibody. Their comparative effectiveness was directly evaluated in the landmark 3C Study, a large, randomised trial in kidney transplant recipients. Alemtuzumab-based induction reduced biopsy-proven acute rejection compared with basiliximab-based induction, without increasing early graft failure or serious infections[19]. These findings illustrate the potential of biological therapies to modulate early alloimmune responses.

Pharmacological immunosuppression remains essential for preventing graft rejection; however, balancing efficacy with long-term safety remains a major challenge. Advances in targeted therapies, including biological agents and co-stimulation blockade, offer opportunities to reduce toxicity and improve long-term outcomes. Continued development of more precise and individualised strategies will be critical to enhancing graft survival and patient quality of life.

1.1.4 Limitations and risks of current immunosuppressive therapies

Despite their critical role in preventing graft rejection, current immunosuppressive therapies are associated with significant limitations and risks. A major concern is increased susceptibility to infections, as immunosuppression impairs host defence against pathogens. Early-onset infections with CMV and Epstein-Barr virus (EBV), occurring within 1-90 days after transplantation, are significant risk factors for antibody-mediated rejection (AMR), highlighting the need for careful monitoring and management to optimise graft outcomes[20]. Beside viral risks, long-term use of immunosuppressive drugs in solid organ transplant recipients is also associated with an elevated incidence of malignancies, particularly skin cancers and

lymphomas, due to immune suppression that impairs the body's ability to recognise and eliminate developing cancer cells[21]. In addition, many immunosuppressive agents exhibit organ-specific toxicities. CNIs, such as cyclosporine and tacrolimus, are associated with nephrotoxicity and contribute to progressive structural kidney damage. Although tacrolimus is linked to reduced acute rejection compared to cyclosporine, both agents are associated with chronic vascular injury and long-term graft dysfunction[22]. Beyond nephrotoxicity, CNIs are associated with metabolic complications, including hypertension, diabetes, and hyperlipidaemia, which increase cardiovascular risk in transplant recipients. Variability in drug exposure can further exacerbate these effects, necessitating careful therapeutic monitoring[23].

These limitations highlight the need for strategies that reduce reliance on long-term immunosuppression while preserving graft function. Emerging approaches, including cellular therapies, aim to promote immune tolerance and provide a more targeted and durable alternative to conventional immunosuppressive regimens[24].

1.1.5 Immune regulation approaches to minimise immunosuppression

Achieving immune tolerance remains a fundamental goal in transplantation to enable graft acceptance without lifelong immunosuppression. Immune regulation strategies focus on modulating immune responses to prevent rejection while maintaining protective immunity. Autologous Treg therapy has emerged as a promising strategy for inducing immune tolerance in kidney transplant recipients by reducing maintenance immunosuppression without increasing rejection risks. Clinical trials such as ONEnTreg13 (ONE Study) and the first cohort of the TWO Study (discussed in more detail in section 1.6) have demonstrated that Treg-treated patients can maintain stable graft function on low-dose tacrolimus monotherapy, minimising the need for standard dual or triple immunosuppressive regimens[25, 26].

In addition, mixed chimerism approaches, involving the introduction of donor haematopoietic cells through combined bone marrow and kidney transplantation, have demonstrated potential to induce tolerance. In some patients, this strategy has enabled complete withdrawal of immunosuppression with sustained graft function for over two to five years. Evidence of donor-specific unresponsiveness and increased Forkhead box P3 (FOXP3) expression in graft biopsies further supports its role in promoting long-term immune regulation[27].

1.2 Key immune cell subsets involved in transplant rejection

1.2.1 Macrophages & Monocytes

Macrophages and monocytes are highly plastic innate immune cells that play a central role in shaping graft outcomes through their ability to regulate inflammation and antigen presentation. During transplant rejection, these cells contribute to local inflammation by secreting pro-inflammatory cytokines such as tumour necrosis factor-alpha (TNF-α), IL-1β, and interleukin-6 (IL-6), and by presenting donor-derived antigens to recipient T cells. This promotes recruitment and activation of additional immune effectors, thereby amplifying the alloimmune response[28].

Macrophages can polarise into distinct functional states, including the pro-inflammatory M1 phenotype, characterised by high IL-12 and low IL-10 production. M1 macrophages are associated with both acute and chronic rejection and contribute to graft injury through the production of reactive oxygen species (ROS) and inflammatory mediators. As such, modulation of macrophage polarisation has emerged as a potential strategy to limit inflammation and improve graft survival[28].

Recent advances in single-cell RNA sequencing (scRNA-seq) have provided high-resolution insight into the immune landscape of transplanted organs. In kidney allografts, scRNA-seq studies have identified substantial immune heterogeneity, including distinct monocyte subsets corresponding to $CD16^+$ nonclassical and $CD16^-$ classical populations[29]. In murine models of renal transplantation, scRNA-seq has further demonstrated expansion of specific macrophage subsets, alongside reductions in naïve $CD8^+$ T cells, B cells, and neutrophils, features associated with progression from acute to chronic rejection[30]. These findings illustrate the dynamic shifts in immune cell composition during rejection and provide insight into the mechanisms driving long-term graft injury.

1.2.2 Natural Killer Cells

NK cells contribute to transplant injury through antibody-independent mechanisms, including direct cytotoxicity and the release of pro-inflammatory cytokines. In kidney transplantation, a subset of $NKG2A^+$ NK cells have been identified that responds to alloantigens and persists despite post-transplant immunosuppression. These cells release the cytotoxic mediator Ksp37, which has been associated with reduced long-term graft function and graft loss, even in the absence of histological rejection. These findings highlight a potential role for NK cells in chronic graft dysfunction and suggest that NK cell activity may serve as a biomarker for transplant outcomes[31].

1.2.3 B Cells

B cells are central to AMR through their differentiation into plasma cells that produce donor-specific antibodies (DSAs). These antibodies target graft endothelial cells, triggering complement activation, endothelial injury, and recruitment of immune cells, including monocytes, macrophages, NK cells, and T cells, leading to graft damage. Acute AMR is typically driven by high-titer DSAs, whereas chronic AMR is associated with persistent, lower-titer antibody responses and progressive graft injury[32]. In addition to antibody production, B cells can function as antigen-presenting cells and cytokine producers, further shaping the alloimmune response[32].

1.2.4 T Cells

T cells are central mediators of transplant rejection, with $CD8^+$ cytotoxic T lymphocytes (CTLs) and $CD4^+$ helper T cells (Th cells) representing the main effector subsets. $CD8^+$ CTLs contribute directly to graft injury by recognising alloantigens presented via MHC class I molecules and inducing apoptosis through perforin-granzyme-mediated cytotoxicity. In parallel, $CD4^+$ Th cells coordinate immune responses by differentiating into pro-inflammatory subsets such as Th1 and T helper 17 (Th17) cells, which secrete interferon-gamma (IFN-γ) and IL-17, respectively, thereby driving tissue inflammation and graft damage[33]. Interactions between these subsets, including cytokine-mediated crosstalk, further amplify the alloimmune response and enhance cytotoxic activity.

While Teff responses drive rejection, Tregs play a critical role in maintaining immune homeostasis and suppressing alloimmune responses by inhibiting Teff activation, modulating antigen-presenting cell (APC) function, and secreting anti-inflammatory cytokines. In addition to immune regulation, Tregs contribute to tissue protection by limiting inflammation and supporting repair processes. The balance between effector T cells (Teffs) and Tregs is therefore a key determinant of graft outcome, highlighting the therapeutic potential of Treg-based approaches to promote tolerance[34]. However, to fully exploit this potential, it is essential to identify the unique phenotypic and functional features of Tregs, particularly *ex vivo*-expanded Tregs, in comparison to Teffs. Notably, there remains a gap in the literature regarding the comprehensive transcriptomic and proteomic characterisation of these cells. The next section will further explore the characteristics and clinical applications of Tregs in transplantation.

1.2.5 Regulatory T Cells (Tregs)

1.2.5.1 Development

Tregs arise through distinct developmental pathways as thymic Tregs (tTregs) or peripherally induced Tregs (pTregs), each contributing to immune homeostasis and transplant tolerance. Their development and functional stability are regulated by cytokine signalling, transcriptional networks, and epigenetic mechanisms[35].

tTregs develop in the thymus following high-affinity recognition of self-antigens presented by thymic epithelial cells, in combination with IL-2 signalling, which induces stable FOXP3 expression. They represent the dominant Treg population in secondary lymphoid organs and play a central role in maintaining immune tolerance by suppressing autoreactive and alloreactive responses. Their lineage stability is supported by epigenetic modifications, including demethylation of the Treg-specific demethylated region (TSDR) within the FOXP3 locus[36, 37]. In contrast, pTregs are generated from conventional $CD4^+$ T cells in peripheral tissues under tolerogenic conditions, primarily driven by Transforming Growth Factor-Beta (TGF-β) and IL-2. These cells help maintain immune tolerance in peripheral tissues, including tolerance to donor antigens after transplantation. However, compared with tTregs, pTregs exhibit greater functional plasticity, as their stability depends on continued antigen and cytokine signalling[35, 38].

iTregs are generated *ex vivo* from conventional $CD4^+$ T cells under tolerogenic conditions, typically through T cell receptor (TCR) stimulation in the presence of TGF-β and IL-2[39]. Although they share FOXP3 expression with tTregs and pTregs, iTregs exhibit greater plasticity due to incomplete TSDR demethylation, making them more susceptible to losing suppressive function in inflammatory environments[39]. Recent work by Sakaguchi and colleagues has demonstrated a novel strategy for generating functionally stable human iTregs by inducing high FOXP3 expression through CDK8/19 inhibition, combined with IL-2 stimulation and deprivation of CD28 co-stimulation during induction[39]. This protocol promotes Treg-specific epigenetic imprinting and yields iTregs with transcriptional and functional properties closely resembling natural Tregs; however, such iTregs have not yet progressed to clinical evaluation. Nonetheless, these advances highlight the therapeutic potential of antigen-specific, *ex vivo*-generated iTregs for future adoptive cell therapy in transplantation.

These distinctions in origin and function underline the complexity of Treg subsets in maintaining immune tolerance. The identification of multiple Treg subpopulations in peripheral blood further emphasises the need to consider both phenotypic and functional markers to accurately define Treg subsets and their roles in immune regulation.

1.2.5.2 Phenotype

Accurate identification of human Tregs requires a combination of phenotypic and functional markers, as no single marker is exclusively definitive[40]. Tregs are identified by high expression of the IL-2R alpha chain (CD25) and the transcription factor FOXP3, which is vital for their development, stability, and suppressive function. However, FOXP3 alone is not a definitive marker in humans, as activated non-Tregs can transiently express FOXP3 without acquiring regulatory properties. To improve specificity, the interleukin-7 receptor alpha chain (CD127) is often included, as FOXP3 and CD127 expression are inversely correlated. $CD4^+CD25^+CD127^{low}$ Tregs have been shown to possess high suppressive activity and are widely used in both research and clinical settings, particularly in Treg-based cellular therapies aimed at inducing immune tolerance in transplantation[40].

In human peripheral blood, $CD4^+FOXP3^+$ Tregs are phenotypically heterogeneous and can be broadly divided into three subsets: $CD45RA^+FOXP3^{lo}/CD25^{lo}$ naïve/resting Tregs, $CD45RA^-FOXP3^{hi}/CD25^{hi}$ effector Tregs, and $CD45RA^-FOXP3^{lo}/CD25^{lo}$ non-suppressive cells, the latter of which are not considered true Tregs[36]. Mass cytometry analyses have identified over 20 Treg phenotypes based on expression of 26 canonical Treg-associated markers, reflecting the extensive heterogeneity within this compartment. This heterogeneity highlights the importance of integrating both phenotypic and functional markers when characterising Treg subsets[36]. CD45RA expression further distinguishes naïve and memory-like subsets with different stability profiles[41].

Beyond core markers, several additional molecules contribute to Treg function, including CTLA-4, glucocorticoid-induced TNFR-related protein (GITR), lymphocyte activation gene 3 (LAG3), glycoprotein A33 (GPA33), and neuropilin-1 (Nrp1); however, none are exclusively expressed by Tregs. Many of these markers, such as GITR and LAG3, are also upregulated on activated effector T cells, complicating their use as definitive identifiers. LAG3, for instance, binds to MHC class II molecules and suppresses early TCR signalling, yet it is also inducible on non-regulatory T cells following activation. This phenotypic overlap underscores that functional capacity, rather than marker expression alone, may provide a more reliable means of characterising Tregs. Consequently, a combination of surface and intracellular markers, together with functional assays, is often necessary to accurately define Tregs and distinguish them from activated Teffs[40].

1.2.5.3 Plasticity and stability

The plasticity of Tregs, particularly pTregs and iTregs, presents both therapeutic opportunities and challenges in transplantation[37]. This plasticity enables adaptation to various microenvironments but also

poses a risk, as Tregs may lose FOXP3 expression and acquire pro-inflammatory characteristics under inflammatory conditions, particularly in the presence of cytokines like IL-6 and IL-1β[35].

Epigenetic regulation at the FOXP3 locus is critical for maintaining Treg identity and suppressive function. Demethylation of the conserved noncoding sequence 2 (CNS2) region is essential for stabilising FOXP3 expression under inflammatory stress[42]. Recent work has demonstrated that pharmacological modulation of CNS2 methylation and chromatin accessibility can enhance FOXP3 imprinting during iTreg induction, promoting the generation of antigen-specific and epigenetically stable iTregs with durable suppressive function[42].

Although tTregs, pTregs, and iTregs share key phenotypic markers such as FOXP3, CD25, and CTLA-4, they differ significantly in their stability due to epigenetic differences. tTregs, which are fully demethylated at the FOXP3 locus, represent the most stable subset, with consistent regulatory function. In contrast, pTregs depend on continuous antigen exposure and cytokine signalling to maintain FOXP3 expression, while iTregs, being artificially induced, exhibit the greatest plasticity and are most susceptible to destabilisation in inflammatory environments[37].

Treg subsets are commonly classified based on the surface expression of CD45RA and the intracellular expression of FOXP3, with each subset exhibiting differing degrees of stability. Naïve/resting Tregs ($CD45RA^+FOXP3^+$) possess a fully demethylated TSDR and demonstrate high lineage stability, whereas effector/memory-like Tregs ($CD45RA^-FOXP3^+$) are more plastic and more vulnerable to functional disruption by environmental stimuli. Notably, exposure to immunosuppressive agents like tacrolimus preferentially affects $CD45RA^-FOXP3^+$ Tregs, reducing their suppressive potential more than that of their $CD45RA^+$ counterparts[41].

Emerging evidence also implicates CD70 in Treg stability. Expanded human Tregs that express CD70 exhibit reduced suppressive function, likely due to changes in activation states and resistance to apoptosis. In contrast, $CD70^-$ Tregs retain a more stable and suppressive phenotype, suggesting that controlling CD70 expression during *ex vivo* expansion may enhance Treg efficacy for therapeutic use in transplantation[43].

Balancing Treg plasticity and stability is essential for maintaining immune tolerance while preventing pathological immune activation. Enhancing the stability of pTregs and iTregs could substantially improve the effectiveness of Treg-based therapies and may reduce reliance on conventional immunosuppression in transplant recipients[35, 37].

A comprehensive understanding of Treg plasticity and stability is essential for optimising their therapeutic application in transplantation. Maintaining Treg stability remains a challenge, highlighting the need for optimised expansion protocols to preserve their identity and function[44]. Furthermore, there remains a gap in understanding how *ex vivo*-expanded Tregs differ from freshly isolated counterparts in terms of their stability, phenotype, and interactions with other immune cells. Defining these differences will be critical for predicting their *in vivo* behaviour, including survival, homing, and suppressive function, and for guiding their effective clinical application.

1.2.5.4 Treg suppressive function

Tregs interact with a wide array of immune cells to enforce immune tolerance in transplantation, employing diverse suppressive mechanisms including cytokine secretion, metabolic disruption, and direct cell-to-cell contact. Through these strategies, Tregs restrain inflammation and promote a regulatory environment that supports long-term graft survival[45].

Tregs closely interact with DCs to promote immune tolerance. They induce a tolerogenic DC (tol-DC) phenotype by downregulating co-stimulatory molecules such as CD80 and CD86 and enhancing the secretion of immunoregulatory cytokines including IL-10 and TGF-β. This interaction limits alloimmune responses by promoting T cell anergy, suppressing Teff's activation, and expanding the Treg pool. In turn, tol-DCs reinforce Treg function, creating a self-sustaining regulatory loop crucial for graft survival[46]. Tregs can further stabilise this tolerogenic state through induction of indoleamine 2,3-dioxygenase (IDO). Experimental models confirm that DC-induced Tregs can suppress Teff proliferation and promote transplant tolerance[46].

Tregs also exert direct suppressive effects on Teffs through cytokine deprivation and co-stimulation blockade[40]. By expressing high-affinity IL-2R, Tregs act as an IL-2 sink, limiting Teff proliferation and survival[40]. In addition, CTLA-4 expression enables Tregs to outcompete Teffs for CD80/CD86 binding on antigen-presenting cells, reducing co-stimulatory signalling[47]. Notably, IL-2 produced by activated T cells simultaneously supports Treg expansion and FOXP3 stability, creating a feedback loop that reinforces immune regulation[46]. Disruption of these pathways can lead to uncontrolled Teff activation and promote graft rejection[46, 47]. Alos, Tregs contribute to the regulation of humoral immunity by promoting the development and function of regulatory B cells (Bregs)[48]. In particular, IL-10^{+} Bregs suppress effector immune responses and modulate antigen-presenting cell activity, thereby reinforcing Treg-mediated immune regulation. This reciprocal interaction between Tregs and IL-10^{+} Bregs represents an additional layer of control relevant to limiting alloimmunity and promoting transplant tolerance[48, 49].

Tregs also modulate monocyte and macrophage function to promote immune regulation within the graft[50]. Through IL-10 secretion and contact-dependent mechanisms, they support macrophage polarisation towards anti-inflammatory, tissue-repair phenotypes[50]. A key example is the induction of DC-SIGN$^+$ regulatory macrophages, which suppress CD8$^+$ T cell responses and promote the expansion of CD4$^+$FOXP3$^+$ Tregs[50]. Costimulatory blockade has been shown to favour the accumulation of these macrophages and enhance IL-10 production associated with prolonged allograft survival[50]. Disruption of this pathway abrogates tolerance, highlighting the central role of these macrophages in shaping a regulatory microenvironment[50]. Despite these insights, bidirectional interactions between monocytes and *ex vivo*-expanded clinical Tregs remain incompletely understood, particularly with respect to how monocytes influence Treg phenotype and stability, and how expanded Tregs in turn shape monocyte differentiation. This represents an important gap in the literature with direct implications for optimising Treg-based cell therapies in transplantation.

1.3 Immune cell crosstalk in transplantation

Cellular interactions are central to the outcome of organ transplantation, determining whether the immune system tolerates or rejects the graft. The immune system relies on a complex network of antigen presentation, direct cell-to-cell communication, and soluble mediators such as cytokines and chemokines to coordinate immune responses. Understanding these signalling pathways and mechanisms of immune cell crosstalk is essential for developing strategies aimed at enhancing graft survival and preventing rejection[2].

1.3.1 Antigen-presenting cells (APCs)

The immune response to allogeneic transplants is initiated through three primary mechanisms of antigen presentation and recognition: direct, indirect, and semi-direct. In direct allorecognition, recipient T cells recognise intact donor MHC molecules on donor-derived APCs, such as dendritic cells. This leads to rapid T cell activation and is the primary driver of acute rejection[51, 52]. Direct allorecognition bypasses antigen processing, allowing a broad range of T cells to respond due to the high determinant density of allogeneic MHC molecules[51]. In indirect allorecognition, recipient APCs internalise, process, and present donor-derived peptides on self-MHC molecules. This pathway predominantly activates CD4$^+$ T cells, promoting alloantibody production and chronic rejection[51, 52]. Unlike direct allorecognition, this mechanism generates a slower but sustained immune response. The semi-direct pathway, also referred to as cross-dressing, represents an intermediate mechanism where recipient APCs acquire intact donor MHC-peptide complexes via trogocytosis or extracellular vesicles. These "cross-dressed" APCs then present unprocessed alloantigens

directly to recipient T cells, sustaining immune activation even after donor APCs are eliminated[53]. This mechanism has been observed in both human and murine transplantation models, where cross-dressed recipient APCs can prime T cells in a donor MHC-restricted manner[53]. However, some studies suggest they may be insufficient to induce full T cell proliferation without concurrent antigen processing via the indirect pathway[54]. The relative contribution of each pathway to acute and chronic rejection remains an area of active investigation.

1.3.2 Direct cell-to-cell communication

Beyond antigen presentation, direct cell-to-cell communication between immune cells plays a fundamental role in transplant immunity. Central to this process is the immune synapse, a specialised junction between T cells and APCs that facilitates signal transmission. Here, TCRs engage MHC-peptide complexes on APCs, initiating T cell activation, proliferation, and differentiation. This interaction is strengthened by costimulatory molecules, such as CD28-CD80/CD86 and CD40-CD40L, which amplify immune responses and are key targets for immunosuppressive therapies like belatacept[51, 52].

Mechanisms such as trogocytosis, described above in the context of semi-direct allorecognition, also contribute to cell-cell communication by transferring membrane fragments, including MHC-peptide complexes, between interacting cells. In the regulatory setting, Tregs exhibit enhanced trogocytosis activity compared with other T cell subsets. Through this process, Tregs can remove MHC class II and costimulatory molecules from APC surfaces, thereby limiting antigen presentation and dampening effector T cell activation[53]. This capacity to directly modulate APC function underscores the dual role of cell-cell interactions in transplantation, both as drivers of immune activation and as mechanisms for promoting tolerance.

1.3.3 Soluble mediators: cytokines and chemokines

1.3.3.1 Cytokine networks in transplantation

Beyond physical interactions, the immune response is orchestrated by a rich milieu of soluble mediators. Cytokines are key regulators of immune responses, facilitating intercellular communication and influencing immune cell activation, differentiation, and function[55]. They are classified based on their receptor families and biological effects, with members of the common cytokine receptor γ chain (γc) family, including IL-2, IL-4, IL-7, IL-9, IL-15, and IL-21, playing central roles in T cell homeostasis and immune regulation[55]. Cytokines act through complex signalling pathways, directing immune responses in both homeostasis and

inflammation. Their dysregulation can lead to excessive immune activation, resulting in a pathological cytokine storm, which has been implicated in autoimmune diseases, sepsis, and transplant rejection[56].

1.3.3.1.1 Pro-inflammatory cytokines in graft rejection

In the context of transplantation, cytokine networks influence immune activation, tolerance, and graft survival. Pro-inflammatory cytokines such as IL-6, TNF-α, and IFN-γ, are key drivers of alloimmune responses, amplifying T cell activation, antigen presentation, and inflammatory cell recruitment to the graft[57]. IL-6 plays a pivotal role in transplant rejection by promoting Th17 differentiation while inhibiting Treg expansion. Studies in murine models have demonstrated that IL-6 blockade can prevent co-stimulation blockade-resistant rejection and enhance immune regulation within the graft[58]. Similarly, TNF-α contributes to endothelial dysfunction, increases leukocyte adhesion, and exacerbates chronic allograft injury, making it a critical target for therapeutic intervention[57]. IFN-γ further amplifies rejection by upregulating major MHC expression and enhancing cytotoxic T cell responses, reinforcing its role in acute and chronic rejection[57].

1.3.3.1.2 Regulatory cytokines and immune tolerance

In contrast to the pro-inflammatory cytokines that drive rejection, regulatory pathways mediated by Tregs rely on anti-inflammatory cytokines such as TGF-β, IL-10, IL-35, and IL-2 to maintain immune tolerance and promote allograft survival[35]. These cytokines sustain FOXP3 expression, suppress effector T cell activation, and regulate the Treg/Th17 balance.

TGF-β is central to Treg differentiation and function, promoting FOXP3 expression and regulating the Treg-Th17 axis, favouring Treg expansion under steady-state conditions but supporting Th17 differentiation in inflammatory environments[59]. IL-10 enhances Treg-mediated suppression and inhibits pro-inflammatory cytokine production, while also supporting the differentiation of Tr1 regulatory cells that contribute to transplant tolerance[35, 59]. IL-35 further augments Treg suppressive capacity by inducing the conversion of conventional $CD4^+$ T cells into IL-35-producing regulatory cells (iTr35)[59]. It has also been linked to increased Treg accumulation in tumours[35]. IL-2 is essential for Treg survival and proliferation, signalling through CD25 and the transcription factor STAT5 to maintain FOXP3 expression, with low levels favouring Tregs and higher levels promoting effector T cell expansion[35, 59]. These cytokines shape a regulatory immune environment that limits effector responses and supports graft acceptance. Therapeutic modulation of these pathways, particularly targeting IL-2 and TGF-β signalling, is being explored to enhance Treg function in transplantation.

Overall, the balance between pro-inflammatory and regulatory cytokines is a key determinant of transplant outcome, influencing whether immune responses progress towards rejection or tolerance. This cytokine

milieu also shapes the recruitment and function of immune cells within the graft, linking cytokine regulation to the chemokine networks discussed below.

1.3.3.2 Chemokine networks in transplantation

1.3.3.2.1 Overview of chemokines

Chemokines are a family of small cytokines that regulate immune cell migration and play a central role in immune surveillance, inflammation, and tissue homeostasis. Since their discovery, extensive research has underscored their importance in leukocyte trafficking under both physiological and pathological conditions. Their primary function is to induce chemotaxis, guiding immune cells to sites of inflammation or injury to ensure effective immune responses and maintain tissue integrity. Additionally, chemokines contribute to lymphoid organ development and immune cell maturation by directing cellular movement through a complex chemokine-receptor system, where chemokine ligands bind to G protein-coupled receptors (GPCRs), initiating intracellular signalling cascades that mediate cell migration[60]. This signalling network enables immune cells to dynamically respond to both homeostatic and inflammatory stimuli[60]. The chemokine system in humans and mice comprises approximately 50 ligands and 20 signalling receptors, reflecting its high degree of specificity and complexity in immune regulation[61].

1.3.3.2.2 Chemokine classification and structure

Chemokines are classified into four subfamilies based on the arrangement of conserved cysteine residues near the N-terminus: CC, CXC, CX3C, and C chemokines. CC chemokines, which contain two adjacent cysteines, primarily attract monocytes, DCs, and NK cells. In CXC chemokines, the cysteines are separated by a single amino acid and are typically involved in the recruitment of neutrophils[60]. CX3C chemokines, characterised by three amino acids between the cysteines, serve both as chemoattractants and adhesion molecules, facilitating leukocyte-endothelial interactions. The C chemokine family, which includes XCL1 and XCL2, is defined by the presence of only two cysteines, one near the N-terminus and one downstream, and is involved in T cell recruitment[60].

Structurally, chemokines share a conserved fold comprising a β-sheet and an α-helix, stabilised by disulfide bonds that are critical for receptor binding and downstream signalling. Functionally, chemokines can be categorised as either homeostatic or inflammatory. Homeostatic chemokines control the steady-state trafficking of immune cells, supporting immune surveillance and tissue maintenance under non-inflammatory conditions. In contrast, inflammatory chemokines are rapidly induced in response to tissue damage or infection and mediate the recruitment of immune cells to sites of inflammation[60, 62].

1.3.3.2.3 Chemokines in transplant rejection

Chemokines play a crucial role in transplant rejection by mediating immune cell recruitment and amplifying local inflammatory responses. Among them, CXCL9, CXCL10, and CXCL11 have emerged as key mediators in this process[30, 63]. Recent scRNA-seq analyses in murine models of renal and cardiac transplantation have demonstrated significant upregulation of these chemokines, correlating with increased infiltration of monocytes, T cells, and NK cells into the graft, thereby contributing to acute rejection episodes[30, 63].

Teffs are central to allograft rejection, with CXCR3 acting as a critical receptor in Th1-mediated responses. High expression of CXCR3 on Teffs facilitates their migration toward inflamed graft tissue, intensifying graft inflammation and the risk of acute rejection. In cardiac transplant models, $CXCR3^+$ Teffs have been shown to infiltrate grafts extensively, underscoring their role in alloreactivity and tissue damage[63]. In addition to T cells, monocytes contribute significantly to the inflammatory milieu in liver transplantation. Recruited via CCR2 and CCR5, these cells traffic to the graft site where they exacerbate immune-mediated injury by promoting inflammation and fibrosis, processes that have been implicated in worsening rejection outcomes[62].

These findings highlight the critical role of chemokine-receptor signalling in alloreactive immune responses and suggest that targeting specific chemokine pathways may be an effective strategy to mitigate immune-mediated graft injury and improve transplant outcomes.

1.3.3.2.4 Chemokines in immune cell recruitment

Chemokines are essential regulators of immune cell trafficking, guiding leukocyte migration during both homeostatic and inflammatory processes. Although their function extends beyond transplantation, chemokines play a significant role in immune responses during graft acceptance and rejection. Several chemokine receptors contribute to transplant immunity by directing specific immune cell subsets to specific tissue sites, as outlined in Table 1.2.1.

For instance, CXCR3, which binds CXCL9, CXCL10, and CXCL11, directs Th1 cells to inflamed tissues and has been strongly implicated in graft rejection[64]. CXCR4 interacts with CXCL12 to regulate stem cell homing, lymphocyte trafficking, and tissue repair. CXCR5 guides B and Tfh cells localisation via CXCL13, playing a central role in lymphoid follicle organisation. Additionally, CXCR6 contributes to the positioning of tissue-resident T cells and NK cells within inflamed grafts. CCR2 and CCR5 promote the infiltration of monocytes and T cells, thereby exacerbating inflammation and tissue injury. In contrast, CCR7 directs T cells and DCs to secondary lymphoid organs, facilitating antigen presentation and T cell priming[61, 64].

CCR4 and CCR8 are closely associated with the migration of Tregs and immune modulation, underscoring their role in maintaining tolerance. Together, these receptor-ligand interactions highlight the complex and cell-specific contributions of chemokine pathways in shaping transplant outcomes[61, 64].

Table 1.3.1. Chemokines and their roles in immune cell migration.

Chemokine Receptor	Ligands	Primary Immune Cells Recruited	Key Functions
CXCR3	CXCL9, CXCL10, CXCL11	Th1, Th17, Tregs, CD8+ T cells, NK cells	Th1 and Th17 immune responses, T cell recruitment
CXCR4	CXCL12	B cells, leukocytes	Bone marrow homing, haematopoiesis
CXCR5	CXCL13	B cells, Tfh cells, Tfr cells	B cell and T cell trafficking in lymphoid tissues
CXCR6	CXCL16	T cells, NK cells	NK and T cell recruitment
CCR2	CCL2, CCL7, CCL8, CCL12, CCL13	Monocytes, macrophages	Monocyte trafficking and inflammation
CCR3	CCL5, CCL7, CCL11, CCL13, CCL15, CCL24, CCL26	Eosinophils, basophils	Eosinophil trafficking, type 2 immunity
CCR4	CCL17, CCL22	Tregs, Th2 cells, Th17 cells, CD8+ T cells	Treg recruitment and retention, Th2 responses
CCR5	CCL3, CCL4, CCL5, CCL8	Monocytes, T cells, NK cells, Tregs	Monocyte and macrophage recruitment, Th1 responses
CCR6	CCL20	Th17 cells, DCs, B cells, Tregs	Th17 responses, DC and B cell trafficking
CCR7	CCL19, CCL21	T cells, DCs, B cells, Tregs	T cell and DC homing to lymphoid tissues
CCR8	CCL1, CCL18 (human)	Th2 cells, Tregs	Th2 responses, immune surveillance in skin
CCR9	CCL25	T cells, thymocytes	T cell homing to the gut

(Adapted from Ozga, A.J., Chow, M.T., & Luster, A.D. (2021). Chemokines and the immune response to cancer[64]. Immunity, 54(5), 859-874. https://doi.org/10.1016/j.immuni.2021.01.012) (Licensed under 6086030641408).

Within these chemokine-regulated pathways, Tregs are of particular importance in transplantation, as their trafficking to inflamed tissues is essential for suppressing alloimmune responses and promoting tolerance. This process is tightly governed by chemokine networks, which guide their migration and enable local immune regulation. These networks facilitate Treg recruitment to inflamed tissues such as the skin, liver, and kidney allografts, where they help balance immune activation and suppression, thereby supporting graft survival[62, 65, 66].

In the context of psoriasis, Tregs exhibit impaired skin-homing capacity due to reduced expression of CCR4 and cutaneous lymphocyte-associated antigen (CLA), alongside increased CCR7 levels. This altered chemokine receptor profile hinders their accumulation in inflamed skin and compromises their ability to

suppress local inflammation[65]. Although psoriasis is not a transplant-related condition, it illustrates how chemokine dysregulation can impair Treg trafficking, a mechanism that is also relevant in transplantation, particularly for skin graft outcomes. Additionally, innate immune cells contribute to Treg recruitment through chemokine signalling. Gr-1$^+$ innate cells enhance Treg trafficking to skin grafts, while the CCR4 ligands CCL17 and CCL22 promote Treg migration. Activated neutrophils and monocytes also facilitate Treg migration, likely via GPCR-mediated signalling pathways[67].

In liver transplantation, Tregs recruited to the graft express high levels of CXCR3, enabling their transmigration across hepatic vasculature, while CCR4-CCL17/CCL22 interactions support their retention in chronically inflamed liver tissue[62]. Similarly, in kidney transplantation, chemokine gradients such as CCL5 are critical for intragraft Treg localisation. Notably, myeloid-derived suppressor cells (MDSCs) regulate CCL5 levels, establishing a chemotactic gradient that promotes Treg accumulation within the graft. Disruption of this gradient reduces intragraft Treg numbers and impairs graft survival[66].

These findings highlight the coordinated roles of chemokines, Tregs, innate immune cells, and MDSCs in regulating immune responses during transplantation. A deeper understanding of these pathways could refine the development of Treg-based therapies and contribute to improved long-term graft outcomes.

1.4 Homing and chemokine receptor expression

1.4.1 Leukocyte homing

The migration of immune cells from circulation into tissues is a tightly regulated process known as transendothelial migration (TEM). This mechanism enables leukocytes to exit blood vessels and reach peripheral tissues[68]. TEM involves several sequential steps: rolling, adhesion, crawling, and transmigration across the endothelial barrier[69], as illustrated in Figure 1.4.1. These stages are controlled by interactions between chemokines, adhesion molecules, and local inflammatory cues, ensuring precise immune cell recruitment during both homeostasis and inflammation[52].

In the rolling phase, selectins expressed on endothelial cells mediate transient interactions with circulating leukocytes, slowing their movement through the vasculature[68]. This initial contact transitions to firm adhesion, triggered by endothelial-derived chemokines that bind to leukocyte receptors and activate integrins[69, 70]. Activated integrins, such as VLA-4, then bind to their ligands (e.g., VCAM-1) on endothelial

cells. Following adhesion, leukocytes undergo crawling, scanning the endothelial surface to locate optimal sites for transmigration, guided by local chemokine gradients[52, 70].

In the final step, transmigration, leukocytes cross the endothelial layer via paracellular (between cells) or transcellular (through cells) pathways, facilitated by chemokine receptor engagement and adhesion molecule interactions[68, 70].

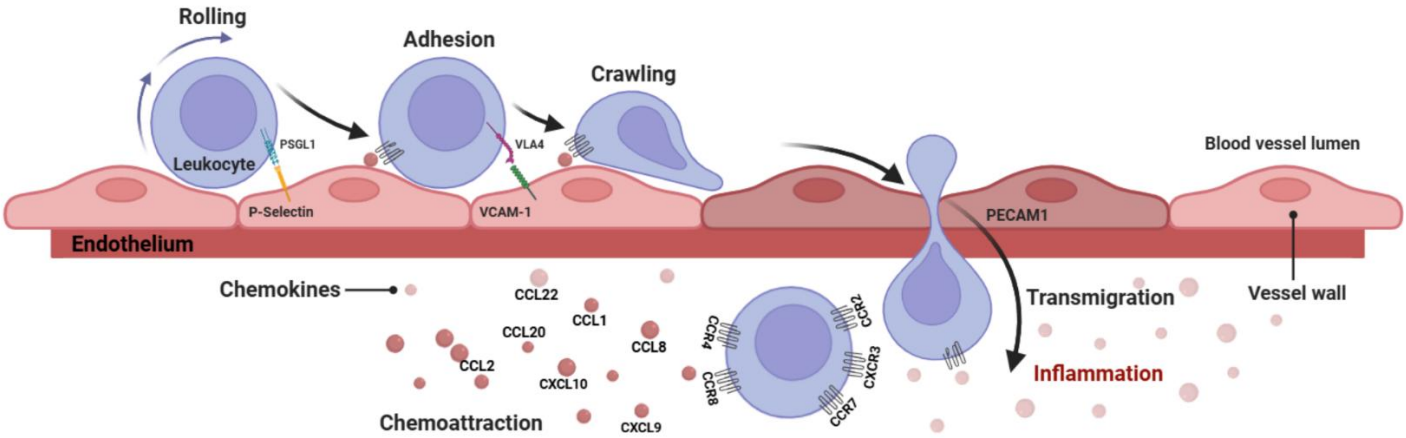


Figure 1.4.1 Leukocyte migration across endothelium.

Leukocyte migration across the endothelium involves a series of sequential steps to facilitate immune surveillance and inflammation. The process begins with rolling, where leukocytes are slowed by interactions between selectins (such as P-selectin) on endothelial cells and ligands like PSGL-1 on leukocytes. This is followed by activation, where chemokines on the endothelial surface bind to leukocyte chemokine receptors, triggering intracellular signalling that induces conformational changes in integrins. During the adhesion phase, activated integrins such as VLA-4 bind to endothelial ligands like VCAM-1, allowing leukocytes to adhere firmly to the endothelium. Once adhered, leukocytes undergo crawling, moving laterally along the endothelial surface to locate optimal sites for transmigration. Finally, during the migration phase, leukocytes cross the endothelium via paracellular pathways (between endothelial cells) or transcellular pathways (directly through endothelial cells), guided by chemokines. Created by Biorender.

While TEM is a shared feature among leukocytes, T cells exhibit unique trafficking programs that allow them to navigate complex tissue environments efficiently. These processes are guided by the expression of specific chemokine receptors and integrins in response to local inflammatory signals[69].

1.4.2 T cell homing

Upon activation, Teffs, including $CD4^+$ Th cells and $CD8^+$ CTLs, upregulate chemokine receptors that enable migration towards inflamed tissues. A key example is CXCR3, commonly expressed by Th1 cells and $CD8^+$ T cells, which responds to CXCL9 and CXCL10 released at sites of tissue injury[69, 71]. These chemokines establish gradients that guide $CXCR3^+$ T cells from the circulation into inflamed tissues. In kidney transplantation, early elevations in CXCL9 and especially CXCL10 are associated with subsequent acute rejection and reduced allograft survival, supporting their role as biomarkers of alloimmune activation[72]. Other T cell subsets display distinct homing profiles: Th2 cells express CCR4, responding to CCL17 and CCL22, while Th17 cells

express CCR6 and are recruited via CCL20 to mucosal and inflamed tissues. In autoimmune kidney disease, local production of CCL20 promotes the recruitment of $CCR6^+$ Th17 cells, which contribute to renal tissue damage through the secretion of pro-inflammatory cytokines such as IL-17A and IL-17F[71]. Additionally, $CXCR6^+$ T cells, interacting with CXCL16, have been implicated in the recruitment of invariant natural killer T (iNKT) cells during nephritis[71].

This targeted migration ensures that Teffs efficiently localise to antigen-rich sites to exert effector functions. While chemokine-receptor interactions, such as CXCR3-CXCL9/CXCL10 and CCR6-CCL20, promote T cell recruitment and tissue entry, endothelial-derived signals can also limit inappropriate T cell infiltration[73]. For example, changes in chemokine gradients and reduced expression of adhesion molecules such as ICAM-1 and VCAM-1 can restrict T cell extravasation. Together, this balanced regulation of recruitment and exclusion is central to controlling T cell trafficking and may inform strategies to modulate immune cell migration in autoimmune disease and transplantation[69, 71].

1.4.3 Treg homing

Unlike Teffs, which primarily migrate to inflamed tissues to mediate immune responses, Tregs rely on finely tuned homing mechanisms to access sites of immune activation or tolerance, where they suppress inflammation and maintain immune homeostasis. This tissue-specific migration is regulated, although not exclusively, by chemokine receptor expression, alongside contributions from adhesion molecules, endothelial cues, and local tissue-derived signals, enabling Tregs to respond to distinct inflammatory environments and exert localised immunosuppressive effects[74].

Tregs expressing CCR7 preferentially home to secondary lymphoid organs, where they suppress activation of autoreactive Teffs[71]. In inflamed renal tissues, $CCR6^+$ Tregs are recruited via CCL20, modulating Th17-mediated responses and limiting tissue damage, while $CXCR3^+$ Tregs co-localise with $CXCR3^+$ Teffs in Th1-driven inflammation to restrain excessive immune activation[71]. In experimental crescentic glomerulonephritis, loss of CXCR3 impaired Treg recruitment and exacerbated renal injury, highlighting the importance of chemokine-guided trafficking in controlling inflammation[71].

Moreover, recent studies demonstrate that effective Treg-mediated immune regulation in the skin is critically dependent on their acquisition of tissue-specific homing programmes[75, 76]. IL-33 activation induces a distinct transcriptional signature in mouse Tregs, characterised by upregulation of key graft and lymph node-homing chemokine receptors, including CCR4, CCR5, CCR2 and CCR7, while simultaneously enhancing expression of the IL-33 receptor ST2[75]. These IL-33-expanded Tregs exhibit increased proportions of

$CCR4^+FOXP3^+$ cells, facilitating migration towards skin- and graft-associated chemokine gradients. Notably, this enhanced homing capacity translates into superior *in vivo* suppressive activity and prolonged skin allograft survival, despite no measurable increase in suppressive function *in vitro*[75]. Human studies further reinforce the importance of tissue-specific homing[76]. Peripheral blood-derived Tregs, which express higher levels of CLA and CCR4, efficiently migrate into human skin and prevent alloimmune-mediated tissue damage, whereas cord blood-derived Tregs lacking these homing receptors fail to confer protection[76]. Thus, the efficacy of skin-homing Tregs in cutaneous transplantation depends not only on their suppressive capacity but also on the acquisition of appropriate chemokine receptor profiles that direct migration into the skin.

To enhance the effectiveness of Treg-based therapies, strategies aimed at preserving or restoring chemokine receptor expression during *ex vivo* expansion are under investigation. Tailoring culture conditions to maintain responsiveness to key chemokines, as well as genetic or pharmacological manipulation of homing receptor profiles, has shown promise in improving Treg localisation, persistence, and immunoregulatory function within graft tissues[74, 77]. Nevertheless, there remains limited understanding of the chemokine receptor landscape of *ex vivo*-expanded clinical Tregs, representing an important gap in optimising their trafficking and functional integration post-transfer.

1.5 Cellular therapy in transplantation

1.5.1 Types of cellular therapies used in transplantation

Several types of cellular therapies have been explored to enhance graft survival and immune tolerance in transplantation. Hematopoietic stem cell transplantation (HSCT) has traditionally been utilised to restore immune function following myeloablation, and in transplantation, it has been investigated to induce donor-recipient mixed chimerism. Clinical studies demonstrated that combined kidney and hematopoietic-cell transplantation using low-intensity conditioning regimens could establish persistent mixed chimerism, enabling withdrawal of immunosuppression without triggering rejection or graft-versus-host disease[78].

Mesenchymal stem cells (MSCs) have also emerged as promising candidates because of their immunomodulatory properties. MSCs suppress pro-inflammatory responses, modulate T cell proliferation, and interact with innate immune cells such as macrophages and DCs, shifting immunity towards a tolerogenic state[79]. Preclinical transplantation models have shown that MSCs can prolong graft survival

across multiple organs despite their short-lived persistence after infusion, likely through induction of regulatory phenotypes in APCs and macrophages[80]. Clinical trials have confirmed the safety and feasibility of MSC administration, although variability in function, optimal dosing, timing, and delivery methods remain under investigation[79, 80].

Regulatory immune cell-based therapies, including tol-DCs and regulatory macrophages, have likewise been investigated in transplantation. Tol-DCs promote graft tolerance by dampening T cell activation and enhancing regulatory pathways, whereas regulatory macrophages support an anti-inflammatory microenvironment favourable to long-term graft acceptance. The ONE Study, a multi-centre clinical trial, provided evidence for the safety and feasibility of these therapies in kidney transplantation, with encouraging preliminary findings suggesting reduced dependence on conventional immunosuppression without increased rejection and with fewer infectious complications[80, 81].

Alongside these approaches, adoptive transfer of Tregs has gained significant attention as a more targeted strategy to promote graft tolerance. Unlike conventional immunosuppression, Tregs offer a more precise approach by selectively inhibiting donor-reactive immune responses while preserving broader immune competence. Optimised protocols for generating and expanding polyclonal or donor-specific Tregs have shown potent inhibition of alloimmune responses, suggesting their potential to promote long-term tolerance while preserving protective immunity against infections and malignancies[82].

These diverse cellular therapies represent a shift in transplantation, moving from broad immunosuppression toward targeted immune modulation strategies aimed at achieving long-term graft survival with minimal side effects. As ongoing research refines these approaches, the integration of cellular therapies into routine transplant protocols could transform the field, offering patients more effective and less toxic alternatives to conventional immunosuppressive regimens.

1.5.2 Treg therapy in transplantation

As mentioned above, Treg therapy involves the isolation, *ex vivo* expansion, and reinfusion of autologous Tregs into the recipient instead of using conventional immunosuppressive drugs. Recent clinical studies, including those in living donor renal transplantation, demonstrated that infusion of autologous expanded Tregs following alemtuzumab induction therapy is safe and facilitates the minimisation of maintenance immunosuppression[83]. These studies showed that recipients could successfully transition to tacrolimus monotherapy without increased acute rejection risk. By promoting immune tolerance, Treg therapy offers a promising strategy to mitigate the long-term complications associated with lifelong immunosuppressive

regimens and provides opportunities to refine timing and protocols for cellular therapies in transplantation[83].

In addition to peripheral blood-derived Tregs, alternative cellular sources are also being explored. A recent first-in-human study demonstrated the feasibility and safety of using thymic-derived regulatory T cells (thyTregs), isolated from thymic tissue routinely removed during paediatric cardiac surgeries[84]. Autologous thyTregs exhibited potent suppressive function, maintained phenotypic stability, and restored the peripheral Treg pool in paediatric transplant recipients. These results highlight thyTregs as a promising alternative source that may help overcome limitations of peripheral blood-derived Tregs, including lower cell yield and phenotypic instability[84].

Recent advances in genetic engineering have also enabled the development of chimeric antigen receptor (CAR) Tregs, which offer enhanced antigen specificity and functional precision. CAR-Tregs are designed to recognise donor-specific alloantigens, thereby improving their targeted suppressive capacity and potential persistence *in vivo*[85]. Preclinical studies using CAR-Tregs targeting HLA-A*02 alloantigens demonstrated potent immunosuppressive function, antigen-specific stability, and robust suppression of alloimmune responses in humanised transplantation models[85]. Nevertheless, CAR-Treg therapies face key challenges, including restricted antigen specificity, maintaining stability, and demonstrating clinical efficacy.

Among the emerging Treg-based strategies discussed above, polyclonal autologous Tregs currently appear to be the most clinically advanced approach, with established feasibility and encouraging safety data in transplantation. While thymic-derived Tregs and CAR-Tregs offer attractive future alternatives, particularly in relation to cell yield or antigen specificity, their broader clinical applicability remains less well defined. Overall, polyclonal Treg therapy currently seems to represent the most practical and translationally mature platform for targeted immune modulation in transplantation.

1.6 The Transplantation Without Overimmunosuppression (TWO) study trial

The TWO Study is a phase IIb, single-centre, randomised controlled trial designed to evaluate the safety and efficacy of autologous Treg therapy in enabling immunosuppression minimisation in living donor kidney transplant recipients[25]. Given the established immunoregulatory role of Tregs in promoting graft tolerance, the trial aimed to determine whether Treg infusion could reduce the need for conventional immunosuppressive therapy. However, emerging safety concerns related to alemtuzumab prompted substantial protocol modifications, resulting in distinct pre- and post-COVID-19 study protocols[83].

1.6.1 Initial study protocol: Alemtuzumab induction with delayed Treg infusion

The initial protocol of the TWO Study randomised living donor kidney transplant recipients into two groups. The control group received standard immunosuppressive therapy, while the experimental group underwent alemtuzumab induction at the time of transplantation, followed by an infusion of autologous, *ex vivo* expanded polyclonal Tregs at six months post-transplant[83]. This strategy was based on the hypothesis that delayed Treg infusion during the lymphocyte repopulation phase following alemtuzumab-induced depletion would create a Treg-favourable immune environment, thereby enabling immunosuppression minimisation without compromising graft function[83].

The primary endpoint was to assess the feasibility and safety of Treg therapy, with key outcome measures including patient and graft survival, biopsy-proven acute rejection, and immunological markers of tolerance. Secondary endpoints included long-term graft function, immunosuppressive burden, and drug-related complications[83].

The results demonstrated that Treg infusion was both feasible and safe, even up to 12 months after cell manufacture. Successful cell expansion and cryopreservation were achieved, and all patients in the Treg-treated group exhibited 100% graft survival with no acute rejection events at 18 months post-transplant. However, due to emerging safety concerns, alemtuzumab was withdrawn from use in UK transplant centres, prompting a revision of the study protocol to adopt an alternative immunosuppressive regimen[83].

1.6.2 Modified study protocol: Basiliximab induction with early Treg infusion

Following the withdrawal of alemtuzumab from clinical use, the TWO Study protocol was revised to implement a basiliximab-based immunosuppressive regimen. In the modified protocol, control arm participants received basiliximab induction alongside tacrolimus, MMF, and prednisolone, followed by gradual tapering to dual maintenance therapy using tacrolimus and MMF[25]. In the Treg therapy arm, patients received an infusion of 5 to 10 million autologous *ex vivo* expanded Tregs per kilogram of body weight on day 5 post-transplantation, serving as a replacement for monoclonal antibody induction. This modification aimed to evaluate whether early Treg administration could enhance immune regulation and support immunosuppression minimisation during the critical early post-transplant period[25].

The revised protocol retained the primary endpoints of safety and feasibility, while secondary outcomes included graft function, rates of acute rejection, and the potential to reduce long-term immunosuppressive therapy[25]. Early Treg infusion was designed to exert immunomodulatory effects during the peak of alloimmune activation. Preliminary results suggest that this approach is well tolerated, with no immediate

safety concerns; however, its long-term efficacy in promoting immune tolerance and sustaining graft function remains under evaluation[25].

1.6.3 Manufacturing and Treg Therapy

The TWO Study was developed on the hypothesis that autologous Tregs could promote immune tolerance and reduce reliance on conventional immunosuppression in kidney transplantation. To test this, Tregs were isolated from transplant recipients before surgery, expanded *ex vivo* under Good Manufacturing Practice (GMP) conditions, and infused either at 6 months post-transplant in the original protocol[83] or on day 5 post-transplant in the revised protocol[25], as shown in Figure 1.6.4. Although the timing of infusion differed between the two protocols, the Treg manufacturing and expansion strategy remained the same[25, 83]. The study further incorporated comprehensive immune monitoring to assess Treg persistence, phenotypic stability, and interactions with other immune cell subsets.

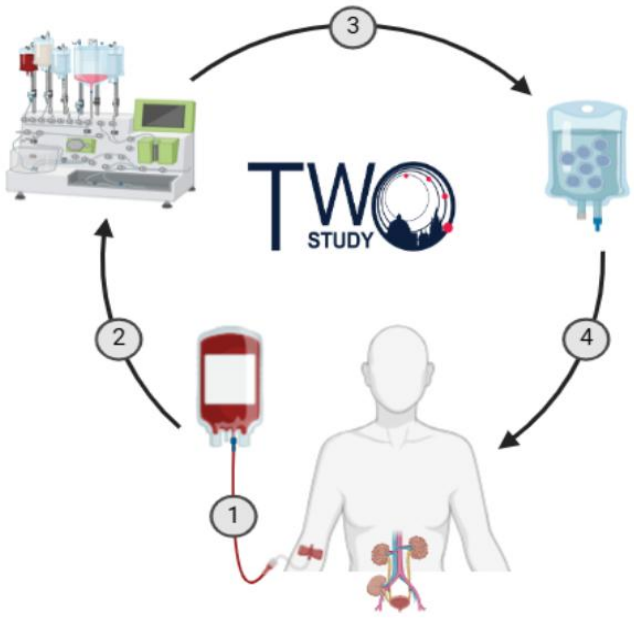


Figure 1.6.4 Schematic representation of Treg therapy in the TWO Study.

*(1) **Treg Isolation**: Whole blood (370 mL) is collected from patients at least three weeks before transplantation to produce the autologous Treg product. (2) **Treg Enrichment**: CD8+ cells are depleted, and CD25+ cells are positively selected, yielding an enriched population of $CD4^+CD25^+FOXP3^+$ regulatory T cells (~75% of cells entering expansion). (3) **Treg Expansion**: Cells undergo multiple rounds of polyclonal expansion using anti-CD3 and anti-CD28 bead stimulation in the presence of IL-2. Rapamycin is included in the culture process to enhance Treg stability and suppress contaminant effector cells. (4) **Treg Infusion**: The final product, containing 5-10 × 10^6 cells/kg, is cryopreserved and later administered to the kidney transplant recipient. Created by Biorender.*

Following randomisation, peripheral blood was collected from recipients assigned to the Treg therapy arm and transferred to a GMP facility for processing. Tregs were manufactured by initial blood volume reduction,

followed by immunomagnetic isolation through CD8 depletion and CD25 enrichment, and subsequent *ex vivo* expansion to the target dose using repeated anti-CD3/anti-CD28 stimulation in the presence of rapamycin and IL-2[25, 83]. The final cell product underwent phenotypic and functional characterisation before cryopreservation, transport under controlled ultra-low-temperature conditions, bedside thawing, and intravenous administration, either at week 26 following withdrawal of MMF in the original protocol or on day 5 post-transplant in the revised protocol[25, 83] (Figure 1.6.4).

1.6.4 Summary and implications for future research

Results from the initial protocol demonstrated favourable graft survival and stable immune profiles, supporting the feasibility and safety of Treg-based immunotherapy[83]. Ongoing analysis of the revised protocol will help determine the optimal timing of Treg infusion and its long-term effects on graft outcomes[83].

A key priority for future research is improving Treg homing and persistence, as these factors are critical for sustained therapeutic efficacy. Achieving efficient trafficking and retention within the graft requires a deeper understanding of the chemokine-receptor networks that regulate Treg migration, which remain incompletely defined. Identifying the key chemokines and receptors involved in Treg localisation to renal allografts may inform strategies to enhance their functional stability and suppressive capacity within the graft microenvironment[86]. In addition, elucidating interactions between Tregs and other immune subsets, particularly monocytes and/or APCs, may reveal further mechanisms underlying immune regulation and transplant tolerance.

Collectively, findings from the TWO Study provide a framework for refining Treg-based therapies. Improvements in trafficking, persistence, and functional stability will be central to advancing these approaches towards clinical application and immunosuppression minimisation[25, 83, 86, 87].

1.7 Thesis aims & objectives

- Examine the homing potential and cellular interactions of human expanded Tregs to gain insight into their immunoregulatory characteristics, including their trafficking, stability, and interactions with immune cells in the transplant environment (Chapters 3 and 4).

- Investigate the impact of Treg therapy on immune modulation in renal transplantation, focusing on its effects on circulating and graft-infiltrating leukocytes, with the goal of refining and optimising clinical Treg-based therapies (Chapter 5).

1.8 Thesis hypotheses

- Clinically expanded Tregs exhibit distinct homing properties, and a unique molecular profile compared to freshly isolated Tregs and conventional T cells, influencing their migration and functional capacity in transplantation (Chapter 3).

- Monocytes play a key role in enhancing the immunosuppressive function of Tregs through direct and indirect cellular interactions, contributing to immune regulation in the transplant environment (Chapter 4).

- Treg infusion may support immune regulation without inducing significant alterations in circulating immune cell populations, while shaping graft-infiltrating leukocyte organisation and transcriptional profiles within the renal allograft (Chapter 5).

---

2 Chapter 2: Materials and Methods

2.1 Human material

2.1.1 TWO Study clinical trial protocol

The TWO Study (REC ref: 18/SC/0054, Eudract number 2017-001421-41) is a single-centre, phase II randomised trial investigating the safety and efficacy of autologous polyclonally expanded Tregs in living donor kidney transplant recipients. Ethical approval was obtained from the South Central - Oxford A Research Ethics Committee, and written informed consent was collected from all participants[25]. Under the original protocol, patients received alemtuzumab induction followed by Treg infusion six months post-transplant. Due to the increased risk of severe COVID-19 in lymphodepleted patients, the protocol was subsequently revised to incorporate basiliximab-based induction. In the revised protocol, patients in the Treg therapy arm received autologous polyTregs alongside tacrolimus monotherapy, while control patients received standard immunosuppression with tacrolimus and MMF. All participants received basiliximab induction and were followed for up to 78 weeks post-transplant[83]. This thesis includes biopsy data from the original protocol and immune monitoring analyses from the revised protocol (Chapter 5).

2.1.2 Healthy blood donors

Peripheral blood mononuclear cells (PBMCs) were isolated from blood cones obtained from healthy donors (NHS Blood and transplant [NHSBT] UK).

2.2 General laboratory methods

2.2.1 Isolation of PBMC by density gradient centrifugation

PBMCs were isolated from blood cones using a lymphocyte separation medium (LSM), (25-072-CV, Corning) for density gradient centrifugation at 2200rpm, at room temperature, for 30mins. Buffy coats were collected and washed with PBS buffer. Erythrocytes were lysed by incubating the PBMCs for 5mins in PharmLyse lysing buffer (BD biosciences, Franklin Lakes, NJ, USA). PBMCs were counted and subsequently used in PBMCs-based assays or cryopreserved for later use.

2.2.2 Cryopreservation and thawing of human leukocytes

Cells were resuspended in a freezing medium composed of 45% RPMI, 45% Foetal Calf Serum (FCS), 10% DMSO at 50-100x10^6cell/mL for PBMCs or 2-10x10^6cell/mL for Tregs. Cells were frozen in 2ml cryovials as 500µl aliquots in freezing boxes at -80°C for 48 hours, before being transferred to liquid nitrogen (-160°) for long-term storage. For thawing cells, frozen vials were transferred to -80°C for at least one hour before thawing at 37°C. Thawed cells were immediately washed in 10ml RPMI, added dropwise.

2.3 Cell isolation and sorting

2.3.1 Isolation and expansion of human Tregs

$CD25^+$ cells were isolated from PBMCs by incubating PBMCs with Miltenyi CD25 microbeads (130-092-983, Miltenyi Biotec, Bergisch Gladbach, Germany), for 15mins at 4°C, cell suspension was washed and applied to Miltenyi LS column on a MACS magnet (Mitenyi), following the manufacturer's protocol. $CD25^+$ cells were stained with 7-aminoactinomycin D (7AAD) viability dye (00-6993-50, eBioscience), anti-CD4 PE-eFluor™ 647 (61-0049-42, eBioscience), anti-CD25 PE-Cy7 (557741, BD Biosciences), and anti-CD127 PE (557938, BD Biosciences). Cells were incubated for 30mins at 4°C, then washed with MACS buffer to remove unbound antibodies. Cells were resuspended in complete RPMI and filtered using sterile 70-micron filter (BD). Then, $CD4^+CD25^+CD127^{low}$ Treg cells were FACS-sorted from $CD25^+$-enriched cells by BD FACSAria II cell sorter (BD). The Treg expansion was performed according to established protocols[88]. Sorted Tregs were expanded (0.5x10^5 cells in 200µl in 96 well plates) in X-Vivo 15 culture medium (Lonza, BE02-060F) supplemented with 5% pooled AB human serum (SeraLab, SM-122-H-30266), 1000U/mL of recombinant human IL-2 (Chiron, Proleukin), and anti-CD3/CD28 beads (Invitrogen, ref:11132D) at a 1:3 cell:bead ratio. Every two days, cultures were split, and fresh medium was added when needed. Cells were re-stimulated with beads (at 1:1 ratio) for the second round of expansion following to the protocol. Cells were cultured for total of 14 days before being harvested and cryopreserved in liquid nitrogen.

2.3.2 Isolation of human myeloid cells and monocytes

Myeloid cells were isolated from PBMCs using CD33 MicroBeads (MACS), following the manufacturer's protocol. Monocytes were isolated from PBMCs using CD14 MicroBeads (MACS) following the manufacturer's protocol.

2.4 *In vitro* suppression assays

2.4.1 Treg *in vitro* suppression assay

Treg suppressive function was assessed using an *in vitro* suppression assay driven by anti-CD3/anti-CD28 stimulating beads with autologous PBMCs as responders, in a dose-dependent manner. Variable numbers of Tregs were incubated with PBMCs (responders) labelled with VPD proliferation dye in triplicate wells containing anti-CD3/anti-CD28 coated beads (1:5 bead ratio). Labelled responders cultured alone or with stimulating beads (without Tregs) were used as negative or positive controls, respectively. Serial dilutions of Tregs were incubated with autologous PBMCs (responders) in triplicate wells containing anti-CD3/anti-CD28 coated beads (1:5 bead ratio). Following 72-96 hours of incubation, co-cultures were stained with 7-AAD viability staining solution (00-6993-50, eBioscience), anti-CD3 APC-eFluor™ 780 (47-0037-42, eBioscience), anti-CD4 PE-eFluor™ 610 (61-0049-42, eBioscience), and anti-CD8 FITC (11-0087-42, eBioscience). Cells were fixed with 1% paraformaldehyde (PFA) and analysed by flow cytometry (BD FACSCanto II).

2.4.2 Treg-monocyte suppression assay

Treg activity was studied by *in vitro* suppression assay driven by anti-CD3/anti CD28 stimulating beads in three different conditions: PBMCs (control), $CD14^+$-depleted PBMCs (PBMCs -/- $CD14^+$), and $CD14^+$-reconstituted PBMCs (PBMCs +/+ $CD14^+$). Variable numbers of Treg were incubated with autologous PBMCs (responders) labelled with VPD proliferation dye in triplicate wells containing anti-CD3/anti CD28 coated beads (1:5 bead: cell ratio). Labelled responders cultured alone or with stimulating beads (without Tregs) were used as a negative or positive control, respectively. Serial dilutions of Tregs were incubated with autologous PBMCs -/- $CD14^+$ or PBMCs +/+ $CD14^+$ (responders) in triplicate wells containing anti-CD3/anti CD28 coated beads (1:5 bead: cell ratio). Following 72-96 hours of incubation, co-cultures were stained with 7-AAD viability staining solution (00-6993-50, eBioscience), anti-CD3 APC-eFluor™ 780 (47-0037-42, eBioscience), anti-CD4 PE-eFluor™ (61-0049-42, eBioscience), and anti-CD8 FITC (11-0087-42, eBioscience). Cells were fixed with 1% paraformaldehyde (PFA) and analysed by flow cytometry (BD FACSCanto II). The same experimental design was used in experiments using CD33 marker for isolating myeloid cells. Supernatants were collected and kept in -20°C for cytokine analysis.

2.5 *In vitro* stimulation assays

To compare chemokine receptor expression across clinical Tregs, PBMCs, conventional T cells, and freshly isolated *ex vivo* Tregs, cells were stimulated with anti-CD3/CD28 Dynabeads (Invitrogen, Cat. 11132D) at a bead-to-cell ratio of 1:5 or left unstimulated. In some conditions, conventional T cells were co-cultured with $CD14^+$ monocytes for allo-stimulation. All cell types were cultured in complete RPMI 1640 medium (R0883, Sigma-Aldrich Co Ltd) supplemented with 100 U/ml penicillin (P4333, Sigma-Aldrich), 10 mg/ml streptomycin (P4333, Sigma-Aldrich), L-glutamine (G7513, Sigma-Aldrich), and 10% heat-inactivated foetal calf serum (FCS; heat-inactivated for 20 min at 56 °C) for 72-96 h.

After incubation, cells were stained with LIVE/DEAD Near-IR viability dye (L10119, Invitrogen) and an antibody panel (Table 2.5.1), incubated at 37 °C for 30 min in the dark, washed with PBS or FACS buffer, fixed in 200 µl of 1% paraformaldehyde (PFA), and acquired on a BD FACS Canto II (BD Biosciences). Data were analysed using FlowJo software. All experimental conditions were performed in at least triplicate, with some conditions conducted with up to seven biological replicates.

2.5.1 Cell source and preparation

Clinical Tregs vs PBMCs: Frozen clinical Tregs were thawed and plated at 2×10^4 cells/well in 24-well flat-bottom plates (662160, Greiner). PBMCs were seeded at 1×10^6 cells/well in parallel, with or without anti-CD3/CD28 stimulation.

Clinical Tregs vs conventional T cells: PBMCs -/- $CD14^+$ were obtained from PBMCs using MACS CD14 microbeads and LS columns (Miltenyi Biotec). Then, $CD4^+$ T cells were isolated using MACS CD4 microbeads (Cat. 130-045-101, Miltenyi Biotec) and $CD8^+$ T cells using MACS CD8 microbeads (Cat. 130-045-201, Miltenyi Biotec), following the manufacturer's protocol. Purity (>95%) was confirmed by flow cytometry. Cells were plated at 2×10^5 cells/well in 96-well flat-bottom plates (655180, Greiner) under the three stimulation conditions: anti-CD3/CD28 stimulation, unstimulated, and co-culture with $CD14^+$ monocytes.

Clinical Tregs vs *ex vivo* Tregs: *Ex vivo* Tregs were prepared as described in section 2.3.1, including $CD25^+$ enrichment, FACS-sorting of $CD4^+CD25^+CD127^{low}$ cells, and 14-day expansion in X-Vivo 15 medium supplemented with pooled human AB serum, IL-2, and anti-CD3/CD28 Dynabeads. Expanded Tregs were then plated under the same three stimulation conditions described above.

Table 2.5.1. Antibodies used for flow cytometric analysis.

Marker	Clone	Fluorochrome	Manufacturer	Catalogue No.
CD3	UCHT1	FITC	BioLegend	300406
CD4	OKT4 (OKT-4)	BV786	eBioscience	417-0048-42
CD8	SK1	BV711	BioLegend	344734
CD62L	DREG-56	BV605	BioLegend	304834
CCR7	G043H7	APC	BioLegend	353214
CCR4	L291H4	PE-Cy7	BioLegend	359410
CCR8	S19016H	BV421	BioLegend	365814
CCR2	K036C2	PE-Cy7	BioLegend	357212
CCR6	REA190	APC	Miltenyi Biotec	130-117-524
CXCR3	G025H7	PE	BioLegend	353706
CXCR5	J252D4	BV421	BioLegend	356920
Viability dye	--	Near-IR	Invitrogen	L10119

2.5.2 Assessment of chemokine and cytokine production

2.5.2.1 Clinical Tregs and conventional T cells chemokine production

Supernatants were collected from cell cultures described in section 2.5.1 under three conditions: stimulated with anti-CD3/CD28 beads (Invitrogen Dynabeads), unstimulated, and co-cultured with $CD14^+$ monocytes for allo-stimulation, using clinical Tregs and conventional T cells. The supernatants were stored at -20°C until use. Thawed supernatants were probed using a multiplex bead-based immunoassay. The LEGENDplex™ Human Proinflammatory Chemokine Panel 1 Standard (cat: 740987, BioLegend) was used to assess supernatants from stimulation assays. This panel includes 10 human proteins: CXCL8 (IL-8), CXCL10 (IP-10), CCL11 (Eotaxin), CCL17 (TARC), CCL5 (RANTES), CCL3 (MIP-1α), CXCL9 (MIG), CCL20 (MIP-3α), CXCL1 (GROα), CXCL11 (I-TAC), CCL4 (MIP-1β), CCL2 (MCP-1), CXCL5 (ENA-78). Additionally, the LEGENDplex™ Human Proinflammatory Chemokine Panel 2 Standard (cat: 741160, BioLegend) was used, containing 12 human proteins: CCL1 (I-309), CCL13 (MCP-4), CCL22 (MDC), CCL7 (MCP-3), CCL24 (Eotaxin-2), CCL19 (ELC), CXCL13 (BLC), CCL8 (MCP-2), CX3CL1 (Fractalkine), CXCL12 (SDF-1), CXCL2 (GRO-β), and CCL18 (PARC). Samples were

acquired using a BD FACSCanto II instrument, and data analysis was performed using LEGENDplex™ software (BioLegend) to compare results between clinical Tregs and conventional T cells.

2.5.2.2 Cytokine production in Treg and monocyte co-culture

Supernatants were collected from cell culture described in section 2.4.2 and stored at -20°C until use. Thawed supernatants were probed using a multiplex bead-based immunoassay. A LEGENDplex™ Human Th Cytokine Panel (cat: 740722, BioLegend) was used to analyse supernatants from suppression assays. This bead-based multiplex assay quantifies 12 human cytokines: IL-2, IL-4, IL-5, IL-6, IL-9, IL-10, IL-13, IL-17A, IL-17F, IL-22, IFN-γ, and TNF-α, which are collectively produced by Th1, Th2, Th9, Th17, and Th22 subsets. Samples were acquired using BD FACS Canto II instrument, and data were analysed using LEGENDplex software (BioLegend).

2.6 Flow cytometry analysis

2.6.1 Staining with cell proliferation dye

For staining with violet proliferation dye (VPD) (ref: 562158, BD Bioscience), cells were washed twice with PBS and incubated with 1µM VPD for 10 minutes at 37°C before being washed in media with FCS.

2.6.2 Clinical Treg staining

Frozen clinical Tregs were thawed and washed with PBS or FACS buffer, then plated in 96-well v-bottom plates at a density of 1×10^5 cells per well. Fluorochrome-conjugated antibodies, such as anti-CD25 PE-Cy7 (557741, BD Biosciences), were added to the cells and incubated for 20-30 minutes at 4°C in the dark. After incubation, cells were washed with PBS or FACS buffer to remove unbound antibodies. Washing involved adding PBS or FACS buffer to each well, centrifuging at 1500 rpm for 5 minutes at 4°C, and discarding the supernatant. After washing, cells were fixed in 200 µl of 1% paraformaldehyde (PFA) and analysed on a FACS Canto II instrument (BD). The LIVE/DEAD™ Fixable dye Aqua (Invitrogen™) was used to identify live cells in all flow cytometry assays. Unstained controls and fluorescence minus one (FMO) control were included to enable accurate gating of positive and negative populations. Cells were stained for surface markers as described, then fixed and permeabilized using FixPerm FOXP3 staining buffer (eBioscience, UK, 00-5523-00) for 1 hour or overnight at 4°C, following the manufacturer's instructions. Perm buffer (eBioscience, UK, 00-5523-00) was used to wash cells twice, followed by a 15-minute incubation with 2% mouse or rat serum (eBioscience) at 4°C. Cells were then stained with FOXP3 APC (17-5773-82, eBioscience) and Helios PE (12-

9883-42, eBioscience) antibodies at 1-2 µL per well or with appropriate FMO controls. After 45 minutes of incubation at 4°C in the dark, cells were washed and fixed in 1% PFA, as done for surface marker staining.

2.6.3 *Ex vivo* Treg staining

Ex vivo Tregs were sorted as described in detail in section 2.3.1 from $CD25^+$ cells isolated from PBMCs using Miltenyi CD25 microbeads (130-092-983, Miltenyi Biotec). After staining with viability dye (7AAD) and antibodies (anti-CD4, anti-CD25, anti-CD127), the cells were washed and filtered. $CD4^+CD25^+CD127^{low}$ Tregs were then sorted using a BD FACSAria II cell sorter (BD). Sorted Tregs were expanded in X-Vivo 15 media (Lonza) supplemented with 5% pooled AB human serum, 1000 U/mL IL-2, and anti-CD3/CD28 beads at a 1:3 cell-to-bead ratio. Cultures were split every two days, with fresh medium added as needed. For the second expansion round, cells were re-stimulated with beads at a 1:1 ratio. After 14 days, the expanded Tregs were harvested and cryopreserved in liquid nitrogen.

2.6.4 Chemokine receptor staining

Chemokine receptor staining was performed on clinical Tregs, $CD4^+$ T cells, $CD8^+$ T cells, and *ex vivo* Tregs to compare their expression profiles. Cells were stained with a panel of chemokine receptor antibodies, including anti-CD62L BV605, anti-CCR7 APC, anti-CCR4 PE-Cy7, anti-CCR8 BV421, anti-CCR2 PE-Cy7, anti-CCR6 APC, anti-CXCR3 PE, and anti-CXCR5 BV421 (Table 2.5.1). Staining was conducted at 37°C for 30 minutes in the dark, washed with PBS or FACS buffer to remove unbound antibodies, and fixed in 1% paraformaldehyde. Details of cell preparation and staining protocols are provided in Section 2.5 Data acquisition was carried out using a BD FACS Canto II, and analysis was performed using FlowJo software.

2.7 TWO Study peripheral blood immunomonitoring

2.7.1 Peripheral blood sampling for immune monitoring

Peripheral blood samples were collected from eligible participants at the Oxford Transplant Centre (Churchill Hospital, Oxford, UK) in sodium-EDTA vacutainer tubes, following institutional ethical guidelines. Samples were transported to the Translational Research and Immunology Group (TRIG) laboratory for immediate processing and analysis. Eligibility criteria were clearly defined. Inclusion criteria required recipients to be aged 18-70 years, receiving a first kidney transplant from a living donor, with a panel-reactive antibody (PRA) level of <30%, and negative crossmatch. Participants had to demonstrate stable cardiovascular and metabolic status. Exclusion criteria included prior transplant history, autoimmune or infectious diseases

(e.g., HIV, hepatitis B/C), use of investigational agents within the last 30 days, and significant comorbidities that could interfere with study participation or Treg production. Women who were pregnant or lactating were also excluded[25, 83].

2.7.2 Staining whole blood with DuraClone Antibody Cocktail Panels

As part of the revised protocol, longitudinal immune monitoring was performed on a broader cohort of patients enrolled in the TWO Study. For the analysis presented in Chapter 5, a subset of nine patients (for whom a whole set of immunomonitoring samples was available at the time) was analysed: five from the Treg therapy group (Patients 112, 113, 116, 117, and 124) and four from the control group (Patients 114, 118, 120, and 122). Peripheral blood was collected at predefined trial visits, including pre-transplant (baseline), day 4 post-transplant, and weeks 2, 4, and 78, to assess longitudinal immunological changes.

For flow cytometry, 100 µL of EDTA-treated whole blood was used for the Basic panel and 50 µL for the Treg panel. Samples were stained using commercially prepared lyophilised antibody panels (DuraClone, Beckman Coulter), which included markers for T cells, B cells, monocytes, and Tregs. The markers included in each panel are detailed in (Table 2.8.1). Staining was performed according to the manufacturer's instructions, and cell pellets were resuspended in PBS containing IO fixation solution.

Table 2.7.1. DURAClone panels used for immune phenotyping in the TWO Study clinical trial.

Fluorochrome	**FITC**	**PE**	**EDC**	**PC5.5**	**PC7**	**APC**	**APC-AF700**	**APC-AF750**	**Pacific blue**	**Krome orange**
Basic Phenotype	CD16	CD56	CD19	*NA*	CD14	CD4	CD8	CD3	*NA*	CD45
T cell subsets	CD45RA	CCR7	CD28	PD-1	CD27	CD4	CD8	CD3	CD57	CD45
TCR	TCR γδ	TCR αβ	HLA-DR	*NA*	TCR-VD1	CD4	CD8	CD3	TCR VD2	CD45
Treg	CD45RA	CD25	*NA*	CD39	CD4	FOXP3	*NA*	CD3	Helios	CD45
B cell	IgD	CD21	CD19	*NA*	CD27	CD24	*NA*	CD38	IgM	CD45

For basic phenotyping, T cell subsets, TCR, Treg, B cells, as well as an in-house developed panel for Tfh cells.

Data acquisition was performed on a Navios flow cytometer (Beckman Coulter), with FlowCheck Pro and FlowSet Pro beads used for quality control prior to each run. Data were analysed using Kaluza software v1.2 (Beckman Coulter), and absolute cell counts were calculated based on clinical haematology reports.

Downstream data visualisation and statistical comparisons were performed using GraphPad Prism 9. Clinical parameters including serum creatinine, eGFR, and tacrolimus trough levels were recorded alongside immunological data for integrated analysis.

2.8 Gene expression analysis using the nCounter Nanostring technology

2.8.1 Overview of nCounter technology

NanoString's nCounter (NanoString Technologies) technology offers a precise and efficient approach to gene expression analysis by digitally detecting and directly barcoding target molecules. Each target is identified by a unique pair of probes, ensuring specificity and accuracy. The data are processed by the nCounter instrument, which generates digital images and converts them into quantifiable counts, conveniently exported in CSV format for analysis. These results can be analysed using nSolver Analysis Software v4.0 (NanoString Technologies). This technology simplifies laboratory workflows and sample analysis by minimising experimental variability. The result is highly precise and accurate gene expression measurements, making it an invaluable tool for generating high-quality data in molecular research.

2.8.2 RNA isolation

RNA isolation was performed by snap freezing 1.0×10^5 cells in liquid nitrogen, followed by processing with the RNeasy® Mini Kit (Qiagen). The RNA's quality and quantity were measured using a Qubit™ Flex Fluorometer (Q33327, Invitrogen™).

2.8.3 nCounter gene expression analysis

Tregs were cultured as previously described under normal media conditions supplemented with IL-2 (300U/mL). On day 14, cells were collected, and RNA was isolated. RNA expression was quantified using the nCounter® Human Immunology V2 panel (NanoString Technologies) following the manufacturer's protocol. Data normalisation was performed using nSolver Analysis Software v4.0 (NanoString Technologies), applying the recommended settings, including positive controls and housekeeping genes. Heatmaps were initially generated within nSolver software using built-in visualisation options. Both nSolver 4.0 and Rosalind software were utilised to generate heatmaps based on Z-scores, which are always positive as the barcode detection output for each gene provides a positive target count. Normalisation was carried out with 15 reference genes, such as TUBB, OAZ1, GAPDH, PPIA, ABCF1, and RPL19. Genes with low expression and less than 85% identity to human sequences were excluded. The analysis process began by running the analysis

function in nSolver 4.0, where Agglomerative Cluster analysis and Z-score transformations were applied to center and scale the heatmap.

2.9 Spatial transcriptomics analysis of kidney biopsies using 10X Xenium

2.9.1 Platform overview

The 10X Xenium platform is a high-resolution spatial transcriptomics technology that enables precise mapping of gene expression within intact tissues (10x Genomics). It combines advanced imaging and barcoding techniques to spatially resolve transcripts at subcellular resolution. The platform supports comprehensive analysis of cell types, states, and spatial interactions within the tissue microenvironment. Its versatility and scalability make it a powerful tool for understanding complex biological systems and diseases.

2.9.2 Sample preparation

Kidney biopsies were collected from the TWO Study groups: control patients who received standard therapy, and patients from the Treg therapy group. The collected tissues were formalin-fixed and paraffin-embedded (FFPE) to preserve cellular and structural integrity. For analysis, tissue sections were prepared by sectioning FFPE blocks and mounting the sections onto Xenium slides. Each Xenium slide has an imageable area of 12 mm by 24 mm, providing a defined spatial platform for downstream transcriptomic analysis.

2.9.3 Spatial analysis using the Xenium in situ platform

The original protocol of the TWO Study incorporated alemtuzumab induction followed by delayed Treg infusion at six months post-transplantation. This strategy aimed to leverage the lymphocyte repopulation phase as a favourable window for adoptive Treg therapy, as detailed in Brook et al. (2024)[83]. In this context, protocol kidney biopsies were performed to assess graft integrity and inform immunosuppression minimisation. In the Treg arm, MMF dosing was tapered from week 12 and discontinued entirely by week 26, provided the week-22 protocol biopsy (Visit 7) showed no evidence of acute rejection. Patients remained on tacrolimus monotherapy thereafter. A second protocol biopsy was performed at week 38 (Visit 13) to assess graft integrity prior to further immunosuppression minimisation. In the control arm, patients remained on combination immunosuppression throughout the trial period, with a single protocol biopsy also performed at week 38. The trial was designed with a total duration of 78 weeks to capture most primary endpoint events.

For the spatial transcriptomic analyses presented in this thesis, high-quality protocol biopsy samples were selected from two patients within the original trial cohort. Patient 102 (Treg therapy arm) contributed two biopsies: one collected prior to Treg infusion at week 22 and a second at week 38. Patient 104 (control arm) contributed a biopsy obtained at the scheduled 9-month (week 38) protocol timepoint. Both Patient 102 and Patient 104 therefore had biopsies available at the week 38 timepoint. Demographic and histopathological details for these patients are summarised in (Table 2.10.1). Patient 102 received Treg infusion at a dose of 5-10 × 10^6 cells/kg at week 26 following confirmation of stable graft function and absence of rejection. Patient 104, in the control arm, received standard immunosuppression throughout.

Table 2.9.1. Demographics of patients included in the trial.

"	Treatment Group	Age (y)	Sex	Race	Transplant Type	Donor CMV Status	Recipient CMV Status	No. of Mismatches	cRF (%)
102	Cell Therapy	32	Female	White	LRD	Pos	Pos	2	3
104	Control	30	Male	White	LRD	Pos	Neg	2	0

Demographics of patients included in the spatial transcriptomic analysis. Data are derived from the original clinical trial as reported by Brook et al. (2024). CMV, cytomegalovirus; cRF, calculated reaction frequency; Tx, transplantation.

To define the cellular composition of kidney allografts at high resolution, spatial transcriptomic profiling was performed using the 10x Genomics Xenium platform on three biopsy samples (two technical replicates per sample), totalling six sections that represented distinct clinical conditions: one control sample from the standard therapy group, one biopsy collected prior to Treg infusion (Pre-Treg), and one biopsy collected six months post-Treg infusion (Post-Treg-1 and Post-Treg-2).

Tissue sections, cut at 6 µm thickness, were transferred onto 10x Genomics Xenium sample slides. The tissues were deparaffinised, decrosslinked, and stained using a customised DNA probe panel and the pre-designed Xenium Human Multi-Tissue and Cancer Gene Expression panel comprising 377 genes (1000626, 10x Genomics), following the manufacturer's protocols. Circularisable DNA probes were hybridised to the tissue, followed by enzymatic ligation and amplification. The slides were then processed using the Xenium Analyzer, which performs iterative rounds of fluorescent probe hybridisation, imaging, and stripping to generate gene-specific optical barcodes. These signals were decoded onboard the instrument to reconstruct spatial maps of transcript expression across the entire tissue section.

Transcriptomic data were obtained from all samples and visualised using Xenium Explorer software. Hematoxylin and Eosin (H&E) staining was conducted after the Xenium run, and the resulting data were

exported for further analysis. H&E images were converted into a pyramidal format using QuPath v0.5.1 and overlaid onto the dataset.

Following quality control and pre-processing, transcriptomic data were converted into Seurat objects and integrated using canonical correlation analysis. Cell type annotations were transferred via Azimuth reference mapping, using a combined human kidney and PBMC single-cell dataset[89], enabling detailed classification of both parenchymal and immune populations. In addition to Seurat v5.0.3 in R v4.3.3, spatial analyses were also conducted using Scanpy and Squidpy in Python, which allowed for advanced spatial neighbourhood quantification and gene co-localisation analyses. Cells with zero transcript counts were excluded, and SCTransform() was applied to normalise the remaining data. Dimensionality reduction was performed using UMAP (RunUMAP(dims = 1:20)), with principal components selected based on an elbow plot. Clustering was performed using FindNeighbours() and FindClusters(resolution = 0.2), and marker genes for each cluster were identified using FindAllMarkers(only.pos = TRUE). Cell types were manually annotated based on the top differentially expressed genes and validated using the Azimuth reference. Visualisations were generated using ggplot(), Squidpy, and Xenium Explorer.

2.10 Statistical analysis

GraphPad Prism software was used for statistical analyses of flow cytometry and immunomonitoring data. Paired comparisons were analysed using paired t-tests. Comparisons across multiple groups were performed using two-way ANOVA with multiple comparisons (simple effects within rows), followed by Dunnett's multiple-comparisons test. Flow cytometric suppression and cytokine data were analysed using two-way mixed-effects models (REML) with donor-matched repeated measures and Sidak's multiple-comparisons test. Longitudinal immunomonitoring data were analysed using REML to account for repeated measures and missing values, with time treated as a repeated factor and treatment group as a fixed effect where appropriate; multiple comparisons were performed using Sidak's test. Spatial transcriptomic data were processed in Seurat and annotated using Azimuth reference mapping, followed by downstream analysis and visualisation using Scanpy and Squidpy. Differential gene expression, clustering, and neighbourhood enrichment analyses were performed within these pipelines. Spatial interaction strength was represented by Z-scores or differential Z-scores, and marker identification was based on ranked differential expression analysis. A p value of <0.05 was considered statistically significant.

---

3 Chapter 3: Homing Potential and Molecular Phenotype of Clinically Expanded Tregs

3.1 Introduction

Regulatory T cells (Tregs) are a subset of $CD4^+$ T cells characterized by the expression of CD25 and the transcription factor FOXP3. They play a central role in maintaining immune tolerance and preventing excessive immune activation[35]. Tregs exert their suppressive effects through various mechanisms, including cytokine secretion, metabolic disruption, and direct cell-to-cell interactions, thereby modulating both innate and adaptive immune responses[45].

Polyclonal Treg-based adoptive cell therapy has shown potential in promoting graft survival while minimising the need for conventional immunosuppression[37, 87]. However, the efficacy of Treg-based therapies is influenced by several factors, including Treg stability, phenotypic plasticity, and tissue homing capacity[37]. Importantly, effective migration to target tissues is crucial for Tregs to exert their regulatory functions at sites of inflammation or transplantation[74]. Chemokine receptors play a vital role in guiding Treg homing, enabling them to migrate to inflamed or tolerogenic sites where they can modulate immune responses[68, 76]. Treg-derived chemokines, particularly CCL3 and CCL4, have been shown to promote the recruitment of $CD4^+$ and $CD8^+$ T cells via CCR5, facilitating close proximity between Tregs and their target cells, a mechanism that is critical for effective suppression in preclinical models of autoimmunity and transplantation[90].

Clinically expanded Tregs, used in therapeutic applications, may differ from both their *ex vivo* counterparts and conventional T cells (including $CD4^+$ and $CD8^+$ T cells) regarding homing potential, receptor expression, and transcriptional profile. Studies have shown that *ex vivo* expansion can alter the expression of key chemokine receptors, potentially impacting the ability of Tregs to localise to graft sites[76, 91]. For instance, the downregulation of CCR5 and CCR4 after expansion may reduce Treg migration to inflamed tissues, while the upregulation of CXCR4 could enhance homing to lymphoid organs[91]. Additionally, clinically expanded Tregs are transcriptionally distinct from conventional T cells, highlighting the need to assess their gene expression patterns and homing characteristics[35]. Identifying unique markers and understanding the impact of *ex vivo* expansion on Treg function and trafficking are essential for improving the clinical application of Treg therapies[37].

Given the importance of homing receptor expression and chemokine production in guiding Treg localisation, this chapter investigates the homing potential and molecular phenotype of clinically expanded Tregs. By comparing the gene expression profiles, surface protein phenotypes, and chemokine secretion of GMP-grade Tregs with those of freshly isolated *ex vivo* Tregs and conventional T cells, this chapter aims to provide insight into the migratory capabilities and potential functional differences of these cells[74, 91].

I hypothesise that clinically expanded GMP-grade Tregs (Clinical-Tregs) have distinct homing properties compared with freshly isolated *ex vivo* Tregs and conventional T cells.

3.1.1 Chapter aims

1) Examine the gene expression profile of Clinical-Tregs versus conventional T cells as well as e*x vivo* Tregs.
2) Compare the protein expression of homing receptors between clinically expanded Tregs and conventional T cells.
3) Identify the chemokines produced by clinically expanded Tregs.

3.2 Results

3.2.1 Clinically expanded Tregs are transcriptionally similar to non-expanded Tregs but differ significantly from conventional T cells

As part of the ongoing Phase II clinical trial, the TWO Study, we are evaluating the safety and efficacy of *ex vivo* expanded polyclonal Treg therapy in living donor kidney transplantation. A key aim of this trial is to assess whether Treg infusion supports immunosuppression minimization while preserving long-term graft function[25]. To characterize the infused cell product, I investigated the homing capacity and molecular phenotype of Clinical-Tregs generated in the TWO Study. Tregs were isolated from patients and expanded *ex vivo* using a standardised protocol at the Guy's and St. Thomas's Hospital GMP Unit[25]. Frozen aliquots of the expanded Tregs were thawed for downstream analysis of gene expression profiles, homing receptor expression, and chemokine secretion.

Gene expression was analysed using the NanoString nCounter platform. Specifically, 11 clinical Treg products from the TWO Study were included. In parallel, $CD4^+$ and $CD8^+$ T cells were sorted from PBMCs, and freshly isolated *ex vivo* Tregs were included as a comparator. Total RNA (25 ng per sample) was extracted from each

population (Figure 3.2.1). The NanoString nCounter system utilizes a direct hybridization method in which a Reporter CodeSet and a Capture ProbeSet bind specifically to target messenger RNA (mRNA) sequences, enabling multiplexed, amplification-free detection of gene expression. Following hybridization, samples were processed and analysed to generate comprehensive transcriptional profiles, as described in Materials & Methods section 2.8.

This methodology enabled a detailed comparison of the transcriptional profiles of Clinical-Tregs, conventional T cells, and *ex vivo* Tregs, providing insights into the transcriptional adaptations associated with *ex vivo* expansion and their potential implications for therapeutic efficacy. Clinical-Tregs were GMP-grade expanded Tregs provided by the GMP unit and were derived from the same therapeutic product manufactured for use in the clinical trial, with surplus cells stored for clinical or research purposes. In contrast, *ex vivo* Tregs were freshly isolated from PBMCs obtained from healthy donors and had not undergone expansion. Conventional $CD4^+$ and $CD8^+$ T cells were also isolated from PBMCs and used as comparator populations.

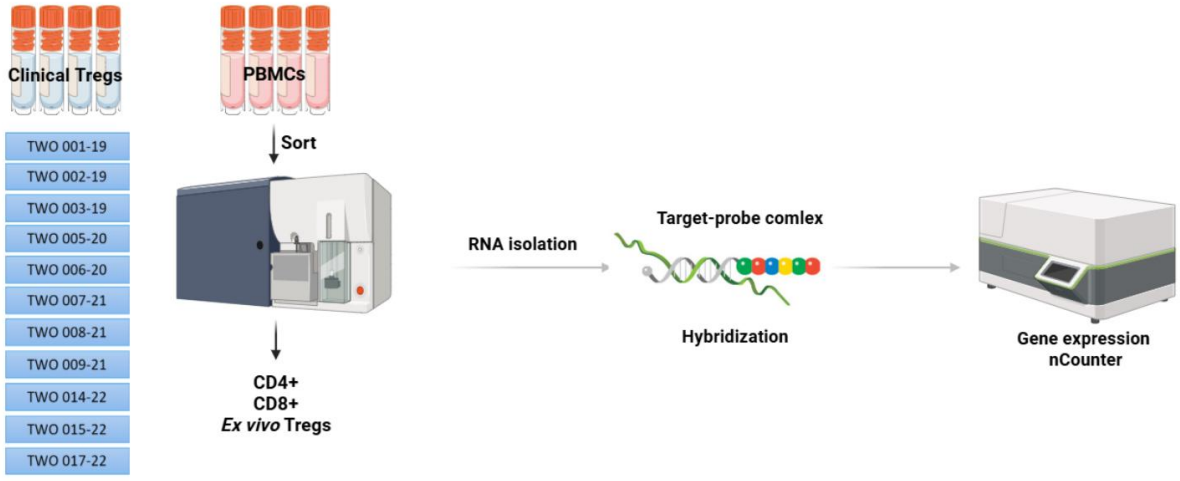


Figure 3.2.1 Workflow for gene expression profiling of clinical Tregs, ex vivo Tregs, and conventional T cells (CD4⁺ and CD8⁺) using the NanoString nCounter platform.

Clinical-grade Tregs from 11 GMP-expanded products obtained from the TWO Study were thawed for RNA extraction. In parallel, peripheral blood mononuclear cells (PBMCs) were processed to isolate CD4⁺, CD8⁺, and ex vivo (freshly isolated) Tregs using the BD FACSAria™ Cell Sorter. A total of 25 ng of RNA from each population was hybridized with a Reporter CodeSet and Capture ProbeSet, forming target-probe complexes. Samples were scanned on the NanoString nCounter system to quantify gene expression and compare transcriptional profiles across cell types.

3.2.1.1 Comparison to conventional CD4+ T cells

Previous studies have shown that Tregs can be distinguished from conventional $CD4^+$ T cells by their expression of key regulatory markers, such as FOXP3, CD25, and CTLA-4, which are essential for their suppressive function and lineage identity[35, 40]. Furthermore, phenotypic characterisation of Tregs reveals distinct profiles in chemokine receptor expression that influence their tissue homing properties[68, 91].

To determine the transcriptional differences between clinically expanded Tregs and conventional $CD4^+$ T cells, I performed a comparative gene expression analysis using nCounter technology (Figure 3.2.1). A total of 108 genes were differentially expressed between the two populations, with 43 genes upregulated in clinical Tregs and 65 genes upregulated in $CD4^+$ T cells (Annex Table A3.1). Clinical Tregs showed significantly higher expression of classical Treg-associated markers, including *FOXP3*, *CD25*, *TIGIT*, and *CD80*, confirming their regulatory identity and functional stability. Notably, several homing and adhesion-related genes were also upregulated in clinical Tregs compared to $CD4^+$ T cells, including *CCR8*, *CXCR6*, *ITGAX*, *ITGAM*, and *CEACAM1* (Figure 3.2.2), suggesting an enhanced capacity for tissue migration and interaction within the graft microenvironment. Adhesion molecules are cell-surface proteins that facilitate cell-cell interactions, migration and tissue localisation. ITGAX and ITGAM encode the integrins CD11c and CD11b, while CEACAM1 mediates cell-cell adhesion, potentially supporting Treg migration and tissue interaction[70]. In contrast, *CXCR4*, typically associated with lymphoid tissue homing, was downregulated in clinical Tregs (Figure 3.2.2). This downregulation of CXCR4, a receptor typically associated with lymphoid trafficking, suggests an adaptive shift facilitating Treg migration toward sites of inflammation, potentially enhancing their functional integration within graft microenvironments[86, 92, 93].

These findings highlight key phenotypic distinctions between clinical Tregs and conventional $CD4^+$ T cells, particularly in regulatory and homing markers, reinforcing their identity as a distinct and therapeutically relevant cell population.

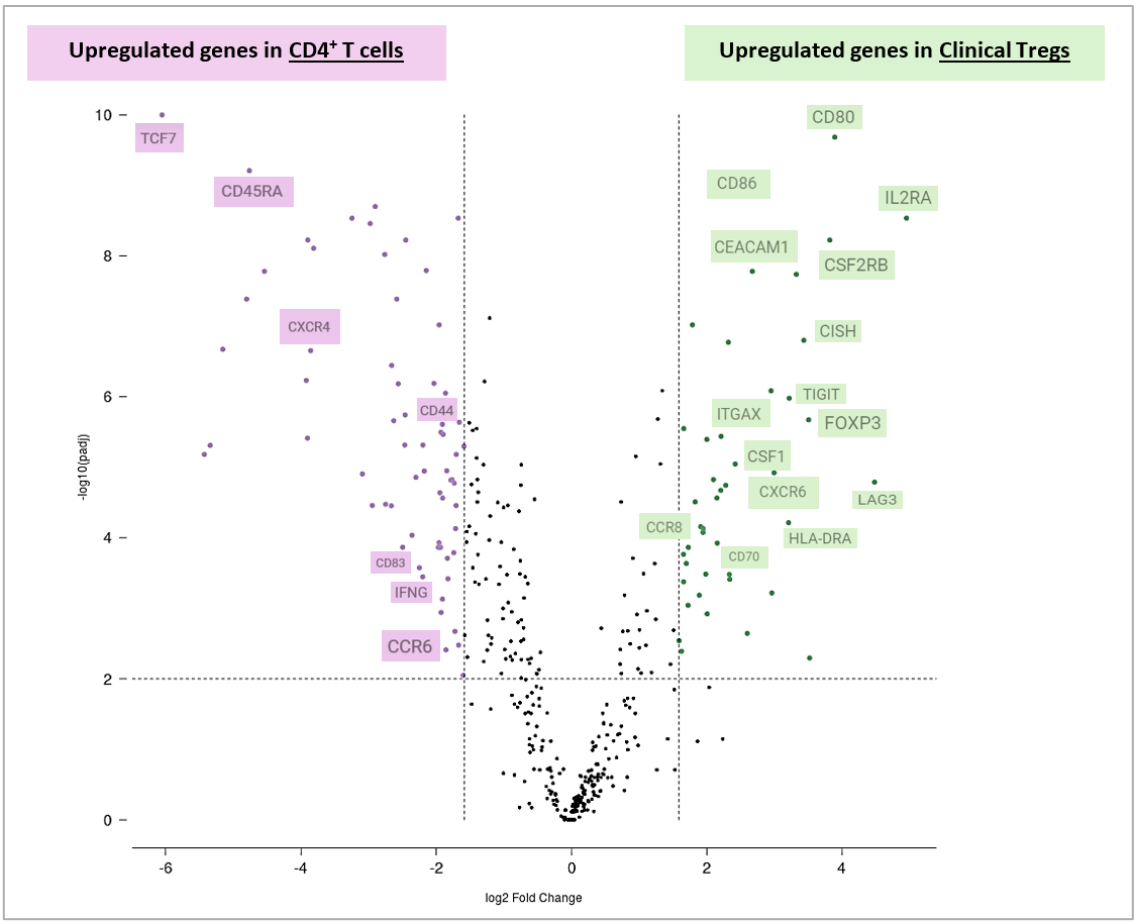


Figure 3.2.2 Volcano plot showing differential gene expression between clinical (GMP-grade) Tregs and CD4⁺ T cells.

Clinical-grade Tregs are characterised by higher expression (green) of typical Treg markers, including FOXP3, IL2RA (CD25), TIGIT, and CD80. Homing receptors CXCR6 and CCR8 are also elevated in clinical Tregs, while CXCR4 is more highly expressed in CD4⁺ T cells (purple). Genes associated with adhesion and migration, such as ITGAX, ITGAM, and CEACAM1, are also upregulated in clinical Tregs. A total of 108 genes were differentially expressed, with 43 genes upregulated in clinical Tregs and 65 in CD4⁺ T cells (fold change > 1.5, -log$_{10}$(adjusted p value) > 2).

3.2.1.2 Differences in gene expression between clinical Tregs & CD8⁺ T cells

Following the comparison between clinical Tregs and conventional CD4⁺ T cells, I next examined their transcriptional differences relative to CD8⁺ T cells to further delineate their molecular identity and differences in homing potential. CD8⁺ T cells are cytotoxic effectors central to antiviral and antitumor immunity, with distinct transcriptional programs and surface markers compared to Tregs[35, 40].

The comparison between clinical Tregs & CD8⁺ T cells revealed results consistent with those observed in section 3.2.1.1, reinforcing the transcriptional distinctiveness of Tregs from conventional effector subsets CD4⁺ and CD8⁺. Specifically, typical Treg markers such as FOXP3, CD25, TIGIT, and CD80 were significantly higher expressed in clinical Tregs, confirming their regulatory identity and suppressive potential (Figure 3.2.3). Several homing receptors, including CXCR6, CCR8, and CXCR3, were also more highly expressed in clinical Tregs than in CD8⁺ T cells, suggesting enhanced potential for tissue-specific migration (Figure 3.2.3).

This pattern of elevated CXCR6 and CCR8 expression in clinical Tregs mirrors transcriptional programs observed in tissue-resident Treg populations, such as those described in visceral adipose tissue and skin, where Tregs express high levels of CXCR6, CCR8, and other tissue-homing molecules to adapt to local microenvironments[94].

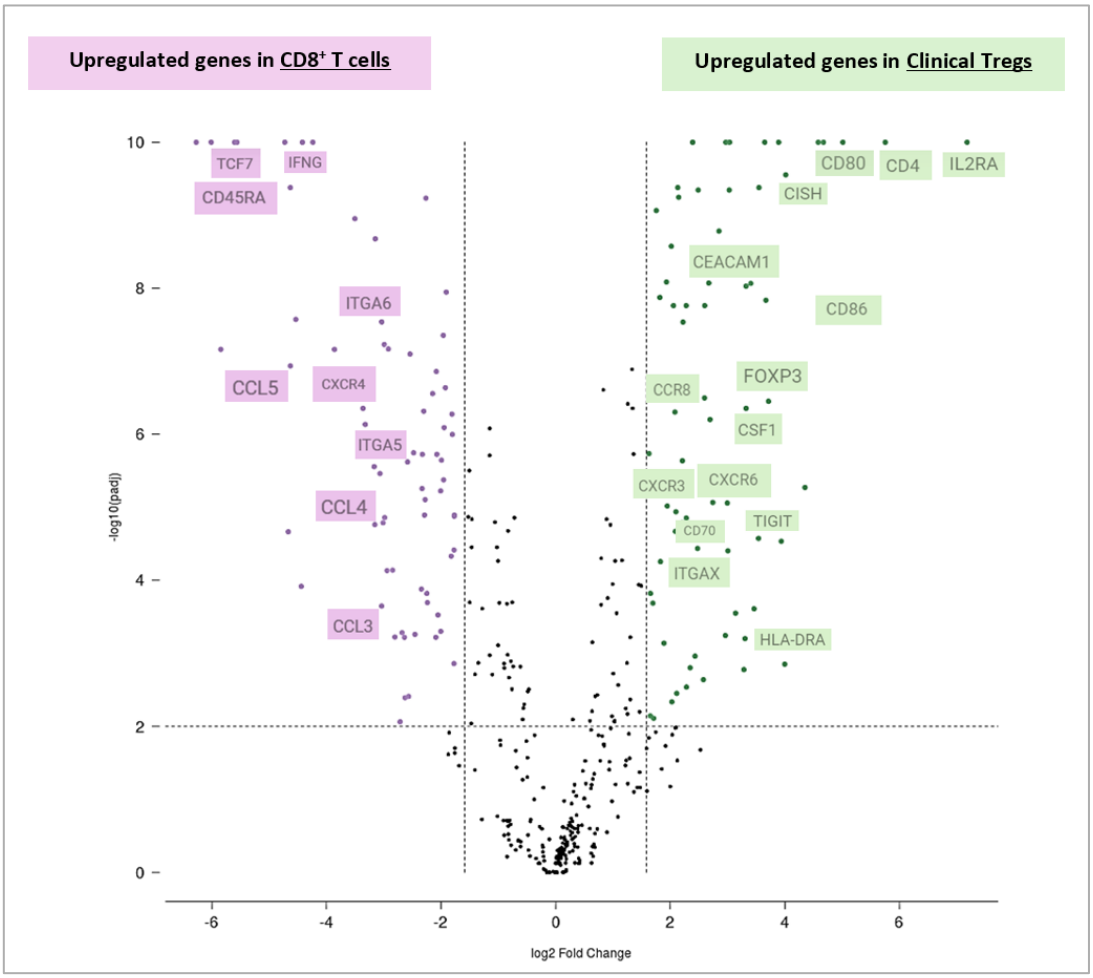


Figure 3.2.3 Volcano plot showing differential gene expression between clinical (GMP-grade) Tregs and CD8⁺ T cells.

Clinical-grade Tregs upregulate (green) characteristic regulatory markers, including FOXP3, IL2RA (CD25), TIGIT, and CD80. Homing receptors such as CXCR6, CCR8, and CXCR3 are also more highly expressed in clinical Tregs. In contrast, genes more strongly expressed in CD8⁺ T cells (purple) reflect their cytotoxic profile and functional divergence. A total of 136 genes were differentially expressed, with 68 genes upregulated in each population (fold change > 1.5, $-\log_{10}$(adjusted p value) > 2).

Genes involved in adhesion and cell trafficking, such as integrins and co-stimulatory molecules, were similarly enriched in clinical Tregs. In total, 136 genes were differentially expressed between the two populations, with 68 genes upregulated in clinical Tregs and 68 upregulated in CD8⁺ T cells (Figure 3.2.3 and Annex Table A3.2). These transcriptional differences underscore the distinct regulatory and functional markers expressed by the clinical Tregs compared to CD8⁺ effector cells.

3.2.1.3 Assessment of transcriptional changes in *ex vivo* and clinical Tregs

Freshly isolated *ex vivo* Tregs should present their authentic transcriptional profile, with rich regulatory markers and homing receptors, reflective of their stable immunosuppressive phenotype. On the other hand, clinical-grade Tregs, subjected to prolonged *ex vivo* expansion and repeated stimulation, may undergo transcriptional shifts that influence their stability and function[95, 96].

To evaluate the impact of *ex vivo* expansion on Treg transcriptional profiles, I compared gene expression between unexpanded *ex vivo* Tregs and clinical-grade Tregs. This analysis identified 129 differentially expressed genes: 43 genes were upregulated in clinical Tregs, while 86 genes were upregulated in ex vivo Tregs as shown in Figure 3.2.4 and Annex Figure A3.1 (fold change > 1.5, $\log_{10}$-adjusted p value > 2).

Core Treg markers such as FOXP3 were not differentially expressed between the two populations, indicating that the fundamental regulatory identity of Tregs is preserved during expansion. However, CD25, LAG3, and TNFRSF4 (OX40) were more highly expressed in clinical Tregs, suggesting enhanced activation or effector characteristics. In contrast, *ex vivo* Tregs exhibited higher expression of IKZF2 (Helios), Transcription factor 7 (TCF7), PTPRC (CD45RA), and ICOS, consistent with a more naïve and potentially more stable phenotype. These differences reflect shifts in activation state, differentiation, and functional capacity resulting from the expansion process.

Chemokine receptors and ligands, including *CCR6*, *CCR8*, *CXCR4*, *XCR1*, and *CXCR1*, were more highly expressed in *ex vivo* Tregs, reflecting differences in homing capabilities. Conversely, clinical Tregs showed upregulation of adhesion molecules such as *ITGAX*, *ITGAM*, and *CEACAM1*, which may facilitate tissue retention and migration. These findings highlight the transcriptional adaptations that occur during Treg expansion, which are thought to support the efficacy of Treg-based therapies. [86, 92, 93]. This downregulation of CXCR4, a receptor typically associated with lymphoid trafficking, suggests an adaptive shift facilitating Treg migration toward sites of inflammation, potentially enhancing their functional integration within graft microenvironments.

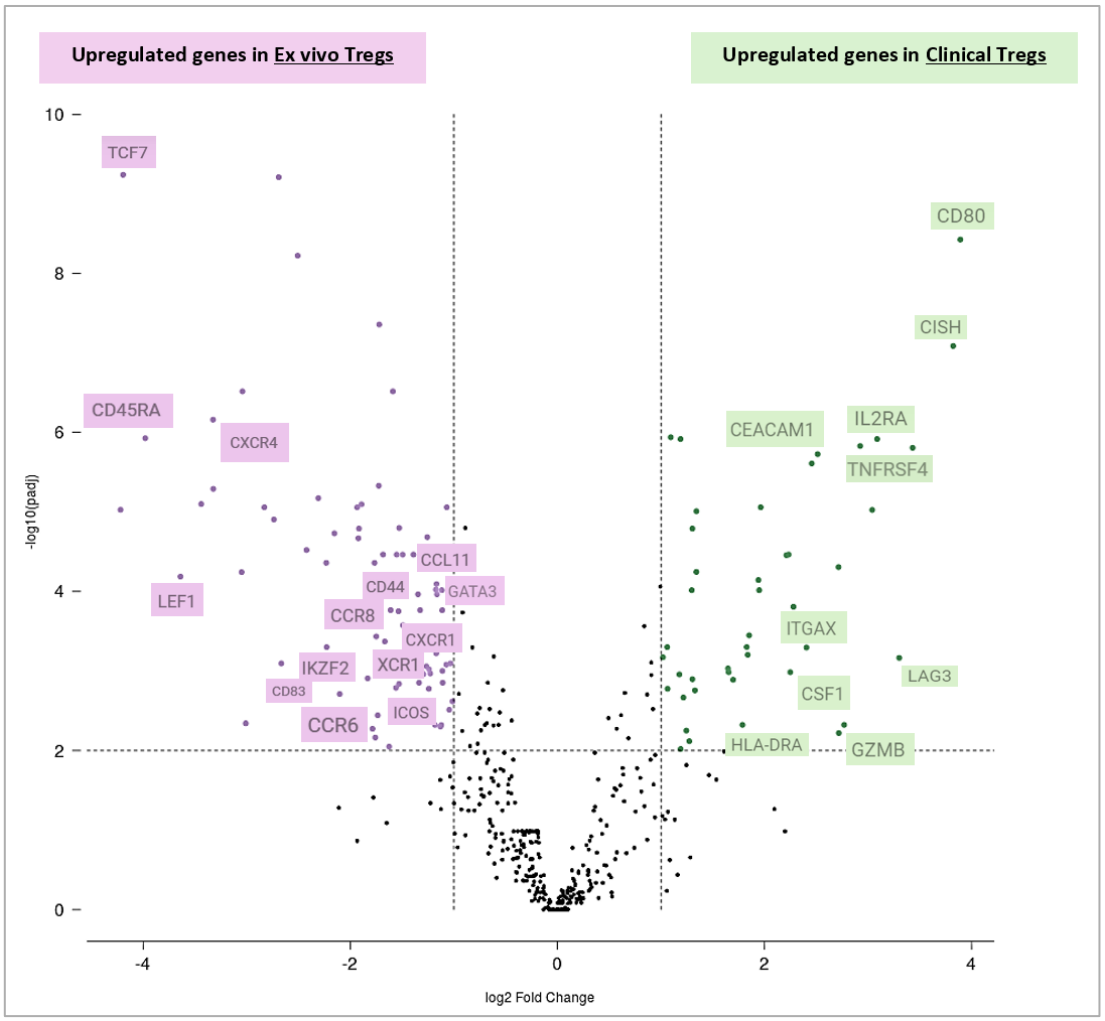


Figure 3.2.4 Volcano plot showing differential gene expression between clinical (GMP-grade) Tregs and Ex vivo Tregs.

Clinical-grade Tregs upregulate (green) adhesion and trafficking markers, including ITGAX, ITGAM, and CEACAM1. In contrast, ex vivo Tregs show higher expression (purple) of key markers such as IKZF2 (Helios), ICOS, TCF7, and CD45RA, indicative of greater lineage stability and a more naïve phenotype. A total of 129 genes were differentially expressed, with 43 genes upregulated in clinical Tregs and 86 genes upregulated in ex vivo Tregs (fold change > 1.5, -log$_{10}$(adjusted p value) > 2).

3.2.2 Expression of homing receptors

The ability of Tregs to exert their immunosuppressive function at target sites is contingent upon their capacity to migrate effectively to lymphoid and peripheral tissues. This process is regulated by the expression of specific chemokine receptors and adhesion molecules, which enable Tregs to home to sites of inflammation and graft in the context of transplantation[86, 92]. Alterations in the expression of these homing molecules following *ex vivo* expansion may influence the therapeutic efficacy of adoptively transferred Tregs.

To investigate the expression of homing receptors in clinical-grade Tregs, I performed surface staining for a panel of chemokine receptors on clinical Tregs, freshly isolated *ex vivo* Tregs, CD4$^+$ T cells, and CD8$^+$ T cells. Receptor expression was assessed under both unstimulated conditions and following stimulation with anti-CD3/CD28 antibodies. Cells were cultured for 3 days, either in medium alone or in the presence of

αCD3/CD28 stimulation and then subjected to chemokine receptor staining and flow cytometric analysis. Details of the staining panel and protocol are provided in Materials & Methods section 2.6.4.

3.2.2.1 Basic characteristics of clinical Tregs

To assess the phenotype of the Clinical Tregs used in this study, flow cytometric analysis was performed on thawed cell products. Cells were stained for CD25, FOXP3, and Helios expression as detailed in Materials & Methods section 2.6.2. The LIVE/DEAD™ Fixable Aqua dye was used to exclude non-viable cells, and fluorescence-minus-one (FMO) controls were included to ensure accurate gating.

Flow cytometry revealed that the majority of the expanded clinical Treg population expressed high levels of CD25 and FOXP3, with a median expression exceeding 80%, confirming the expected regulatory phenotype. However, Helios expression was relatively low, with a median of approximately 25%, suggesting a possible shift in phenotypic profile following *ex vivo* expansion (Figure 3.2.5). Reduced Helios expression following *in vitro* expansion has been previously reported and may reflect phenotypic plasticity or the influence of repeated stimulation and culture [97].

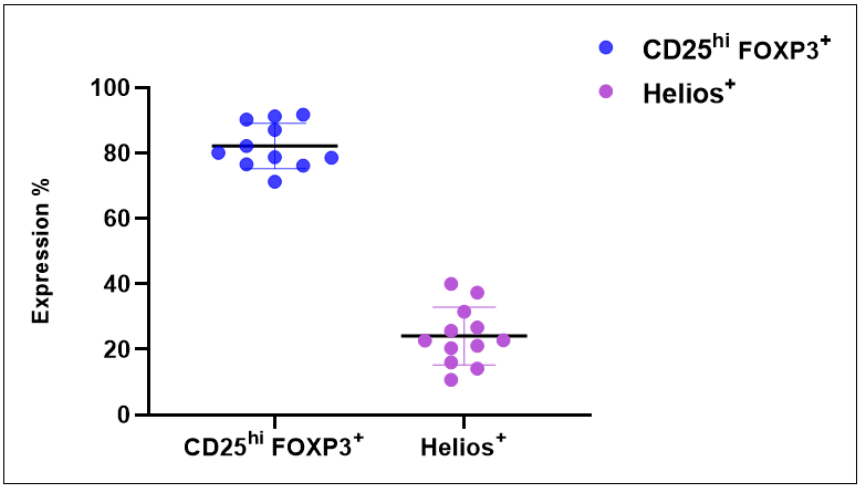


Figure 3.2.5 Frequency of CD25^{hi} FOXP3^{+} and Helios^{+} cells within the clinical (GMP-grade) Treg population.

Clinical-grade Tregs were thawed and stained for intracellular markers following fixation and permeabilization. CD25^{hi} FOXP3^{+} Tregs were consistently observed at high frequencies across donors, whereas Helios^{+} expression was significantly lower, suggesting a phenotypically mixed population. Data represent 11 Treg products from the TWO Study.

3.2.2.2 Differences in homing markers on Tregs and T cells

The trafficking and localisation of T cells are governed by their expression of chemokine receptors, which facilitate tissue-specific migration and immune surveillance. The expression patterns of these receptors differ between circulating Tregs and conventional CD4^{+} and CD8^{+} T cells, reflecting their distinct functional roles and tissue tropisms[92].

To further investigate these phenotypic differences, I assessed the surface expression of a panel of chemokine receptors on clinical Tregs, $CD4^+$, and $CD8^+$ T cells with and without TCR/CD28 stimulation to mimic a steady state and full activation. Chemokine receptor staining was conducted as outlined in Materials & Methods section 2.6.4. Cells were stained with antibodies targeting key receptors including CCR7, CD62L, CCR4, CCR8, CCR2, CCR6, CXCR3, and CXCR5. Viability dyes and fluorescence-minus-one (FMO) controls were employed to ensure accuracy. These receptors were selected based on established evidence for their roles in Treg trafficking, including migration to lymphoid tissues (CCR7, CD62L), inflammatory/peripheral tissues (CCR4, CCR8, CCR2, CCR6 and CXCR3), and B-cell follicles (CXCR5)[64]. A schematic of the experimental workflow is shown in Figure 3.2.6.

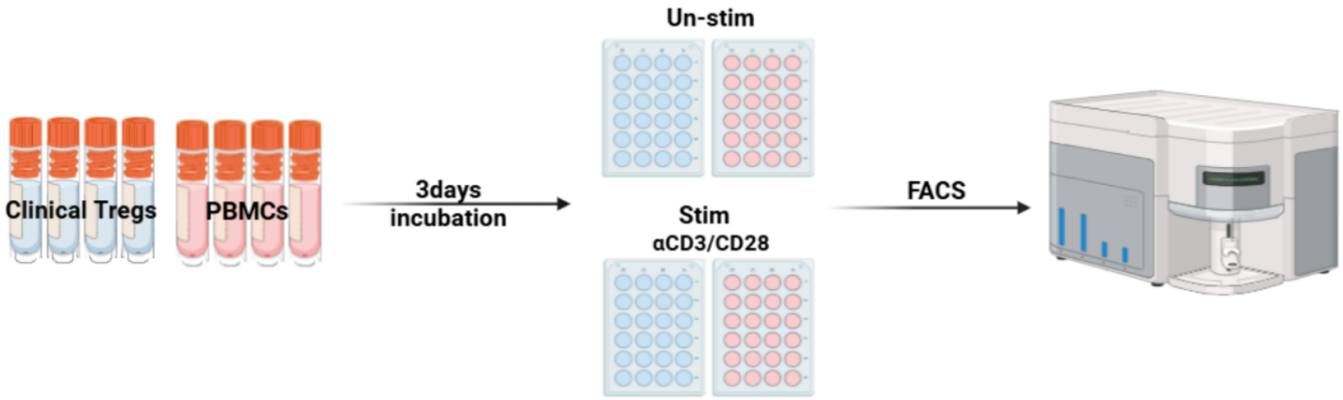


Figure 3.2.6 Experimental workflow for assessment of chemokine receptor expression on T cell subsets.

Clinical Tregs and PBMCs were thawed and cultured under unstimulated or αCD3/CD28-stimulated conditions for 3 days. Post-incubation, cells were stained with a panel of chemokine receptor antibodies and analysed by flow cytometry using the Invitrogen™ Attune™ NxT Flow Cytometer. This workflow enabled the evaluation of homing receptor expression across clinical Tregs, $CD4^+$ T cells, $CD8^+$ T cells, and ex vivo Tregs under resting and activated conditions.

3.2.2.2.1 Impact of activation on expression of homing markers in clinical Tregs

First, to assess how stimulation influences homing receptor expression in Clinical-Tregs, I compared chemokine receptor profiles before and after activation. Paired flow cytometry analysis revealed distinct modulation of several key receptors following stimulation. Specifically, the expression of CCR7 and CCR8 increased significantly after stimulation (72 hours; p=0.0004 and p=0.0097, respectively). In contrast, the expression levels of CD62L, CCR2, and CCR6 were notably reduced. These findings suggest that activation induces dynamic changes in the homing signature of clinical Tregs, which may impact their migratory potential and tissue localisation following infusion and *in vivo* activation (Figure 3.2.7). Interestingly, activated Clinical-Tregs seem to be able to retain the ability to home to the lymph nodes, with a modest decrease in CD62L expression being compensated by an increase in CCR7 expression as well as home to peripheral tissues with a significant increase in CCR8 expression. CCR7 has been shown to enable expanded

human peripheral blood-derived Tregs expressing high levels of this receptor to prevent graft rejection in a murine model[76].

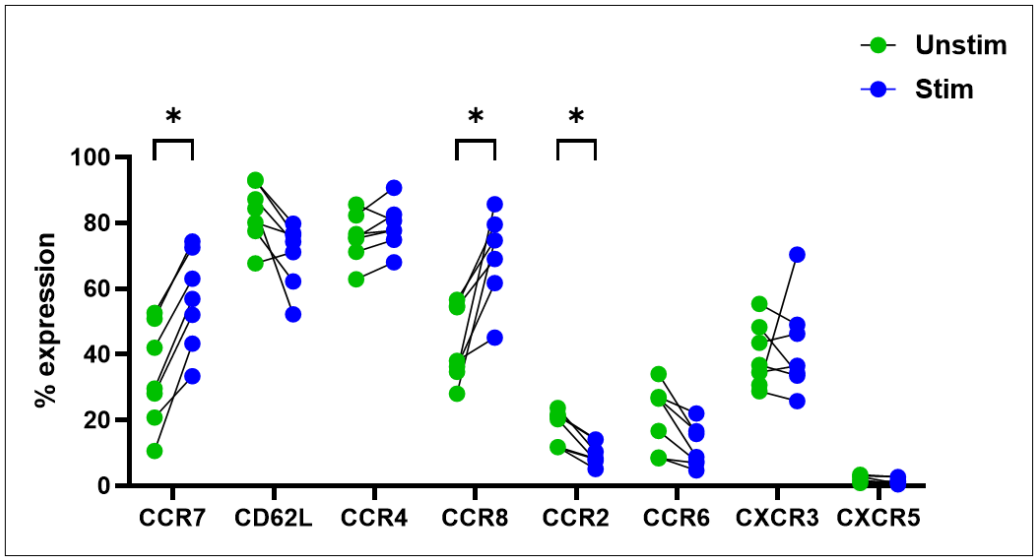


Figure 3.2.7 Paired comparison of homing receptor expression in clinical Tregs under unstimulated (green) and anti-CD3/CD28-stimulated (blue) conditions.

*Stimulation led to a significant upregulation of CCR7 and CCR8, while expression of CD62L, CCR2, and CCR6 decreased. Flow cytometry was performed using chemokine receptor-specific antibody panels, (n=7). Unstim: beads unstimulated, Stim: beads stimulated. Data were analysed and visualised using GraphPad Prism. Statistics: Paired t-test; *p < 0.05.*

3.2.2.2.2 Expression of homing receptors on $CD4^+$ and $CD8^+$ T cells

Next, I studied the expression of homing receptors in a steady state, comparing unstimulated $CD4^+$ and $CD8^+$ T cells and clinical Tregs. In these conditions, clinical Tregs exhibited a distinct homing receptor profile compared to conventional T cell subsets. Relative to $CD4^+$ T cells, clinical Tregs expressed significantly higher levels of peripheral tissues homing receptors CCR4, CCR8, CCR6, and CXCR3, while showing lower expression of a lymph node homing receptor, CCR7 ($p< 0.0001$, $p< 0.0001$, $p=0.0160$, $p=0.0005$, respectively). Compared to $CD8^+$ T cells, Tregs displayed significantly elevated expression of a lymph node homing CD62L and tissue homing CCR4, CCR8, and CCR6 ($p< 0.0001$, $p< 0.0001$, $p< 0.0001$, $p=0.0036$, respectively). This differential expression highlights the unique migratory programming of Clinical-Tregs and supports their capacity to localise to sites of immune activation and inflammation (Figure 3.2.8). Importantly, high frequency of CCR4 and CCR8 expressing (over 60% and 30-60%, respectively) Clinical-Tregs is consistent between different donors and likely to contribute to the *in vivo* efficacy of Tregs, providing them with advantage in terms of homing to the inflamed tissues.

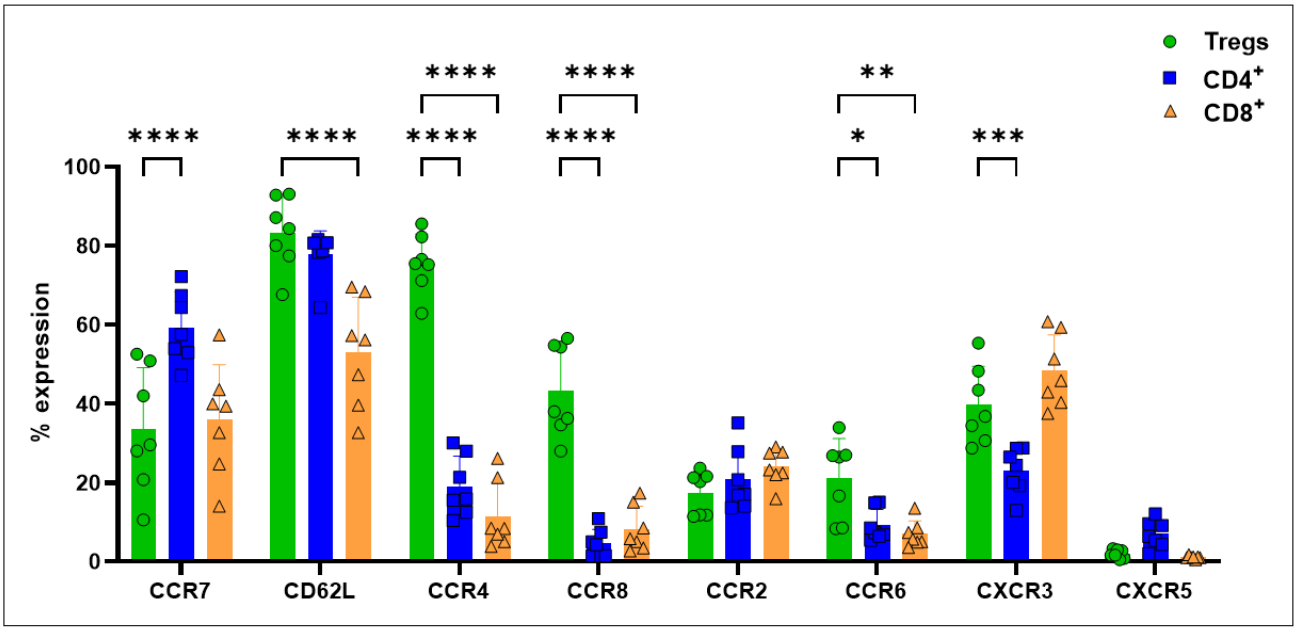


Figure 3.2.8 Surface expression of homing receptors on clinical Tregs (green), CD4⁺ T cells (blue), and CD8⁺ T cells (orange) without stimulation.

*Clinical Tregs exhibited increased expression of CCR4, CCR8, CCR6, and CXCR3 compared to CD4⁺ T cells, and higher levels of CCR4, CCR8, CD62L, and CCR6 relative to CD8⁺ T cells. Flow cytometric analysis was performed, data are presented as mean ± SD (n=7), and plots were generated using GraphPad Prism. Statistics: Two-way ANOVA with multiple comparisons (simple effect within rows), followed by Dunnett's multiple comparisons test, *p < 0.05, **p < 0.01, ****p < 0.0001.*

3.2.2.2.3 Differences in homing receptors expression between Tregs and conventional T cells in response to stimulation

To assess the impact of activation on homing receptor expression, clinical Tregs were compared with $CD4^+$ and $CD8^+$ T cells following anti-CD3/CD28 stimulation for 72 hours. Consistent with the unstimulated condition, CCR4 and CCR8 remained prominently expressed on clinical Tregs relative to both T cell subsets ($p< 0.0001$ for both). Although CCR7 remained significantly higher in $CD4^+$ T cells, its expression increased in clinical Tregs after stimulation, narrowing the difference ($p=0.0229$), and suggesting partial induction upon activation. CD62L expression also remained significantly higher in Tregs compared to $CD8^+$ T cells ($p< 0.0001$). Conversely, CCR2 expression was significantly elevated in $CD8^+$ T cells compared to Tregs post-stimulation ($p< 0.0001$). Altogether, these findings highlight CCR4 and CCR8 as the most stably and distinctly expressed homing receptors in clinical Tregs following activation (Figure 3.2.9) and in a steady state (Figure 3.2.8), underscoring their relevance as phenotypic markers with potential implications for targeted migration in therapeutic applications. Also, upregulation of CCR4 and CCR8 is a recognised feature of tissue-adapted Tregs, reflecting their migratory programming towards non-lymphoid sites[98].

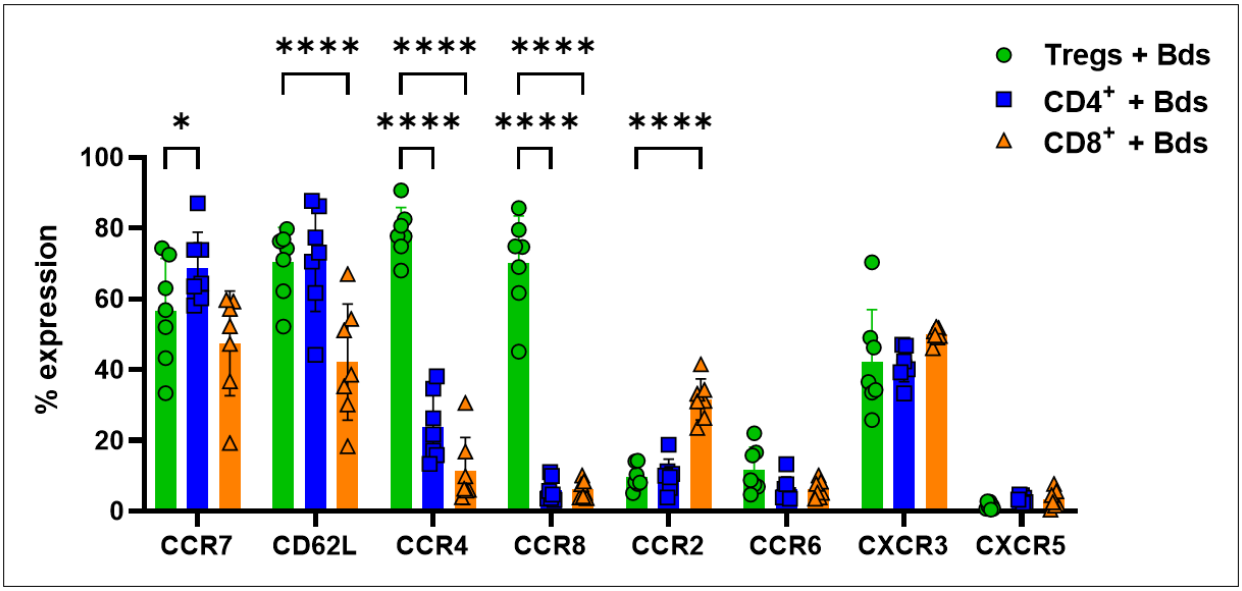


Figure 3.2.9 Surface expression of homing receptors on clinical Tregs (green), CD4⁺ T cells (blue), and CD8⁺ T cells (orange) after 72-hour anti-CD3/CD28 stimulation.

*Clinical Tregs maintained significantly higher levels of CCR4 and CCR8 compared to both conventional T cell subsets. CCR7 expression increased in clinical Tregs but remained higher in CD4⁺ T cells, while CD62L expression was elevated in Tregs relative to CD8⁺ T cells. CCR6 no longer differed significantly post-stimulation, suggesting activation-induced modulation. CCR2 expression remained higher in CD8⁺ T cells than in Tregs. Flow cytometric analysis was performed; data are presented as mean ± SD (n = 7). Plots were generated using GraphPad Prism. Statistics: Two-way ANOVA with multiple comparisons (simple effect within rows), followed by Dunnett's multiple comparisons test; *p < 0.05, ***p < 0.0001.*

When displaying side by side changes in the chemokine receptor expression upon activation in the Clinical-Tregs and conventional CD4⁺ T cells, I can observe similar dynamics with notable exception of CCR8 (significant increase on Tregs but not conventional CD4⁺ T cells upon stimulation) and CCR4 (overall higher expression on Tregs) (Figure 3.2.9). Together, findings from sections 3.2.2.2.2 and 3.2.2.2.3 illustrate that the migratory phenotype of clinical Tregs is distinctly shaped by both their lineage and activation status, with potential implications for their function in therapeutic settings.

3.2.2.3 Similarities in homing markers on *ex vivo* and clinical Tregs

Successful therapeutic application of Tregs relies not only on their suppressive function but also on their capacity to migrate to relevant tissue sites. This migratory potential is governed by the coordinated expression of chemokine receptors and adhesion molecules that enable Tregs to respond to local chemokine gradients[77]. Preserving or enhancing the expression of these receptors during *ex vivo* expansion is crucial for optimising Treg-based therapies, particularly in the context of transplantation where targeted suppression of alloimmune responses is required. To investigate whether Clinical-Tregs maintain similar homing profiles to their freshly isolated counterparts, I analysed the expression of key homing markers on *ex vivo* Tregs, followed by a relative comparison across both populations.

3.2.2.3.1 Impact of activation on homing markers on *ex vivo* Tregs

Flow cytometric analysis revealed that freshly isolated *ex vivo* Tregs exhibited relatively low baseline expression of homing receptors such as CCR4, CCR7, CD62L, and CXCR5 under unstimulated conditions. However, upon stimulation with anti-CD3/CD28 beads, there was a marked upregulation of these receptors, which could indicate enhancement of migratory phenotype (Annex Figure A3.4). I assessed changes in homing receptor expression in *ex vivo* Tregs following activation. As shown in Figure 3.2.10, stimulation with anti-CD3/CD28 beads significantly increased the expression of CCR7 ($p < 0.05$), CD62L ($p < 0.01$), and CXCR5 ($p < 0.05$), suggesting enhanced potential for lymphoid and peripheral tissue trafficking post-activation. CCR7, CD62L, and CXCR5 receptors are involved in lymphoid and peripheral tissue trafficking, indicating that stimulation enhances Tregs' ability to home to both secondary lymphoid organs and inflammatory sites. This quantitative confirmation supports earlier findings and aligns with previous literature suggesting that activation can promote Treg tissue-specific migration potential[77].

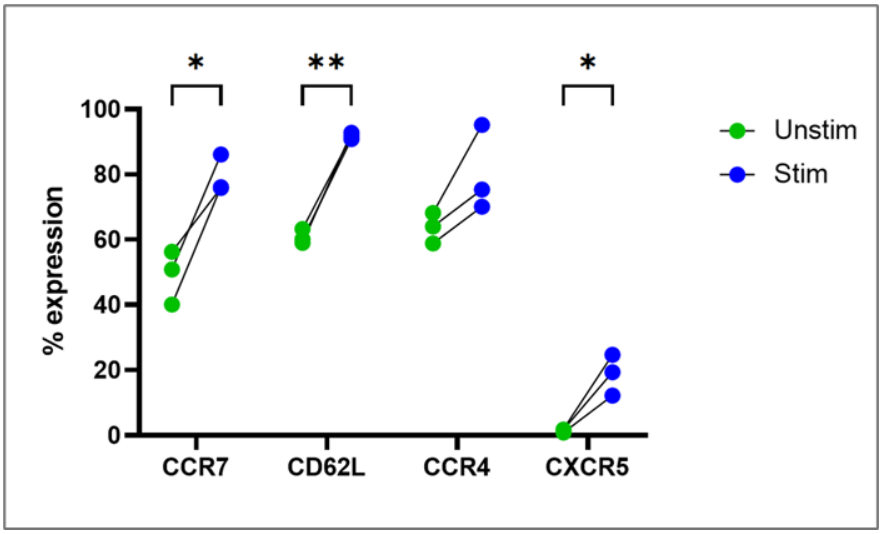


Figure 3.2.10 Quantitative analysis of homing receptor expression in ex vivo Tregs before and after stimulation.

*Expression levels of CCR7, CD62L, CCR4, and CXCR5 were measured in freshly isolated Tregs under unstimulated (green) and anti-CD3/CD28-stimulated (blue) conditions. CCR7, CD62L, and CXCR5 were significantly upregulated following stimulation, while CCR4 showed modest increases. Unstim: beads unstimulated, Stim: beads stimulated. Data were analysed and visualized using GraphPad Prism. Statistics: Paired t-test; * = $p < 0.05$, ** = $p < 0.01$.*

3.2.2.3.2 Differences of homing receptors expression between clinical Tregs and *ex vivo* Tregs in response to stimulation

To assess whether clinical-grade expansion alters the responsiveness of Tregs to activation in terms of homing receptor expression, I compared surface levels of CCR7, CD62L, and CCR4 in Clinical-Tregs and freshly isolated *ex vivo* Tregs before and after anti-CD3/CD28 stimulation (Figure 3.2.11). At baseline, both Treg

populations expressed relatively high levels of CCR7 and CD62L. Upon stimulation, CCR7 was significantly upregulated in both clinical and *ex vivo* Tregs ($p < 0.05$), indicating preserved activation responsiveness. In contrast, CD62L expression significantly increased in *ex vivo* Tregs ($p < 0.05$), but declined in clinical Tregs, suggesting that prolonged *in vitro* expansion may attenuate CD62L maintenance following activation. These results highlight key differences in homing receptor dynamics between freshly isolated *ex vivo* Tregs and Clinical-Tregs that may influence their tissue-targeting potential and therapeutic efficacy *in vivo*. Importantly, the expression of CCR4, a well-known Treg-associated homing receptor, remained high upon stimulation on both Treg populations.

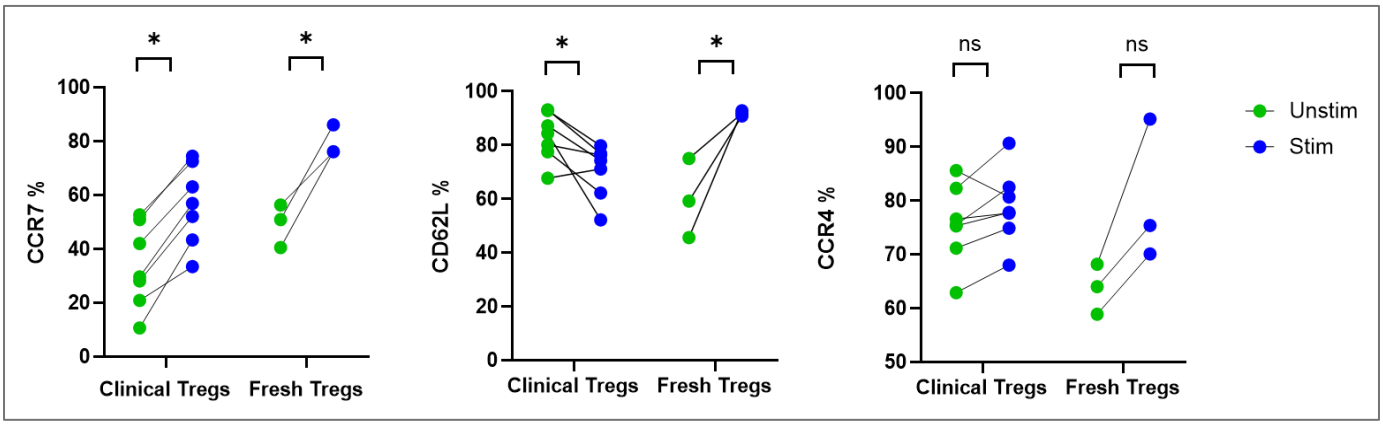


Figure 3.2.11 Comparison of homing receptor expression in clinical (GMP-grade) versus ex vivo (freshly isolated) Tregs before (green) and after (blue) anti-CD3/CD28 stimulation.

*Flow cytometry analysis of CCR7, CD62L, and CCR4 revealed that CCR7 expression increased in both Treg populations following stimulation. CD62L was upregulated in ex vivo Tregs but declined in clinical Tregs. Data were analysed using GraphPad Prism. Statistics: Unpaired t-test; *p < 0.05. ns = not significant.*

3.2.3 Production of chemokines

Having explored the expression of homing receptors, I next investigated the ability to produce chemokines by Tregs and conventional T cells following anti-CD3/CD28 or polyclonal donor-specific stimulations, with or without IL-2.

3.2.3.1 Effect of IL-2 on chemokine production by Tregs

First, I investigated chemokine secretion by clinical-grade Tregs assessing the impact of polyclonal (anti-CD3/CD28 beads) and allogeneic (allogeneic monocytes) stimulation of Tregs in the presence or absence of IL-2 supplementation (a key Treg growth and survival factor). Chemokine secretion following anti-CD3/CD28 stimulation is shown in Figure 3.2.12A, while secretion in response to allogeneic monocytes is presented in (Figure 3.2.12B) The results demonstrate that IL-2 did not alter chemokine secretion by clinical Tregs under either stimulation condition. Across both settings, levels of key chemokines, including CCL1, CCL22, CCL24,

CXCL13, CXCL2, and CCL18, remained comparable regardless of IL-2 presence. These findings suggest that while IL-2 is critical for Treg survival and expansion, it does not directly modulate their chemokine production profile. Interestingly, while levels of tested chemokines were relatively low (below 100pg/ml) upon polyclonal stimulation with beads; stimulation with allogeneic monocytes resulted in a relatively high production of CCL22 (CCR4 ligand) and CCL24 (CCR3 ligand) (Figure 3.2.12).

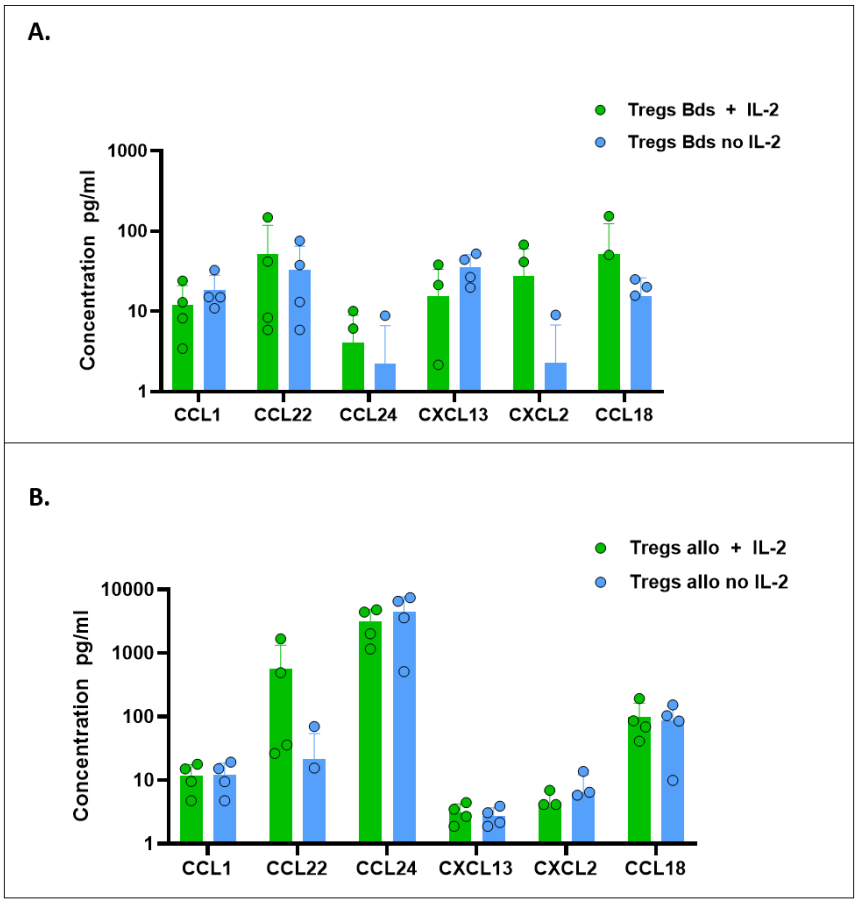


Figure 3.2.12 Effect of IL-2 on chemokine production by clinical Tregs.

Chemokine secretion by clinical-grade Tregs was measured following stimulation with (A) anti-CD3/CD28 beads (Tregs Bds) or (B) allogeneic monocytes (Tregs allo), in the presence (green) or absence (blue) of IL-2. Levels of selected chemokines were quantified from culture supernatants. No consistent differences were observed between IL-2-treated and untreated conditions across donors, indicating that IL-2 did not significantly alter the chemokine secretion profile. Data are presented as mean ± SD (n = 3-4), and plots were generated using GraphPad Prism. Statistics: Two-way ANOVA with multiple comparisons.

3.2.3.2 Comparison of chemokine secretion by Tregs and conventional T cells

To further characterise the secretory profile of clinical-grade Tregs, I compared chemokine production following anti-CD3/CD28 stimulation between Tregs, $CD4^+$, and $CD8^+$ T cells. As shown in Figure 3.2.13, Tregs secreted significantly higher levels of CXCL8 (IL-8) compared to both $CD4^+$ and $CD8^+$ T cells ($p < 0.0001$ for both). CXCL8 is a potent neutrophil chemoattractant that signals through CXCR1 and CXCR2 and plays established roles in leukocyte recruitment, tissue injury, and inflammation[99, 100]. Its elevated secretion by

Tregs suggests a context-dependent role in modulating inflammation and may contribute to immune cell recruitment via chemokine release.

In addition, secretion of CCL5 (RANTES), which promotes leukocyte recruitment through CCR1 and CCR5[101], was significantly higher in Tregs compared to CD4⁺ T cells ($p = 0.0206$), although CD8⁺ T cells exhibited the highest overall CCL5 levels ($p < 0.0001$ vs. CD4⁺ T cells) (Figure 3.2.13). CCL3, another CCR1/CCR5-binding chemokine[101], was elevated in CD8⁺ T cells relative to CD4⁺ T cells ($p = 0.062$), suggesting a more pro-inflammatory characteristics of the CD8⁺ subset (Figure 3.2.13). These data suggest that, although Tregs are not classically defined by chemokine secretion, they may actively shape immune cell trafficking via selective production of inflammatory mediators, particularly CXCL8.

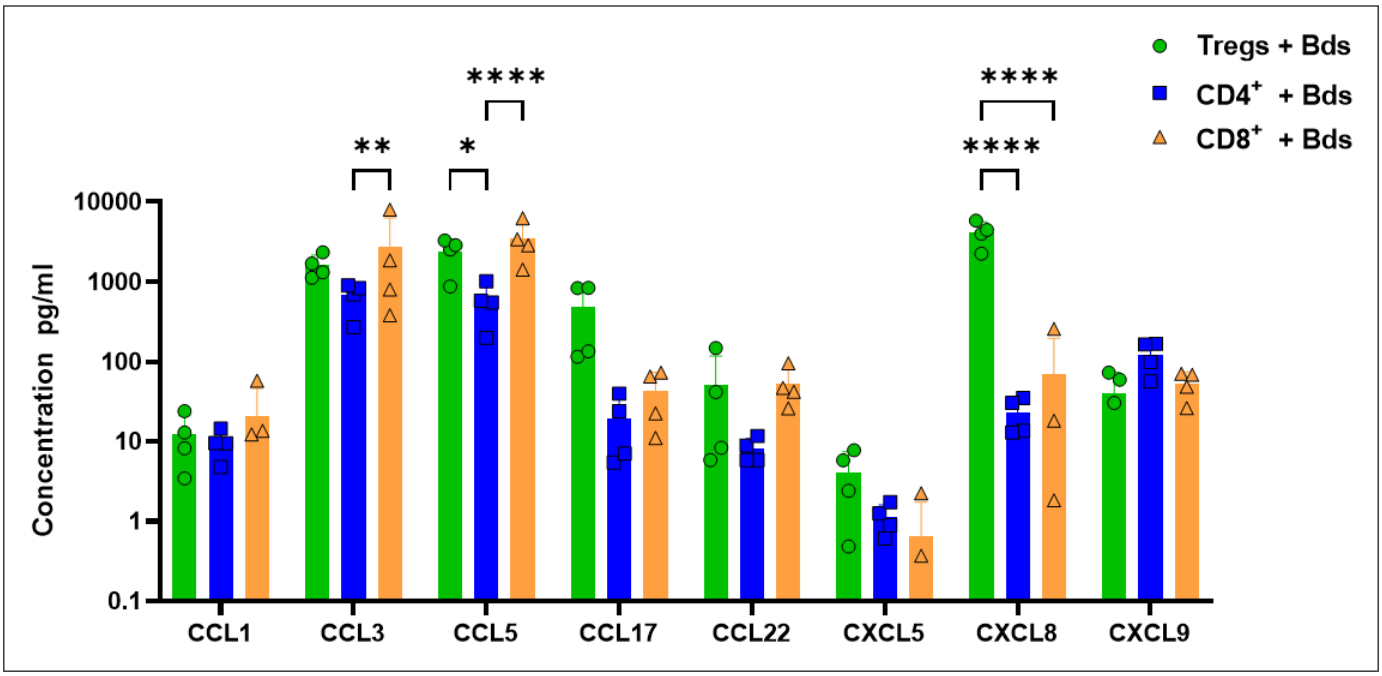


Figure 3.2.13 Chemokine secretion by Tregs, CD4⁺, and CD8⁺ T cells following CD3/CD28 stimulation.

*Supernatants were collected after stimulation with anti-CD3/CD28 beads, and levels of selected chemokines were measured. Tregs showed significantly elevated secretion of CXCL8 compared to both CD4⁺ and CD8⁺ T cells. CCL5 levels were modestly increased in Tregs compared to CD4⁺ T cells, with the highest levels observed in CD8⁺ T cells. CCL3 was significantly higher in CD8⁺ than in CD4⁺ T cells. Data represent mean ± SD; n = 4 donors. Graphs were generated using GraphPad Prism. Statistics: Two-way ANOVA with multiple comparisons; *p < 0.05, **p < 0.01, ****p < 0.0001. anti-CD3/CD28 beads (Bds).*

3.2.3.3 Impact of allogeneic stimulation on chemokines produced by conventional T cells and Tregs

To assess the differential chemokine secretion profiles among T cell subsets upon allogeneic stimulation, I co-cultured clinical-grade Tregs, CD4⁺, and CD8⁺ T cells with allogeneic CD14⁺ monocytes. As depicted in Figure 3.2.14, Tregs exhibited a significantly higher production of CCL24 compared to both CD4⁺ and CD8⁺ T cells (72 hours; p=0.0090 and p=0.0093, respectively). CCL24, also known as eotaxin-2, is a CCR3-binding chemokine traditionally linked to eosinophil recruitment but also implicated in chronic inflammation and

tissue remodelling[102]. The elevated secretion of CCL24 by clinical Tregs suggests a broader immunomodulatory function, potentially contributing to immune cell trafficking and tissue-specific responses during allogeneic stimulation. Interestingly, CCL2 (ligand of CCR2) and CXCL9 (ligand for CXCR3) production was significantly lower in Tregs as compared to CD8+ T cells, with both chemokines previously linked with kidney injury following ischemia reperfusion (CCR2)[103], or kidney rejection (CXCL9)[72].

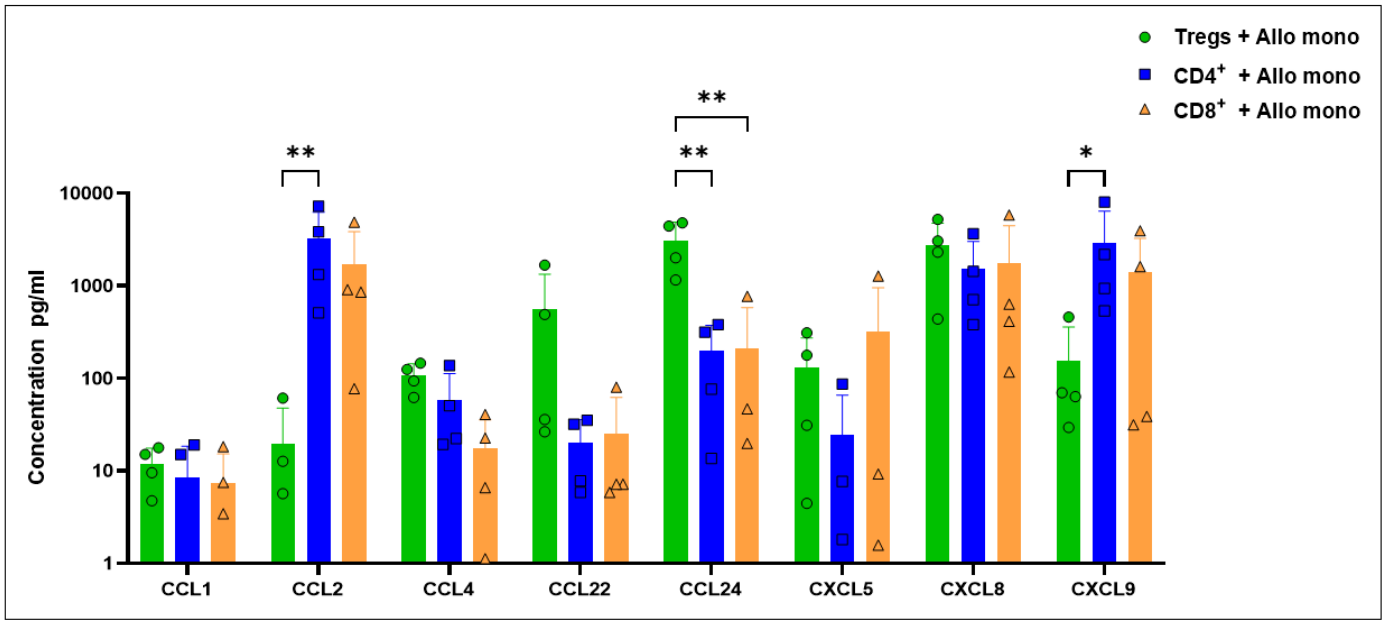


Figure 3.2.14 Chemokine secretion by Tregs, CD4⁺, and CD8⁺ T cells following allogeneic stimulation.

*Supernatants were collected after stimulation with allogeneic CD14⁺ monocytes, and levels of selected chemokines were measured. Tregs demonstrated significantly higher secretion of CCL24 compared to both CD4⁺ and CD8⁺ T cells. Data represent mean ± SD; n = 4 donors. Graphs were generated using GraphPad Prism. Statistics: Two-way ANOVA with multiple comparisons; *p < 0.05, **p < 0.01. Allogeneic monocytes (Allo mono).*

3.3 Discussion

Tregs are critical mediators of immune tolerance, exerting suppressive functions that maintain immune homeostasis and prevent tissue damage. In the context of transplantation, polyclonal Treg-based therapies have emerged as a promising approach to enhance graft survival while reducing the reliance on conventional immunosuppression[25]. However, the success of Treg therapy is highly dependent on the cells' ability to maintain a stable regulatory phenotype and to efficiently migrate to sites of inflammation, a process guided by chemokine receptor expression[76]. Understanding how clinical expansion alters Treg transcriptional profiles, homing receptor expression, and chemokine production is therefore essential to optimize their therapeutic potential. Herein, I want to examine the gene expression profile of clinical Tregs compared to conventional T cells and *ex vivo* Tregs and compare the protein expression of homing receptors between

clinically expanded Tregs and conventional T cells, finally, identify the chemokines produced by clinically expanded Tregs.

Comparative transcriptomic analysis revealed that clinically expanded Tregs maintain a robust regulatory identity distinct from conventional $CD4^+$ and $CD8^+$ T cells. Expanded Tregs demonstrated elevated expression of canonical regulatory markers such as FOXP3, CD25, TIGIT, and CD80 compared to both $CD4^+$ and $CD8^+$ T cell subsets (Figure 3.2.2 and Figure 3.2.3). These results emphasise FOXP3 and CD25 as a unique markers that are known for sustaining Treg lineage and suppressive functionality[104, 105]. Upregulation of TIGIT, a key co-inhibitory receptor mediating Treg suppression, further reinforces the regulatory stability of our clinical-grade Treg products[106]. In addition to maintaining classical regulatory markers, clinical Tregs exhibited enhanced expression of and trafficking molecules, such as ITGAX, ITGAM, and CEACAM1, compared to both conventional $CD4^+$ and $CD8^+$ T cells (Figure 3.2.2 and Figure 3.2.3). These molecules are critical for tissue retention and migration to sites of inflammation, processes essential for the therapeutic efficacy of Tregs in transplantation settings[70]. Consistent with clinical observations in kidney and liver transplantation, where efficient Treg trafficking and tissue localisation are key to successful tolerance induction and graft protection[26, 107], the enhanced expression of adhesion and migratory molecules observed in clinical Tregs could underscore their potential for effective tissue integration.

Moreover, clinical Tregs demonstrated higher expression of homing receptors such as CXCR6 and CCR8, further distinguishing them from conventional $CD4^+$ and $CD8^+$ T cells and aligning with findings that tissue-adapted Tregs are transcriptionally primed for migration to inflamed sites[94, 108]. Additionally, studies in effector $CD8^+$ T cells have reported that CXCR6 expression is driven by strong TCR signalling to promote tissue residency through chemotactic reprogramming[108], suggesting that similar signals might enhance Treg tissue localisation and functional adaptation post-expansion. These parallels reinforce the concept that GMP-expanded Tregs are transcriptionally primed for effective tissue infiltration and immunomodulation, an essential feature for successful tolerance induction in transplantation. Notably, clinical Tregs exhibited reduced expression of CXCR4 compared to conventional $CD4^+$ and $CD8^+$ T cells, consistent with previous observations that *ex vivo* expansion can remodel chemokine receptor profiles to favour peripheral tissue homing over lymphoid tissue retention[93]. Together, these comparative transcriptional profiles support the concept that Clinical-Tregs undergo selective modulation of adhesion and migratory molecules, optimising their adaptation to inflammatory tissues and possibly improving their therapeutic efficacy in transplantation contexts.

Preservation of key Treg markers following expansion is a critical indicator of their expected *in vivo* behaviour in recipients of Treg therapy. In this study, direct comparison between Clinical-Tregs and freshly isolated *ex vivo* counterparts revealed that, while core regulatory identity was maintained, expansion-induced phenotypic adaptations were evident. *Ex vivo* Tregs expressed higher levels of Helios, TCF7, and CD45RA (Figure 3.2.4), markers associated with a naïve and stable phenotype[109], whereas clinical Tregs showed enhanced expression of activation markers like LAG3 and OX40 (Figure 3.2.4), molecules broadly associated with T cell activation and improved immune regulation in inflammatory contexts[110]. These findings are consistent with prior observations that prolonged *ex vivo* expansion and specific cytokine conditioning can induce an effector-like transcriptional program in Tregs, enhancing their suppressive capacity while selectively modifying their homing receptor expression[77]. Overall, this adaptive transcriptional reprogramming indicates that Clinical-Tregs remain aligned with their regulatory lineage while selectively acquiring features that may optimise their therapeutic performance post-infusion.

I next investigated how *ex vivo* expansion impacts the trafficking potential of clinical Tregs through surface homing receptor profiling. Flow cytometric analysis confirmed that the majority of Clinical-Tregs maintained high expression of CD25 and FOXP3 after expansion, consistent with a preserved regulatory identity. However, a notable reduction in Helios expression was observed (Figure 3.2.5), aligning with previous studies suggesting that Helios, predominantly associated with thymic-derived Tregs, can be downregulated following prolonged culture and repeated stimulation[97, 111, 112], reflecting phenotypic plasticity and adaptation to the *in vitro* environment.

Surface profiling of clinical Tregs under both unstimulated and anti-CD3/CD28-stimulated conditions revealed that *ex vivo* stimulation significantly modulated chemokine receptor expression (Figure 3.2.7). Consistent with earlier observations from our group by Issa et al., showing that expanded human peripheral blood-derived Tregs expressing high levels of CCR7 and CD62L could prevent graft rejection in a murine model[76], the data here demonstrated stimulation-induced upregulation of CCR7 (Figure 3.2.7). The increase in CCR7 expression post-stimulation compared to unstimulated clinical Tregs suggests that activated Tregs exhibit enhanced potential for trafficking to lymphoid tissues, despite a long *in vitro* culture, that may contribute to better immunoregulation *in vivo*.

When examining chemokine receptor expression compared between Clinical-Tregs and conventional $CD4^+$ and $CD8^+$ T cells under unstimulated conditions, clinical Tregs displayed a distinct migratory signature (Figure 3.2.8). They exhibited significantly higher expression of CCR4, CCR8, CCR6, and CXCR3 compared to $CD4^+$ T cells, and elevated levels of CCR4, CCR8, CD62L, and CCR6 relative to $CD8^+$ T cells. Following anti-CD3/CD28

stimulation, dynamic shifts in chemokine receptor expression were observed across all T cell subsets (Figure 3.2.9). Clinical Tregs maintained high levels of CCR4 and CCR8 relative to conventional $CD4^+$ and $CD8^+$ T cells, while expression of CCR6 and CCR2 was further reduced. Despite activation-induced changes, CCR4 and CCR8 remained stable and prominently expressed in clinical Tregs, emphasising their potential role in directing Treg migration to inflamed peripheral tissues[98]. Moreover, the stable expression of CCR4 and CCR8 on Clinical-Tregs reflects the migratory adaptations observed in tissue-resident Tregs inhabiting barrier tissues such as the skin and gut, where these receptors contribute to selective recruitment and retention under both homeostatic and inflammatory conditions[92, 98]. Comparison of Clinical-Tregs to freshly isolated *ex vivo* Tregs revealed important differences upon stimulation. Both populations upregulated CCR4 and CCR7 proteins following activation; however, CD62L expression diverged, increasing in *ex vivo* Tregs while declining in clinical Tregs (Figure 3.2.11). This divergence suggests that prolonged *in vitro* expansion may selectively alter the responsiveness of specific homing receptors to activation, potentially affecting the recirculation and lymph node homing capabilities of infused Tregs[92, 113]. These expansion-related adaptations must be considered when optimising Treg manufacturing protocols for therapeutic applications.

In the flow cytometric analysis of surface homing receptors, my findings demonstrate that Clinical-Tregs retain a highly adaptable migratory profile. This is characterised by a notable increase in CCR7 expression following anti-CD3/CD28 stimulation, alongside stable expression of CCR4 and CCR8 compared with conventional T cells, supporting their capacity to localise to peripheral inflamed tissues. Importantly, CCR8 was significantly upregulated in clinical Tregs at both the transcriptomic level (Figure 3.2.2 and Figure 3.2.4) and the protein level (Figure 3.2.8), highlighting this chemokine receptor as a potential signature marker of clinical Tregs with therapeutic relevance.

To complement the transcriptional and surface-protein phenotyping analysis, chemokine secretion was assessed to further characterise the functional properties of Clinical-Tregs. Chemokine production represents a critical but less extensively characterised aspect of Treg biology, with potential implications for shaping immune cell recruitment and modulating tissue microenvironments during transplantation[90]. Lim, Tiong Y., et al. demonstrated that Tregs are highly sensitive to very low doses of IL-2, which effectively expanded the circulating Treg pool[114]. However, this expansion of Treg circulation did not increase the frequency of donor-specific Tregs, nor did it promote their trafficking to the transplanted liver. Their findings underscore the critical role of IL-2 in enhancing Treg survival and expansion in circulation, as observed in liver transplant recipients. Interestingly, my results show that IL-2 had no measurable effect on the secretion of chemokine ligands by Tregs under both anti-CD3/CD28 bead stimulation and allogeneic stimulation with

monocytes (Figure 3.2.12), which could potentially explain why IL-2 did not promote Treg trafficking in the mentioned study.

Clinical-Tregs secrete significantly elevated levels of CXCL8 (IL-8) following anti-CD3/CD28 stimulation when compared to conventional T cells (Figure 3.2.13). A pivotal study demonstrated that, despite their inability to produce classic proinflammatory cytokines, human Tregs secrete considerable amounts of chemokines, notably CXCL8, along with others such as CCL2-5, CCL7, and CXCL10[115]. This chemokine secretion profile equips Tregs with the ability to influence the cellular composition of inflamed tissues by attracting immune cells, particularly neutrophils, via CXCL8-mediated mechanisms. My findings corroborate these insights by showing that clinical-grade Tregs retain or even enhance this capacity under stimulatory conditions. The fact that CXCL8 secretion was observed even in the context of clinical manufacturing underscores its potential functional relevance *in vivo*, especially in modulating local immune cell recruitment during inflammation or transplantation. These findings may contribute to a growing recognition that chemokine production by Tregs is not simply a byproduct of activation but a functionally significant aspect of their immunoregulatory role.

Following allogeneic stimulation by $CD14^+$ monocytes, clinical Tregs secreted significantly higher levels of CCL24 compared to conventional $CD4^+$ and $CD8^+$ T cells (Figure 3.2.14). Although the role of CCL24 secretion by Tregs remains unclear, limited evidence suggests a potential function in Treg recruitment to inflammatory sites[116]. CCL24 may contribute to Treg recruitment to inflamed tissues, as protein array analysis showed an increase in its levels in lung tissue during neutrophilic inflammation; however, the study did not identify the cellular source of CCL24 or directly demonstrate its role in Treg recruitment[116]. The fact that Tregs themselves can produce CCL24, as shown here (Figure 3.2.14), further suggests an autocrine or paracrine loop through which Tregs may promote their own recruitment or retention within inflamed tissues. These findings position CCL24 as a potentially important mediator in Treg homing and function under inflammatory conditions, getting further mechanistic investigation in immune-mediated disease settings. Although no individual molecule was assessed both as a surface protein and as a secreted chemokine, the data together indicate that Clinical-Tregs combine a Treg-skewed chemokine receptor profile (high CCR4/CCR8 with inducible CCR7) with a distinctive chemokine secretion programme (CXCL8 and CCL24), that could support both their migratory specialisation and their capacity to shape the inflammatory milieu.

To sum up, in transcriptomic, surface-protein, and functional chemokine-secretion analyses, Clinical-Tregs demonstrated a highly consistent profile characterised by preserved regulatory identity and a coordinated shift towards enhanced migratory and tissue-adaptation potential. Transcriptomic analysis showed sustained expression of core regulatory genes such as FOXP3, CD25 and TIGIT (Figure 3.2.2 and 3.2.3),

alongside selective upregulation of trafficking and adhesion pathways including CCR8, CXCR6, ITGAM and CEACAM1 (Figure 3.2.2 and 3.2.4). These transcriptional signatures were mirrored at the protein level, where flow cytometry confirmed stable expression of CCR4 and CCR8 and stimulation-induced upregulation of CCR7 (Figure 3.2.7 and 3.2.9), as well as differential responsiveness of CD62L in clinical versus *ex vivo* Tregs (Figure 3.2.11). Complementing these phenotypic findings, the chemokine-secretion assays demonstrated that clinical Tregs retained functional competence, producing CXCL8 following TCR stimulation (Figure 3.2.13) and uniquely secreting CCL24 in response to allogeneic $CD14^{+}$ monocytes (Figure 3.2.14). Notably, IL-2 had no measurable effect on chemokine secretion under any stimulatory condition (Figure 3.2.12), aligning with external evidence that IL-2 expands circulating Tregs without enhancing trafficking. Collectively, these multimodal datasets show that expanded Tregs maintain lineage stability while adopting a specialised homing and chemokine-communication programme that is conserved across transcriptomic signatures, surface-receptor expression, and chemokines released by Tregs, supporting their suitability for therapeutic deployment in transplantation.

---

4 Chapter 4: *In vitro* Interactions Between Tregs and Monocytes

4.1 Introduction

The therapeutic potential of Tregs in transplantation is increasingly recognised for their capacity to suppress Teffs and for their broader role in shaping immune response through interactions with other cells. Tregs directly suppress Teffs by limiting IL-2 availability and blocking co-stimulatory signals. Their high expression of CD25 enables them to act as IL-2 sinks, restricting Teff proliferation and survival[47]. Also, Tregs express CTLA-4, which competes with CD28 on Teffs for binding to CD80/CD86 on APCs, effectively reducing co-stimulatory signals required for full T cell activation. These actions promote Teff anergy or apoptosis, particularly in autoreactive $CD8^+$ T cells. Meanwhile, IL-2 from activated Teffs sustains Treg expansion and FOXP3 expression, forming a feedback loop that maintains immune regulation[47].

While the role of Tregs in modulating alloimmunity has been well established, their dynamic crosstalk with myeloid cells particularly monocytes remain less clearly defined. Growing evidence indicates that Tregs can influence the functional state of monocytes and macrophages, driving them toward immunoregulatory phenotypes that reinforce transplant tolerance through IL-10 production and dampened antigen presentation[28, 117]. Conversely, monocytes may also contribute actively to Treg-mediated suppression by providing stabilising cues or participating in feedback loops that sustain the immunosuppressive environment. Recent studies have demonstrated that monocyte-Treg interactions can enhance anti-inflammatory cytokine secretion and promote the expansion or function of Tregs in inflamed tissue microenvironments[117]. *In vitro*-activated monocytes promoted an increase in the production of pro-inflammatory IL-17^+, IFN-γ^+, and TNF-α^+ Tregs, as well as anti-inflammatory IL-10^+ Tregs. This cytokine induction, particularly the rise in IL-17^+ and IFN-γ^+ Tregs, was driven by monocyte-derived IL-1β, IL-6, and TNF-α, and involved both $CD14^+CD16^-$ and $CD14^+CD16^+$ monocyte subsets. Notably, despite the elevated pro-inflammatory cytokine expression, the cells retained their $CD25^+FOXP3^+CD39^+$ regulatory phenotype and demonstrated enhanced suppression of effector T cell proliferation and IL-17 production[118]. However, the direct impact of monocytes on the function of expanded Tregs in controlled *in vitro* settings, remains insufficiently characterised.

Given these observations, this chapter investigates whether monocytes support or enhance the suppressive function of Tregs through direct cellular interactions. Furthermore, I explore whether monocyte presence alters cytokine production within a suppression assay, offering mechanistic insights into how these cells may modulate immune responses in the transplant context. I hypothesise that monocytes may enhance the

immunosuppressive function of Tregs through direct and indirect cellular interactions, contributing to immune regulation in the transplant environment.

4.1.1 Chapter aims

1) To investigate the *in vitro* interactions between polyclonal expanded Tregs and monocytes and to determine whether monocytes are required for optimal Treg-mediated suppression.
2) To assess whether the presence of monocytes alters cytokine production in suppression assays.

4.2 Results

4.2.1 Treg *in vitro* expansion and testing

4.2.1.1 Tregs sorting & expansion

As illustrated in Figure 4.2.1, polyclonal Tregs were successfully expanded from human PBMCs obtained from healthy donors. Briefly, $CD4^+CD25^+CD127^{low}$ cells were isolated using a BD FACSAria cell sorter, consistently achieving purities above 94% in accordance with established protocols[88, 119]. Sorted Tregs were expanded *in vitro* for 14 days using anti-CD3/CD28-coated Dynabeads and 1000 U/mL recombinant human IL-2. This expansion approach yielded a stable, suppressive Treg population suitable for downstream co-culture assays, in line with strategies previously shown to preserve Treg phenotype and function in preclinical transplant models[88, 119].

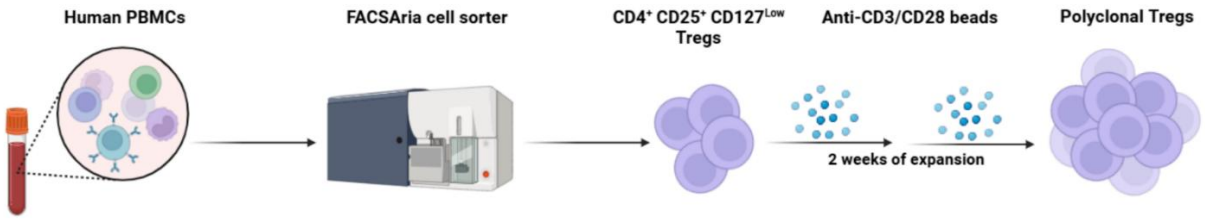


Figure 4.2.1 Human Treg Isolation and Expansion Protocol.

Schematic representation of the workflow used to isolate and expand human regulatory T cells. Tregs were isolated from peripheral blood mononuclear cells (PBMCs) obtained from healthy donors. $CD4^+CD25^+CD127^{low}$ cells were sorted by flow cytometry using a FACSAria cell sorter. The purified Tregs were cultured for 14 days in the presence of anti-CD3/CD28-coated Dynabeads and 1000 U/mL recombinant human IL-2, resulting in a polyclonal Treg population suitable for functional assays. Figure created using BioRender.com.

4.2.1.2 Treg fold expansion and FOXP3 expression analysis

Polyclonal Tregs expanded following stimulation with anti-CD3/CD28 beads and IL-2 over a 14-day culture period. These expanded Tregs were generated in our research laboratory and were not GMP-grade Tregs. They were therefore distinct from the Clinical-Tregs used in Chapter 3, which were manufactured by the GMP unit as the therapeutic product used in the clinical trial. Tregs exhibited a fold expansion ranging from approximately 30 to 120 across three independent donors (Figure 4.2.2.A). Total cell numbers increased significantly, reaching up to 4.6 × 10^7 cells after two weeks of expansion (Figure 4.2.2.B). Importantly, the expanded population retained high FOXP3 expression, with over 60% of cells expressing this key regulatory marker by the end of the culture period (Figure 4.2.2.C). These results confirm the successful expansion and phenotypic stability of the polyclonal Tregs for use in downstream functional assays.

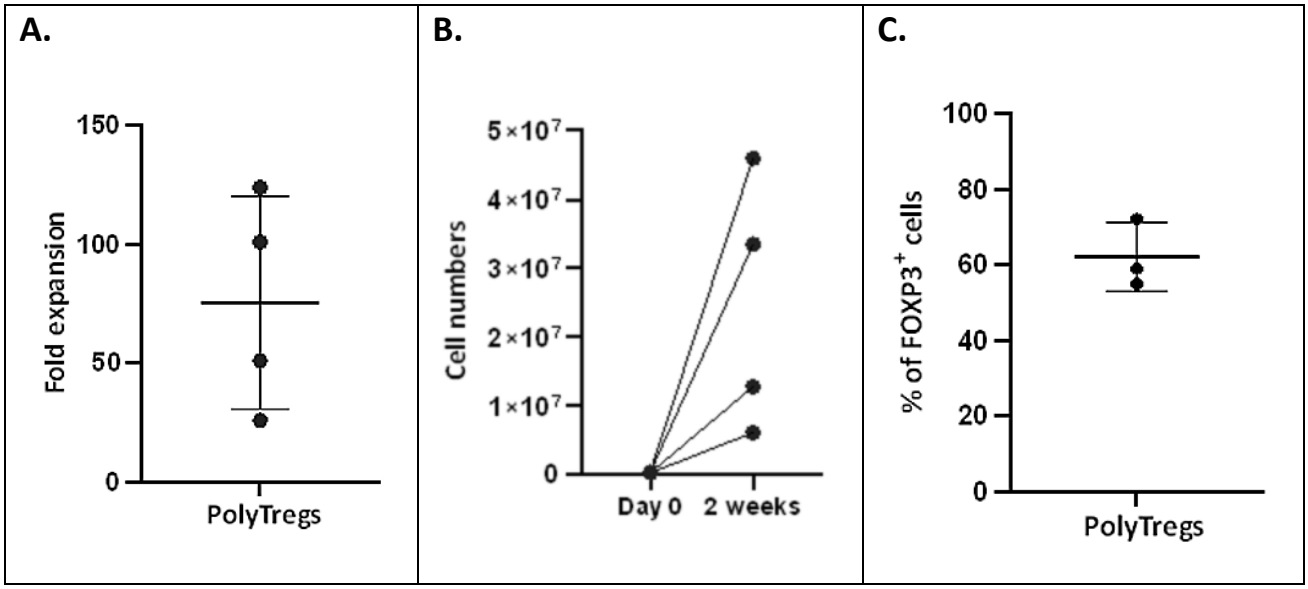


Figure 4.2.2 Expansion and FOXP3 Expression of Polyclonal Tregs.

(A) Fold expansion of polyclonal Tregs over 14 days of in vitro culture with anti-CD3/CD28 beads and IL-2. Data represent n = 4 independent healthy donors. (B) Total cell numbers at day 0 and after 2 weeks of expansion. Data represent n = 4 independent healthy donors. (C) FOXP3 expression was assessed by flow cytometry at the end of the expansion period. One donor sample was excluded from FOXP3 analysis due to inadequate staining quality. Data represent n = 3 independent healthy donors. Error bars indicate mean ± SD.

4.2.1.3 Assessment of Treg suppressive capacity using *in vitro* suppression assays

Following co-culture, cells were analysed using BD FACS Canto II with a standardized flow cytometry gating strategy to identify viable $CD4^+$ and $CD8^+$ T cell subsets (Figure 4.2.3.A). To assess the suppressive capacity of polyclonal expanded Tregs, VPD-labeled PBMCs were co-cultured with Tregs at varying ratios ranging from 1:1 to 1:16. T cell proliferation was monitored based on VPD dye dilution. As shown in Figure 4.2.3.B, Tregs efficiently suppressed responder T cell proliferation in a dose-dependent manner, with the strongest inhibition observed at the 1:1 ratio. Suppressive effects gradually decreased at lower Treg concentrations,

confirming that the polyclonal expanded Tregs retained functional potency across multiple Treg-to-responder conditions.

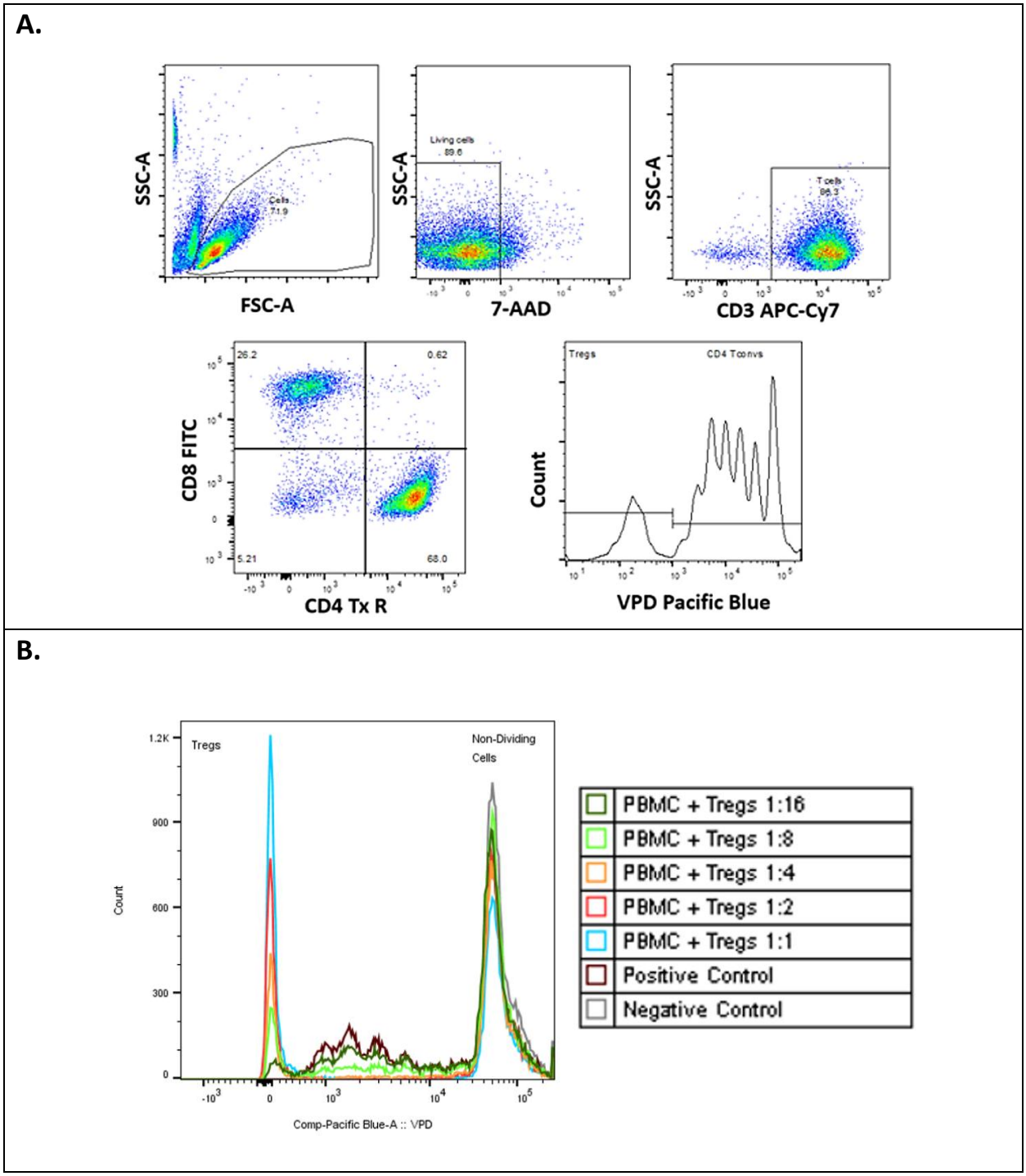


Figure 4.2.3 Flow Cytometry Gating Strategy and Suppressive Function of Polyclonal Expanded Tregs.

(A) Gating strategy used to identify T cell subsets in co-culture samples. Cells were gated using forward scatter (FSC) versus side scatter (SSC) to exclude debris, followed by 7-AAD exclusion to identify viable cells. $CD3^+$ T cells were then gated and further divided into $CD4^+$ and $CD8^+$ subsets. VPD staining was used to distinguish dividing $CD4^+$ effector T cells (VPD^+) from non-dividing Tregs (VPD^-). The same gating strategy was applied consistently across all samples. (B) Treg suppressive capacity was assessed by co-culturing VPD-labeled PBMCs with expanded Tregs at different ratios (1:1, 1:2, 1:4, 1:8, and 1:16). Proliferation of responder T cells was inhibited in a dose-dependent manner, with higher Treg proportions resulting in greater suppression. Positive control (stimulated PBMCs without Tregs) and negative control (unstimulated PBMCs) are shown for comparison. Plots were generated using FlowJo software (BD Biosciences).

4.2.2 Role of monocytes in Treg-mediated suppression

There is growing evidence highlighting the crosstalk between monocytes and Tregs. For instance, it has been reported that clinical Tregs can produce IL-10 to influence monocyte kinetics[28, 117]. On the contrary, monocytes have been shown to support Treg suppressive function in inflamed tissues by enhancing pro-inflammatory cytokine secretion[118].

Here, I explored the contribution of monocytes to Treg-mediated suppression by establishing a co-culture assay system using human PBMCs with or without CD14⁺ monocytes, as schematically illustrated in Figure 4.2.4. In this setup, I compared three experimental conditions. Condition 1 used total PBMCs stimulated with αCD3/CD28 beads and co-cultured with *in vitro* polyclonal expanded Tregs at various ratios (1:2 to 1:16), including positive and negative controls. Condition 2 involved PBMCs depleted of CD14⁺ monocytes (PBMCs -/- CD14⁺), which were then stimulated and co-cultured with Tregs under the same conditions. In Condition 3, CD14⁺ monocytes were isolated and added back to CD14⁺-depleted PBMCs (PBMCs +/+ CD14⁺) before stimulation and co-culture with Tregs, using the same range of cell ratios. After 72-96 hours, T cell proliferation was analysed by flow cytometry, and supernatants were collected and stored for cytokine bead array analysis (Figure 4.2.4).

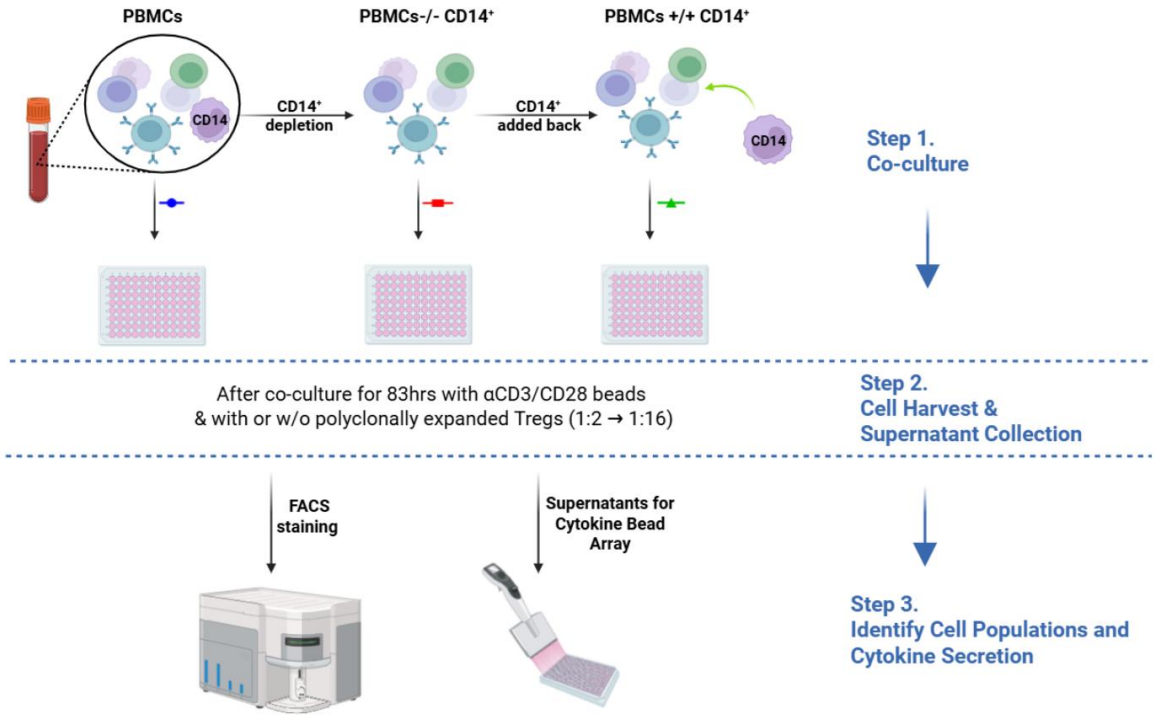


Figure 4.2.4 Experimental Design to Assess the Role of Monocytes in Treg-Mediated Suppression.

Schematic representation of the experimental workflow designed to assess the contribution of CD14⁺ monocytes to Treg-mediated suppression. ***Step 1:*** *Co-culture - Autologous PBMCs were isolated from healthy donors and* labelled *with VPD. CD14⁺ monocytes were either retained (Condition 1: PBMCs, blue), depleted (Condition 2: PBMCs -/- CD14⁺, red), or re-added to depleted PBMCs at*

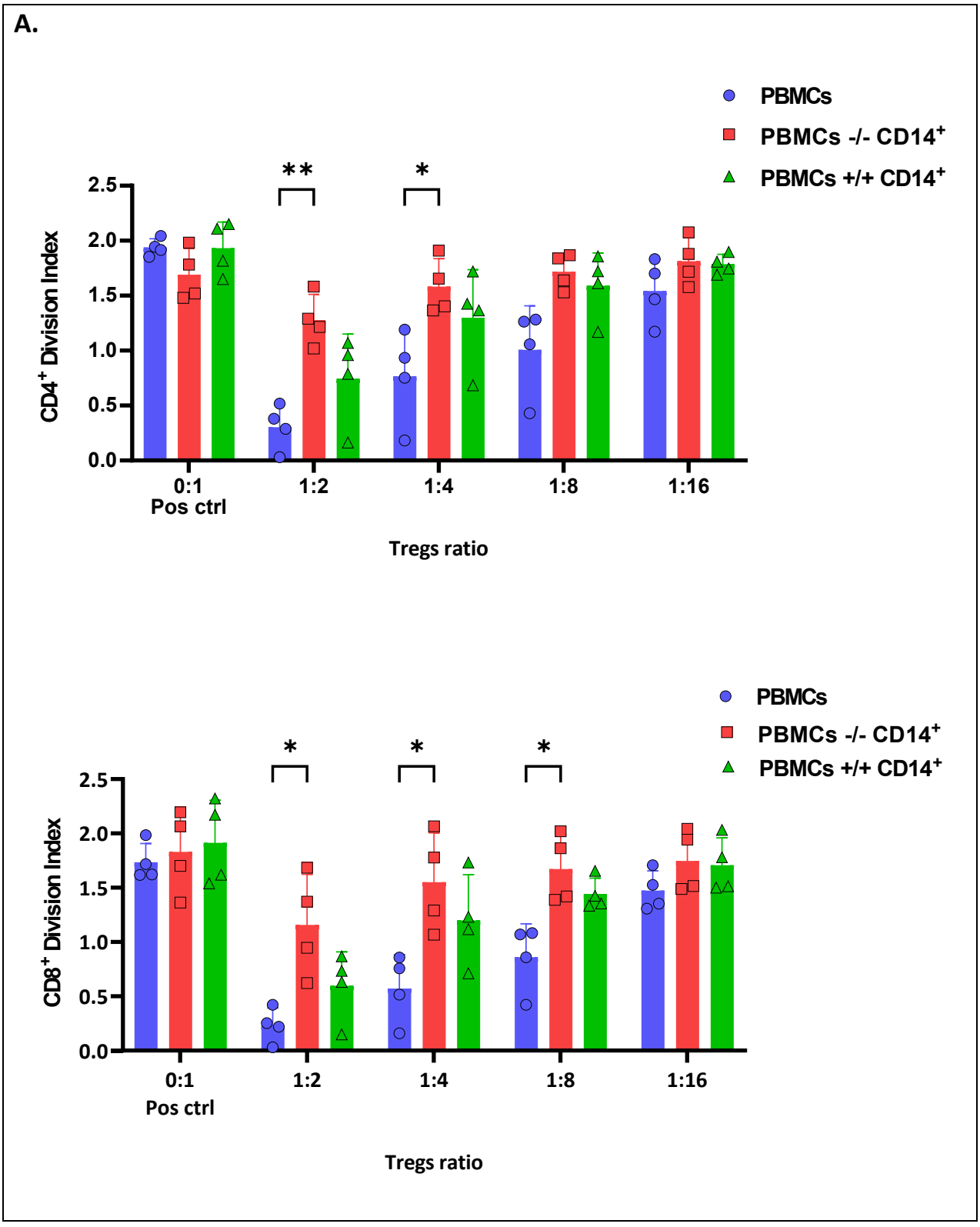
a 1:8 ratio (Condition 3: PBMCs +/+ CD14⁺, green). Cultures were stimulated with αCD3/CD28 beads and co-cultured with or without in vitro polyclonal expanded Tregs at varying Treg-to-responder ratios (1:2 → 1:16). ***Step 2:*** *Cell Harvest & Supernatant Collection - After ~ 83 hours (72-96 hours average) of co-culture, cells were harvested for downstream analysis, and supernatants were collected and stored at -20°C.* ***Step 3:*** *Identify Cell Populations and Cytokine Secretion - T cell proliferation was* analysed *by flow cytometry (FACS Canto II), and cytokine production was measured using a cytokine bead array. Figure created using BioRender.com.*

4.2.2.1 *In vitro* suppression by Tregs in the presence and absence of monocytes

To determine whether the presence of monocytes influences the ability of Tregs to suppress T cell proliferation, I compared $CD4^+$ and $CD8^+$ T cell division across three experimental conditions PBMCs, PBMCs -/- $CD14^+$, and PBMCs +/+ $CD14^+$ at a 1:8 ratio. As expected, T cells in the positive control group (no Tregs, 0:1 ratio) proliferated strongly under all conditions (Figure 4.2.5A). $CD14^+$ monocytes were reconstituted at a 1:8 monocyte-to-responder ratio to approximate the physiological proportion of monocytes within human PBMCs[120].

When Tregs were co-cultured with total PBMCs, I observed suppression of both $CD4^+$ and $CD8^+$ T cell proliferation across the Treg titration, particularly at intermediate Treg-to-responder ratios (Figure 4.2.5A). However, in the absence of $CD14^+$ monocytes, this suppressive capacity was reduced. Strikingly, when $CD14^+$ cells were re-introduced to the $CD14^+$-depleted PBMCs, Treg-mediated suppression was partially restored, most notably at higher Treg-to-responder ratios (Figure 4.2.5A). These effects were reflected in the calculated division index (DI), highlighting reduced suppressive efficiency of Tregs in the absence of monocytes and partial restoration following $CD14^+$ re-addition.

To account for variability in baseline proliferation across conditions, I next calculated the area under the curve (AUC) from division index values[121], normalising suppression relative to the positive control (0:1, no Tregs). As shown in Figure 4.2.5B, Tregs were consistently less effective at suppressing both $CD4^+$ and $CD8^+$ T cell proliferation in the absence of monocytes, while suppression was partially or fully restored when $CD14^+$ cells were reintroduced. These data suggest that monocytes support optimal Treg suppressive function *in vitro*.


A.
PBMCs
PBMCs -/- CD14+
PBMCs +/+ CD14+
**
*
CD4+ Division Index
2.5
2.0
1.5
1.0
0.5
0.0
0:1
Pos ctrl
1:2
1:4
1:8
1:16
Tregs ratio
PBMCs
PBMCs -/- CD14+
PBMCs +/+ CD14+
*
*
*
CD8+ Division Index
2.5
2.0
1.5
1.0
0.5
0.0
0:1
Pos ctrl
1:2
1:4
1:8
1:16
Tregs ratio

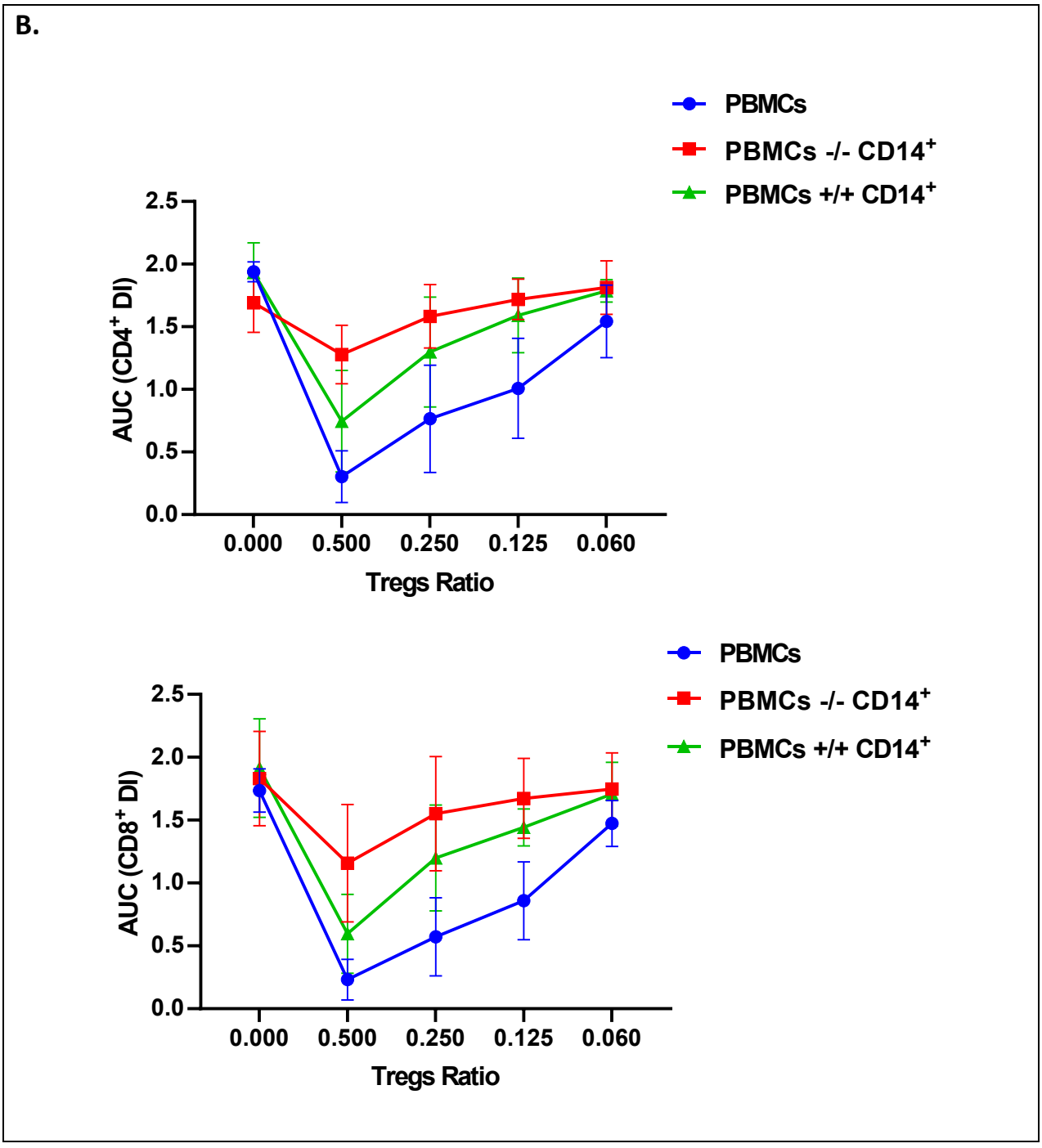


Figure 4.2.5 Effect of Monocytes on Treg-Mediated Suppression of T Cell Proliferation.

*(A) Division index (DI) of responder CD4⁺ (top) and CD8⁺ (bottom) T cells in suppression assays across three experimental conditions: PBMCs (blue), PBMCs depleted of CD14⁺ monocytes (PBMCs −/− CD14⁺, red), and CD14⁺-depleted PBMCs with re-added CD14⁺ cells (PBMCs +/+ CD14⁺, green). Autologous Tregs were co-cultured with αCD3/CD28-stimulated PBMCs at decreasing Treg: responder ratios (1:2 to 1:16). The 0:1 condition represents the positive control (stimulated PBMCs without Tregs). Across the titration, depletion of CD14⁺ monocytes were associated with reduced Treg-mediated suppression, while re-addition of CD14⁺ cells partially restored suppressive capacity, with differences between conditions most evident at intermediate Treg ratios. Data are shown as mean ± SD; n = 4 donors. Statistics: For panel A, division index data were analysed using a two-way mixed-effects model (REML) with donor-matched repeated measures and Sidak's multiple-comparisons test. Graphs were generated using GraphPad Prism. *p < 0.05, **p < 0.01. (B) Suppression of CD4⁺ (top) and CD8⁺ (bottom) T cell proliferation summarised as area under the curve (AUC) of DI across the full Treg titration, calculated for each donor and condition to normalise for baseline proliferation differences. Data are shown as mean ± SD; n = 4 donors.*

4.2.2.2 Investigation of cytokine production within suppression assays

Having observed that monocyte depletion impaired the suppressive ability of Tregs on T cell proliferation, I next investigated whether this effect extended to cytokine production. Cytokine bead array analysis was performed on supernatants collected from suppression assays under three experimental conditions: PBMCs, PBMCs depleted of $CD14^+$ monocytes (PBMCs -/- $CD14^+$), and $CD14^+$-depleted PBMCs with re-added $CD14^+$ cells (PBMCs +/+ $CD14^+$), across multiple Treg-to-effector ratios (1:2, 1:4, 1:8) after 72-96 hours of co-culture (Figure 4.2.6).

Within the Th1 cytokine compartment, IFN-γ and TNF-α remained significantly elevated in $CD14^+$-depleted PBMC cultures compared with total PBMCs at intermediate and higher Treg-to-effector ratios, most notably at 1:4 and 1:8 (Figure 4.2.6A). These differences were attenuated following re-addition of $CD14^+$ monocytes, indicating that monocytes contribute to effective Treg-mediated suppression of pro-inflammatory Th1 cytokine production. IL-2 showed a pronounced increase in the $CD14^+$-depleted positive control condition, with reduced but still detectable levels across Treg-containing cultures, supporting a role for monocytes in regulating baseline IL-2 availability.

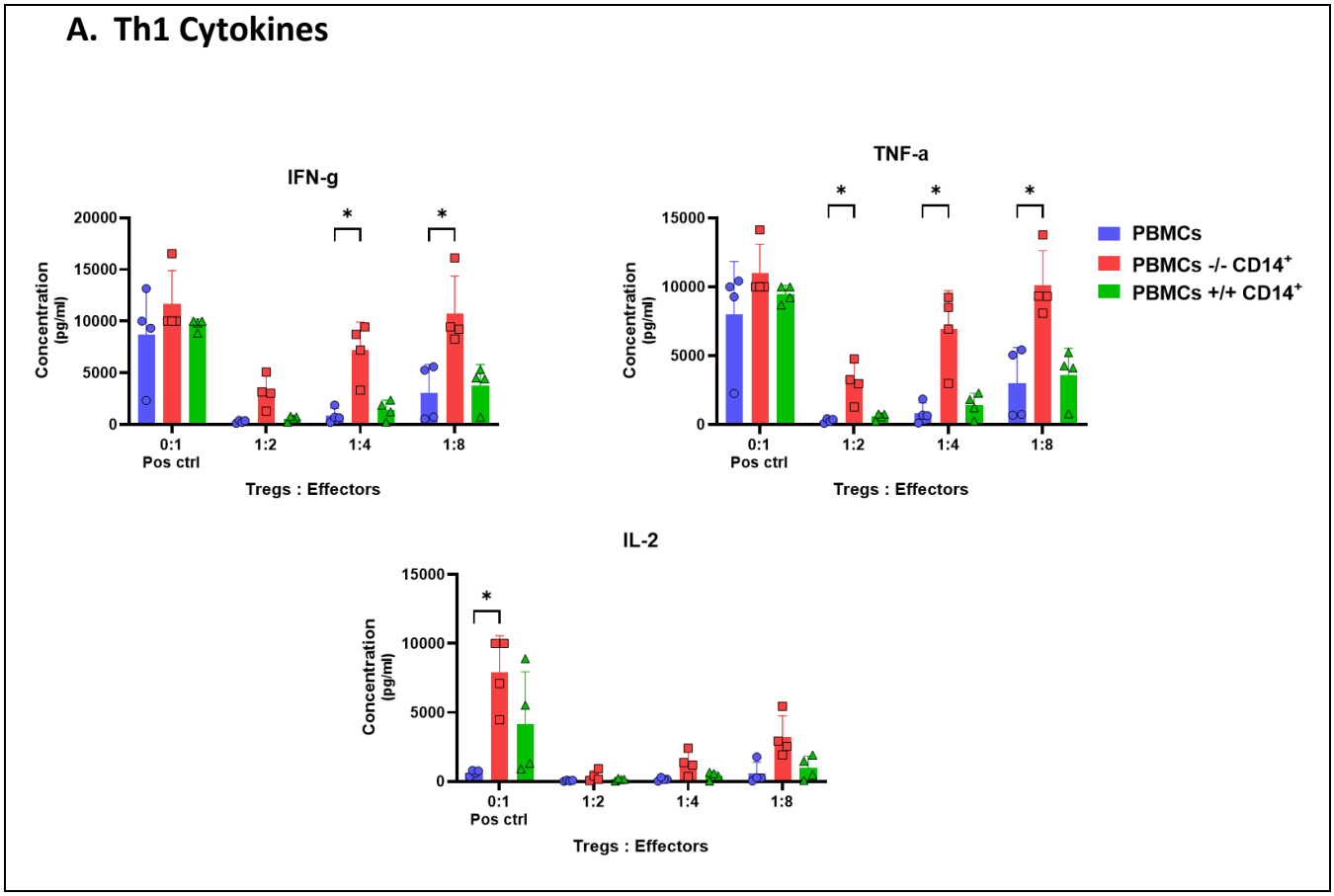
Analysis of Th2 cytokines demonstrated that IL-4 and IL-6 were significantly increased in the absence of $CD14^+$ monocytes, particularly at higher Treg ratios (Figure 4.2.6B). IL-4 displayed consistent elevation at 1:4 and 1:8 in $CD14^+$-depleted cultures, while IL-6 showed marked increases in the positive control and at 1:8. In contrast, IL-5 and IL-13 did not exhibit statistically significant differences across experimental conditions, suggesting that not all Th2-associated cytokines are equally dependent on monocyte-Treg interactions.

A robust and reproducible effect of monocyte depletion was observed within the Th17 cytokine axis. Both IL-17A and IL-17F were significantly elevated in $CD14^+$-depleted cultures across the positive control and all Treg ratios examined (Figure 4.2.6C). Importantly, partial suppression of these cytokines was restored following $CD14^+$ re-addition, highlighting a critical role for monocytes in restraining Th17-associated inflammatory responses in the context of Treg-mediated suppression.

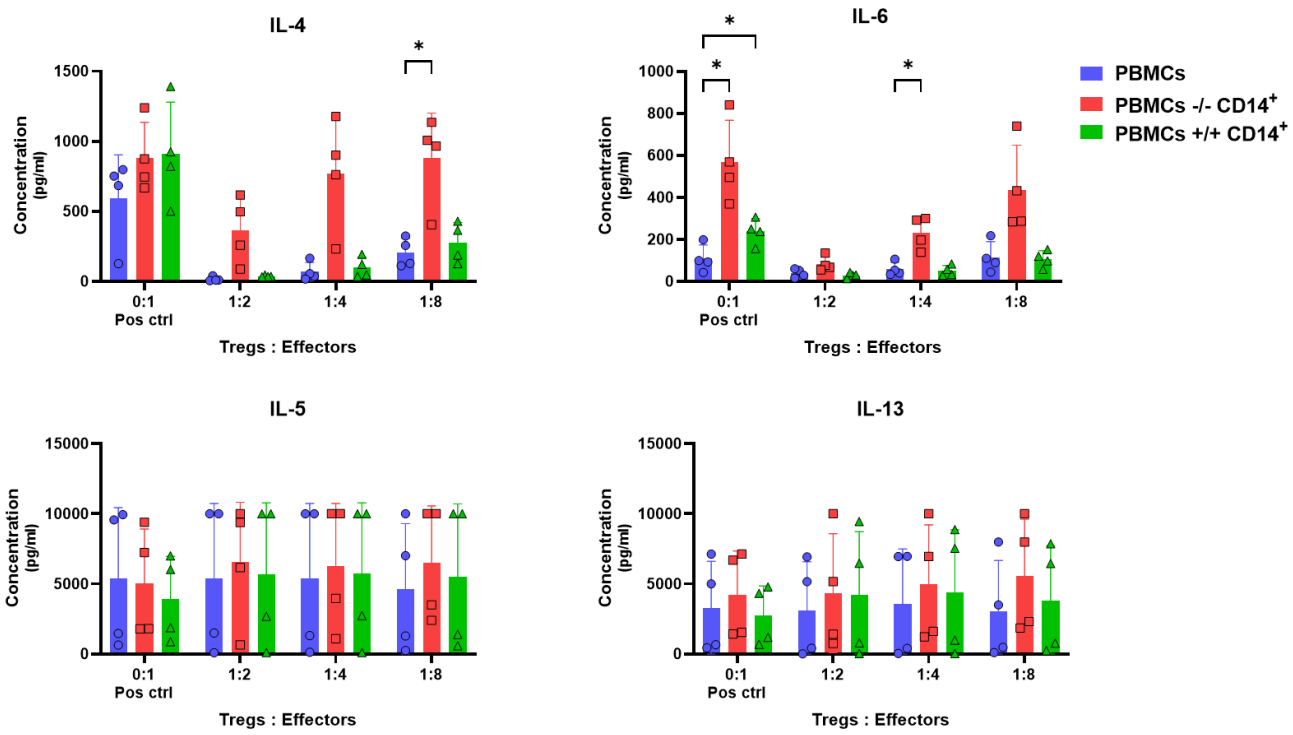
Within the anti-inflammatory cytokine compartment, IL-10 levels were significantly increased in $CD14^+$-depleted conditions, particularly in the absence of Tregs and at intermediate Treg ratios (Figure 4.2.6D). Re-addition of $CD14^+$ monocytes partially normalised IL-10 concentrations, suggesting that monocytes not only support suppression of pro-inflammatory cytokines but also influence the regulation of compensatory anti-inflammatory responses.

Finally, analysis of the remaining cytokines revealed that IL-9, IL-21, and IL-22 were significantly elevated in CD14⁺-depleted cultures, with the strongest effects observed at higher Treg ratios (Figure 4.2.6E). As observed for other cytokine groups, re-introduction of monocytes led to partial restoration of suppression, reinforcing the conclusion that monocytes broadly modulate cytokine control in Treg suppression assays rather than selectively affecting a single cytokine pathway.

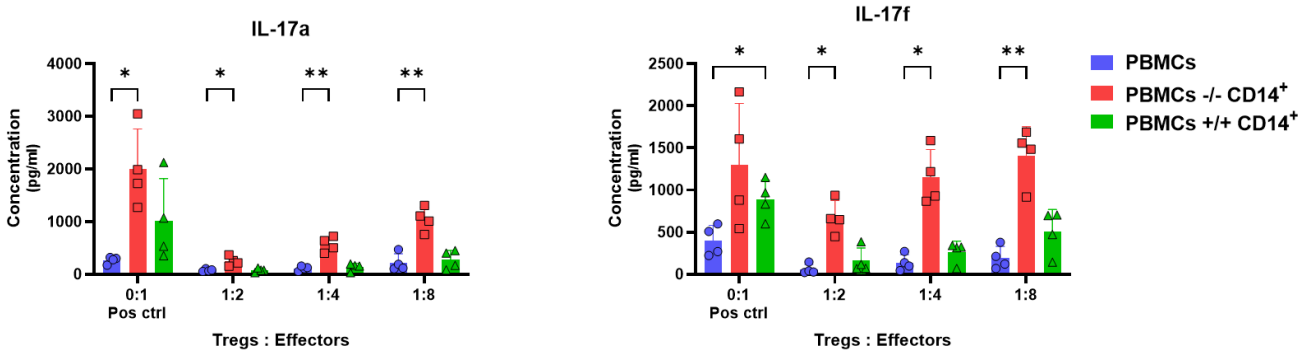
Overall, these data show that removal of monocytes leads to elevated levels of pro-inflammatory cytokines such as IFN-γ, TNF-α, IL-17A, and IL-17F, alongside increased production of the anti-inflammatory cytokine IL-10 and impairs Treg-mediated suppression of cytokine production in co-culture assays. This pattern suggests a loss of coordinated cytokine control in the absence of monocytes, indicating that monocytes are required to support balanced cytokine regulation during Treg-mediated suppression.



B. Th2 Cytokines



C. Th17 Cytokines



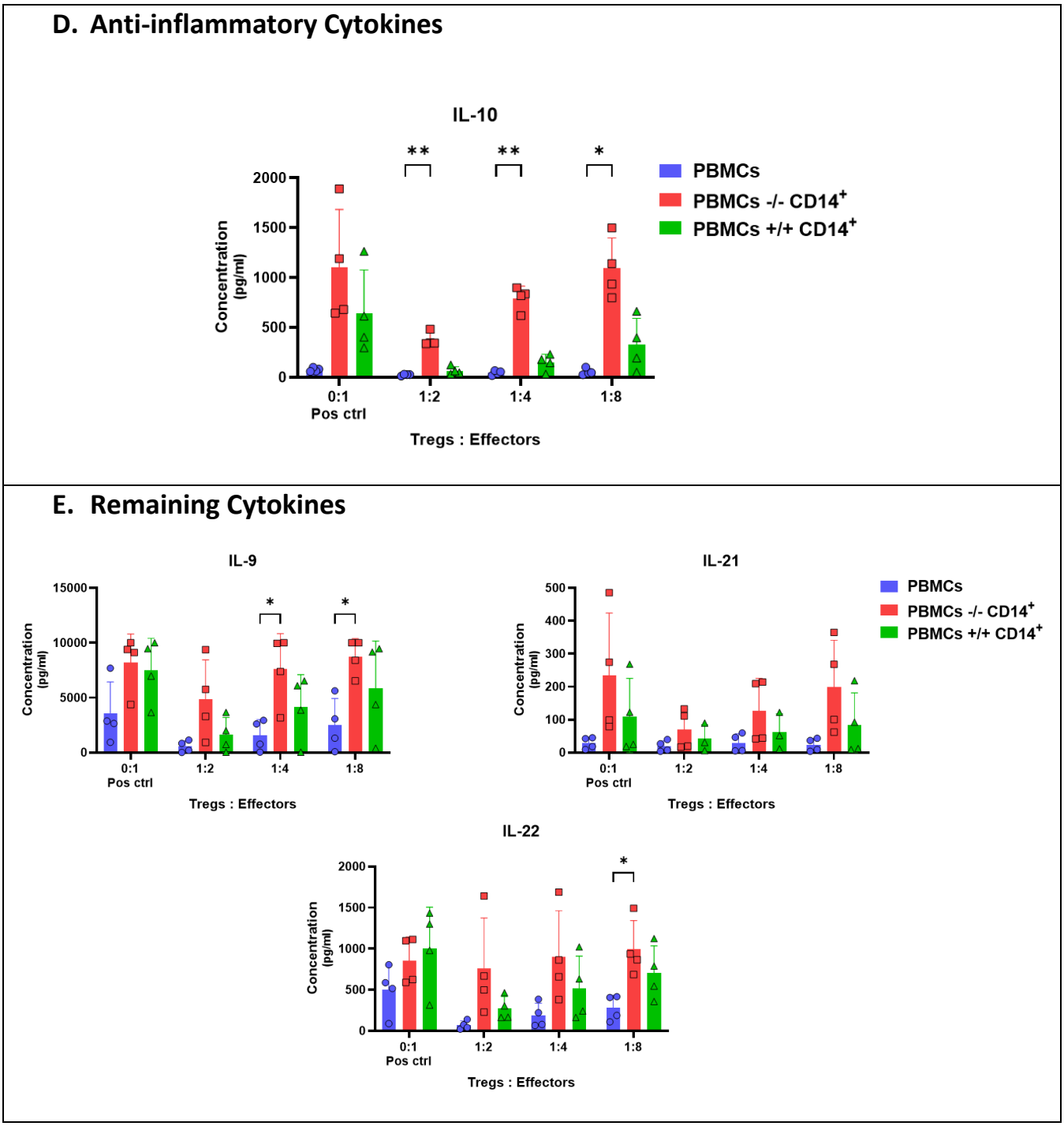


Figure 4.2.6 HU Th Cytokine Panel: Cytokine Profiling in Suppression Assays Across Experimental Conditions.

*Cytokine production was measured by bead-based immunoassay across three experimental conditions: PBMCs (blue), PBMCs −/− CD14⁺ (red), and PBMCs +/+ CD14⁺ (green), after 72-96 hours of co-culture with or without in vitro polyclonal expanded Tregs. Treg-to-effector ratios of 1:2, 1:4, and 1:8 were assessed, with PBMCs without Tregs serving as the positive control (0:1). Cytokine concentrations were determined using LEGENDplex software and are shown as pg/mL. (A) Th1 cytokines: IL-2, IFN-γ, and TNF-α. (B) Th2 cytokines: IL-4, IL-5, IL-6, and IL-13. (C) Th17 cytokines: IL-17A and IL-17F. (D) Anti-inflammatory cytokine: IL-10. (E) Other cytokines: IL-9, IL-21, and IL-22. Data represent mean ± SD; n = 4 donors. Graphs were generated using GraphPad Prism. Statistics: Data were analysed using a two-way mixed-effects model (REML) with donor-matched repeated measures. Post hoc comparisons were performed using Sidak's multiple-comparisons test, with PBMCs used as the control condition. *p < 0.05, **p < 0.01.*

4.3 Discussion

Tregs play a central role in maintaining immune tolerance in transplantation through direct suppression of Teffs and through broader immunomodulatory effects on antigen-presenting cells. By sequestering IL-2 and limiting co-stimulation via CTLA-4-mediated competition for CD80/CD86, Tregs inhibit Teff activation, proliferation, and survival while reinforcing their own expansion and FOXP3 stability through IL-2 feedback[47]. Although Treg-Teff interactions are well described, their crosstalk with myeloid cells, particularly monocytes, remains incompletely understood. Emerging evidence suggests that Tregs can modulate monocyte phenotype and function, promoting anti-inflammatory states that favour tolerance[28, 117], while monocytes may also support Treg stability and enhance their suppressive capacity via cytokine-mediated feedback loops[117, 118]. Yet, how these interactions operate in defined *in vitro* systems, especially when using polyclonal expanded Tregs as applied in clinical protocols, is not fully elucidated. I aimed first to validate the suppressive function of polyclonal expanded Tregs, and then to determine whether monocytes are required for optimal Treg-mediated suppression. Additionally, I investigated whether monocyte presence influences cytokine production within suppression assays. Together, these aims address the bidirectional interplay between Tregs and monocytes and the role they could play in shaping immunoregulation.

There is growing consensus that successful Treg-based therapies require the administration of high cell numbers, which cannot be achieved through isolation alone. Although freshly isolated *ex vivo* Tregs have been used in early-phase clinical trials[122], their limited availability restricts broader therapeutic application. *Ex vivo* expansion protocols have therefore been developed to generate sufficient cell doses for adoptive transfer, and polyclonal expanded Tregs have been shown to exhibit enhanced suppressive capacity compared with freshly isolated cells[123, 124], potentially mediated by upregulation of ectoenzymes such as CD73 and CD39 that promote adenosine generation[123]. Polyclonal expanded Tregs were generated using an established protocol previously associated with enhanced suppressive function, and these cells retained robust FOXP3 expression following two weeks of expansion. Sustained FOXP3 expression is a defining feature of Treg identity and has been linked to long-term persistence and intragraft localisation in humanised mouse models[76]. Consistent with prior literature, the *in vitro* suppression assays conducted here confirmed that the polyclonal expanded Tregs used in this study retained potent suppressive activity, supporting their suitability for downstream functional analyses rather than serving as a primary endpoint of investigation.

The crosstalk between Tregs and monocytes is bidirectional. On one hand, expanded Tregs have been shown to more effectively modulate monocyte phenotype and function than freshly isolated *ex vivo* Tregs,

promoting an alternatively activated, anti-inflammatory state characterised by reduced pro-inflammatory cytokine production and decreased expression of co-stimulatory and MHC class II molecules[125]. In this study, I investigate the reverse interaction, specifically, how monocytes may influence the suppressive function of expanded Tregs.

Tregs play a crucial role in preventing graft rejection by suppressing the proliferation of Teffs, thereby maintaining immune tolerance[126]. Dowling et al. used quantitative modelling to demonstrate that Tregs primarily reduce the magnitude of Teff responses by limiting their *division destiny*, rather than by increasing cell death rates or slowing the pace of cell division[126]. In T cell biology, division destiny refers to the total number of times a T cell will divide before it stops, due to terminal differentiation, senescence, or quiescence, it represents a kind of pre-set limit on proliferative potential[126]. In contrast, the division rate (interdivision time) refers to how fast the divisions occur, and the cell death rate reflects how quickly cells die, reducing population size independently of proliferation. The study found that Tregs do not act primarily by accelerating Teff death or slowing their cycling, but by lowering the total number of divisions each Teff undergoes[126]. This reduction in division destiny functions as a "log-dampener," meaning even small decreases in the number of divisions result in a logarithmic reduction in the final size of the effector T cell population, highlighting the potency of Tregs in modulating immune responses and preventing immune-mediated tissue damage[126]. Herein, I similarly observed that Tregs suppressed Teff division destiny. When Tregs were co-cultured with total PBMCs, I observed significant suppression of both $CD4^+$ and $CD8^+$ T cell proliferation, particularly at a 1:2 Treg-to-responder ratio (Figure 4.2.5.A). The aim of this experiment was to assess the contribution of monocytes to Treg-mediated suppression. Notably, in the absence of monocytes, this suppressive capacity was markedly reduced. When monocytes were reintroduced to monocyte-depleted PBMCs, Treg-mediated suppression was clearly restored, most prominently at a Treg-to-responder ratio of 1:2, with continued suppression observed at 1:4 and 1:8 (Figure 4.2.5.A). These findings were further supported by division index analysis, which reflected reduced Treg function in the absence of monocytes and a recovery of suppressive capacity following monocytes reconstitution. Previous reports have highlighted how monocytes can influence Treg proliferation and have shown that monocyte subsets modulate Treg function[127].

In this study, I demonstrate that the presence of monocytes is essential for maintaining the suppressive capacity of polyclonal expanded Tregs in *in vitro* proliferation tests. This conclusion was further reinforced by AUC analysis of division index values, which accounted for baseline variability and emphasised the role of monocytes in supporting Treg-mediated suppression of Teffs[121]. In line with this, Walter, Gina J., et al.

showed that memory Tregs co-cultured with LPS-activated monocytes exhibited enhanced suppressive activity, particularly in limiting Teff proliferation and IL-17 production, despite increased expression of pro-inflammatory cytokines[118]. These findings suggest that Treg-monocyte crosstalk not only preserves but may even enhance Treg suppressive function under inflammatory conditions, consistent with my observations that monocytes are critical modulators of Treg efficacy. While previous studies have focused on monocyte-mediated modulation of freshly isolated or a subset of Tregs, this study explores this interaction in the context of polyclonally expanded Tregs, which is timely in the context of the increasing interest in Treg cellular therapy in transplantation and autoimmune diseases.

In an attempt to understand how monocytes modulate Treg suppressive function, I examined alterations in cytokine secretion in the presence and absence of monocytes. And the data here, demonstrate that monocytes are required for optimal Treg-mediated regulation not only of T cell proliferation but also of cytokine production. Specifically, depletion of monocytes resulted in elevated levels of both pro-inflammatory cytokines, including IFN-γ, TNF-α, and IL-17A/F, as well as the anti-inflammatory cytokine IL-10, while reconstitution with monocytes partially restored suppression across multiple cytokine axes (Figure 4.2.6A-E).

The precise mechanisms by which monocytes support Treg-mediated suppression in the assays here remain unresolved. One possibility is that monocytes provide accessory cytokine signals that could sustain Treg functional fitness while simultaneously restraining excessive effector cytokine production. In support of this concept, Walter et al. demonstrated that activated human monocytes drive increased cytokine expression in memory Tregs via monocyte-derived IL-1β, IL-6, and TNF-α, yet importantly preserve FOXP3 expression and enhance suppressive capacity[118]. This study highlights that exposure to inflammatory monocyte-derived cytokines does not necessarily destabilise Tregs but instead can enhance their suppressive function under certain conditions. My observation that IL-10 levels increase alongside pro-inflammatory cytokines in monocyte-depleted cultures (Figure 4.2.6D) suggests that, in the absence of monocytes, Tregs alone may be insufficient to coordinate effective suppression of a dysregulated cytokine milieu. This increase in IL-10 may represent a compensatory regulatory response to the heightened inflammatory environment following monocyte depletion. Supporting the importance of IL-10 in Treg–monocyte interactions, Nayer et al. demonstrated in mouse models that Treg-derived IL-10 promotes an anti-inflammatory monocyte/macrophage phenotype[117]. However, the cellular source of the increased IL-10 observed in the present study was not determined.

An alternative, but not mutually exclusive, possible explanation is that monocytes influence Treg stability and suppressive capacity in a subset- and cytokine-dependent manner. Zhong et al. demonstrated that distinct monocyte subsets differentially regulate Helios$^+$ and Helios$^-$ Treg proliferation via IL-12 and TNF-α, respectively[127]. Although Helios expression was not assessed in the present study[127], my data showing elevated IFN-γ and IL-17A/F in the absence of monocytes (Figure 4.2.6A, C) are consistent with a scenario in which loss of specific monocyte-derived signals permits expansion of inflammatory pathways that Tregs are unable to fully restrain. This raises the likelihood that defined monocyte subsets may be required to maintain particular Treg functional states necessary for efficient suppression of effector cytokine responses.

Importantly, monocyte-derived signals may also be detrimental to Treg function depending on inflammatory context. Arterbery et al. demonstrated that in de novo autoimmune hepatitis, monocyte/macrophage-derived IL-12 and IL-6 drive Tregs towards Th1- and Th17-like phenotypes characterised by IFN-γ and IL-17 production, resulting in functional impairment despite preserved FOXP3 demethylation[128]. Partial restoration of suppressive function following IFN-γ blockade in that study highlights the capacity of monocyte-derived cytokines to actively destabilise Treg-mediated regulation in inflammatory settings[128]. Together with my findings, these data suggest that monocytes act as central regulators of the cytokine milieu that can either support or impair Treg suppressive function depending on their activation state and cytokine output. Although *in vivo* and non-human primate studies support interactions between Tregs and myeloid cells within transplanted tissues[129], evidence in humans remains limited, and the more complex cellular and cytokine environment within the graft may influence these interactions differently from the *in vitro* setting.

Further work will be required to dissect the mechanisms underlying the monocyte-dependent effects observed here. This could include selective blockade of candidate monocyte-derived cytokines during suppression assays, assessment of Treg stability markers and transcriptional states following monocyte depletion or reconstitution, and direct comparison of suppressive capacity in the presence of defined monocyte subsets. Such approaches would help clarify whether monocytes primarily act by sustaining Treg functional fitness, shaping the cytokine environment, or directly restraining inflammatory effector pathways. Together, these findings highlight the common and context-dependent nature of Treg-monocyte crosstalk. While previous studies have demonstrated how activated monocytes can enhance or impair Treg function through cytokine-mediated mechanisms[118, 127, 128], my data extend this paradigm by showing that removal of monocytes results in a breakdown of coordinated cytokine regulation that cannot be compensated for by Tregs alone. This underscores the importance of monocytes in enabling effective Treg-mediated immune regulation.

5 Chapter 5: Investigation into Impact of Treg Therapy on Circulating and Graft-Resident Leukocytes in Renal Transplant Recipients

5.1 Introduction

The Transplantation Without Overimmunosuppression (TWO) Study is a phase IIb, single-centre randomised controlled trial aimed at assessing the safety and efficacy of autologous Treg therapy in promoting immunosuppression minimisation following living donor kidney transplantation[25]. This innovative trial was designed in response to the well-established role of Tregs in maintaining immune tolerance and mitigating alloimmune responses, with the hypothesis that adoptive transfer of *ex vivo*-expanded autologous Tregs could reduce the requirement for immunosuppression agents[25].

The trial's original protocol employed an alemtuzumab-based induction strategy, with Treg therapy administered six months post-transplantation during the lymphocyte repopulation phase. This delayed infusion approach was informed by earlier findings suggesting that lymphodepletion via alemtuzumab creates a favourable immunological niche for Treg expansion. In this cohort, control patients received standard immunosuppression, while those in the Treg arm were infused with autologous polyclonal Tregs manufactured under GMP conditions[83] followed by reduction in maintenance immunosuppression. The strategy was designed to maximise Treg efficacy during immune reconstitution. Results demonstrated its feasibility and safety, with 100 percent graft survival and no biopsy-proven rejection at 18 months[83]. As reported by Brook et al., delayed Treg infusion is not only compatible with lymphodepleting induction but may support durable graft outcomes in clinical settings[83].

Additionally, evidence from the study by McCallion et al. further supports the therapeutic role of Tregs in kidney transplantation[130]. This work showed that kidney transplant recipients treated with early Treg infusion exhibit stable long-term graft function with reduced immunosuppressive burden. Notably, focal lymphocytic infiltrates were observed in protocol biopsies of Treg-treated patients, which were phenotypically distinct from acute rejection and were enriched for regulatory markers such as IL-10, PD-L1, and TIGIT[130]. These findings suggest that the beneficial effects of Treg therapy may be mediated by local immunoregulation within the graft microenvironment[130].

While Tregs are known to suppress alloimmunity, their interactions with myeloid cells, particularly monocytes, remain incompletely understood[118]. Evidence suggests that monocyte-Treg crosstalk can

promote anti-inflammatory phenotypes and support the stability of Tregs[118], although the role of monocytes in modulating the function of Tregs used in adoptive cell therapy is not yet fully defined.

Given these observations, this chapter investigates the effects of Treg infusion on both systemic and local immune responses in kidney transplant recipients. I hypothesise that Treg infusion may support immune regulation without inducing significant alterations in circulating immune cell populations, and that within the allograft, Tregs could interact with monocytes to help establish a regulatory microenvironment that favours tolerance.

5.1.1 Chapter aims

1) To investigate the impact of cellular therapy with Tregs on the circulating leukocytes.
2) To explore how cellular therapy with Tregs impacts immune infiltrates in renal allograft biopsies, with a focus on the monocytes.

5.2 Results

5.2.1 Study design

The TWO Study clinical trial was designed to evaluate the efficacy and immunological impact of autologous Treg therapy in kidney transplantation [25, 83] (detailed description in the Material and methods chapter). As illustrated in Figure 5.2.1, patients in the Treg therapy arm underwent leukapheresis at least three weeks prior to transplantation to collect peripheral blood for Treg isolation and *ex vivo* expansion. The final Treg product, comprising 5-10 × 10^6 autologous $CD4^+CD25^+FOXP3^+$ cells per kg body weight, was infused on day five post-transplantation, replacing conventional antibody induction therapy. Participants in the control arm received basiliximab induction and standard triple immunosuppression (tacrolimus, MMF, and prednisolone), with stepwise reduction of prednisolone to dual therapy, whereas in the cell therapy group an additional gradual withdrawal of MMF was intended. Both arms underwent immunomonitoring and protocol biopsies at specified time points up to 78 weeks[25, 83].

Participants were randomised 1:1 to receive either Treg infusion or conventional care, with an aim to recruit 34 patients in each arm. This current cohort (basiliximab cohort) forms the basis of the immunomonitoring analysis as reported in this chapter (Section 5.2.2). An additional seven patients were treated earlier under the original alemtuzumab protocol prior to its discontinuation due to COVID-19 pandemic and

overimmunosuppression concerns. These were reported separately as a cohort demonstrating earlier experience with Treg therapy[25, 83]. Two of these patients were selected for spatial transcriptomic analysis using the 10x Xenium platform, and these data is described later in this chapter (Section 5.2.3).

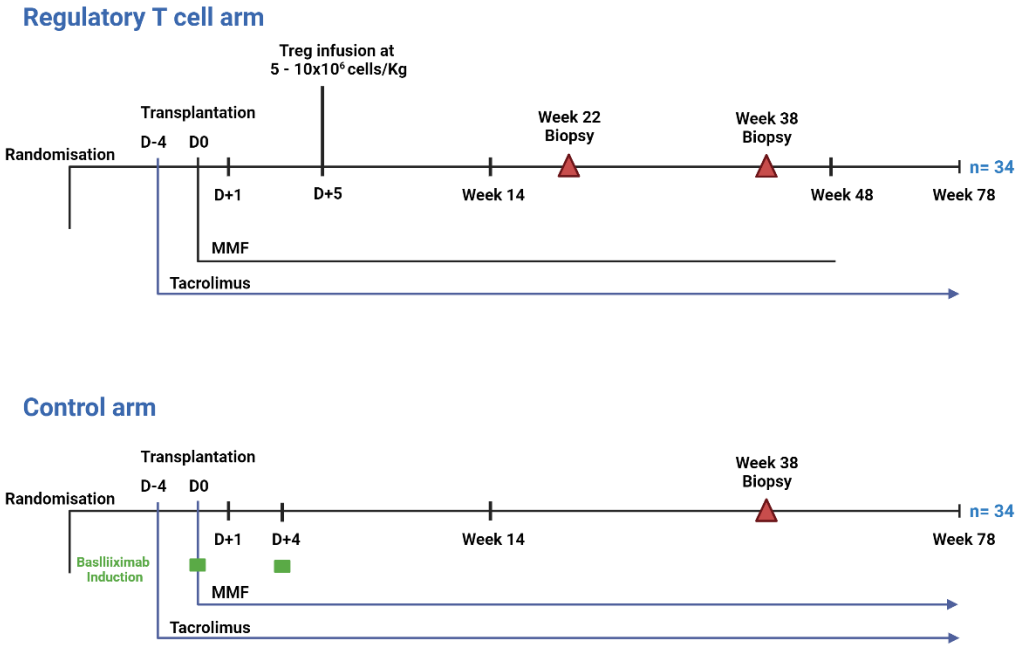


Figure 5.2.1 Diagrammatic representation of the immunosuppressive regimen used in the TWO Study.

The upper panel represents the Treg therapy arm, in which autologous regulatory T cells were infused on day 5 post-transplant following leukapheresis, ex vivo expansion, and cryopreservation. The lower panel shows the control arm, where basiliximab was administered as induction therapy and standard immunosuppression was gradually tapered. Both arms underwent protocol biopsies and follow-up until week 78[25, 83]. Created by Biorender.

5.2.2 Phenotypical analysis of peripheral leukocytes in TWO study participants

To assess longitudinal changes in peripheral immune cell populations following Treg therapy, flow cytometric analysis was performed on blood samples collected from a subset of nine patients enrolled in the revised protocol of the TWO Study. This subset included five participants from the Treg therapy group (Patients 112, 113, 116, 117, and 124) and four from the control group (Patients 114, 118, 120, and 122). Consecutive patients who completed the immunomonitoring period at the time of preparation of this thesis were included in the analysis. Although some included participants had occasional missing visits, they retained sufficient longitudinal data for analysis. Patients were excluded due to multiple missing visits or withdrawal from the study. Patients enrolled from patient 125 onwards had not completed the full immunomonitoring period (up to week 78) at the time of thesis preparation and were therefore not included. All patients

underwent scheduled trial visits at predefined time points: pre-transplant (baseline), Day 4, and weeks 2, 4, and 78 post-transplant (Table 5.2.1).

Table 5.2.1 Schedule of assessments and interventions for participants included in the immunomonitoring sub study.

ASSESSMENTS		V0 Pre-visit	V1 min.-3 weeks	V2 W-2	In-patient			V3 W1	V4 W2	V5 W4	V6 W12	V7 W22	V8 W30	V9 W38	V10 W41	V11 W43	V12 W49	V13 W51	V14 W78
					D0	D4	D5												
STUDY GROUP	Control	X		X	X	X		X	X	X	X		X	X		X		X	X
	Treg therapy	X	X	X	X	X	X	X	X	X	X	X	X	X	X	X	X	X	X
Rx ADMINISTRATIO	Treg/Cell isolation		X																
	TR001 (IMP) administration						X												
	Basiliximab (Control arm)				X	X													
IMMUNE MONITORING				X		X		X	X	X	X	X		X		X		X	X

This diagram outlines the timing of study group assignments, immunosuppressive interventions, and immune monitoring time points in the revised protocol of the TWO Study. Participants in the Treg therapy group underwent leukapheresis for Treg cell isolation at least three weeks prior to transplantation (V1), followed by infusion of the investigational medicinal product (TR001) on day 5 post-transplantation. Control participants received Basiliximab induction therapy at the time of transplant (D0 and D4). Peripheral blood samples were collected for immune monitoring at specified visits, spanning pre-transplant baseline through long-term follow-up. The red "X" marks denote the day of kidney transplantation surgery.

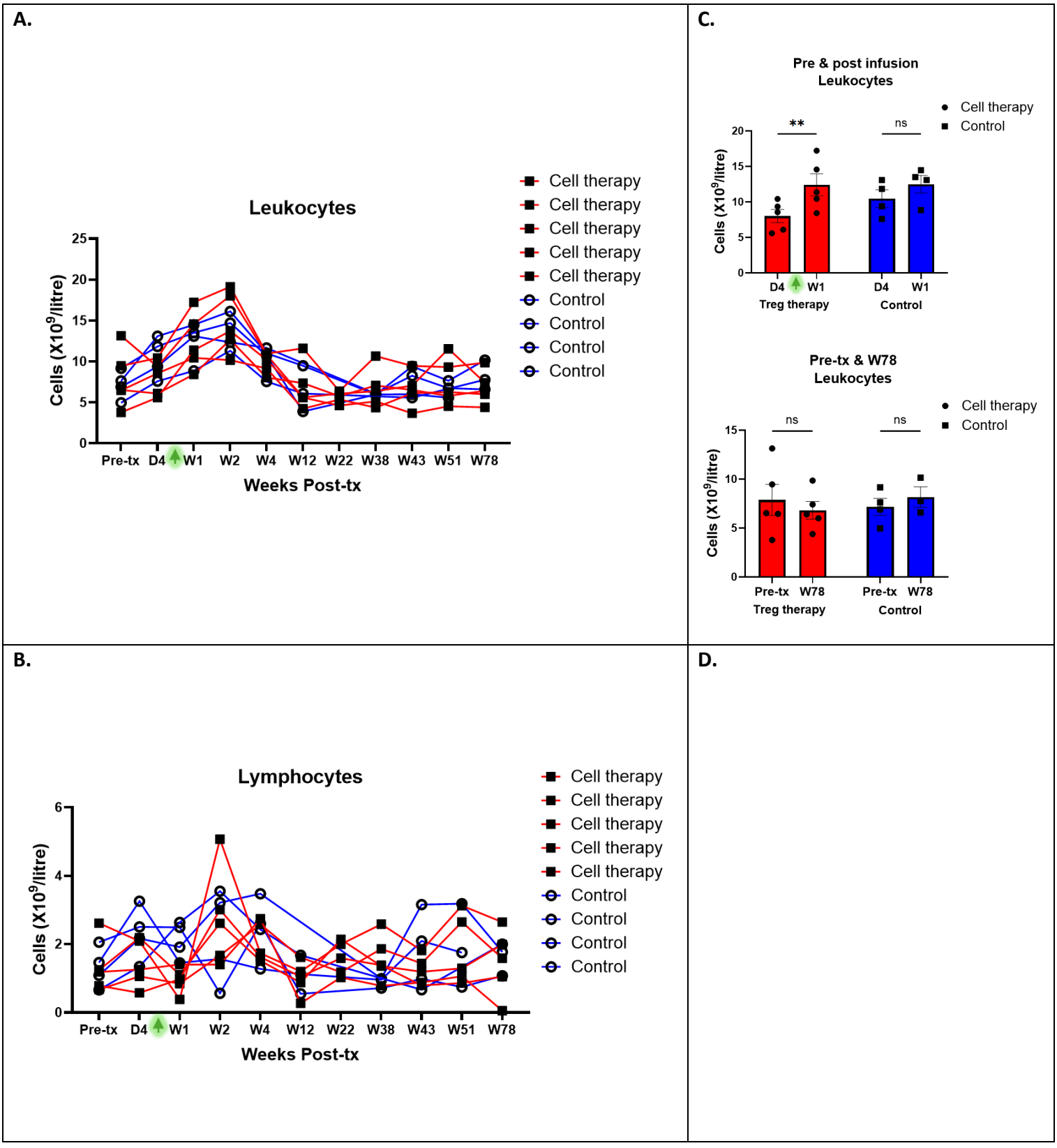
Samples were stained using lyophilised DuraClone antibody panels and analysed on a Navios flow cytometer. Absolute cell counts were calculated using haematology reports, and immune cell frequencies were evaluated to determine the effects of Treg infusion on circulating leukocyte subsets.

5.2.2.1 Analysis of main immune populations post transplantation

5.2.2.1.1 Analysis of leukocyte & lymphocyte levels across all visits

Longitudinal immunomonitoring demonstrated dynamic changes in circulating leukocyte and lymphocyte counts following kidney transplantation (Annex A5.1, and Figure 5.2.2). Leukocyte counts rose over the early post-transplant interval, with a significant increase between day 4 and week 1 observed in the Treg therapy group (Figure 5.2.2A, C), whereas the corresponding change in controls was not significant (Figure 5.2.2C); by late follow-up, leukocyte counts at week 78 were not different from pre-transplant levels in either group (Figure 5.2.2A, C). The early increase in circulating leukocytes is consistent with the expected post-operative inflammatory response to major surgery, where tissue injury and surgical stress induce innate immune activation and transient changes in circulating leukocyte populations[131]. In contrast, lymphocyte counts showed modest inter-individual variability across the sampling period, with no detected differences at the key early (D4 vs week 1) or late (Pre-transplant vs week 78) comparisons, and overall comparable values between the Treg therapy and control groups (Figure 5.2.2B, D). These findings indicate that Treg therapy

was not associated with sustained or global perturbations in circulating leukocyte or lymphocyte numbers, supporting its immunological safety despite a transient early increase in leukocytes following infusion.



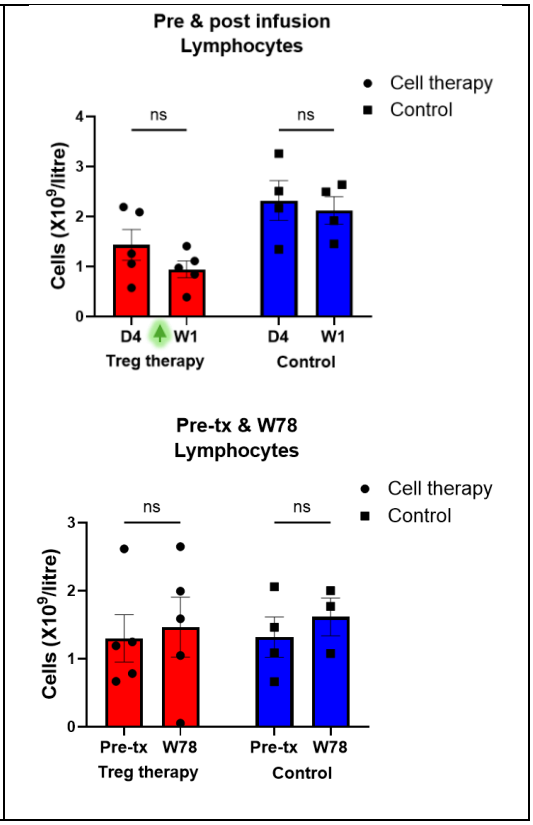


Figure 5.2.2 Absolute counts of circulating leukocytes and lymphocytes in peripheral blood following kidney transplantation.

*(A, B) Line graphs showing absolute numbers of leukocytes (A) and lymphocytes (B) in peripheral blood collected at serial timepoints from patients in the Treg therapy group (red, solid squares) and the control group (blue, open circles). Each line represents an individual patient. Samples were collected pre-transplant (Pretx), at day 4 (D4), and subsequently at weeks 1, 2, 4, 12, 22, 38, 43, 51, and 78 post-transplantation. The green arrow pre-week 1 (day 5 post-transplant) indicates the timing of Treg infusion. (C, D) Bar plots showing group comparisons of leukocyte (C) and lymphocyte (D) counts at two key timepoints: pre- versus post-Treg infusion (D4 vs. week 1), and Pretx versus week 78. Cell therapy patients are shown in red, and control patients in blue. Dots represent individual patients, bars indicate mean ± SEM. Longitudinal data were analysed using a mixed-effects model (REML), with time as a repeated measure and treatment group as a fixed effect. *p < 0.05, **p < 0.01; ns denotes not significant. Tx, transplantation; Pre-tx, pre-transplant; D4, day 4 post-transplant.*

5.2.2.1.2 Investigation of T cell subpopulations ($CD4^+$ and $CD8^+$ T cells)

To determine whether Treg therapy was associated with broader alterations in circulating T cell compartments, longitudinal changes in $CD4^+$ and $CD8^+$ T cell counts were examined following kidney transplantation (Figure 5.2.3). Across the study period, $CD4^+$ T cell counts exhibited temporal fluctuations without evidence of differences at the early post-infusion interval (day 4 versus week 1) or between pre-transplant and late follow-up at week 78, and values remained broadly unchanged in Treg-treated and control patients (Figure 5.2.3A, C). $CD8^+$ T cell counts also varied between individuals over time, with no detectable change immediately following infusion, while a modest increase between pre-transplant and week 78 was observed in the Treg therapy and in control groups (Figure 5.2.3B, D). These findings could indicate that Treg therapy was not associated with marked or sustained perturbations in circulating $CD4^+$ or $CD8^+$ T cell numbers over the course of follow-up.

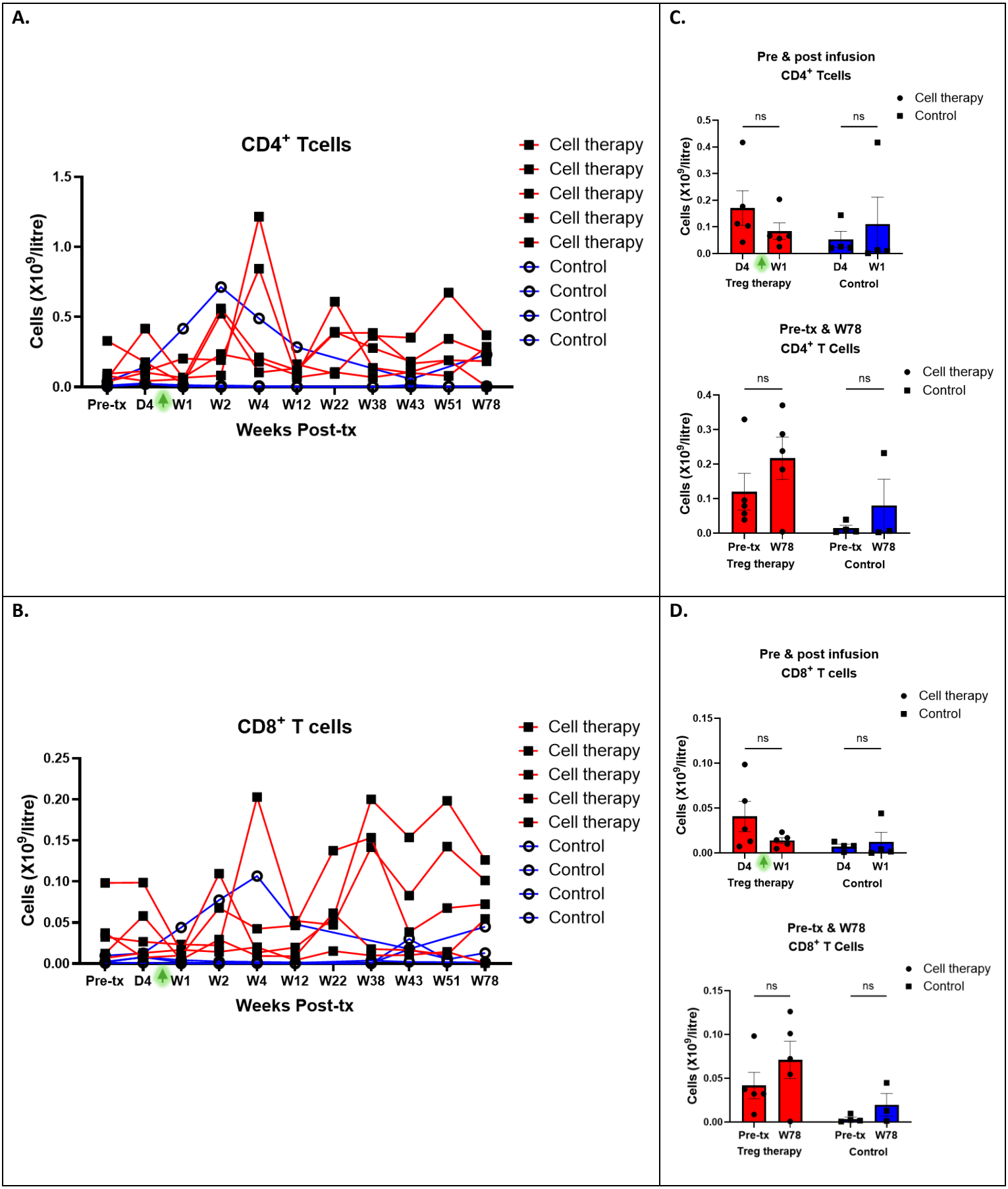
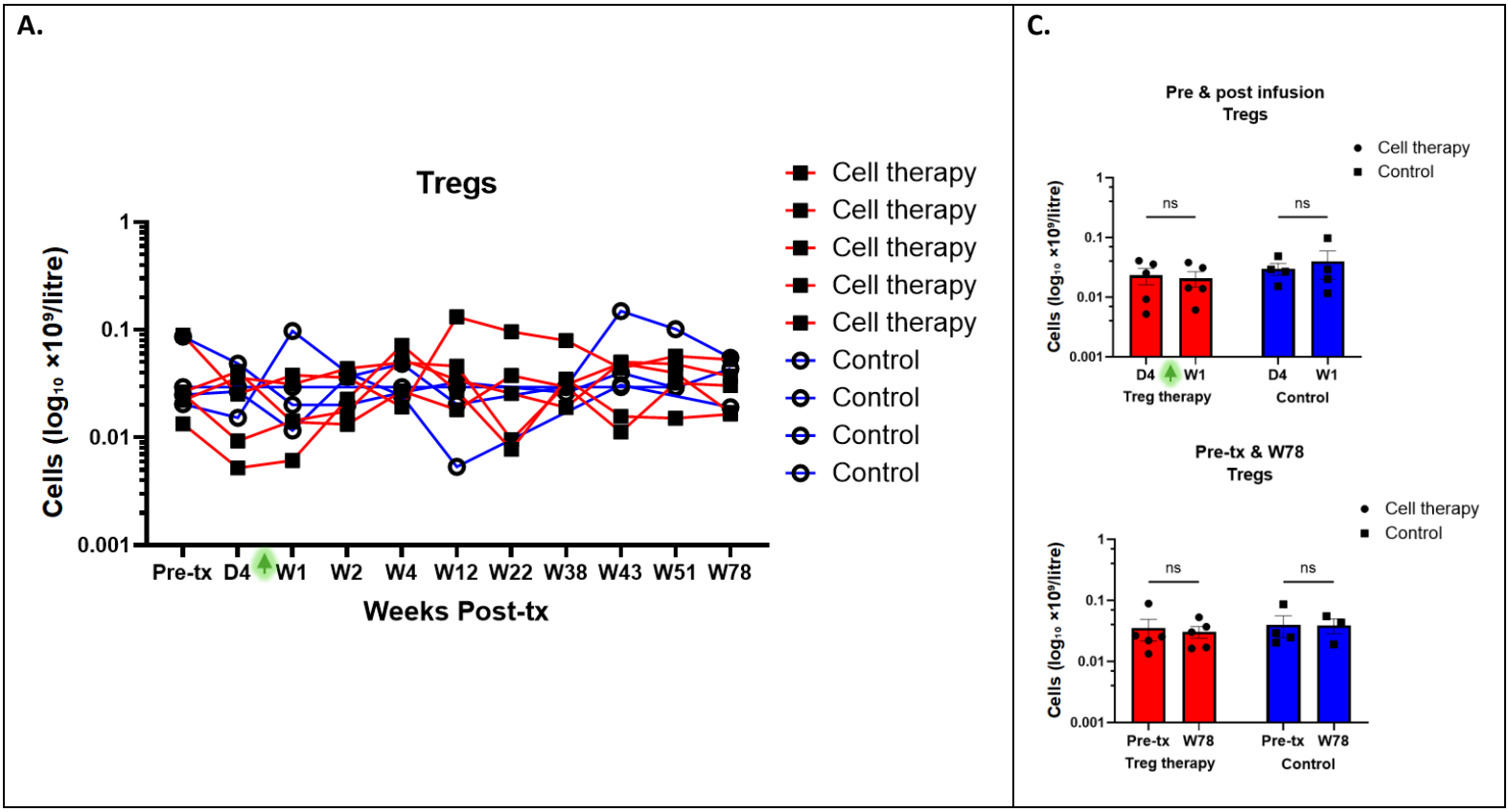


Figure 5.2.3 Longitudinal analysis of CD4+ and CD8+ T cell dynamics in peripheral blood following Treg therapy.

(A, B) Line graphs showing absolute numbers of peripheral CD4⁺ T cells (A) and CD8⁺ T cells (B) from patients in the Treg therapy group (red, solid squares) and control group (blue, open circles), collected pre-transplant (Pretx), at day 4 (D4), and at serial timepoints up to week 78 post-transplantation. Treg infusion occurred on day 5 post-transplant (green arrow, pre-week 1). Each line represents an individual patient. (C, D) Bar plots comparing CD4⁺ (C) and CD8⁺ (D) T cell counts at key timepoints: immediately pre- and post-Treg infusion (D4 vs. week 1) and over the full duration (Pre-tx vs. week 78). Cell therapy patients are shown in red, controls in blue. Dots represent individual patients, bars indicate mean ± SEM. Longitudinal data were analysed using a mixed-effects model (REML), with time as a repeated measure and treatment group as a fixed effect; ns denotes not significant. Tx, transplantation; Pre-tx, pre-transplant; D4, day 4 post-transplant.

5.2.2.1.3 Evaluation of changes in circulating Treg cells overtime

To assess the impact of Treg therapy on circulating Tregs, longitudinal changes in total Tregs and Helios⁺ Tregs were examined following kidney transplantation (Figure 5.2.4). Absolute Treg counts displayed variability over time in both groups, with no significant differences detected at the early post-infusion interval (day 4 versus week 1) or between pre-transplant and late follow-up at week 78, and comparable levels were observed between Treg-treated and control patients throughout follow-up (Figure 5.2.4A, C). Similarly, Helios⁺ Tregs showed inter-individual fluctuations across the post-transplant period without significant changes at early or late timepoints and without divergence between treatment groups (Figure 5.2.4B, D). These data highlight that adoptive Treg therapy was not associated with sustained alterations in circulating total or Helios⁺ Treg frequencies over the course of immunomonitoring.



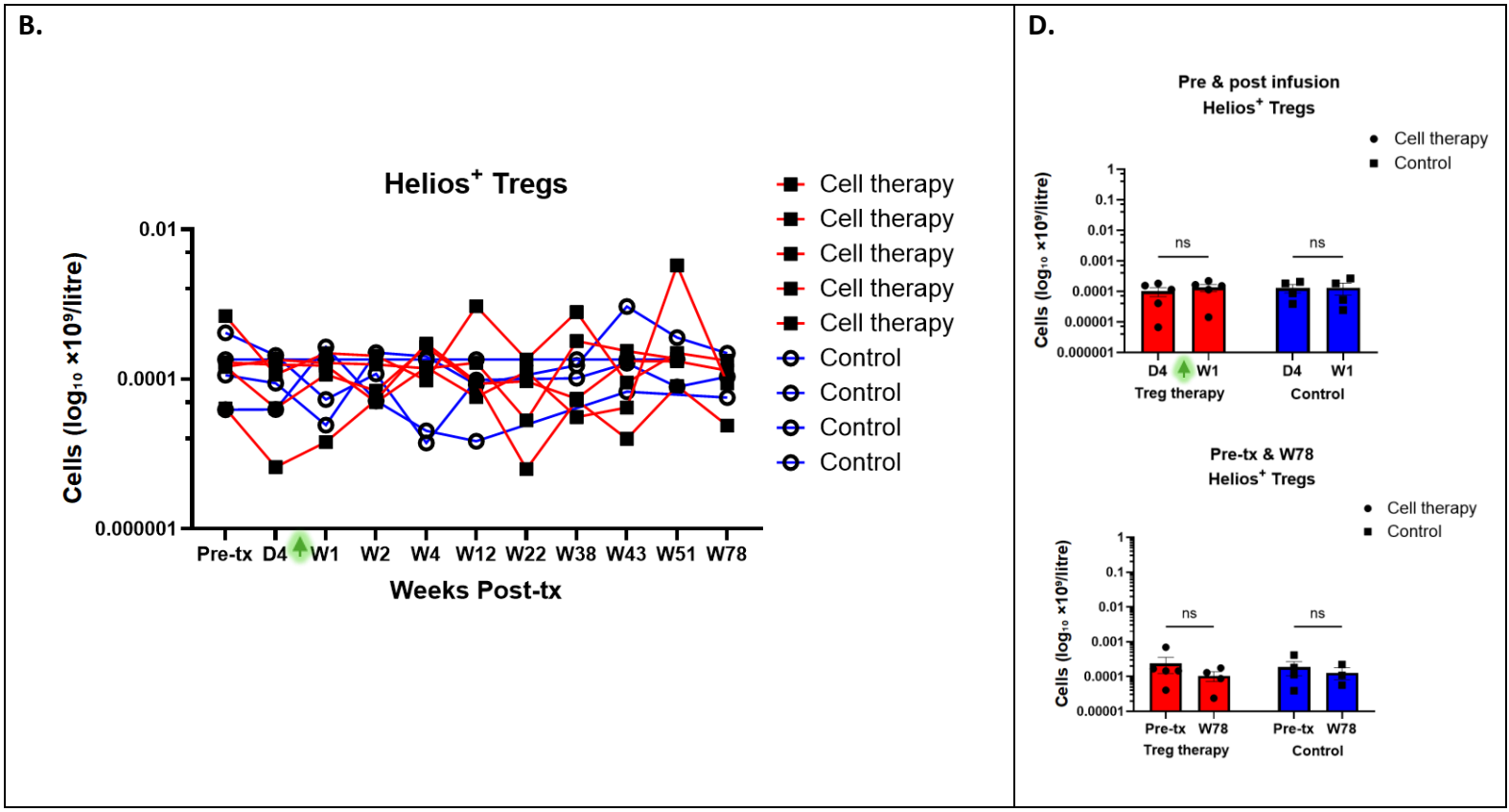


Figure 5.2.4 Longitudinal analysis of peripheral Treg and Helios⁺ Treg dynamics following Treg therapy in kidney transplant recipients.

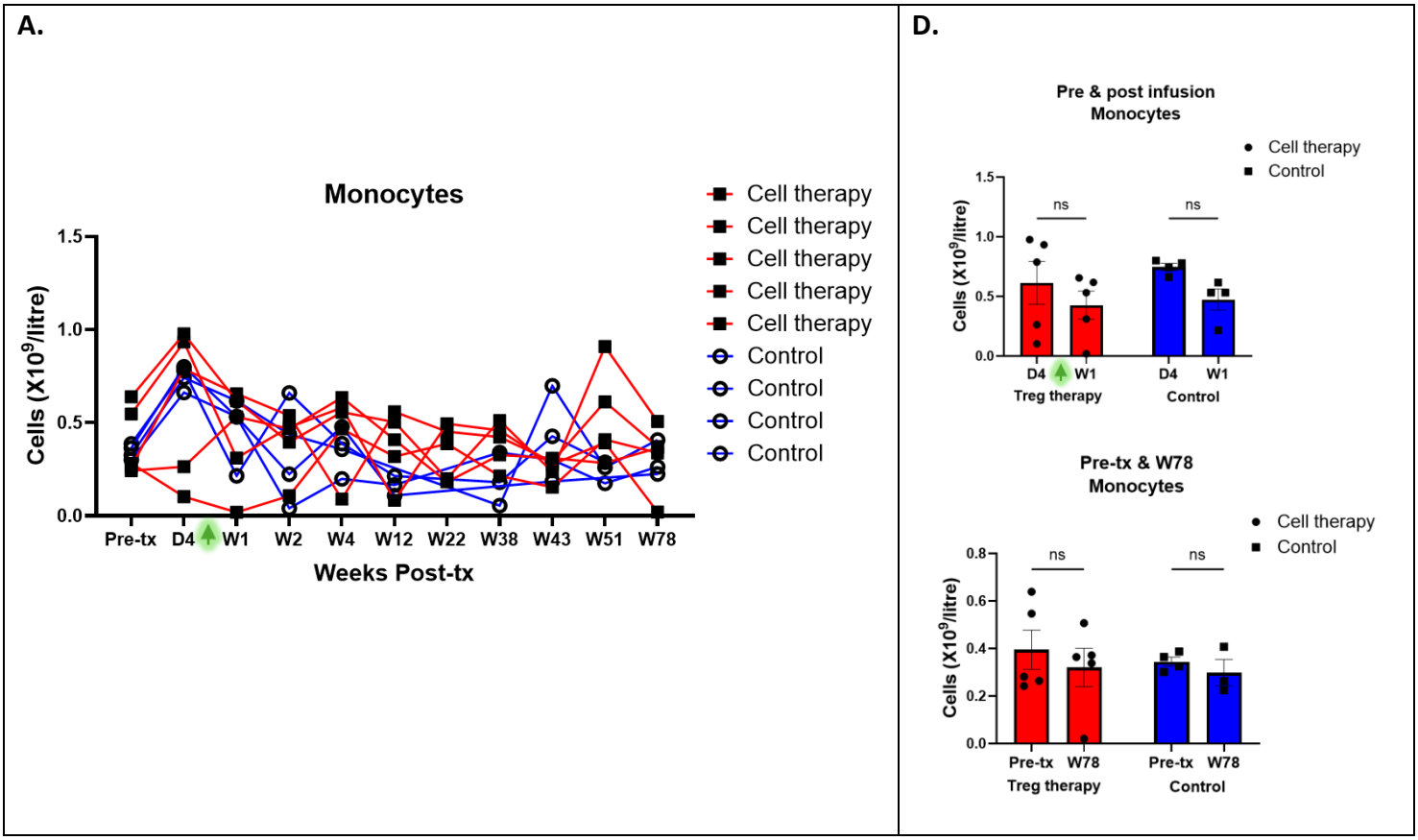
(A) Longitudinal absolute counts of peripheral Tregs in Treg-treated (red, solid squares) and control (blue, open circles) patients from pre-transplant baseline (Pre-tx) through week 78 post-transplantation. Treg infusion was administered on day 5 post-transplant (green arrow). (B) Longitudinal absolute counts of Helios⁺ Tregs across the same timepoints and patient groups. Each line represents an individual patient; cell counts are displayed on a $\log_{10}$ scale (cells ×10⁹/L). (C-D) Summary bar plots comparing Treg and Helios⁺ Treg counts before and after infusion (day 4 vs week 1, top panels) and between baseline and late follow-up (Pre-tx vs week 78, bottom panels). Dots represent individual patients, bars indicate mean ± SEM. Longitudinal data were analysed using a mixed-effects model (REML), with time as a repeated measure and treatment group as a fixed effect; ns denotes not significant. Tx, transplantation; Pre-tx, pre-transplant; D4, day 4 post-transplant.

5.2.2.1.4 Examination of changes in monocytes and monocyte subsets overtime

Given the critical role of monocytes in modulating Treg suppressive function, as demonstrated in the preceding *in vitro* analyses (Chapter 4), longitudinal changes in circulating monocytes and their major subsets were examined following kidney transplantation (Figure 5.2.5). Total monocyte counts showed temporal variability across the post-transplant period in both study groups, with no significant differences detected at the early post-infusion interval (day 4 versus week 1) or between pre-transplant and late follow-up at week 78, and overall comparable levels between Treg-treated and control patients (Figure 5.2.5A, D).

Analysis of monocyte subpopulations revealed similar patterns, with both non-classical $CD14^{+}CD16^{hi}$ and classical $CD14^{+}CD16^{lo}$ monocyte subsets exhibiting inter-individual fluctuations over time but no significant changes at key early or late timepoints and no clear divergence between treatment groups (Figure 5.2.5B, C, E, F). Notably, despite the absence of statistically significant group differences, absolute counts of

CD14^{+}CD16^{hi} monocytes appeared consistently higher in Treg-treated patients compared with controls across multiple timepoints (Figure 5.2.5B, E). This observation may suggest a relative enrichment of non-classical CD14^{+}CD16^{hi} monocytes in Treg-treated patients, indicating a subtle shift in myeloid subset composition without a marked increase in total monocyte numbers.



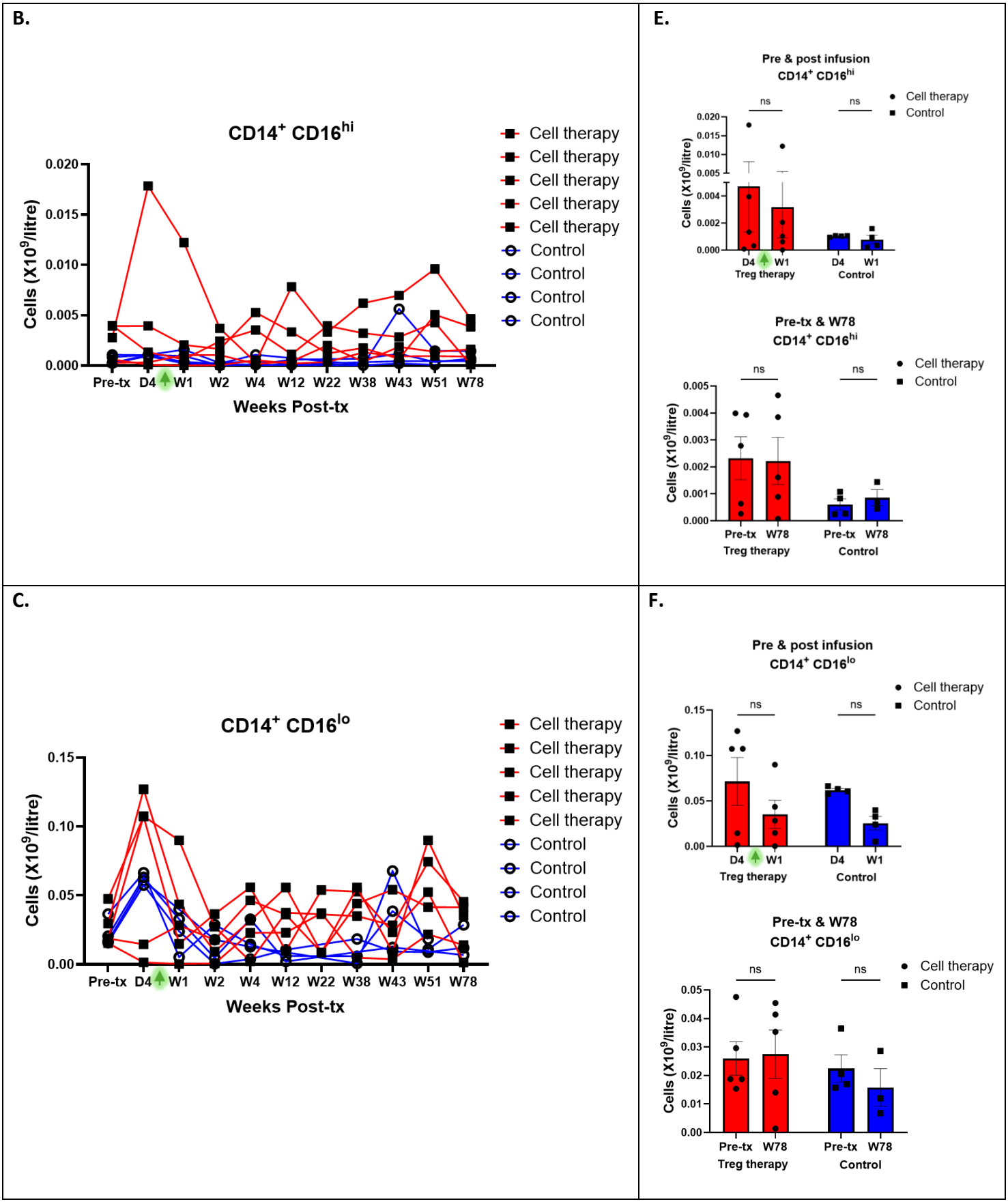


Figure 5.2.5 Longitudinal dynamics of circulating monocytes and their subsets in Treg therapy versus control groups.

(A-C) Line graphs displaying absolute counts of total monocytes (A), CD14^{+}CD16^{hi} non-classical monocytes (B), and CD14^{+}CD16^{lo} classical monocytes (C) over time in peripheral blood. Samples were collected from patients in the Treg therapy group (red, solid squares) and control group (blue, open circles) at baseline (Pretx), day 4 (D4), and multiple post-transplant timepoints up to week 78. Treg infusion was administered on day 5 (green arrow). Each line represents an individual patient. (D-F) Bar plots comparing absolute monocyte counts across defined intervals. Total monocyte counts (D), CD14^{+}CD16^{hi} (E), and CD14^{+}CD16^{lo} (F) subsets are shown for early (D4 vs. week 1, top panels) and late (Pretx vs. week 78, bottom panels) timepoints. Red bars represent Treg therapy group; blue bars represent controls. Dots represent individual patients, bars indicate mean ± SEM. Longitudinal data were analysed using a mixed-effects model (REML), with time as a repeated measure and treatment group as a fixed effect; ns denotes not significant. Tx, transplantation; Pre-tx, pre-transplant; D4, day 4 post-transplant.

Overall, no distinct patterns or changes in the major circulating immune populations were observed. However, given that the immune response to the transplanted tissue is mostly developing in the tissue itself or local lymph nodes, the next step was an assessment of kidney protocol biopsies collected in the TWO Study.

5.2.3 Analysis of graft infiltrating cells in TWO study biopsies using spatial transcriptomics

5.2.3.1 Experimental design

Hypothesising that Tregs confer their regulatory function directly in tissues, I have next utilised the campath cohort of the TWO Study, where I have access to both pre- and post-Treg transplant kidney biopsies. To define the spatial landscape of immune and parenchymal cells within the graft, I performed high-resolution spatial transcriptomic profiling on three protocol kidney biopsies representing three distinct clinical groups/timepoints (Control: control group biopsy week 38; Pre-Treg: week 22 pre-Treg infusion biopsy; and Post-Treg: week 38 post-Treg infusion), using the 10x Genomics Xenium platform (Figure 5.2.6). Given the limited number of protocol biopsies available for spatial analysis, differences observed between the Control and Post-Treg samples may reflect individual patient variability. Therefore, all spatial transcriptomic findings presented below should be considered exploratory and hypothesis-generating rather than definitive conclusions regarding the effects of Treg therapy. Relevant clinical and histopathological characteristics of these patients are provided in Appendix Tables A5.1 and A5.2. At the time of biopsy, renal function was stable and there was no evidence of active infection or rejection; however, differences in graft histopathology were present, including greater tubulointerstitial fibrosis and mild focal tubulitis in the control biopsy, which may also have influenced the observed spatial differences. Tissue processing, hybridisation, imaging, and transcript decoding were carried out according to the manufacturer's protocol. Following quality control, transcriptomic data were integrated using canonical correlation analysis, and cell types were annotated using Azimuth reference mapping (see Chapter 2, Section 2.8.4 for full methodology). Downstream spatial analyses were conducted using Seurat, Scanpy, and Squidpy to characterise cell populations, transcript distributions, and tissue architecture.

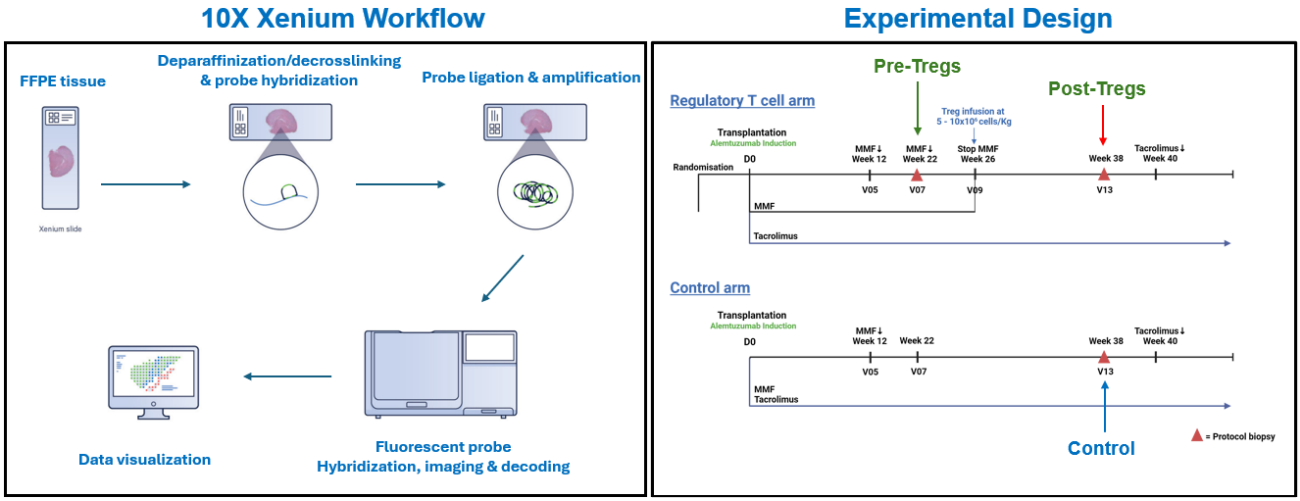


Figure 5.2.6 Workflow overview of 10x Xenium in situ spatial transcriptomics applied to kidney transplant biopsies from the TWO study.

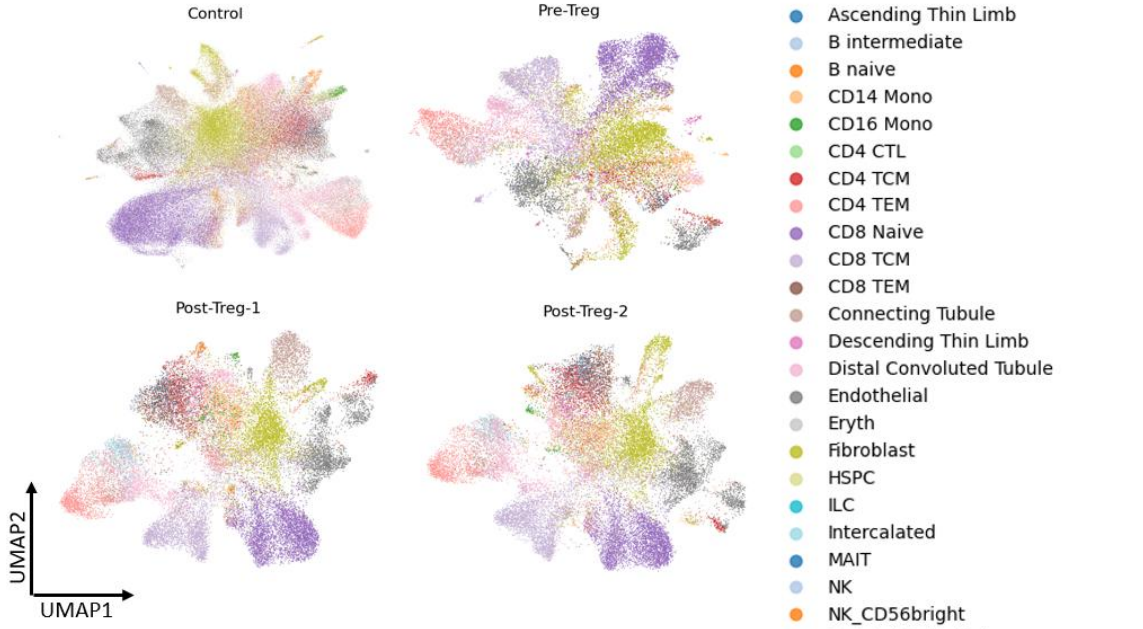
The 10x Xenium platform enables single cell in situ spatial transcriptomic profiling at cellular resolution. Biopsies were collected from TWO study participants, including one control biopsy from the standard therapy group and one biopsy from the Treg therapy group: one pre-Treg infusion and one post-Treg infusion (6 months post-transplantation). Formalin-fixed paraffin-embedded (FFPE) tissue sections were prepared on Xenium slides (12 × 24 mm imageable area), followed by deparaffinisation and decrosslinking to expose RNA targets. Circularisable DNA probes were hybridised and ligated, generating circular DNA templates for enzymatic amplification. The Xenium Analyzer then performed iterative rounds of fluorescent probe hybridisation, imaging, and probe removal, producing high signal-to-noise optical signatures for gene identification. This process generates a spatial transcriptomic map of target gene expression across the entire tissue section in a subcellular resolution.

5.2.3.2 Integration of spatial transcriptomics to define cellular composition in kidney allografts

Integrated analysis of spatial transcriptomic data revealed a complex cellular architecture within the graft, comprising both structural and immune compartments. Azimuth-based annotation identified major parenchymal subsets, including proximal and distal tubular cells, endothelial cells, and fibroblasts, as well as a diverse range of immune cell types, such as T cells, monocytes, and B cells. These populations were consistently detected across all sections, with variation in abundance and localisation depending on the clinical condition.

UMAP dimensionality reduction revealed sample-specific clustering patterns (Figure 5.2.7A), and a total of 165,936 cells were recovered across the four conditions, with the majority from the control biopsy (Figure 5.2.7B). Annotated UMAP plots for individual samples are shown in Figure 5.2.7A, illustrating distribution and diversity of cell types across biopsy conditions. In total, 37 distinct cell clusters were identified, including key immune subsets (e.g., $CD14^+$ monocytes, $CD4^+$ T cells, NK cells, B cell subsets, and Tregs), as well as kidney-resident parenchymal cell types such as proximal tubule, endothelial cells, and podocytes.

A.



B.

Sample Name	Total Number of Cells
Control	90,389
Pre-Treg	22,391
Post-Treg-1	25,791
Post-Treg-2	27,365

Figure 5.2.7 Spatial transcriptomic profiling and cell type annotation of kidney transplant biopsies using 10x Xenium platform.

(A) Annotated UMAP plots: Control (standard therapy), Pre-Treg (biopsy collected before Treg infusion), and Post-Treg-1-2 (sections of 1 biopsy collected 6 months post-Treg infusion), displaying major kidney and immune cell populations identified using hierarchical label transfer from Azimuth reference datasets (Hao et al., Cell 2021). Spatial transcriptomics data were processed as Seurat objects and annotated via Azimuth, followed by advanced spatial analysis and visualisation using Scanpy workflows. (B) Summary table showing the total number of cells profiled per sample.

5.2.3.3 Immune profiling and transcriptional signatures in kidney transplant biopsies

To further explore the immune landscape of the kidney allograft, I performed detailed immune profiling across three biopsies, with two technical replicates analysed per biopsy. Immune cell subsets were extracted and re-clustered based on Azimuth reference mapping, enabling the annotation of major lymphoid and myeloid populations. Immune focused UMAP visualisation revealed the distribution of immune cells within individual samples (Figure 5.2.8A). This analysis highlighted a range of adaptive and innate immune populations, including $CD4^+$ and $CD8^+$ T cell subsets (naïve, central memory, effector memory), NK cells, monocytes ($CD14^+$ and $CD16^+$), plasmablasts, innate lymphoid cells (ILCs), dendritic cells, and Tregs.

Relative immune cell proportions across conditions are shown in the stacked bar plot (Figure 5.2.8B). Interestingly, Post-Treg samples exhibited a notable reduction in CD4⁺ central memory T cells (TCM) compared to both a Pre-Treg sample at an earlier time-point and a Control sample obtained at the same time post transplantation. Moreover, the Post-Treg sample showed a relatively higher proportion of monocytes, including both CD14⁺ and CD16⁺ populations, compared with the control sample (Figure 5.2.8B). Additionally, I assessed the expression of transcriptional features by generating a dot plot to visualise selected signature genes across annotated immune cell types (Figure 5.2.8C). This visualisation provides an overview of subset-specific gene expression patterns, helping to confirm cell type annotations and highlight distinguishing molecular features of individual populations. For example, FCGR3A (encoding CD16) was predominantly expressed in CD16⁺ monocytes, while CD8A showed enriched expression across CD8⁺ T cell subsets. Dot size indicates the proportion of cells within each population expressing the gene, whereas colour intensity reflects the mean normalised expression level.

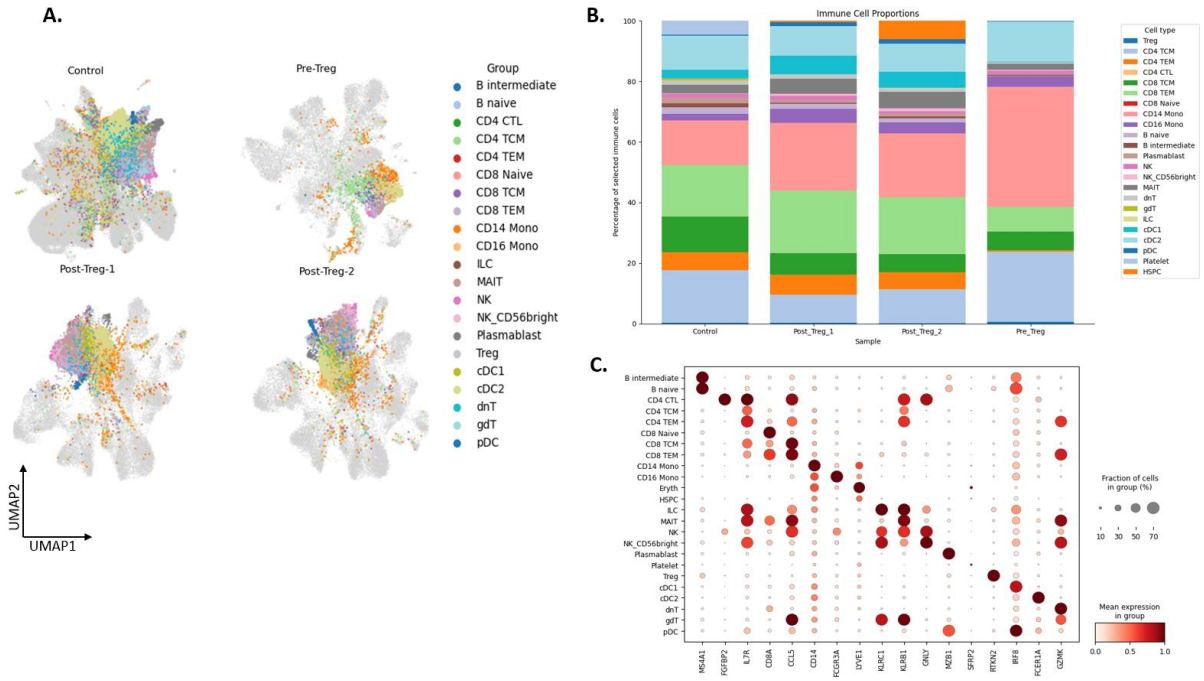


Figure 5.2.8 Characterisation of immune cell populations in kidney transplant biopsies using spatial transcriptomics.

(A) UMAP visualisation of immune cells for individual samples, annotated into major immune subsets using Azimuth reference mapping. The background shows the entire cellular landscape, with immune populations highlighted in colour. (B) Stacked bar plot showing the relative proportions of annotated immune cell types in each biopsy sample (Control, Pre-Treg, and Post-Treg-1-2). (C) Dot plot depicting the expression of key signature genes across immune cell populations. Dot size represents the fraction of cells expressing each gene within the population, and colour intensity indicates the mean normalised expression level. Data processing was performed using Seurat and Azimuth for cell type annotation, and visualisation was carried out using Scanpy.

5.2.3.4 Chemokine expression changes following Treg therapy

Chemokines play an important role in Tregs homing, as discussed in Chapter 3. I profiled a defined panel of chemokine genes available in the spatial transcriptomic assay, including CCL2, CCL5, CCL19, CCL27, CXCL2, CXCL6, CXCL9, CXCL10, and the ligand-receptor pair CCR7 and CCL19. I first visualised the expression of these chemokines across immune cell subsets in all samples, Control, Pre-Treg, Post-Treg-1, and Post-Treg-2, as shown in Figure 5.2.9A, and subsequently performed a comparative analysis between Post-Treg and Control samples (Figure 5.2.9B). This analysis revealed transcriptional differences across multiple immune compartments. $CD14^+$ monocytes demonstrated increased expression of both CCR7 and CCL19 (Figure 5.2.9B). Among T cell subsets, $CD8^+$ TCM showed upregulation of CCR7 and CXCL6, and downregulation of CXCL2, while $CD8^+$ effector memory T cells (TEM) displayed increased expression of CCL19, CCL27, and CXCL6, alongside reduced CXCL2. CD4 TCM cells exhibited decreased CCL19 expression, with elevated levels of CXCL6 and CXCL10. In the dendritic cell compartment, conventional dendritic cells type 1 (cDC1) showed upregulation of CCR7, whereas conventional dendritic cells type 2 (cDC2) demonstrated increased CXCL6 expression without notable changes in CCR7. Within the B cell lineage, B intermediate cells upregulated CCL27 and CXCL9, while B naive cells displayed limited changes across the chemokine panel (Figure 5.2.9B). These transcriptional changes suggest a coordinated chemokine landscape favouring CCR7-CCL19-mediated immune cell positioning and retention within the graft, with prominent contributions from monocytes and selected T-cell and B-cell subsets, potentially supporting structured immune cell organisation in post-Treg therapy environment.

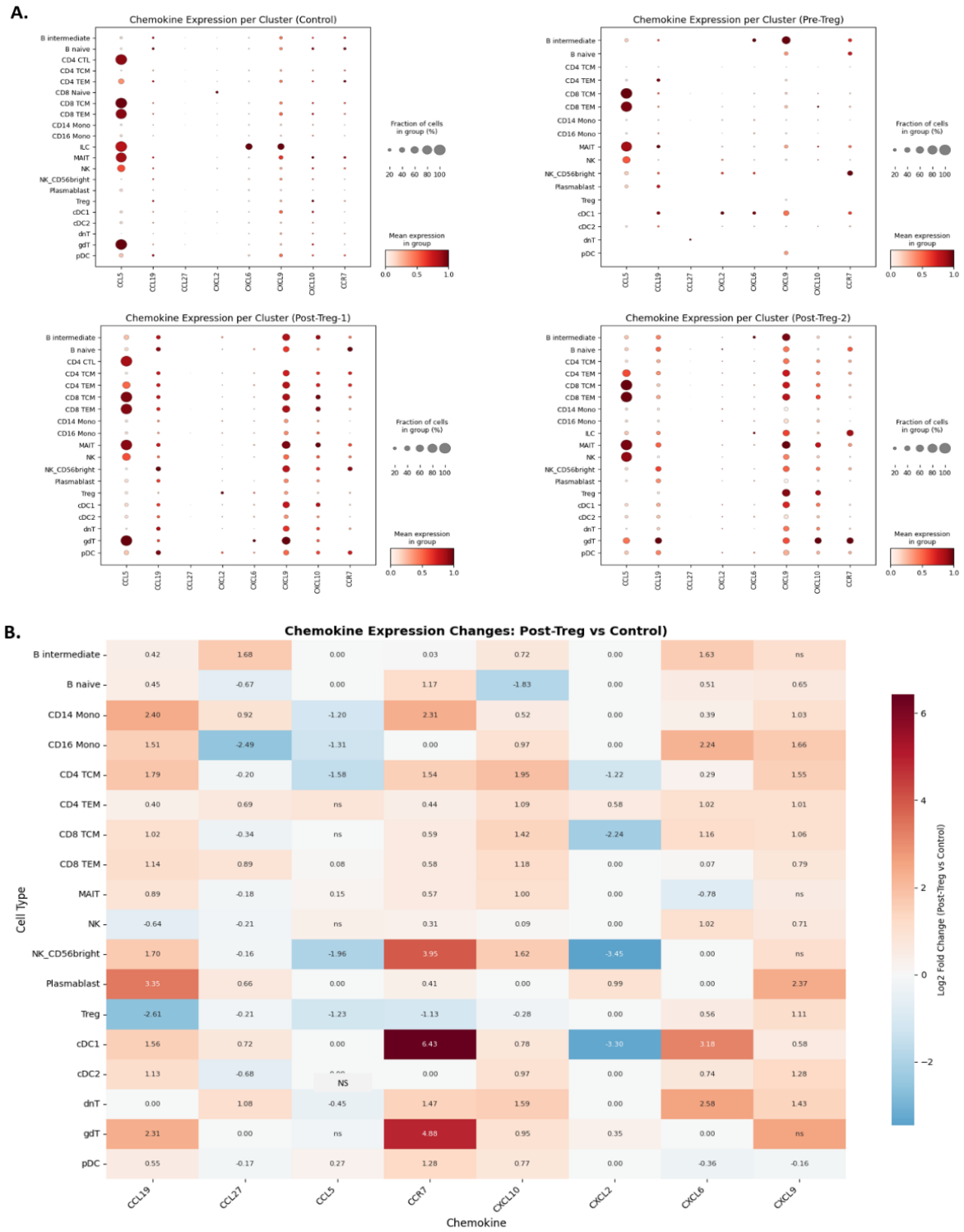


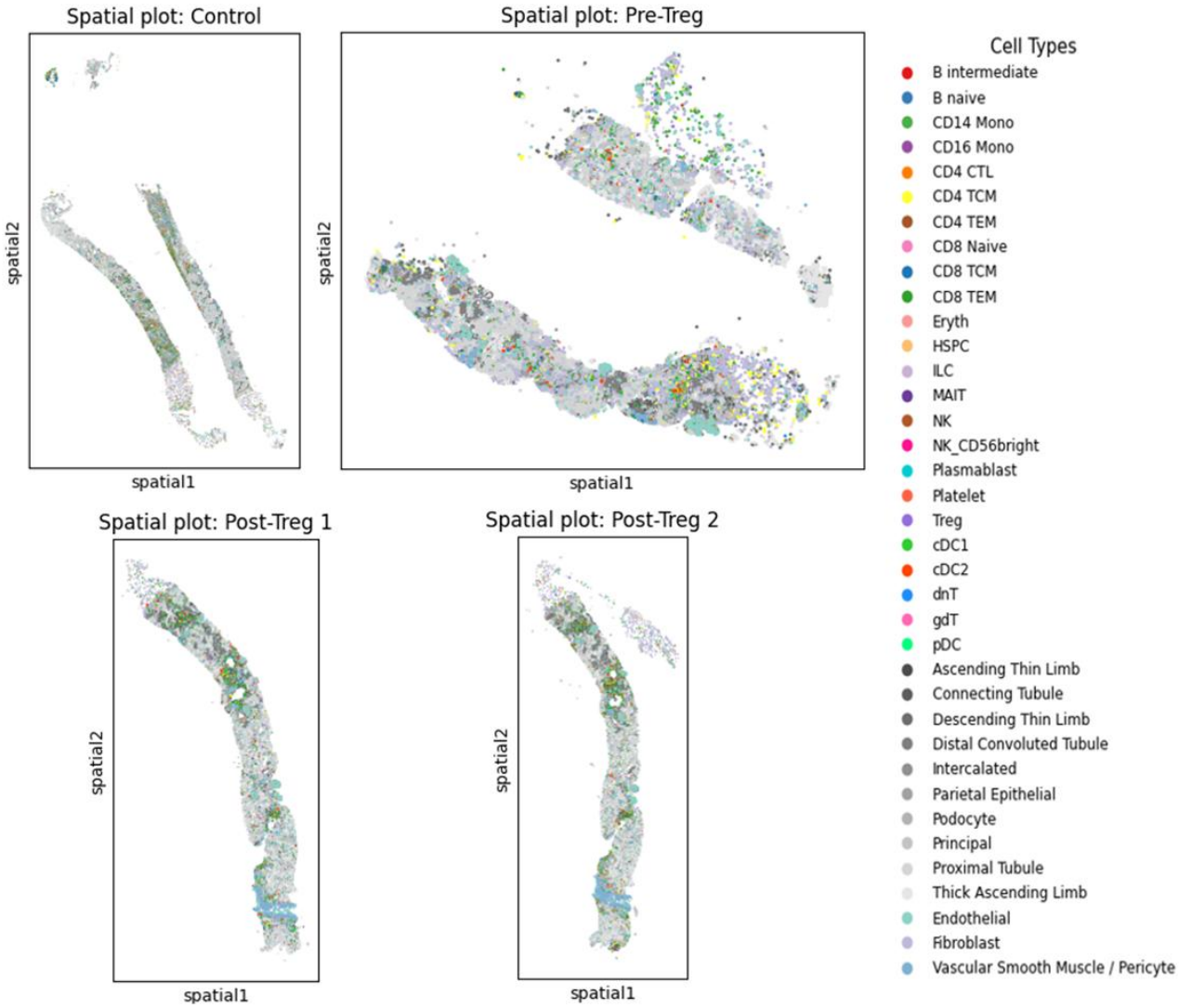
Figure 5.2.9 Differential chemokine expression patterns across experimental conditions and immune cell types.

(A) Dot plots of chemokine expression within annotated immune cell clusters for each biopsy individually conditions (Control, Pre-Treg, and *Post-Treg-1-2), illustrating cluster-specific chemokine expression patterns.(B) Heatmap showing log2 fold changes in chemokine expression in Post-Treg biopsy compared to Control biopsy. Significant changes are colour-coded, while non-significant differences are shown as ns. Data were processed using Seurat for cell type annotation and Scanpy for visualisation and statistical analysis.*

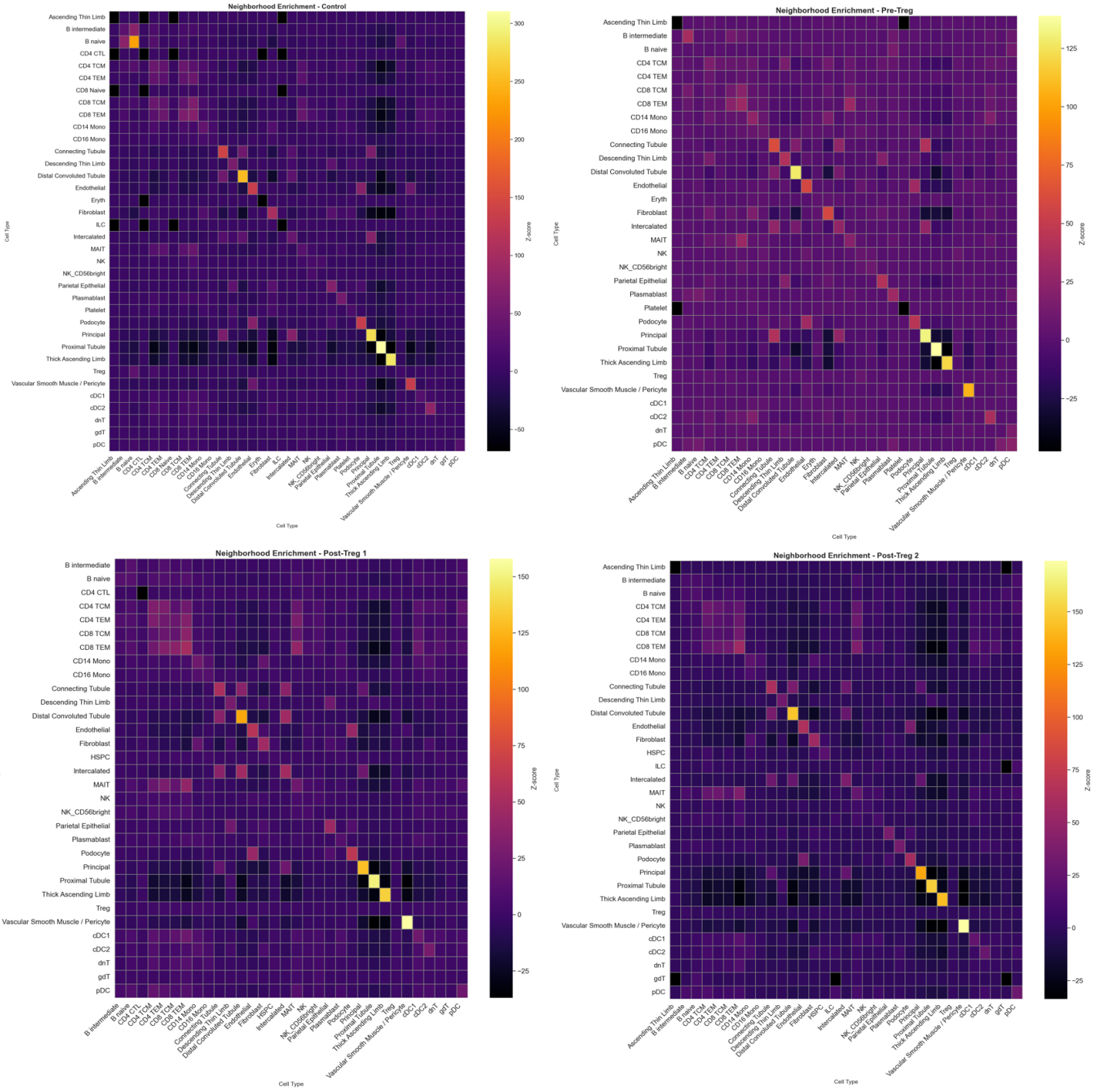
5.2.3.5 Spatial organisation and immune cell neighbourhood remodelling

To investigate tissue-level immune architecture following Treg therapy, I performed spatial mapping and neighbourhood enrichment analyses (Figure 5.2.10). As shown in Figure 5.2.10A, spatial plots of annotated cell types across individual biopsy samples (Control, Pre-Treg, and Post-Treg-1-2) revealed distinct distribution patterns, with cellular identities assigned via Azimuth mapping and spatial coordinates. Figure 5.2.10B illustrates neighbourhood enrichment matrices across the four samples, capturing the frequency of spatial co-localisation between immune and parenchymal cell types. These heatmaps highlight the core structural interactions of the kidney microenvironment and allow comparison of spatial proximity dynamics. In Figure 5.2.10C, differential neighbourhood enrichment (Post-Treg vs Control) identified significant spatial remodelling of immune cell interactions, with Delta Z-scores (ΔZ-scores) representing shifts in spatial proximity. ΔZ-scores exceeding ±1.5 were considered significant. $CD14^+$ and $CD16^+$ monocytes demonstrated reduced co-localisation with effector T cell subsets (CD4 TCM and CD8 TEM), and plasmacytoid DCs (pDCs), while exhibiting increased proximity to B naive, B intermediate, and cDC2 populations. B naive cells showed a loss of self-association (ΔZ-score = -102.5) and diminished interactions with Tregs (ΔZ = -15.1) but gained spatial association with $CD14^+$ monocytes (Figure 5.2.10C).

A.


Spatial plot: Control
Spatial plot: Pre-Treg
Spatial plot: Post-Treg 1
Spatial plot: Post-Treg 2
spatial1
spatial2
Cell Types
B intermediate
B naive
CD14 Mono
CD16 Mono
CD4 CTL
CD4 TCM
CD4 TEM
CD8 Naive
CD8 TCM
CD8 TEM
Eryth
HSPC
ILC
MAIT
NK
NK_CD56bright
Plasmablast
Platelet
Treg
cDC1
cDC2
dnT
gdT
pDC
Ascending Thin Limb
Connecting Tubule
Descending Thin Limb
Distal Convoluted Tubule
Intercalated
Parietal Epithelial
Podocyte
Principal
Proximal Tubule
Thick Ascending Limb
Endothelial
Fibroblast
Vascular Smooth Muscle / Pericyte

B.


Neighborhood Enrichment - Control
Neighborhood Enrichment - Pre-Treg
Neighborhood Enrichment - Post-Treg 1
Neighborhood Enrichment - Post-Treg 2
Cell Type
Z-score

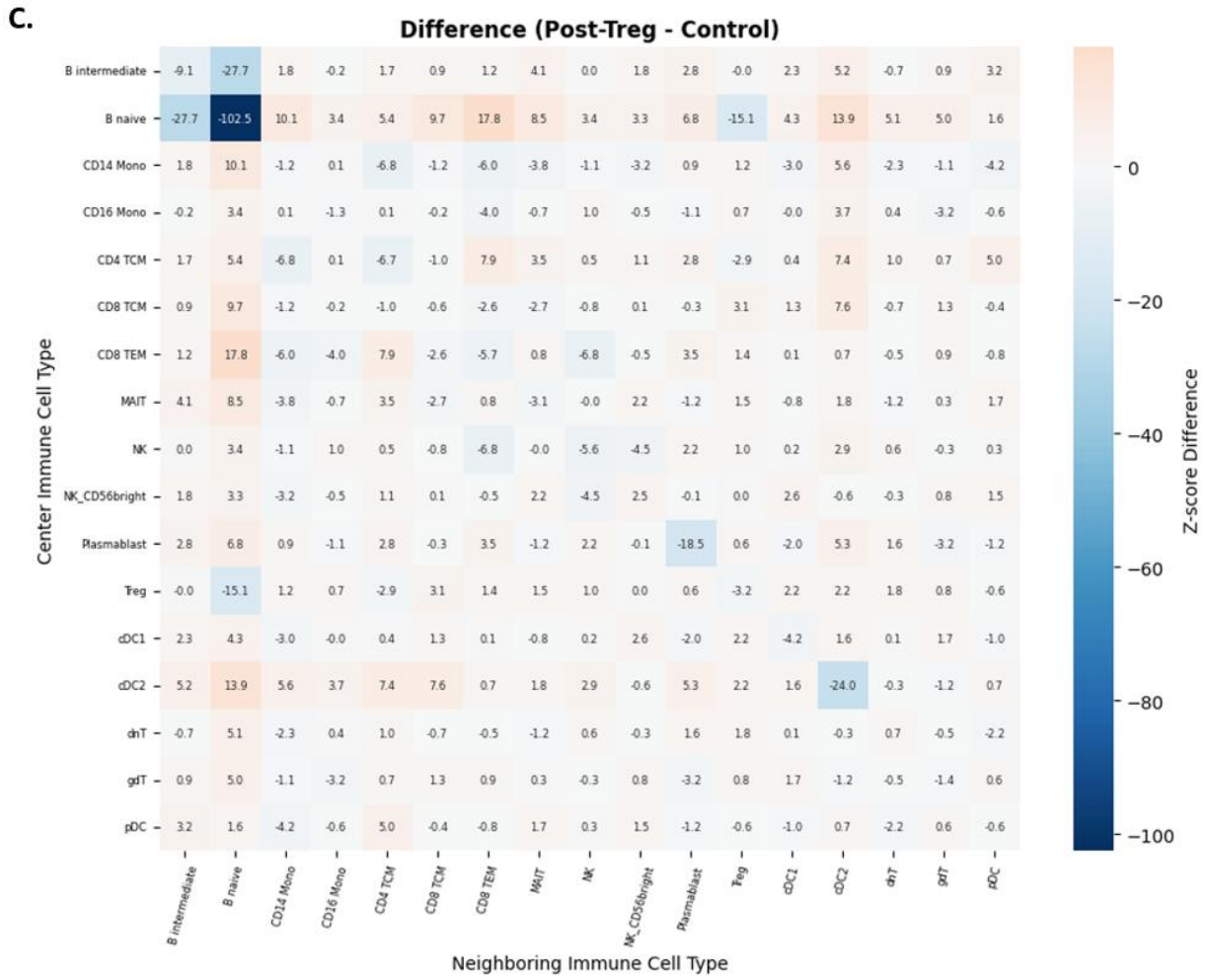
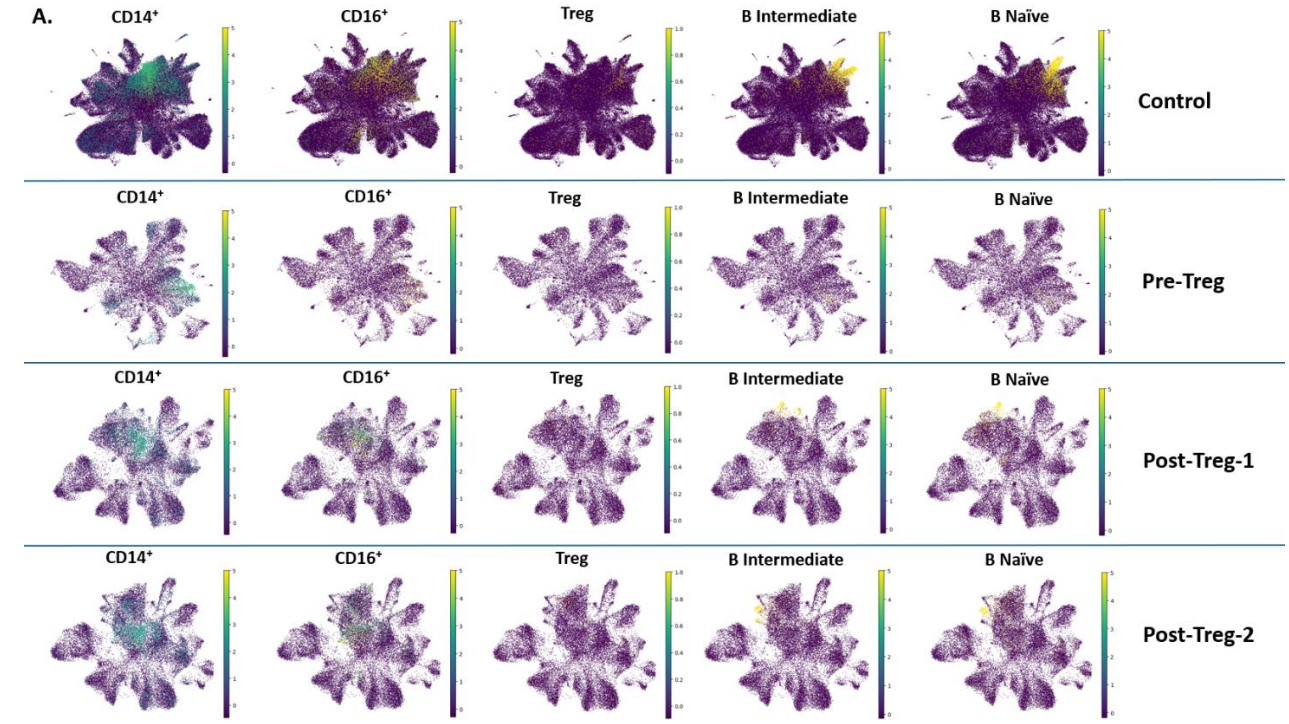


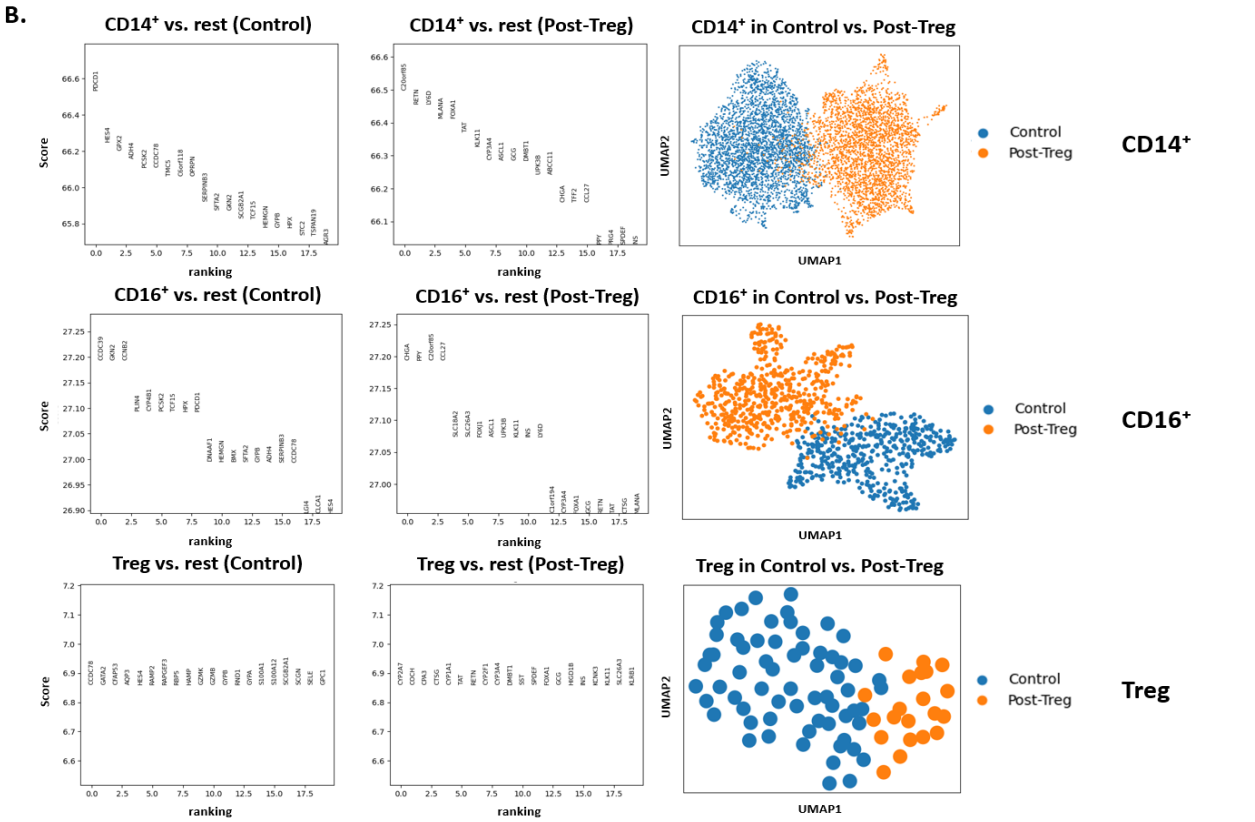
Figure 5.2.10 Spatial plots and neighbourhood enrichment analyses reveal tissue architecture and immune cell interactions in the kidney microenvironment.

(A) Spatial plots of all annotated cell types across individual biopsy samples (Control, Pre-Treg, and *Post-Treg-1-2), visualised using Squidpy. Cell identities were assigned based on Azimuth annotation and spatial coordinates derived from Xenium output. (B) Neighbourhood enrichment heatmaps display the frequency of spatial co-localisation between different cell types in each biopsy, revealing tissue-specific and condition-specific spatial architecture. (C) Heatmap displaying the differential neighbourhood enrichment of immune cell interactions, illustrating changes in spatial proximity between Post-Treg and Control samples (ΔZ-score). Positive ΔZ-scores (light red) indicate increased spatial co-localisation following Treg therapy, whereas negative values (blue) reflect reduced interactions. A threshold of |ΔZ-score| > 1.5 was considered significant.*

5.2.3.6 Differential gene expression and cluster transcriptomic shifts

To characterise cell type-specific transcriptional and compositional changes following Treg therapy, I examined the expression and distribution of key immune subsets across experimental conditions (Figure 5.2.11A). UMAPs in Figure 5.2.11A revealed changes in the abundance of $CD14^+$ monocytes, $CD16^+$ monocytes, Tregs, B intermediate, and B naïve cells across Control, Pre-Treg, and Post-Treg-1-2 samples. Notable redistribution patterns were observed, particularly in $CD14^+$ and $CD16^+$ monocytes, which appeared to maintain a relatively consistent expression profile. This observation aligns with findings presented earlier in Figure 5.2.8B, comparing Post-Treg and Control conditions.


A.
CD14⁺
CD16⁺
Treg
B Intermediate
B Naïve
Control
Pre-Treg
Post-Treg-1
Post-Treg-2


B.
CD14⁺ vs. rest (Control)
CD14⁺ vs. rest (Post-Treg)
CD14⁺ in Control vs. Post-Treg
CD16⁺ vs. rest (Control)
CD16⁺ vs. rest (Post-Treg)
CD16⁺ in Control vs. Post-Treg
Treg vs. rest (Control)
Treg vs. rest (Post-Treg)
Treg in Control vs. Post-Treg
Score
ranking
UMAP1
UMAP2
Control
Post-Treg
CD14⁺
CD16⁺
Treg

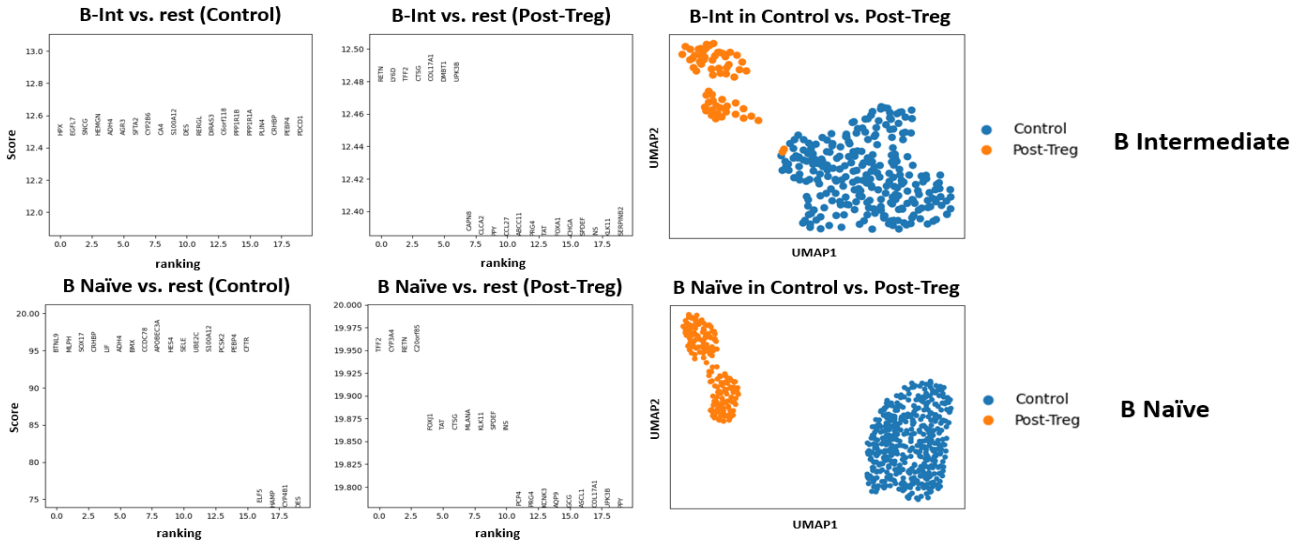


Figure 5.2.11 Transcriptional reprogramming of CD14⁺ monocytes, CD16⁺ monocytes, regulatory T cells (Tregs), and B cells following clinical-grade Treg therapy.

(A) UMAP visualisations showing the expression and distribution of selected immune cell subsets: CD14⁺ monocytes, CD16⁺ monocytes, Tregs, B intermediate, and B naïve cells, across individual biopsy samples (Control, Pre-Treg, and Post-Treg-1-2). Each panel displays log-normalised expression values per cluster, highlighting changes in abundance and localisation across conditions. (B) Differentially expressed genes (DEGs) of each cell type: CD14⁺ monocytes, CD16⁺ monocytes, Tregs, B intermediate, and B naïve cells, the left and middle plots display the top DEGs in Control and Post-Treg samples compared to the rest of the dataset. The accompanying UMAP plots show clear transcriptional separation between Control (blue) and Post-Treg (orange) groups.

Differential gene expression analyses further highlighted condition-specific transcriptional programmes for each immune subset (Figure 5.2.11B). In CD14⁺ monocytes, Post-Treg samples exhibited upregulation of inflammatory genes such as RETN and CCL27, alongside diminished expression of PDCD1 (encoding PD-1), a regulatory marker enriched in the Control group. CD16⁺ monocytes showed increased expression of CHGA, PYY, and CCL27 following Treg therapy, with concurrent downregulation of CCDC93 and GKN2, which were preferentially expressed in the Control condition. For Tregs, cells from Post-Treg biopsy upregulated genes involved in immune signalling and metabolism (e.g., RETN and members of the CYP2 family), whereas Control-derived Tregs retained higher expression of canonical regulatory and homeostatic genes including GZMK and RAPGEF3. Within the B cell compartment, B intermediate cells in Post-Treg samples displayed increased expression of RETN, DMBT1, and CCL27, coupled with reduced expression of regulatory genes such as PD-1 and HPX. Similarly, B naïve cells showed transcriptional activation of RETN, CYP3A4, and CTSG in the Post-Treg group, while expression of markers like BTNL9, SOX17, and APOBEC3A was decreased relative to Controls. The accompanying UMAP plots revealed distinct transcriptional segregation between Control (blue) and Post-Treg (orange) cells across all subsets, further supporting the presence of therapy-associated transcriptional reprogramming (Figure 5.2.11B).

5.3 Discussion

This chapter evaluated the immunological impact of adoptive Treg therapy in the context of the TWO Study, a phase IIb clinical trial investigating the potential of autologous, *ex vivo*-expanded Tregs to enable immunosuppression minimisation following kidney transplantation[25, 83]. Building on previous findings that demonstrated the safety and feasibility of both delayed and early Treg infusion[83, 87], this chapter explores how Treg therapy shapes systemic immune profiles and modulates the graft microenvironment. It considers the interplay between Tregs and monocytes, a myeloid population increasingly recognised for its role in supporting regulatory immune circuits[118, 130]. The results are interpreted considering current understanding of Treg biology and provide mechanistic insights into how cell therapy may contribute to peripheral and local immune regulation in transplant recipients.

To understand the systemic immunological impact of autologous Treg therapy in kidney transplantation, longitudinal immune profiling was performed using flow cytometry on peripheral blood samples from patients enrolled in the revised protocol of the TWO Study. Five patients receiving Treg infusion and four control patients treated with standard basiliximab-based immunosuppression were monitored across defined timepoints up to 78 weeks post-transplantation. Longitudinal immunomonitoring demonstrated dynamic but largely conserved patterns of circulating immune cell counts following kidney transplantation (Figure 5.2.2-5.2.5). Total leukocyte counts showed an early post-transplant increase in the Treg therapy group between day 4 and week 1, with no sustained differences between groups at later timepoints, may indicate preserved white blood cell homeostasis following Treg infusion (Figure 5.2.2A, C). In contrast, lymphocyte counts remained broadly stable over time, with no significant differences detected at early or late follow-up and comparable trajectories between Treg-treated and control patients (Figure 5.2.2B, D). Similarly, circulating $CD4^+$ and $CD8^+$ T cell counts did not differ significantly between groups across the monitoring period (Figure 5.2.3B, D). This may reflect that Treg therapy does not induce sustained alterations in conventional T cell compartments or global leukocyte numbers during long-term immunomonitoring[25, 83].

Infusion of *ex vivo*-expanded polyclonal Tregs was not associated with marked changes in circulating Treg numbers over time, with levels remaining broadly stable across immunomonitoring timepoints (Figure 5.2.4A, C). No consistent increases in peripheral Treg counts were observed following infusion, and values remained comparable to pre-transplant levels throughout follow-up (Figure 5.2.4A, C). This pattern is compatible with physiological homeostatic regulation of the Treg compartment and may also reflect

redistribution of infused cells to peripheral tissues rather than prolonged persistence in the circulation[107], an interpretation supported by recent trial data showing transient peripheral peaks of infused polyclonal Tregs together with evidence of their trafficking into kidney allograft biopsies after infusion[132]. Similar kinetics have been reported previously in the alemtuzumab-conditioned cohort of the TWO Study[83], as well as in other clinical studies of adoptive Treg transfer, including a pilot trial of regulatory T cell-based therapy in living donor liver transplantation, in which infused Tregs did not result in sustained peripheral expansion and were well tolerated[83, 107, 130]. Importantly, Treg infusion was well tolerated, with no evidence of lymphoproliferation or systemic immune dysregulation observed during long-term follow-up.

Analysis of the monocyte compartment revealed temporal variability following transplantation, with broadly comparable total monocyte counts between Treg-treated and control patients over the course of follow-up (Figure 5.2.5A, D). While no statistically significant group differences were detected at key early or late timepoints, total monocyte numbers showed transient fluctuations in both groups before returning towards baseline levels by late follow-up. Examination of monocyte subsets demonstrated that classical $CD14^{+}CD16^{lo}$ monocytes remained relatively stable across time in both treatment arms (Figure 5.2.5C, F). In contrast, non-classical $CD14^{+}CD16^{hi}$ monocytes appeared consistently higher in Treg-treated patients compared with controls across several post-transplant timepoints, despite the absence of statistically significant inter-group differences (Figure 5.2.5B, E). Although exploratory, this pattern may indicate subtle differences in myeloid subset composition following Treg therapy rather than obvious quantitative expansion. This is consistent with preclinical evidence demonstrating that Tregs can promote alternative activation of monocytes and macrophages, favouring $CD163^{+}$ M2-like phenotypes in non-human primates[129] and IL-10-producing macrophages in murine models[117]. These observations could suggest that Treg therapy may engage peripheral myeloid populations to reinforce immune regulation.

Local graft immune landscapes revealed by spatial transcriptomics showed sample-specific clustering, indicating transcriptomic and compositional differences between control and Treg-treated samples. Even though the Control sample had a larger number of cells compared to Post-Treg sample (Figure 5.2.7B), notably, post-Treg therapy biopsy was enriched for monocyte-lineage cells (Figure 5.2.8B). Chemokine expression analysis further illustrated therapy-induced changes. Monocytes in Treg-treated biopsy exhibited expression of CCR7 and its ligand CCL19, molecules associated with lymphoid tissue organisation (Figure 5.2.9B). Similar upregulation of CCR7 was seen in cDC1 dendritic cells, while $CD8^{+}$ TCM displayed increased CCR7 and CXCL6, and reduced CXCL2 (Figure 5.2.9B). $CD8^{+}$ TEM showed elevated CCL19, CCL27, and CXCL6 (Figure 5.2.9B). These transcriptional patterns point towards a tissue environment supporting controlled

immune cell trafficking and lymphoid neogenesis, features typically associated with regulatory rather than inflammatory microenvironments[117, 130].

Spatial neighbourhood analysis underscored the architectural remodelling induced by Treg therapy. In treated samples, $CD14^+$ and $CD16^+$ monocytes displayed reduced proximity to effector T cells (CD4 TCM and CD8 TEM) but increased spatial association with B cells and cDC2 populations (Figure 5.2.10C). Notably, B naïve cells, which typically clustered with themselves or with Tregs in control biopsy, became spatially linked to monocytes in the Treg group (Figure 5.2.10C). The marked change in B-cell spatial interactions may indicate reorganisation of the local immune microenvironment following Treg therapy. This is consistent with previous human kidney transplant studies reporting prominent B-cell signatures within Treg therapy-associated immune infiltrates[130]; however, the functional significance of the increased B cell-monocyte proximity observed here remains unclear and requires further investigation. In contrast, control biopsy exhibited fewer monocytes and lacked B cell and regulatory cell enrichment (Figure 5.2.10C). This aligns with previous spatial and histological studies that describe non-rejection-like immune infiltrates in Treg-treated grafts, characterised by prominent B cells and $IL\text{-}10^+$ regulatory markers[130]. These findings could suggest the emergence of novel immune aggregates within the graft; potentially resembling tertiary lymphoid structures oriented towards regulation rather than inflammation. This concept is supported by spatial transcriptomic data from human kidney transplants undergoing rejection, where immune cell clusters, particularly T and B cells, are found to colocalise with distinct nephron segments in defined spatial patterns[133]. Unlike the regulatory profiles seen in our Treg-treated samples, those rejection-associated infiltrates show a stronger alignment with effector immune activation[133]. Similar tissue-specific regulatory niches have also been described in other organs; for instance, intestinal Tregs require proximity to $CX3CR1^+$ macrophages in the lamina propria to exert full suppressive activity[134]. Analogously, my findings suggest that monocyte-Treg-B cell microniches may form within the kidney following Treg infusion, supporting a local immune regulatory milieu.

Differential gene expression analysis of individual immune cell types further supported a therapy-induced reprogramming. $CD14^+$ monocytes in Treg-treated grafts upregulated RETN and CCL27, alongside reduced expression of PD-1, indicating a shift in transcriptional profile compared with controls (Figure 5.2.11B). $CD16^+$ monocytes showed increased expression of CHGA, PYY, and CCL27 following Treg therapy, with concurrent downregulation of genes such as CCDC93 and GKN2 that were enriched in control samples (Figure 5.2.11B). Tregs in treated grafts upregulated genes associated with immune signalling and metabolic activity (e.g., RETN and members of the CYP2 family), whereas control-derived Tregs retained higher expression of

canonical regulatory and homeostatic markers including GZMK and RAPGEF3 (Figure 5.2.11B). Together, these findings indicate transcriptional reprogramming of both myeloid and regulatory T cell compartments within the graft, potentially reflecting local microenvironmental influences. These changes may reflect an adaptive tissue-resident effector Treg state, consistent with prior reports of metabolic reprogramming in Tregs exposed to inflammatory environments[133, 134]. Although classical pro-inflammatory cytokines such as IL-17 or IFNγ were not detected in Tregs in my dataset, likely due to panel limitations, previous studies have shown that Tregs can transiently express such cytokines without loss of suppressive function, particularly in response to monocyte-derived signals such as IL-1β or IL-6[118]. This may support a bidirectional interaction within the graft, whereby monocytes influence Treg phenotypes, and in turn, Tregs contribute to shaping a locally regulated immune environment.

Several limitations warrant consideration. First, the sample size for both the peripheral and spatial analyses was limited. Although flow cytometry data captured dynamic immune changes, the cohort comprised only nine patients. Similarly, spatial transcriptomics was performed on three biopsies from a subset of two patients, limiting the generalisability of tissue-level findings. Although the immune infiltrates observed in the Treg-treated graft appeared non-rejection-like, the possibility of subclinical rejection cannot be excluded. The small number of biopsies and assessment at a single time point make it difficult to distinguish treatment-associated immune regulation from other underlying immune processes. Additionally, functional validation of transcriptional changes (e.g., cytokine production, suppressive capacity) was not feasible within the scope of this study. Finally, while spatial analyses revealed intriguing patterns, formal identification of tertiary lymphoid structures and regulatory B cells was not performed. Future studies should seek to validate these observations in larger, multicentre cohorts. Integration of spatial transcriptomics with multiplex imaging and functional assays could provide deeper insight into the cellular networks governing tolerance. It will also be important to characterise the role of B cells, within the Treg-induced immune landscape. Investigating how monocyte-Treg-B cell interactions evolve over time and relate to clinical outcomes such as drug minimisation or graft survival could inform personalised immunosuppression strategies.

In summary, this study provides a comprehensive view of the immunological impact of Treg therapy in human kidney transplantation. Peripheral blood monitoring demonstrated that Treg infusion is safe and associated with stable levels of circulating Tregs without disruption of conventional T cell homeostasis. Spatial transcriptomic profiling identified distinct immune niches within the graft, characterised by transcriptional changes in monocytes, Tregs, and B cells, and altered patterns of cell-cell interactions. These findings suggest that Treg therapy may influence not only systemic immunity but also the local tissue

environment within the graft. Collectively, these findings provide insight into the immunological impact of adoptive Treg therapy, demonstrating changes in immune cell composition, transcriptional profiles, and spatial organisation within the graft.

---

6 Chapter 6: General Discussion

6.1 Summary of findings

Regulatory T cells (Tregs) are emerging as a powerful cellular therapy to promote immune tolerance in transplantation. This project investigated how *ex vivo* expanded human Tregs perform in terms of maintaining their regulatory identity, migratory capacities, suppression of effector T cells, and interacting with other immune cells, both *in vitro* and in a clinical transplant setting. The key findings across the experimental chapters highlight that polyclonal Tregs expanded under GMP conditions preserve their core suppressive phenotype and function, acquire homing features compatible with trafficking to inflamed tissues, and engage in beneficial crosstalk with other immune cells (Figure 6.2.1). Below, the summary of the major findings is followed by an appraisal of the study's limitations, future directions, and overall conclusions.

Ex vivo expansion of Clinical-Tregs preserved phenotypic stability and sustained expression of key suppressive markers. Transcriptomic analyses in Chapter 3 showed that Clinical-Tregs retained elevated expression of the canonical regulatory markers FOXP3 and CD25, together with sustained expression of TIGIT and CD80. In parallel, transcriptomic profiling identified selective upregulation of trafficking and adhesion related genes including CCR8, CXCR6, ITGAX, ITGAM, and CEACAM1, compared to both conventional $CD4^+$ and $CD8^+$ T cells. Relative to freshly isolated *ex vivo* Tregs, Clinical-Tregs also showed lower expression of Helios, CD45RA and TCF7, together with increased expression of LAG3 and OX40. At the protein level, Clinical-Tregs showed higher expression of CCR4 and CCR8 than conventional T cells, and stimulation induced upregulation of CCR7 over unstimulated Tregs. Beyond surface phenotype, Chapter 3 further showed that Clinical-Tregs secreted chemokines, with high CXCL8 production following TCR stimulation and CCL24 secretion following allogeneic stimulation with donor monocytes. IL-2 had no measurable effect on chemokine secretion under the stimulatory conditions tested.

In Chapter 4, expanded Tregs potently suppressed proliferation of responder T cells in total PBMCs[123, 124]. A key finding was the dependence on monocytes, depletion of monocytes markedly reduced Treg-mediated suppression, which was restored by monocyte reconstitution, with accompanying dysregulation of cytokine production, including increased IFN-γ, TNF-α, IL-17A/F, and IL-10, that was partially normalised upon monocyte reconstitution. Finally, in chapter 5, I focused on clinical samples of the TWO Study. Treg infusion within this programme was reported to be feasible and safe, with immunosuppression minimisation achieved in a proportion of recipients without excess acute rejection or donor-specific antibodies[25, 26, 83, 107]. Longitudinal immunomonitoring demonstrated variability in circulating Treg counts over time, without evidence of sustained peripheral expansion or significant divergence between Treg-treated and control patients, consistent with regulated homeostasis of the circulating Treg compartment following adoptive transfer[83, 122]. Importantly, conventional T cell reconstitution proceeded without major disruption. At the same time, subtle differences were observed within the monocyte compartment in Treg-treated patients, characterised by relatively higher circulating levels of non-classical $CD14^{+}CD16^{hi}$ monocytes without a corresponding increase in total monocyte counts. Spatial transcriptomic analysis of protocol kidney biopsies, including a biopsy obtained after Treg infusion referred to here as the post-Treg biopsy, revealed regulatory-leaning infiltrates in Treg-treated grafts with higher proportions of monocytes compared to the control. Chemokine analysis showed increased CCR7 and CCL19 expression in the post Treg biopsy. Neighbourhood analysis indicated greater co localisation of $CD14^{+}$ and $CD16^{+}$ monocytes with B cells and cDC2, together with reduced adjacency to effector T cells. Differential expression analysis further showed transcriptional changes in $CD14^{+}$ and $CD16^{+}$ monocytes, alongside altered gene expression in intermediate and naïve B cell subsets in the post Treg biopsy.

6.2 General discussion

Across this thesis, Clinical-Tregs retained core lineage features, including FOXP3 and CD25, together with inhibitory modules such as TIGIT and molecules involved in co-stimulatory regulation, including CD80, that underpin suppressive function[47, 104-106, 123, 124]. This aligns with foundational and translational literature indicating that *ex vivo* expansion can maintain lineage fidelity and functional potency[104, 105, 112, 123, 124]. Phenotypically, expanded cells showed an activated effector Treg profile, for example LAG3 and OX40, whilst preserving FOXP3 and CD25, consistent with reports that transient activation or repeated stimulation can endow Tregs with enhanced *in vivo* performance without eroding regulatory identity[111, 124]. Differences between freshly isolated *ex vivo* Tregs and Clinical-Tregs, including lower expression of Helios, CD45RA and

TCF7 together with increased expression of LAG3 and OX40, are coherent with known human Treg heterogeneity and with culture induced shifts away from naïve and thymic like features[97, 109, 113]. Despite prolonged culture, Clinical-Tregs preserved the key molecular hallmarks that support suppressive identity and anticipated *in vivo* efficacy[47, 104-106, 112, 123, 124].

Effective Treg therapy depends on appropriate trafficking to allografts and inflamed sites[76, 77, 86, 92, 98]. In this thesis, transcriptomic profiling of Clinical-Tregs revealed a trafficking signature consistent with peripheral tissue localisation, characterised by increased expression of chemokine receptors such as CCR8 and CXCR6, together with adhesion molecules including ITGAX, ITGAM, and CEACAM1, alongside reduced expression of CXCR4, a receptor linked to lymphoid and bone marrow retention[70, 77, 86, 92-94, 98]. This coordinated modulation suggests a shift towards enhanced migratory capacity and tissue anchoring within inflamed environments. Although CXCR6 is most commonly associated with tissue residency in highly activated effector $CD8^+$ T cells[108], its expression in Clinical-Tregs aligns with evidence that regulatory T cells can adopt similar tissue-adaptive programmes, supporting persistence within inflamed sites[77, 94, 98]. In parallel, elevated CCR8 expression and upregulation of adhesion molecules such as ITGAX and ITGAM may be consistent with a phenotype equipped for tissue extravasation and retention[69-71]. Collectively, these features may suggest that *ex vivo* expansion not only preserves Treg identity but promotes a coordinated trafficking and adhesion programme that may enhance their localisation and immunoregulatory function within the graft.

At the protein level, flow cytometry demonstrated high expression of CCR4 and CCR8, whereas Treg stimulation led to increased CCR7 expression relative to unstimulated cells. This preserved CCR4 and CCR8 profile in Clinical-Tregs may reflect trafficking features shared with tissue-adapted Tregs at barrier sites, including the skin and gut, where these receptors are thought to facilitate targeted homing and local persistence in both steady-state and inflammatory settings[92, 98]. In line with previous findings from Issa et al.[76], the observed upregulation of CCR7 following stimulation suggests that activated Tregs retain or reacquire lymphoid homing capacity, potentially enhancing their ability to traffic to secondary lymphoid organs and support immune regulation *in vivo* despite prolonged *in vitro* expansion. It is also possible that some of the homing markers identified here could be further tailored through optimisation of expansion conditions, as shown by Hoeppli et al., who demonstrated that *ex vivo* culture conditions can favour some chemokines expression[77]. This raises the possibility that other chemokine receptors could similarly be enriched in Treg populations with enhanced trafficking features and potentially improved migration to inflammatory sites.

In addition to this phenotypic and trafficking profile, Clinical-Tregs retained functional chemokine secreting capacity. High CXCL8 production was observed following TCR stimulation, consistent with reports that human Tregs can produce CXCL8 and recruit neutrophils[115]. More broadly, Treg-derived chemokines can attract pathogenic T cells into proximity, enabling contact-dependent suppression, the "attraction-and-suppression" model[90]. In allogeneic co culture, CCL24 was also detected; although its Treg specific role in humans remains incompletely defined, Tregs are known to restrain airway inflammation across eosinophilic and neutrophilic settings, supporting a context dependent contribution of chemokine mediated regulation[116]. In parallel, low dose IL-2 selectively expands circulating Tregs but did not promote liver allograft tolerance in humans, aligning with my observation that IL-2 did not augment chemokine secretion *in vitro*[114]. Overall, the chemokine data support the position of expanded Tregs as active organisers of the local immune milieu rather than passive suppressors[90, 115, 116].

This thesis also highlighted that expanded Tregs exerted strong suppression of responder Teff proliferation in total PBMCs. Quantitative analysis further suggested that this effect was mediated predominantly through limiting division destiny, rather than by increasing cell death or prolonging interdivision time, consistent with prior modelling studies[121, 126]. A key integrative finding was the requirement for monocytes; depletion reduced suppression, whereas reconstitution restored it. This is consistent with evidence that monocyte derived inflammatory cues, for example IL-1β, IL-6 and TNF-α, can enhance Treg suppressive activity[118], that expanded Tregs can reprogramme monocytes towards alternatively activated, IL-10 biased states[125], and that monocyte subsets modulate Helios$^+$ and Helios$^-$ Tregs via IL-12 and TNF-α respectively[127]. The centrality of monocyte plasticity to tolerance and rejection further underscores a cooperative axis in which Tregs and monocytes reinforce one another's regulatory functions[28, 118, 125, 127].

Within the TWO Study, longitudinal immunomonitoring analysis showed inter-individual fluctuations across the post-transplant period without significant changes in circulating Tregs, while conventional T cell reconstitution was generally maintained, consistent with homing and normal post-transfer kinetics[83, 122]. This is further supported by recent clinical trial data showing that infused polyclonal Tregs peak transiently in the circulation and can be detected at lower frequencies in post-infusion kidney biopsies, highlighting the importance of monitoring Treg trafficking, persistence, and lineage stability after transfer[132]. Spatial profiling of biopsies from TWO Study patients provided complementary tissue-level context. Post-Treg biopsies showed a higher representation of monocyte lineage cells, including CD14$^+$ and CD16$^+$ populations, whereas these features were less prominent in the control biopsy; this pattern is supported by evidence showing that repeated Treg infusions enrich myeloid populations and are associated with improved allograft

outcomes[117, 129]. Neighbourhood analysis indicated greater co-localisation of monocytes with B cells and cDC2, alongside reduced adjacency to effector T cells. At the transcriptional level, post-Treg samples showed increased CCR7-CCL19 receptor-ligand signalling across immune cell populations, as well as elevated CXCL6 with reduced CXCL2 in selected T cell subsets, while B cell subsets exhibited increased CCL27 and CXCL9[64]. Although CXCL9 and CXCL10 are often associated with rejection, previous studies suggest that transient increases followed by resolution may instead reflect self-limiting immune activation rather than persistent alloimmunity, particularly when graft function remains stable[72]. The presence of CCR7-CCL19 signalling across these populations suggests coordinated chemokine networks that may contribute to immune cell positioning and crosstalk within the graft, potentially supporting Treg and antigen-presenting cell interactions in lymphoid-like niches[117, 130, 135]. Together, these findings are consistent with a reorganised tissue environment in which lymphoid and myeloid cells are spatially arranged in a manner that may favour immune regulation. This interpretation aligns with the concept of immune microniches, where close proximity between lymphocytes and myeloid cells is required for optimal Treg function within tissues[134]. Additionally, the differential gene expression analysis showed distinct transcriptional changes in intragraft monocyte subsets following Treg therapy, including altered expression of RETN, CCL27, PD-1, CHGA, and PYY compared with controls, suggesting reprogramming of the local myeloid compartment. This view is supported by recent non-human primate data in which repeated infusions of *ex vivo* expanded Tregs increased myeloid populations and were associated with improved kidney allograft survival[129], reinforcing the idea that Treg therapy may act in part through regulatory remodelling of myeloid cells within the graft.

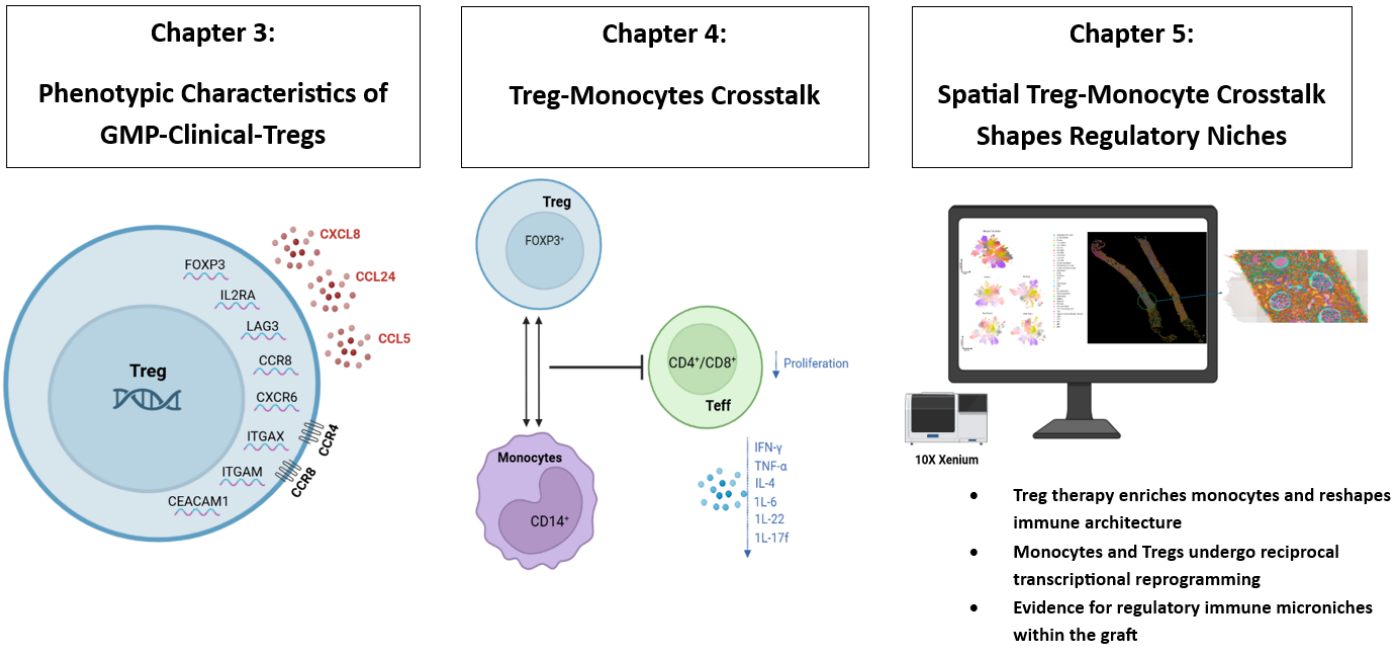


Figure 6.2.1 Summary of the main findings across experimental chapters.

This figure integrates key results from Chapters 3-5. GMP-grade Tregs maintained a stable regulatory phenotype and expressed homing-associated chemokines (Chapter 3). Their suppressive function was enhanced by CD14$^+$ monocytes, revealing bidirectional crosstalk that regulated Teff proliferation and cytokine production (Chapter 4). Spatial transcriptomics of post-Treg grafts showed monocyte enrichment, regulatory chemokine profiles, and formation of Treg-monocyte-B cell microniches (Chapter 5), highlighting tissue-level reprogramming associated with tolerance.

6.3 Limitations

Several limitations should be considered when interpreting the findings of this thesis. First, the study size was modest across both the experimental and clinical components. Although the *in vitro* analyses provided consistent phenotypic and functional signals, the clinical immunomonitoring cohort was small, which limits statistical power and the extent to which systemic immune trends can be generalised across a broader transplant population. This was particularly relevant for the spatial transcriptomic component, which was performed on a very limited number of protocol kidney biopsies. As a result, the tissue level observations are best interpreted as hypothesis generating rather than definitive, since sample specific effects, inter patient variability, and biopsy timing may all have influenced the observed spatial organisation and transcriptional profiles. In addition, the analysis was based on protocol biopsies from a restricted clinical context and therefore may not capture the full range of graft immune states over time. A further limitation is that the study design did not allow direct tracking of the infused Treg product. Consequently, it was not possible to distinguish with certainty between infused and endogenous Tregs within the circulation or graft, nor to define the persistence, localisation, or fate of the therapeutic cells after transfer, which remains an important challenge for interpreting the *in vivo* behaviour of adoptively transferred Tregs.

Second, there are important methodological limitations in relation to validation and mechanistic resolution. The spatial transcriptomic platform enabled detailed analysis of transcriptional patterns and cellular neighbourhoods, but it did not provide protein level confirmation of cell identity, activation state, or receptor expression. In particular, multiplex protein imaging or other protein-based approaches were not performed, so findings such as the inferred regulatory nature of intragraft immune aggregates, the expression of checkpoint molecules, and the potential presence of tertiary lymphoid like structures could not be formally validated at the protein level. Similarly, although the monocyte depletion and reconstitution experiments strongly supported a role for monocytes in optimising Treg suppressive function, these assays were conducted in reductionist *in vitro* systems and therefore cannot fully recapitulate the complexity of the *in vivo* graft microenvironment, where stromal cells, dendritic cells, endothelial compartments, and local cytokine gradients are also likely to contribute. Finally, although chemokine secretion and transcriptional changes were clearly observed, the functional consequences of specific molecules such as CXCL8, CCL24, and

CCR7-CCL19 were not directly tested. For this reason, the mechanistic links proposed in this thesis are biologically plausible and supported by the literature, but they require further validation in larger cohorts and with integrated functional and protein-based approaches.

6.4 Future directions

Future work should build on these findings by strengthening both mechanistic resolution and clinical validation. A first priority will be to dissect the Treg and monocyte axis in greater detail using perturbation based co cultures and *ex vivo* human tissues. This would help define which monocyte derived signals, including IL-1β, IL-6, TNF-α and IL-10, are necessary or sufficient to reinforce Treg suppressive activity, and whether distinct monocyte subsets differentially shape Treg phenotype and function. Given the strong signal emerging from the spatial analyses, it will also be important to validate therapy associated immune aggregates within the graft using spatially resolved protein-based methods. Combining spatial transcriptomics with multiplex protein imaging would allow more confident confirmation of cell identity and functional state, including the presence of IL-10$^+$ B cells, PD-L1$^+$ myeloid cells, and TIGIT or Helios$^+$ Tregs, and would help determine whether the observed aggregates meet formal criteria for tertiary lymphoid like structures.

A second priority will be to clarify the fate and behaviour of the infused Treg product *in vivo*. Although technically challenging, future studies incorporating safe labelling, barcoding, or other tracking approaches, together with longitudinal sampling, could define persistence, trafficking between blood, graft, and lymphoid tissues, and stability of the expanded phenotype over time. This would help distinguish infused from endogenous Tregs and refine understanding of when and where the therapeutic product exerts its effects. In parallel, larger clinical cohorts will be needed to confirm the systemic and tissue level findings described here and to assess how they relate to clinical outcomes such as immunosuppression minimisation, graft function, and long-term allograft survival. Finally, the homing receptor profile identified in this thesis, including CCR7, CCR4, and CCR8, may be further optimised through *ex vivo* expansion conditions to enrich Treg populations with enhanced migratory capacity and potentially improved localisation to relevant inflammatory sites.

6.5 Conclusion

This thesis demonstrated that GMP-expanded, autologous Tregs retained lineage defining markers and inhibitory modules, displayed trafficking profiles compatible with peripheral tissue localisation, and exerted potent suppression that was amplified by monocytes. Using samples from kidney transplant recipients enrolled in the TWO Study, this work further showed that Treg therapy was associated with regulatory leaning tissue architectures and systemic immune changes consistent with a tolerogenic shift. Taken together, these observations provide mechanistic insight into how expanded Tregs function and how could monocytes contribute to their suppressive activity in transplantation, while underscoring the need for larger cohorts, and mechanistic validation of tissue regulatory niches before broader generalisation.

References

1. Garcia GG, Harden P, Chapman J. The global role of kidney transplantation. The Lancet. 2012;379(9820):e36-e8.
2. Li Q, Lan P. Activation of immune signals during organ transplantation. Signal transduction and targeted therapy. 2023;8(1):110.
3. Liu Y, Feng H, Li K, Li R, Zhang X-J, Tian Y, et al. Donor MHC-specific thymus vaccination allows for immunocompatible allotransplantation. Cell Research. 2025:1-13.
4. Wang Y, Ullah MA, Waltner OG, Bhise SS, Ensbey KS, Schmidt CR, et al. Calcineurin inhibition rescues alloantigen-specific central memory T cell subsets that promote chronic GVHD. The Journal of clinical investigation. 2024;134(11).
5. Griffith BP, Goerlich CE, Singh AK, Rothblatt M, Lau CL, Shah A, et al. Genetically modified porcine-to-human cardiac xenotransplantation. New England Journal of Medicine. 2022;387(1):35-44.
6. Dumbill R, Knight S, Hunter J, Fallon J, Voyce D, Barrett J, et al. Prolonged normothermic perfusion of the kidney prior to transplantation: a historically controlled, phase 1 cohort study. Nature Communications. 2025;16(1):4584.
7. Bikbov B, Purcell CA, Levey AS, Smith M, Abdoli A, Abebe M, et al. Global, regional, and national burden of chronic kidney disease, 1990–2017: a systematic analysis for the Global Burden of Disease Study 2017. The lancet. 2020;395(10225):709-33.
8. Guglin M, Zucker MJ, Borlaug BA, Breen E, Cleveland J, Johnson MR, et al. Evaluation for heart transplantation and LVAD implantation: JACC council perspectives. Journal of the American College of Cardiology. 2020;75(12):1471-87.
9. Kupiec-Weglinski J. Grand Challenges in Organ Transplantation. Front Transplant 1: 897679 doi: 103389/frtra. 2022.
10. Spardy J, Concepcion J, Yeager M, Andrade R, Braun H, Elkbuli A. National analysis of recent trends in organ donation and transplantation in the United States: toward optimizing care delivery and patient outcomes. The American Surgeon™. 2023;89(12):5201-9.
11. Transplantation GOoDa. Total Kidney (Total Deceased + Total Living): GODT; 2023 [Available from: https://www.transplant-observatory.org/data-charts-and-tables/chart/.
12. Anand RP, Layer JV, Heja D, Hirose T, Lassiter G, Firl DJ, et al. Design and testing of a humanized porcine donor for xenotransplantation. Nature. 2023;622(7982):393-401.
13. Wisel SA, Borja-Cacho D, Megna D, Adjei M, Kim IK, Steggerda JA. Organ Utilization Rates from Non-Ideal Donors for Solid Organ Transplant in the United States. Journal of Clinical Medicine. 2024;13(11):3271.
14. Diker Cohen T, Dotan I, Calvarysky B, Robenshtok E. Endocrine effects of long-term calcineurin inhibitor use in solid organ transplant recipients. European Journal of Endocrinology. 2025;193(3):R1-R16.
15. Guerra G, Ciancio G, Gaynor JJ, Zarak A, Brown R, Hanson L, et al. Randomized trial of immunosuppressive regimens in renal transplantation. Journal of the American Society of Nephrology. 2011;22(9):1758-68.
16. van Alem CM, Schmidbauer M, Rong S, Derlin K, Schmitz J, Bräsen JH, et al. Liposomal delivery improves the efficacy of prednisolone to attenuate renal inflammation in a mouse model of acute renal allograft rejection. Transplantation. 2020;104(4):744-53.
17. Bak S, Tischer S, Dragon A, Ravens S, Pape L, Koenecke C, et al. Selective effects of mTOR inhibitor sirolimus on naïve and CMV-specific T cells extending its applicable range beyond immunosuppression. Frontiers in immunology. 2018;9:2953.

18. Vincenti F, Rostaing L, Grinyo J, Rice K, Steinberg S, Gaite L, et al. Belatacept and long-term outcomes in kidney transplantation. New England Journal of Medicine. 2016;374(4):333-43.
19. Group CSC. Alemtuzumab-based induction treatment versus basiliximab-based induction treatment in kidney transplantation (the 3C Study): a randomised trial. The Lancet. 2014;384(9955):1684-90.
20. Saldan A, Mengoli C, Sgarabotto D, Fedrigo M, Angelini A, Feltrin G, et al. Human cytomegalovirus and Epstein–Barr virus infections occurring early after transplantation are risk factors for antibody-mediated rejection in heart transplant recipients. Frontiers in Immunology. 2023;14:1171197.
21. Sargen MR, Cahoon EK, Kelly JY, Madeleine MM, Zeng Y, Rees JR, et al. Spectrum of nonkeratinocyte skin cancer risk among solid organ transplant recipients in the US. JAMA dermatology. 2022;158(4):414-25.
22. Nankivell BJ, P'Ng CH, O'Connell PJ, Chapman JR. Calcineurin inhibitor nephrotoxicity through the lens of longitudinal histology: comparison of cyclosporine and tacrolimus eras. Transplantation. 2016;100(8):1723-31.
23. Neuberger JM, Bechstein WO, Kuypers DR, Burra P, Citterio F, De Geest S, et al. Practical recommendations for long-term management of modifiable risks in kidney and liver transplant recipients: a guidance report and clinical checklist by the consensus on managing modifiable risk in transplantation (COMMIT) group. Transplantation. 2017;101(4S):S1-S56.
24. Bottomley MJ, Brook MO, Shankar S, Hester J, Issa F. Towards regulatory cellular therapies in solid organ transplantation. Trends in immunology. 2022;43(1):8-21.
25. Brook MO, Hester J, Petchey W, Rombach I, Dutton S, Bottomley MJ, et al. Transplantation Without Overimmunosuppression (TWO) study protocol: a phase 2b randomised controlled single-centre trial of regulatory T cell therapy to facilitate immunosuppression reduction in living donor kidney transplant recipients. BMJ open. 2022;12(4):e061864.
26. Roemhild A, Otto NM, Moll G, Abou-El-Enein M, Kaiser D, Bold G, et al. Regulatory T cells for minimising immune suppression in kidney transplantation: phase I/IIa clinical trial. bmj. 2020;371.
27. Kawai T, Cosimi AB, Spitzer TR, Tolkoff-Rubin N, Suthanthiran M, Saidman SL, et al. HLA-mismatched renal transplantation without maintenance immunosuppression. New England Journal of Medicine. 2008;358(4):353-61.
28. Panzer SE. Macrophages in transplantation: a matter of plasticity, polarization, and diversity. Transplantation. 2022;106(2):257-67.
29. Wu H, Malone AF, Donnelly EL, Kirita Y, Uchimura K, Ramakrishnan SM, et al. Single-cell transcriptomics of a human kidney allograft biopsy specimen defines a diverse inflammatory response. Journal of the American Society of Nephrology. 2018;29(8):2069-80.
30. Shen Q, Wang Y, Chen J, Ma L, Huang X, Tang SC, et al. Single-cell RNA sequencing reveals the immunological profiles of renal allograft rejection in mice. Frontiers in Immunology. 2021;12:693608.
31. Ruan DF, Fribourg M, Yuki Y, Park Y-H, Martin MP, Yu H, et al. High-dimensional analysis of NK cells in kidney transplantation uncovers subsets associated with antibody-independent graft dysfunction. JCI insight. 2024;9(21):e185687.
32. Chong AS. Mechanisms of organ transplant injury mediated by B cells and antibodies: Implications for antibody-mediated rejection. American Journal of Transplantation. 2020;20:23-32.
33. Short S, Lewik G, Issa F. An immune atlas of T cells in transplant rejection: pathways and therapeutic opportunities. Transplantation. 2023;107(11):2341-52.
34. Mikami N, Sakaguchi S. Regulatory T cells in autoimmune kidney diseases and transplantation. Nature Reviews Nephrology. 2023;19(9):544-57.
35. Zong Y, Deng K, Chong WP. Regulation of Treg cells by cytokine signaling and co-stimulatory molecules. Frontiers in Immunology. 2024;15:1387975.

36. Luo Y, Xu C, Wang B, Niu Q, Su X, Bai Y, et al. Single-cell transcriptomic analysis reveals disparate effector differentiation pathways in human Treg compartment. Nature communications. 2021;12(1):3913.
37. Shevach EM, Thornton AM. tTregs, pTregs, and iTregs: similarities and differences. Immunological reviews. 2014;259(1):88-102.
38. Waldmann H, Hilbrands R, Howie D, Cobbold S. Harnessing FOXP3+ regulatory T cells for transplantation tolerance. The Journal of clinical investigation. 2014;124(4):1439-45.
39. Mikami N, Kawakami R, Sugimoto A, Arai M, Sakaguchi S. Generation of antigen-specific and functionally stable Treg cells from effector/memory T cells for cell therapy of immunological diseases. bioRxiv. 2025:2025.06. 13.659621.
40. Gootjes C, Zwaginga JJ, Roep BO, Nikolic T. Defining Human Regulatory T Cells beyond FOXP3: The Need to Combine Phenotype with Function. Cells. 2024;13(11):941.
41. Hornero RA, Betts GJ, Sawitzki B, Vogt K, Harden PN, Wood KJ. CD45RA distinguishes CD4+ CD25+ CD127−/low TSDR demethylated regulatory T cell subpopulations with differential stability and susceptibility to tacrolimus-mediated inhibition of suppression. Transplantation. 2017;101(2):302-9.
42. Chen S, Zhang L, Ying Y, Wang Y, Arnold PR, Wang G, et al. Epigenetically modifying the Foxp3 locus for generation of stable antigen-specific Tregs as cellular therapeutics. American Journal of Transplantation. 2020;20(9):2366-79.
43. Arroyo Hornero R, Georgiadis C, Hua P, Trzupek D, He L-Z, Qasim W, et al. CD70 expression determines the therapeutic efficacy of expanded human regulatory T cells. Communications biology. 2020;3(1):375.
44. Zhou X, Bailey-Bucktrout S, Jeker LT, Bluestone JA. Plasticity of CD4+ FoxP3+ T cells. Current opinion in immunology. 2009;21(3):281-5.
45. Dikiy S, Rudensky AY. Principles of regulatory T cell function. Immunity. 2023;56(2):240-55.
46. Thomson AW, Turnquist HR, Zahorchak AF, Raimondi G. Tolerogenic dendritic cell-regulatory T-cell interaction and the promotion of transplant tolerance. Transplantation. 2009;87(9S):S86-S90.
47. Kennedy A, Waters E, Rowshanravan B, Hinze C, Williams C, Janman D, et al. Differences in CD80 and CD86 transendocytosis reveal CD86 as a key target for CTLA-4 immune regulation. Nature immunology. 2022;23(9):1365-78.
48. Shankar S, Stolp J, Juvet S, Beckett J, Macklin P, Issa F, et al. Ex vivo-expanded human CD19+ TIM-1+ regulatory B cells suppress immune responses in vivo and are dependent upon the TIM-1/STAT3 axis. Nature Communications. 2022;13(1):3121.
49. Beckett J, Hester J, Issa F, Shankar S. Regulatory B cells in transplantation: roadmaps to clinic. Transplant International. 2020;33(11):1353-68.
50. Conde P, Rodriguez M, van der Touw W, Jimenez A, Burns M, Miller J, et al. DC-SIGN+ macrophages control the induction of transplantation tolerance. Immunity. 2015;42(6):1143-58.
51. Carnel N, Lancia HH, Guinier C, Benichou G. Pathways of antigen recognition by T cells in allograft rejection. Transplantation. 2023;107(4):827-37.
52. Duneton C, Winterberg PD, Ford ML. Activation and regulation of alloreactive T cell immunity in solid organ transplantation. Nature Reviews Nephrology. 2022;18(10):663-76.
53. Nakayama M, Hori A, Toyoura S, Yamaguchi S-I. Shaping of T cell functions by trogocytosis. Cells. 2021;10(5):1155.
54. Markey KA, Koyama M, Gartlan KH, Leveque L, Kuns RD, Lineburg KE, et al. Cross-dressing by donor dendritic cells after allogeneic bone marrow transplantation contributes to formation of the immunological synapse and maximizes responses to indirectly presented antigen. The Journal of Immunology. 2014;192(11):5426-33.
55. Lin J-X, Leonard WJ. The common cytokine receptor γ chain family of cytokines. Cold Spring Harbor perspectives in biology. 2018;10(9):a028449.

56. Jarczak D, Nierhaus A. Cytokine storm—definition, causes, and implications. International journal of molecular sciences. 2022;23(19):11740.
57. Bartekova M, Radosinska J, Jelemensky M, Dhalla NS. Role of cytokines and inflammation in heart function during health and disease. Heart failure reviews. 2018;23:733-58.
58. Muckenhuber M, Mengrelis K, Weijler AM, Steiner R, Kainz V, Buresch M, et al. IL-6 inhibition prevents costimulation blockade-resistant allograft rejection in T cell-depleted recipients by promoting intragraft immune regulation in mice. Nature Communications. 2024;15(1):4309.
59. Wang J, Zhao X, Wan YY. Intricacies of TGF-β signaling in Treg and Th17 cell biology. Cellular & molecular immunology. 2023;20(9):1002-22.
60. Xu H, Lin S, Zhou Z, Li D, Zhang X, Yu M, et al. New genetic and epigenetic insights into the chemokine system: the latest discoveries aiding progression toward precision medicine. Cellular & Molecular Immunology. 2023;20(7):739-76.
61. Griffith JW, Sokol CL, Luster AD. Chemokines and chemokine receptors: positioning cells for host defense and immunity. Annual review of immunology. 2014;32(1):659-702.
62. Chaudhry S, Emond J, Griesemer A. Immune cell trafficking to the liver. Transplantation. 2019;103(7):1323-37.
63. Chen Z, Xu H, Li Y, Zhang X, Cui J, Zou Y, et al. Single-Cell RNA sequencing reveals immune cell dynamics and local intercellular communication in acute murine cardiac allograft rejection. Theranostics. 2022;12(14):6242.
64. Ozga AJ, Chow MT, Luster AD. Chemokines and the immune response to cancer. Immunity. 2021;54(5):859-74.
65. Lee BH, Bang YJ, Lim SH, Kang S-J, Kim SH, Kim-Schulze S, et al. High-dimensional profiling of regulatory T cells in psoriasis reveals an impaired skin-trafficking property. EBioMedicine. 2024;100.
66. Dilek N, Poirier N, Usal C, Martinet B, Blancho G, Vanhove B. Control of transplant tolerance and intragraft regulatory T cell localization by myeloid-derived suppressor cells and CCL5. The Journal of Immunology. 2012;188(9):4209-16.
67. Jacob J, Nadkarni S, Volpe A, Peng Q, Tung SL, Hannen RF, et al. Spatiotemporal in vivo tracking of polyclonal human regulatory T cells (Tregs) reveals a role for innate immune cells in Treg transplant recruitment. Molecular Therapy Methods & Clinical Development. 2021;20:324-36.
68. Alcaide P. Mechanisms Regulating T Cell–Endothelial Cell Interactions. Cold Spring Harbor Perspectives in Medicine. 2022;12(7):a041170.
69. Fowell DJ, Kim M. The spatio-temporal control of effector T cell migration. Nature Reviews Immunology. 2021;21(9):582-96.
70. Ley K, Laudanna C, Cybulsky MI, Nourshargh S. Getting to the site of inflammation: the leukocyte adhesion cascade updated. Nature reviews immunology. 2007;7(9):678-89.
71. Riedel J-H, Turner J-E, Panzer U. T helper cell trafficking in autoimmune kidney diseases. Cell and Tissue Research. 2021:1-12.
72. Rabant M, Amrouche L, Morin L, Bonifay R, Lebreton X, Aouni L, et al. Early low urinary CXCL9 and CXCL10 might predict immunological quiescence in clinically and histologically stable kidney recipients. American Journal of Transplantation. 2016;16(6):1868-81.
73. Certo M, Elkafrawy H, Pucino V, Cucchi D, Cheung KC, Mauro C. Endothelial cell and T-cell crosstalk: Targeting metabolism as a therapeutic approach in chronic inflammation. British journal of pharmacology. 2021;178(10):2041-59.
74. Mempel TR, Marangoni F. Guidance factors orchestrating regulatory T cell positioning in tissues during development, homeostasis, and response. Immunological reviews. 2019;289(1):129-41.
75. Kawai K, Uchiyama M, Hester J, Issa F. IL-33 drives the production of mouse regulatory T cells with enhanced in vivo suppressive activity in skin transplantation. American Journal of Transplantation. 2021;21(3):978-92.

76. Issa F, Hester J, Milward K, Wood KJ. Homing of regulatory T cells to human skin is important for the prevention of alloimmune-mediated pathology in an in vivo cellular therapy model. PloS one. 2012;7(12):e53331.
77. Hoeppli RE, MacDonald KN, Leclair P, Fung VC, Mojibian M, Gillies J, et al. Tailoring the homing capacity of human Tregs for directed migration to sites of Th1-inflammation or intestinal regions. American journal of transplantation. 2019;19(1):62-76.
78. Scandling JD, Busque S, Dejbakhsh-Jones S, Benike C, Millan MT, Shizuru JA, et al. Tolerance and chimerism after renal and hematopoietic-cell transplantation. New England Journal of Medicine. 2008;358(4):362-8.
79. Song N, Scholtemeijer M, Shah K. Mesenchymal stem cell immunomodulation: mechanisms and therapeutic potential. Trends in pharmacological sciences. 2020;41(9):653-64.
80. Hoogduijn MJ, Issa F, Casiraghi F, Reinders ME. Cellular therapies in organ transplantation. Transplant International. 2021;34(2):233-44.
81. Sawitzki B, Harden PN, Reinke P, Moreau A, Hutchinson JA, Game DS, et al. Regulatory cell therapy in kidney transplantation (The ONE Study): a harmonised design and analysis of seven non-randomised, single-arm, phase 1/2A trials. The Lancet. 2020;395(10237):1627-39.
82. Mathew JM, Voss JH, McEwen ST, Konieczna I, Chakraborty A, Huang X, et al. Generation and characterization of alloantigen-specific regulatory T cells for clinical transplant tolerance. Scientific reports. 2018;8(1):1136.
83. Brook MO, Hennessy C, Hester J, Hammad S, Alzhrani A, Rombach I, et al. Late Treatment With Autologous Expanded Regulatory T-cell Therapy After Alemtuzumab Induction Is Safe and Facilitates Immunosuppression Minimization in Living Donor Renal Transplantation. Transplantation. 2024:10.1097.
84. Bernaldo-de-Quirós E, Camino M, Martínez-Bonet M, Gil-Jaurena JM, Gil N, Hernández-Flórez D, et al. First-in-human therapy with Treg produced from thymic tissue (thyTreg) in a heart transplant infant. Journal of Experimental Medicine. 2023;220(12):e20231045.
85. Proics E, David M, Mojibian M, Speck M, Lounnas-Mourey N, Govehovitch A, et al. Preclinical assessment of antigen-specific chimeric antigen receptor regulatory T cells for use in solid organ transplantation. Gene Therapy. 2023;30(3):309-22.
86. Burrell BE, Nakayama Y, Xu J, Brinkman CC, Bromberg JS. Regulatory T cell induction, migration, and function in transplantation. The Journal of Immunology. 2012;189(10):4705-11.
87. Harden PN, Game DS, Sawitzki B, Van der Net JB, Hester J, Bushell A, et al. Feasibility, long-term safety, and immune monitoring of regulatory T cell therapy in living donor kidney transplant recipients. American Journal of Transplantation. 2021;21(4):1603-11.
88. Hester J, Schiopu A, Nadig S, Wood K. Low-dose rapamycin treatment increases the ability of human regulatory T cells to inhibit transplant arteriosclerosis in vivo. American Journal of Transplantation. 2012;12(8):2008-16.
89. Hao Y, Hao S, Andersen-Nissen E, Mauck WM, Zheng S, Butler A, et al. Integrated analysis of multimodal single-cell data. Cell. 2021;184(13):3573-87. e29.
90. Patterson SJ, Pesenacker AM, Wang AY, Gillies J, Mojibian M, Morishita K, et al. T regulatory cell chemokine production mediates pathogenic T cell attraction and suppression. The Journal of clinical investigation. 2016;126(3):1039-51.
91. Chakraborty R, Rooney C, Dotti G, Savoldo B. Changes in chemokine receptor expression of regulatory T cells after ex vivo culture. Journal of Immunotherapy. 2012;35(4):329-36.
92. Campbell DJ. Control of regulatory T cell migration, function, and homeostasis. The Journal of Immunology. 2015;195(6):2507-13.
93. Huang M, Ke Z, Lyu M-A, Masarova L, Sadeghi T, Flowers CR, et al. CXCR4-enriched T regulatory cells preferentially home to bone marrow and resolve inflammation. Iscience. 2024;27(9).
94. Muñoz-Rojas AR, Mathis D. Tissue regulatory T cells: regulatory chameleons. Nature Reviews Immunology. 2021;21(9):597-611.

95. Rossetti M, Spreafico R, Moshref M, van Loosdregt J, Albani S. Ex Vivo-Expanded, but Not in Vitro-Induced, Human Regulatory T Cells Are Suitable for Cell Therapy in Rheumatological Autoimmune Diseases Thanks to Stable FOXP3 Demethylation.: 1455. Arthritis & Rheumatology. 2014;66:S641.
96. Hippen KL, Merkel SC, Schirm DK, Sieben CM, Sumstad D, Kadidlo DM, et al. Massive ex vivo expansion of human natural regulatory T cells (Tregs) with minimal loss of in vivo functional activity. Science translational medicine. 2011;3(83):83ra41-83ra41.
97. Thornton AM, Korty PE, Tran DQ, Wohlfert EA, Murray PE, Belkaid Y, et al. Expression of Helios, an Ikaros transcription factor family member, differentiates thymic-derived from peripherally induced Foxp3+ T regulatory cells. The Journal of Immunology. 2010;184(7):3433-41.
98. Miragaia RJ, Gomes T, Chomka A, Jardine L, Riedel A, Hegazy AN, et al. Single-cell transcriptomics of regulatory T cells reveals trajectories of tissue adaptation. Immunity. 2019;50(2):493-504. e7.
99. De Oliveira S, Reyes-Aldasoro CC, Candel S, Renshaw SA, Mulero V, Calado A. Cxcl8 (IL-8) mediates neutrophil recruitment and behavior in the zebrafish inflammatory response. The Journal of Immunology. 2013;190(8):4349-59.
100. Cambier S, Gouwy M, Proost P. The chemokines CXCL8 and CXCL12: molecular and functional properties, role in disease and efforts towards pharmacological intervention. Cellular & molecular immunology. 2023;20(3):217-51.
101. Schaller TH, Batich KA, Suryadevara CM, Desai R, Sampson JH. Chemokines as adjuvants for immunotherapy: implications for immune activation with CCL3. Expert review of clinical immunology. 2017;13(11):1049-60.
102. Greenman R, Segal-Salto M, Barashi N, Hay O, Katav A, Levi O, et al. CCL24 regulates biliary inflammation and fibrosis in primary sclerosing cholangitis. JCI insight. 2023;8(12):e162270.
103. Li L, Huang L, Sung S-SJ, Vergis AL, Rosin DL, Rose Jr CE, et al. The chemokine receptors CCR2 and CX3CR1 mediate monocyte/macrophage trafficking in kidney ischemia–reperfusion injury. Kidney international. 2008;74(12):1526-37.
104. Sakaguchi S, Mikami N, Wing JB, Tanaka A, Ichiyama K, Ohkura N. Regulatory T cells and human disease. Annual review of immunology. 2020;38(1):541-66.
105. Morikawa H, Sakaguchi S. Genetic and epigenetic basis of Treg cell development and function: from a FoxP3-centered view to an epigenome-defined view of natural Treg cells. Immunological reviews. 2014;259(1):192-205.
106. Bin Dhuban K, d'Hennezel E, Nashi E, Bar-Or A, Rieder S, Shevach EM, et al. Coexpression of TIGIT and FCRL3 identifies Helios+ human memory regulatory T cells. The Journal of Immunology. 2015;194(8):3687-96.
107. Todo S, Yamashita K, Goto R, Zaitsu M, Nagatsu A, Oura T, et al. A pilot study of operational tolerance with a regulatory T-cell-based cell therapy in living donor liver transplantation. Hepatology. 2016;64(2):632-43.
108. Abdelbary M, Hobbs SJ, Gibbs JS, Yewdell JW, Nolz JC. T cell receptor signaling strength establishes the chemotactic properties of effector CD8+ T cells that control tissue-residency. Nature communications. 2023;14(1):3928.
109. Himmel ME, MacDonald KG, Garcia RV, Steiner TS, Levings MK. Helios+ and Helios− cells coexist within the natural FOXP3+ T regulatory cell subset in humans. The Journal of Immunology. 2013;190(5):2001-8.
110. Ohmura H, Yamaguchi K, Hanamura F, Ito M, Makiyama A, Uchino K, et al. OX40 and LAG3 are associated with better prognosis in advanced gastric cancer patients treated with anti-programmed death-1 antibody. British journal of cancer. 2020;122(10):1507-17.
111. Raffin C, Vo LT, Bluestone JA. Treg cell-based therapies: challenges and perspectives. Nature Reviews Immunology. 2020;20(3):158-72.
112. Wiesinger M, Stoica D, Roessner S, Lorenz C, Fischer A, Atreya R, et al. Good manufacturing practice-compliant production and lot-release of ex vivo expanded regulatory T

cells as basis for treatment of patients with autoimmune and inflammatory disorders. Frontiers in Immunology. 2017;8:1371.
113. Smigiel KS, Srivastava S, Stolley JM, Campbell DJ. Regulatory T-cell homeostasis: steady-state maintenance and modulation during inflammation. Immunological reviews. 2014;259(1):40-59.
114. Lim TY, Perpiñán E, Londoño M-C, Miquel R, Ruiz P, Kurt AS, et al. Low dose interleukin-2 selectively expands circulating regulatory T cells but fails to promote liver allograft tolerance in humans. Journal of Hepatology. 2023;78(1):153-64.
115. Himmel ME, Crome SQ, Ivison S, Piccirillo C, Steiner TS, Levings MK. Human CD4+ FOXP3+ regulatory T cells produce CXCL8 and recruit neutrophils. European journal of immunology. 2011;41(2):306-12.
116. Jang E, Nguyen QT, Kim S, Kim D, Le THN, Keslar K, et al. Lung-infiltrating Foxp3+ regulatory T cells are quantitatively and qualitatively different during eosinophilic and neutrophilic allergic airway inflammation but essential to control the inflammation. The Journal of Immunology. 2017;199(12):3943-51.
117. Nayer B, Tan JL, Alshoubaki YK, Lu Y-Z, Legrand JM, Lau S, et al. Local administration of regulatory T cells promotes tissue healing. Nature Communications. 2024;15(1):7863.
118. Walter GJ, Evans HG, Menon B, Gullick NJ, Kirkham BW, Cope AP, et al. Interaction with activated monocytes enhances cytokine expression and suppressive activity of human CD4+ CD45RO+ CD25+ CD127low regulatory T cells. Arthritis & Rheumatism. 2013;65(3):627-38.
119. Nadig SN, Więckiewicz J, Wu DC, Warnecke G, Zhang W, Luo S, et al. In vivo prevention of transplant arteriosclerosis by ex vivo–expanded human regulatory T cells. Nature medicine. 2010;16(7):809-13.
120. Nardiello S, Pizzella T, Russo M, Galanti B. Percentage of monocytes in preparations of mononuclear cells from normal subjects: evaluation by a new rapid method for the identification of esterase-positive cells. Bollettino Della Societa Italiana di Biologia Sperimentale. 1982;58(8):467-70.
121. Akimova T, Levine MH, Beier UH, Hancock WW. Standardization, evaluation, and area-under-curve analysis of human and murine Treg suppressive function. Suppression and Regulation of Immune Responses: Methods and Protocols, Volume II. 2016:43-78.
122. Di Ianni M, Falzetti F, Carotti A, Terenzi A, Castellino F, Bonifacio E, et al. Tregs prevent GVHD and promote immune reconstitution in HLA-haploidentical transplantation. Blood, The Journal of the American Society of Hematology. 2011;117(14):3921-8.
123. Jarvis LB, Rainbow DB, Coppard V, Howlett SK, Georgieva Z, Davies JL, et al. Therapeutically expanded human regulatory T-cells are super-suppressive due to HIF1A induced expression of CD73. Communications biology. 2021;4(1):1186.
124. Issa F, Milward K, Goto R, Betts G, Wood KJ, Hester J. Transiently activated human regulatory T cells upregulate BCL-XL expression and acquire a functional advantage in vivo. Frontiers in immunology. 2019;10:889.
125. Romano M, Fanelli G, Tan N, Nova-Lamperti E, McGregor R, Lechler R, et al. Expanded regulatory T cells induce alternatively activated monocytes with a reduced capacity to expand T helper-17 cells. Front Immunol. 2018; 9: 1625. 2018.
126. Dowling M, Kan A, Heinzel S, Marchingo J, Hodgkin P, Hawkins E. Regulatory T cells suppress effector T cell proliferation by limiting division destiny. Front. Immunol. 9: 2461. 2018.
127. Zhong H, Yazdanbakhsh K. Differential control of Helios+/− Treg development by monocyte subsets through disparate inflammatory cytokines. Blood, The Journal of the American Society of Hematology. 2013;121(13):2494-502.
128. Arterbery AS, Osafo-Addo A, Avitzur Y, Ciarleglio M, Deng Y, Lobritto SJ, et al. Production of proinflammatory cytokines by monocytes in liver-transplanted recipients with de novo autoimmune hepatitis is enhanced and induces TH1-like regulatory T cells. The Journal of Immunology. 2016;196(10):4040-51.

129. Sasaki K, Kubo M, Wang Y-c, Lu L, Vujevich V, Wood-Trageser MA, et al. Multiple infusions of ex vivo-expanded regulatory T cells promote CD163+ myeloid cells and kidney allograft survival in non-lymphodepleted non-human primates. Kidney International. 2024;105(1):84-98.
130. McCallion O, Cross AR, Brook MO, Hennessy C, Ferreira R, Trzupek D, et al. Regulatory T cell therapy is associated with distinct immune regulatory lymphocytic infiltrates in kidney transplants. Med. 2025;6(5).
131. Alhayyan A, McSorley S, Roxburgh C, Kearns R, Horgan P, McMillan D. The effect of anesthesia on the postoperative systemic inflammatory response in patients undergoing surgery: A systematic review and meta-analysis. Surgery Open Science. 2020;2(1):1-21.
132. Chandran S, Leung JC, Vu A, Lee K, Fitch M, Esensten JH, et al. Pharmacokinetics, lineage identity, and trafficking of ex vivo expanded polyclonal regulatory T cells in a prospective randomized clinical trial of kidney transplant recipients with allograft inflammation. American Journal of Transplantation. 2026.
133. Martin-Martin C, Suarez-Alvarez B, González M, Torres IB, Bestard O, Martín JE, et al. Exploring kidney allograft rejection: A proof-of-concept study using spatial transcriptomics. American Journal of Transplantation. 2024;24(7):1161-71.
134. Gu Y, Bartolomé-Casado R, Xu C, Bertocchi A, Janney A, Heuberger C, et al. Immune microniches shape intestinal Treg function. Nature. 2024;628(8009):854-62.
135. Zhang Y, Liu G, Zeng Q, Wu W, Lei K, Zhang C, et al. CCL19-producing fibroblasts promote tertiary lymphoid structure formation enhancing anti-tumor IgG response in colorectal cancer liver metastasis. Cancer cell. 2024;42(8):1370-85. e9.

Appendix

Lists of differentially expressed genes across the indicated populations.

A.

43 Genes ^ UP		
IL2RA	LAG3	CD80
CISH	HLA-DQA1	FOXP3
ITGAM	CSF2RB	TIGIT
HLA-DRA	CXCR6	SPP1
LGALS3	CSF1	CEACAM1
GZMB	TGFBR1	STAT1
HLA-DRB3	CTSC	ITGAX
HAVCR2	TNFRSF9	CD70
NCF4	IL1A	TNFSF13B
CD59	TNFRSF4	TNFRSF1B
MAF	CD79B	HLA-DPA1
TNFRSF11A	IRF4	LY96
HLA-DMB	IL1R1	CTLA4-TM
CCR8	IL1R2	NT5E
HLA-DMA		

B.

65 Genes v DOWN		
TCF7	IL7R	IFIT2
GPR183	TNFAIP3	CD45RA
PTGER4	TAGAP	LEF1
IL6ST	CXCR4	ITGA6
IL23A	EGR1	GZMK
IFITM1	BCL6	ADGRE5
CD40LG	NFKBIA	AHR
TGFBR2	ATG16L1	SOCS3
CD83	CDKN1A	IFNGR1
MALT1	KLRB1	TRAF4
MX1	IKZF3	RELB
NFKBIZ	MCL1	NOD2
BCL3	RARRES3	BTLA
XBP1	SKI	CD44
IFIH1	CD99	IFNG
MBP	CEBPB	SIGIRR
CCR6	ITGA5	CD48
TNF	NFKB1	RELA
ZEB1	ILF3	TNFRSF13C
TGFB1	IL11RA	TICAM1
FCGRT	ITGB1	ADA
TNFSF8	MAPKAPK2	

Table A3.1 Differentially expressed genes between clinical Tregs and CD4⁺ T cells.

Tables A and B list genes differentially expressed between clinical regulatory T cells and CD4⁺ T cells. A total of 108 genes were identified, of which 43 were upregulated in clinical Tregs (Table A, highlighted in green) and 65 were upregulated in CD4⁺ T cells (Table B, highlighted in purple).

A.

68 Genes ^ UP		
IL2RA	LGALS3	CD4
CTLA4-TM	IRF4	CTLA4_ALL
CISH	HLA-DQA1	CD59
CD80	FOXP3	CD27
TP53	TNFRSF4	TIGIT
HLA-DRB3	TGFBR1	CSF1
CSF2RB	HLA-DRA	DUSP4
TMEM173	PSMB5	BATF
CD2	CXCR6	NCF4
SPP1	NOTCH2	TNFSF13B
MAF	CEACAM1	CD79B
ICAM2	TNFRSF1B	TNFSF12
STAT1	DPP4	CXCR3
BST2	CD70	PSMB10
BCL2	ITGAX	IL12RB1
IKBKE	HAVCR2	TNFRSF9
IFI35	CASP2	HLA-DMA
IL1A	HLA-DMB	CCR8
TBK1	BCAP31	UBE2L3
TNFRSF11A	CD82	CD40LG
LY96	TOLLIP	TRAF2
JAK2	IL1R1	IL1R2
IL18R1	CTSC	

B.

68 Genes v DOWN		
KLRK1	CD8A	IFIT2
CD45RA	TCF7	KLRC4
IL7R	GZMK	CCL5
TNFAIP3	GNLY	IFNG
KLRG1	PTGER4	ADGRE5
CXCR4	TBX21	TAGAP
GPR183	ATG16L1	CCL4
KLRD1	ITGA6	IKZF3
IFNGR1	CD83	CCL3
IL6ST	LEF1	IL18RAP
GZMA	CD8B	BCL6
GZMB	ITGA5	EGR1
TGFBR2	TRAF4	SLAMF7
NFKBIA	TGFB1	TNF
NFATC2	NFKB1	NFKBIZ
MCL1	SKI	MX1
NFKB2	IFITM1	FYN
AHR	PRF1	ILF3
BCL3	TRAF6	STAT4
ZAP70	SIGIRR	JAK1
MALT1	CDKN1A	MAPKAPK2
CEBPB	KLRB1	LITAF
SOCS3	PTPRC_ALL	

Table A3.2 Differentially expressed genes between clinical Tregs and CD8⁺ T cells.

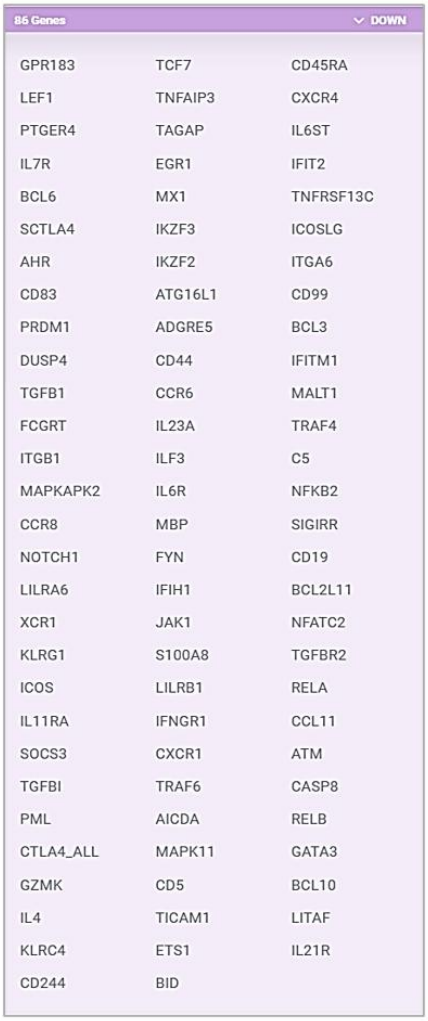
Tables A and B list genes differentially expressed between clinical regulatory T cells and CD8⁺ T cells. A total of 136 genes were identified, with 68 genes upregulated in clinical Tregs (Table A, highlighted in green) and 68 genes upregulated in CD8⁺ T cells (Table B, highlighted in purple).

A.



43 Genes		UP
CD80	CISH	ITGAM
LAG3	IL2RA	DPP4
TNFRSF4	SPP1	GZMB
STAT1	CD59	CEACAM1
TNFSF13B	ITGAX	CSF1
LGALS3	HAVCR2	CTSC
LTA	TGFBR1	PSMB5
IL1A	LY96	HLA-DRA
IL1R1	IL1R2	TNFRSF11A
PYCARD	JAK2	B2M
ITGA4	PSMB9	TP53
BAX	CD86	CSF2RB
TNFRSF1B	PSMB8	CASP3
CD53	TNFRSF8	TMEM173
PSMB10		

B.



86 Genes		DOWN
GPR183	TCF7	CD45RA
LEF1	TNFAIP3	CXCR4
PTGER4	TAGAP	IL6ST
IL7R	EGR1	IFIT2
BCL6	MX1	TNFRSF13C
SCTLA4	IKZF3	ICOSLG
AHR	IKZF2	ITGA6
CD83	ATG16L1	CD99
PRDM1	ADGRE5	BCL3
DUSP4	CD44	IFITM1
TGFB1	CCR6	MALT1
FCGRT	IL23A	TRAF4
ITGB1	ILF3	C5
MAPKAPK2	IL6R	NFKB2
CCR8	MBP	SIGIRR
NOTCH1	FYN	CD19
LILRA6	IFIH1	BCL2L11
XCR1	JAK1	NFATC2
KLRG1	S100A8	TGFBR2
ICOS	LILRB1	RELA
IL11RA	IFNGR1	CCL11
SOCS3	CXCR1	ATM
TGFBI	TRAF6	CASP8
PML	AICDA	RELB
CTLA4_ALL	MAPK11	GATA3
GZMK	CD5	BCL10
IL4	TICAM1	LITAF
KLRC4	ETS1	IL21R
CD244	BID	

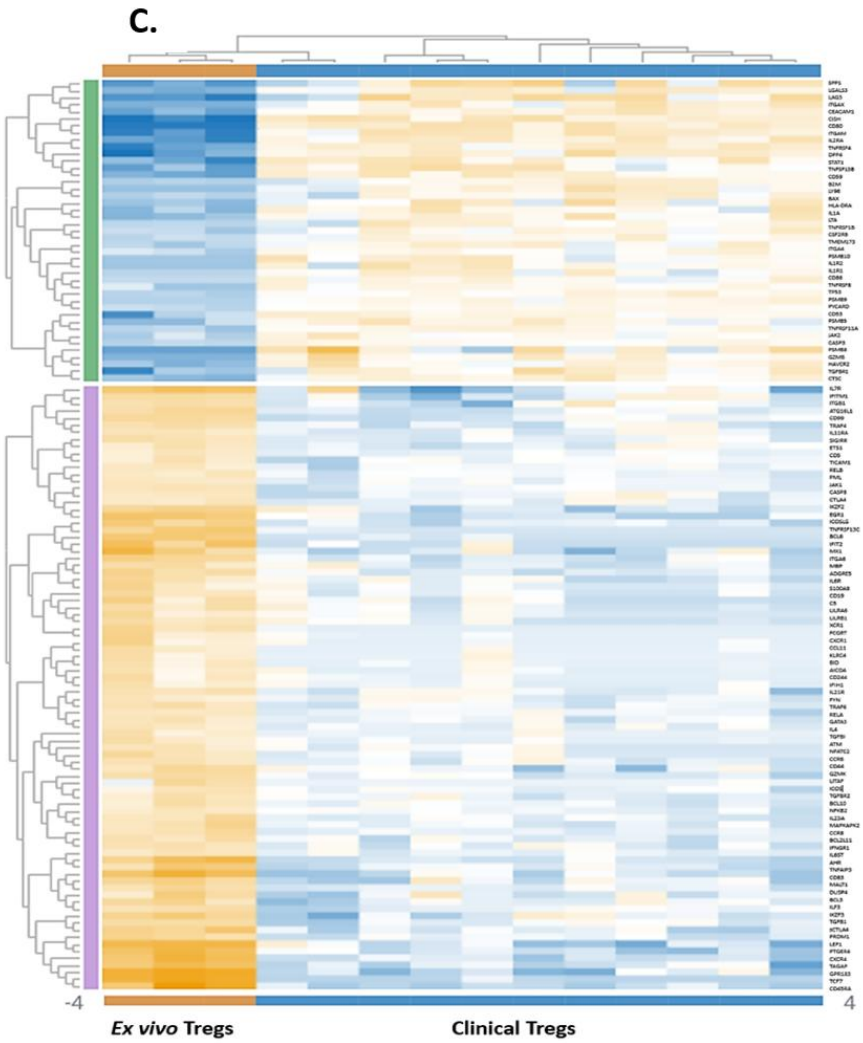


Figure A3.1 Gene expression differences between clinical and ex vivo-expanded Tregs.

Tables A and B list genes differentially expressed between clinical regulatory T cells and ex vivo-expanded Tregs. A total of 129 genes were identified, with 43 genes upregulated in clinical Tregs (Table A, highlighted in green) and 86 genes upregulated in ex vivo Tregs (Table B, highlighted in purple). (C) Heat map of the same dataset, providing an alternative visualisation of transcriptional differences between the two populations.

Overview of the gating strategy for homing receptor expression analysis.

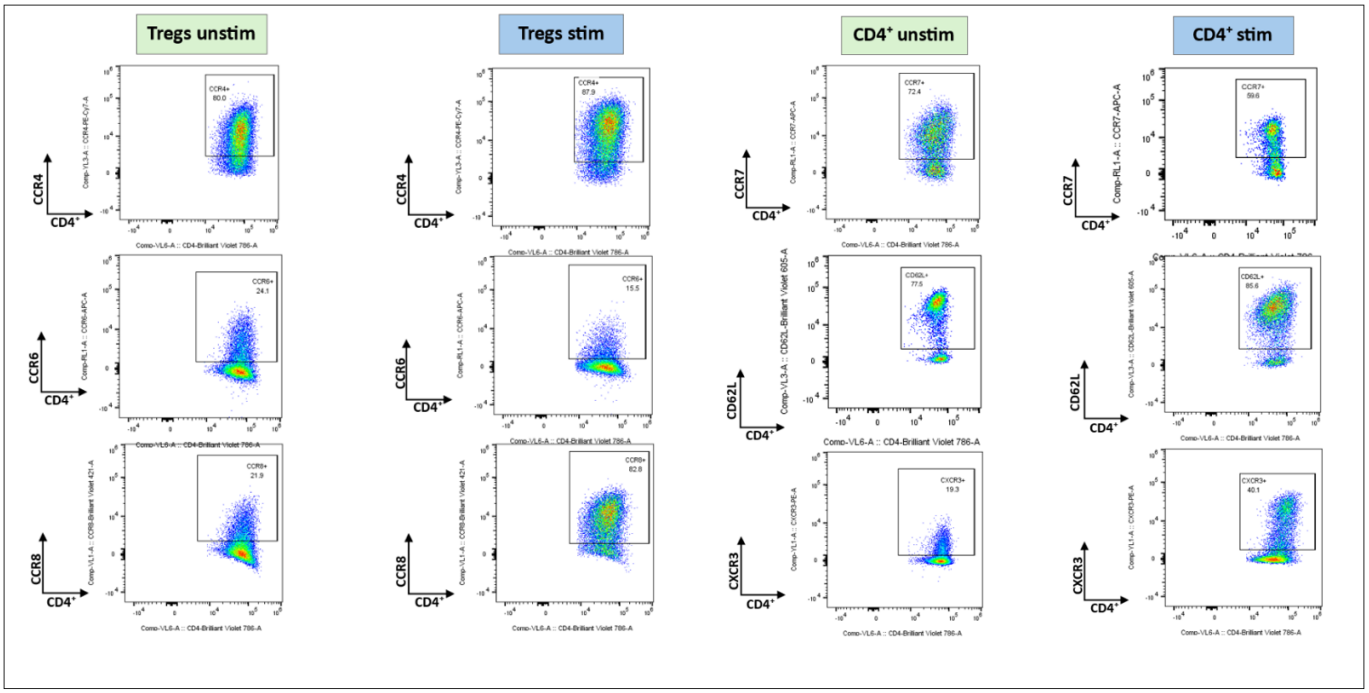


Figure A3.3 Examples of homing receptor expression in clinical Tregs and CD4⁺ T cells.

Individual expression profiles for each homing receptor. Flow cytometric analysis was performed using the Attune™ NxT Flow Cytometer, and plots were generated using FlowJo software. Unstim: beads unstimulated, Stim: beads stimulated

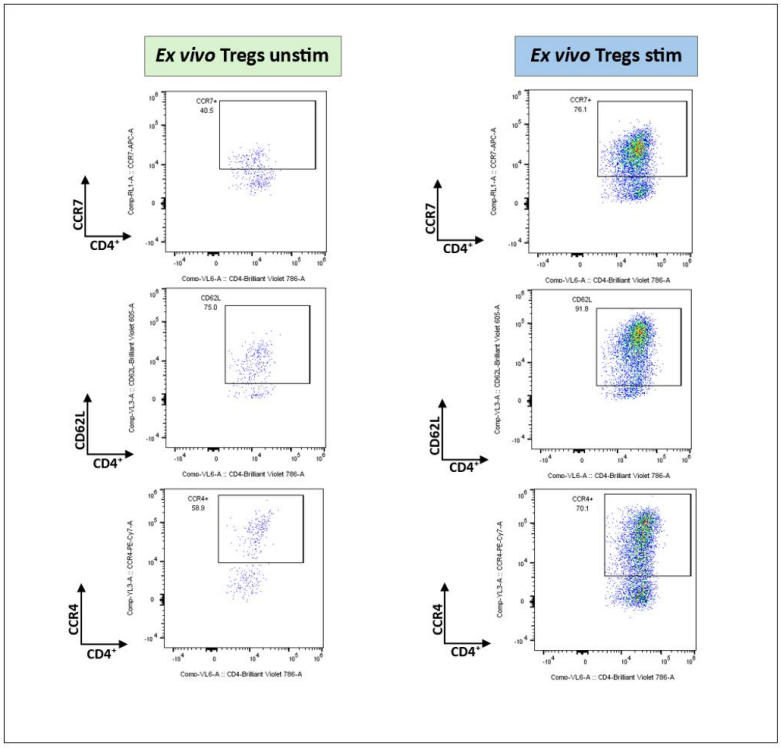
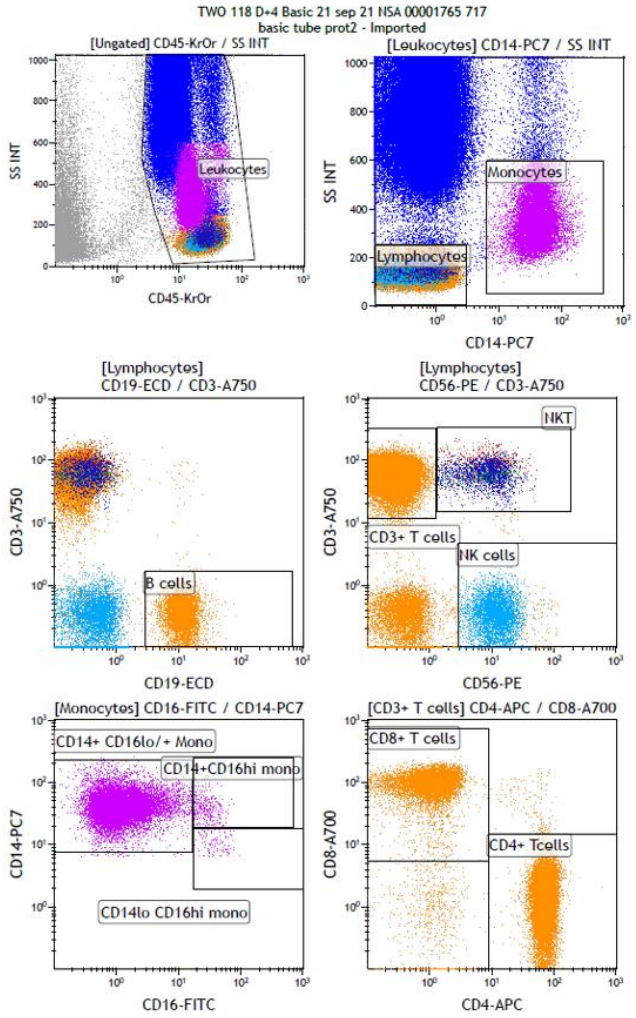


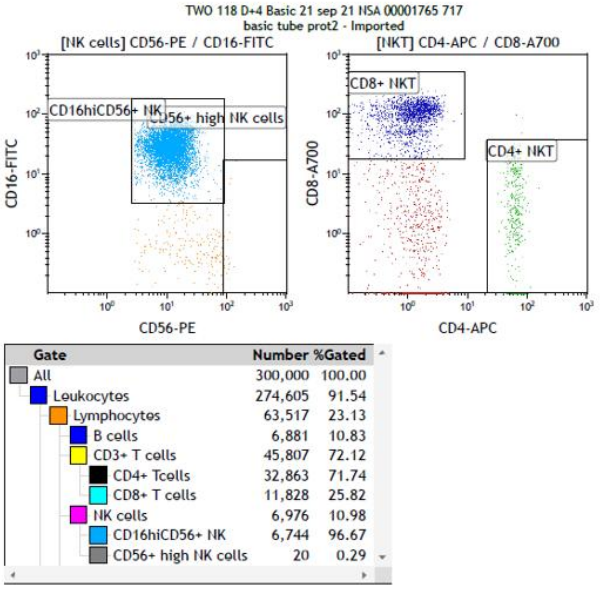
Figure A3.4 Homing receptor expression profile of ex vivo Tregs.

Flow cytometric analysis of CCR7, CD62L, and CCR4 surface expression in freshly isolated (ex vivo) Tregs under unstimulated and anti-CD3/CD28-stimulated conditions. Data acquired using the Attune™ NxT Flow Cytometer; plots generated in FlowJo software. Unstim: beads unstimulated, Stim: beads stimulated.

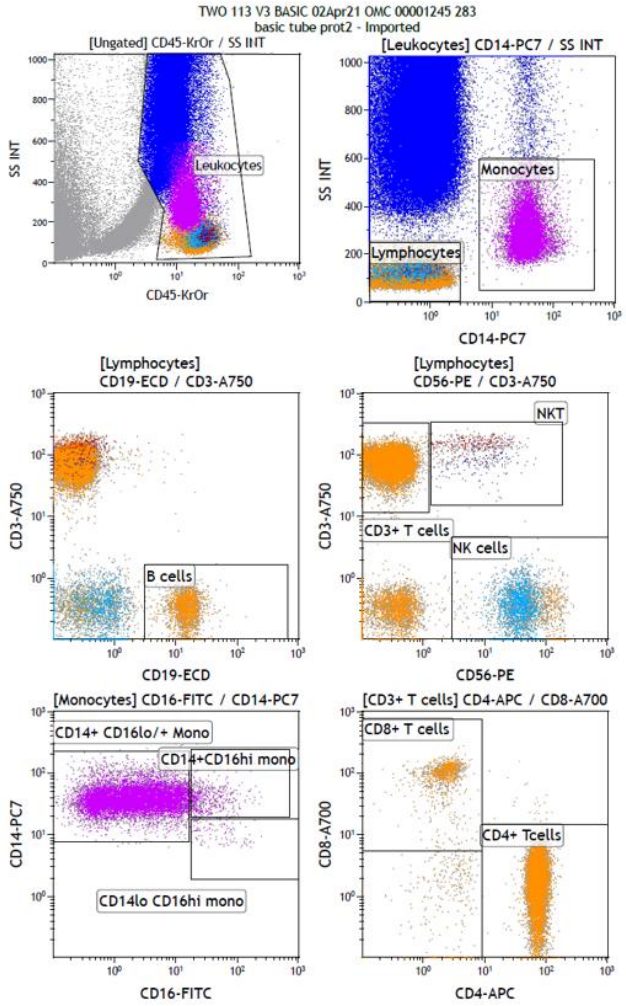
Representative gating strategies for longitudinal immunomonitoring analysis.

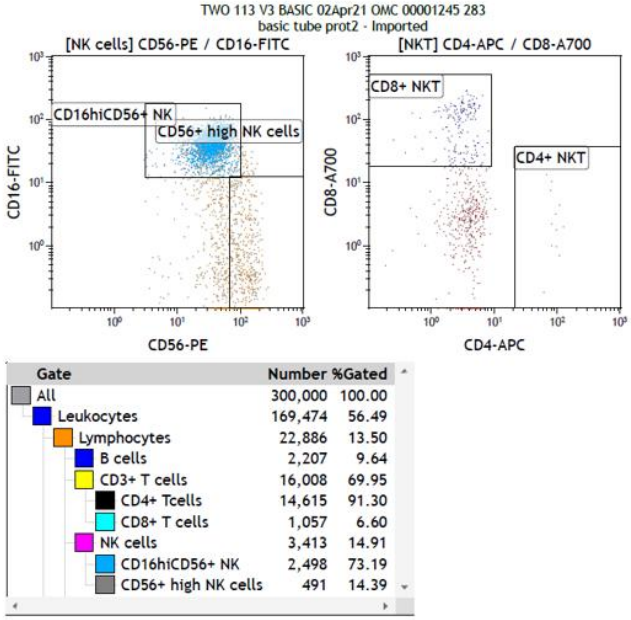
A.





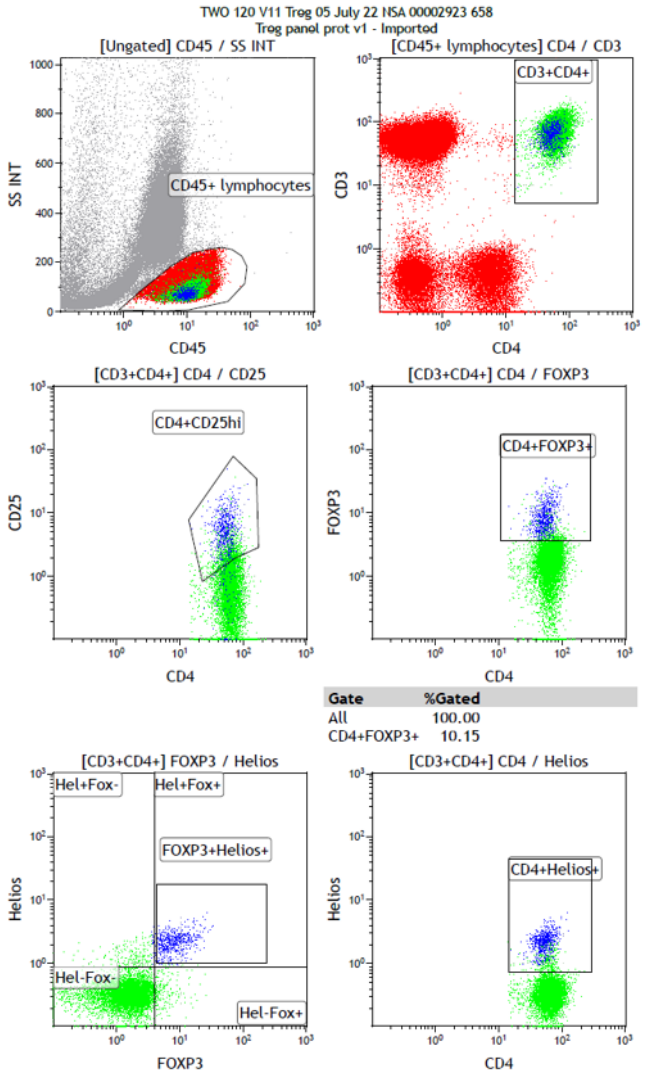
B.

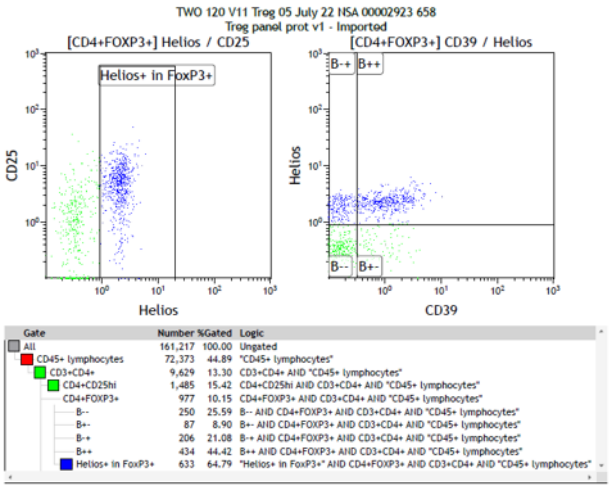




Gate	Number	%Gated
All	300,000	100.00
Leukocytes	169,474	56.49
Lymphocytes	22,886	13.50
B cells	2,207	9.64
CD3+ T cells	16,008	69.95
CD4+ Tcells	14,615	91.30
CD8+ T cells	1,057	6.60
NK cells	3,413	14.91
CD16hiCD56+ NK	2,498	73.19
CD56+ high NK cells	491	14.39

C.


TWO 120 V11 Treg 05 July 22 NSA 00002923 658
Treg panel prot v1 - Imported
[Ungated] CD45 / SS INT
CD45+ lymphocytes
SS INT
CD45
[CD45+ lymphocytes] CD4 / CD3
CD3+CD4+
CD3
CD4
[CD3+CD4+] CD4 / CD25
CD4+CD25hi
CD25
CD4
[CD3+CD4+] CD4 / FOXP3
CD4+FOXP3+
FOXP3
CD4
Gate %Gated
All 100.00
CD4+FOXP3+ 10.15
[CD3+CD4+] FOXP3 / Helios
Hel+Fox-
Hel+Fox+
FOXP3+Helios+
Hel-Fox-
Hel-Fox+
Helios
FOXP3
[CD3+CD4+] CD4 / Helios
CD4+Helios+
Helios
CD4


TWO 120 V11 Treg 05 July 22 NSA 00002923 658
Treg panel prot v1 - Imported
[CD4+FOXP3+] Helios / CD25
Helios+ in FoxP3+
CD25
Helios
[CD4+FOXP3+] CD39 / Helios
B-+
B++
B--
B+-
Helios
CD39
Gate Number %Gated Logic
All 161,217 100.00 Ungated
CD45+ lymphocytes 72,373 44.89 "CD45+ lymphocytes"
CD3+CD4+ 9,629 13.30 CD3+CD4+ AND "CD45+ lymphocytes"
CD4+CD25hi 1,485 15.42 CD4+CD25hi AND CD3+CD4+ AND "CD45+ lymphocytes"
CD4+FOXP3+ 977 10.15 CD4+FOXP3+ AND CD3+CD4+ AND "CD45+ lymphocytes"
B-- 250 25.59 B-- AND CD4+FOXP3+ AND CD3+CD4+ AND "CD45+ lymphocytes"
B+- 87 8.90 B+- AND CD4+FOXP3+ AND CD3+CD4+ AND "CD45+ lymphocytes"
B-+ 206 21.08 B-+ AND CD4+FOXP3+ AND CD3+CD4+ AND "CD45+ lymphocytes"
B++ 434 44.42 B++ AND CD4+FOXP3+ AND CD3+CD4+ AND "CD45+ lymphocytes"
Helios+ in FoxP3+ 633 64.79 "Helios+ in FoxP3+" AND CD4+FOXP3+ AND CD3+CD4+ AND "CD45+ lymphocytes"

D.

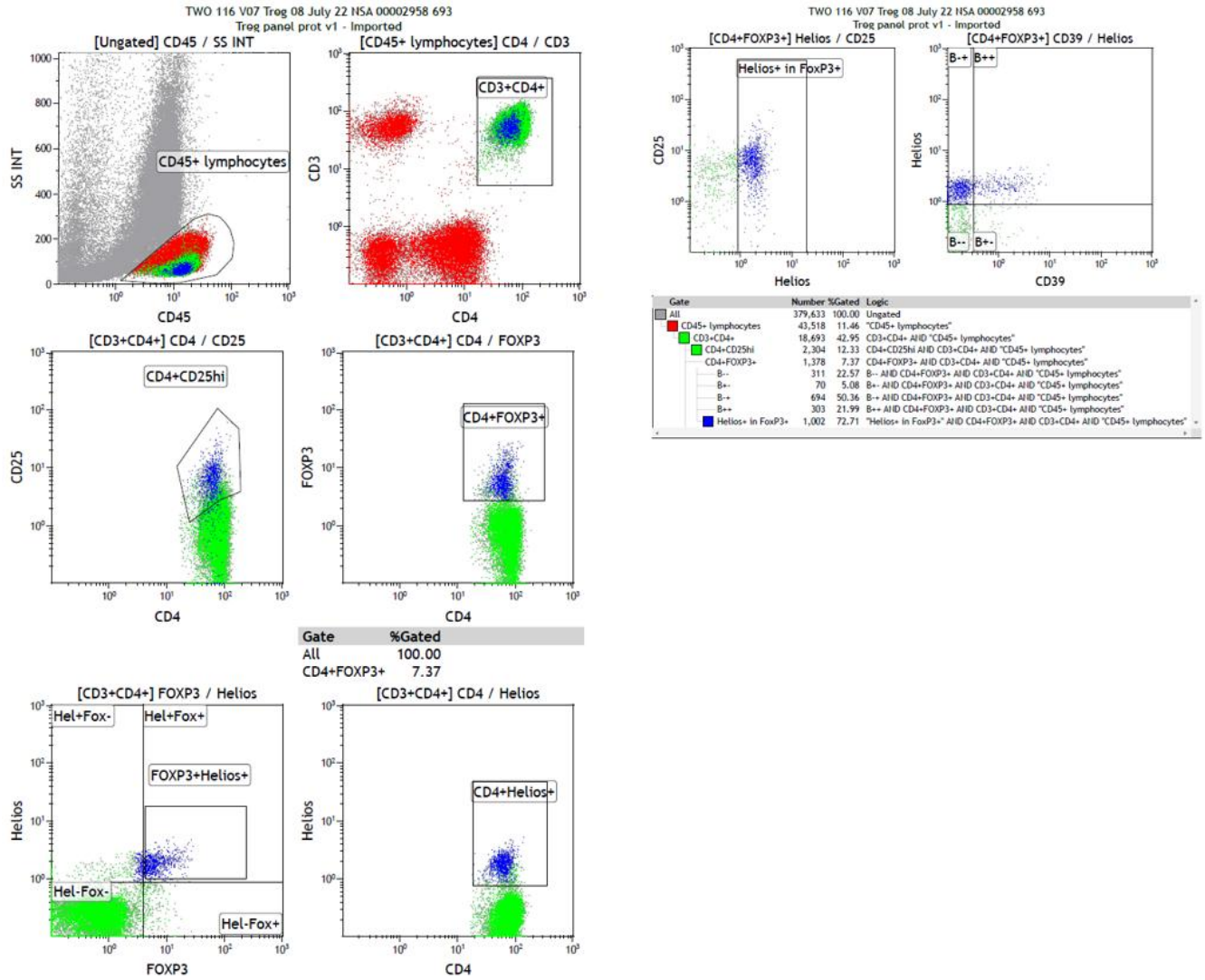


Figure A5.1 Flow cytometric gating strategies for immunomonitoring panels.

Representative flow cytometry plots illustrating the gating strategies used for peripheral blood immunomonitoring. (A, B) Gating strategy for the Basic immunophenotyping panel, shown for a representative control patient (TWO118; A) and a Treg therapy patient (TWO113; B). Leukocytes were identified based on forward and side scatter, followed by sequential gating of major immune populations including lymphocytes, monocytes, B cells, NK cells, and CD3⁺ T cells. Monocyte subsets were further delineated based on CD14 and CD16 expression to identify CD14⁺CD16^{lo} and CD14⁺CD16^{hi} populations, while CD4⁺ and CD8⁺ T cells were gated within the CD3⁺ compartment. (C, D) Gating strategy for the Treg panel, shown for a representative control patient (TWO120; C) and a Treg therapy patient (TWO116; D). Following identification of CD45⁺ lymphocytes and CD3⁺CD4⁺ T cells, regulatory T cells were defined by expression of CD25 and FOXP3, with further subdivision based on Helios expression to distinguish Helios⁺ and Helios⁻ Treg subsets. These gating strategies were applied consistently across all samples included in the immunomonitoring analyses.

Longitudinal dynamics of B cells and NK cells following Treg therapy.

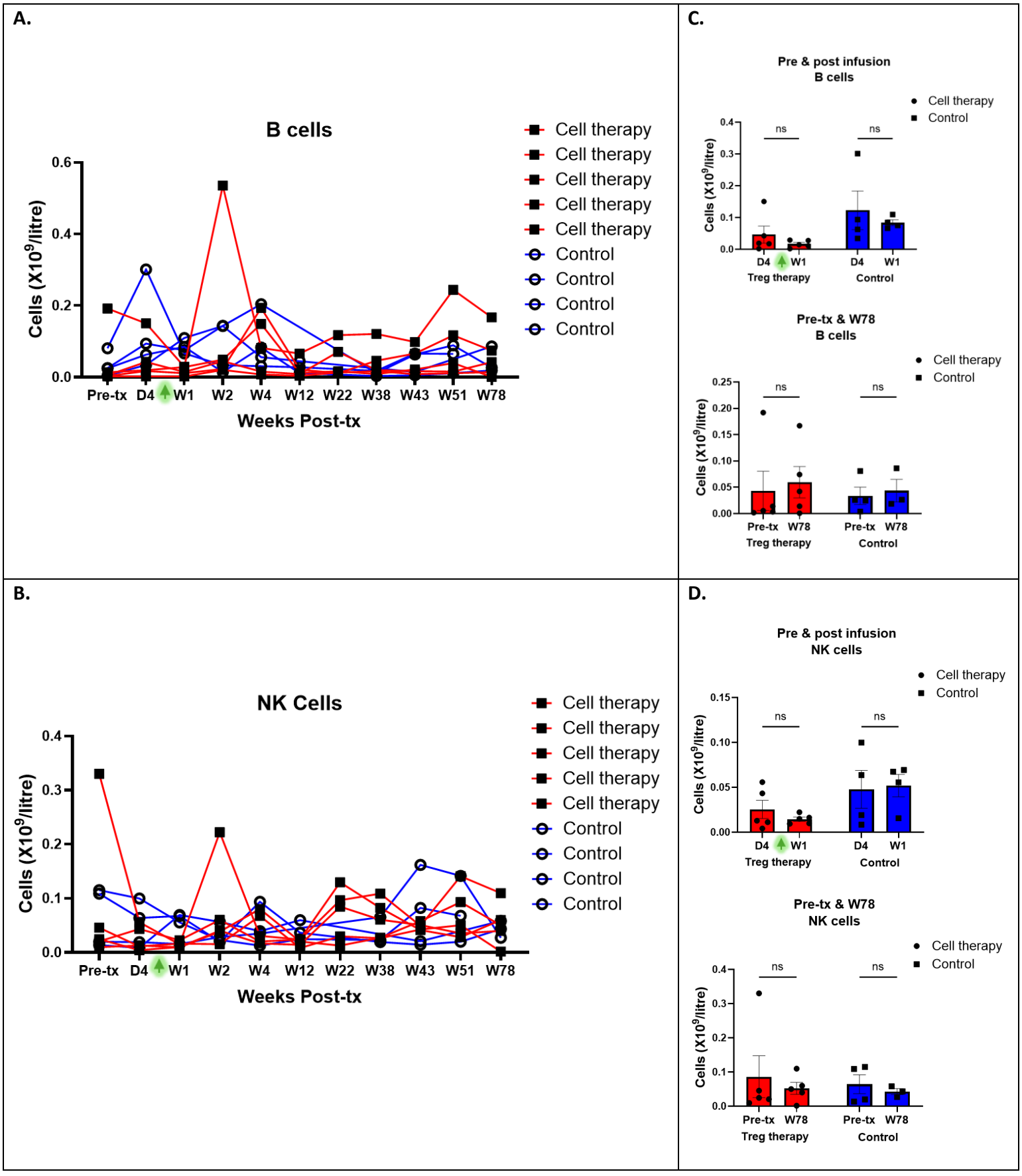


Figure A5.2 Longitudinal analysis of peripheral B cell and NK cell dynamics following Treg therapy in kidney transplant recipients.

(A) Longitudinal absolute counts of peripheral B cells in Treg-treated (red, solid squares) and control (blue, open circles) patients from pre-transplant baseline (Pre-tx) through week 78 post-transplantation. Treg infusion was administered on day 5 post-transplant (green arrow). (B) Longitudinal absolute counts of NK cells across the same timepoints and patient groups. Each line represents an individual patient, and cell counts are expressed as cells ×10⁹/L. (C-D) Summary bar plots comparing B cell (C) and NK cell (D) counts before and after infusion (day 4 vs week 1, top panels) and between baseline and late follow-up (Pre-tx vs week 78, bottom panels). Dots represent individual patients and bars indicate mean ± SEM. Longitudinal data were analysed using a mixed-effects model (REML), with time as a repeated measure and treatment group as a fixed effect; ns denotes not significant. Tx, transplantation; Pre-tx, pre-transplant; D4, day 4 post-transplant.

Table A5.1 Demographics of patients included in the spatial transcriptomics analysis

Patient	Treatment Group	Age (y)	Sex	Race	Transplant Type	Donor CMV Status	Recipient CMV Status	No. of Mismatches	cRF (%)
102	Cell Therapy	32	Female	White	LRD	Pos	Pos	2	3
104	Control	30	Male	White	LRD	Pos	Neg	2	0

Demographic data shown here correspond to the two patients included in the current spatial transcriptomic analysis: Patient 102 (Treg cell therapy) and Patient 104 (control). These data are derived from the original clinical trial as reported by Brook et al. (2024). CMV, cytomegalovirus; cRF, calculated reaction frequency; Tx, transplantation

Table A5.2 Histopathological findings from protocol biopsies in Treg-treated and control patients

Treatment Group	Cell therapy Patient (102)	Control Patient (104)
Microscopic description	14 glomeruli	16 glomeruli
Glomerular sclerosis: Global	2/14	Neg
Glomerular sclerosis: segmental	NA	Neg
Glomerulitis	Neg	Mild in 1
Basement membrane	Normal	Normal
Tubulointerstitial fibrosis	10%	40%
Tubulitis	None	Mild focal lymphocytic
Vessels	Mild fibroelastosis	Normal
Rejection	No	No
C4d staining	Neg	Neg
SV40 staining	Neg	Neg
Comment	Mild acute tubular injury. Mild chronic damage	Moderate chronic damage. Extensive mononuclear infiltrate in areas of fibrosis

Biopsies shown here were obtained as part of the scheduled 9-month protocol biopsies, as previously described by Brook et al. (2024). These samples were selected for inclusion based on quality and availability for downstream spatial transcriptomic analysis. C4d, complement split product; marker of antibody-mediated rejection in transplantation. SV40, simian virus 40.

Top marker genes across immune cell clusters in individual samples.

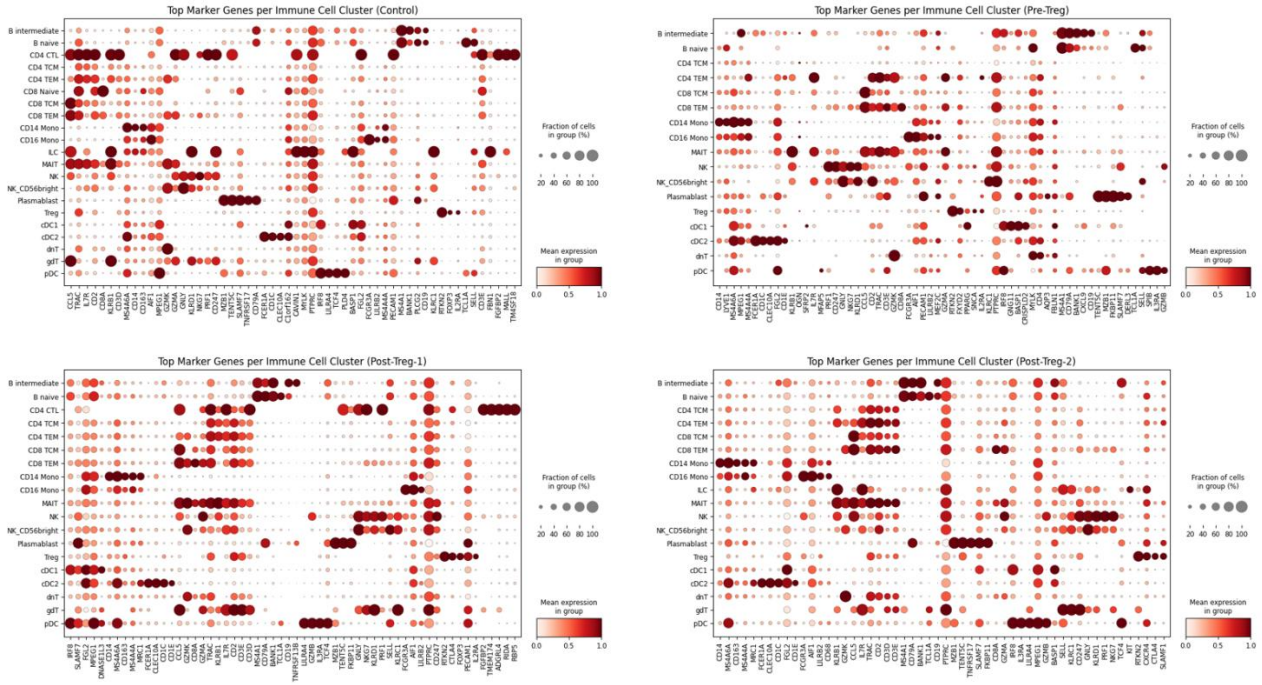


Figure A5.3 Representation of top marker genes across immune cell clusters in kidney transplant biopsies.

Dot plots display the expression of selected marker genes across annotated immune cell subsets within each biopsy condition: Control (top left), Pre-Treg (top right), and Post-Treg-1-2 (bottom). Marker gene expression was assessed using transcriptomic data and plotted for each immune cluster identified by Azimuth-based annotation. Each dot represents a gene's expression within a given cell type; the size of the dot indicates the proportion of cells within that cluster expressing the gene, while the colour intensity reflects the average normalised expression level.

Chemokine Expression Heatmaps: Control vs Post-Treg.

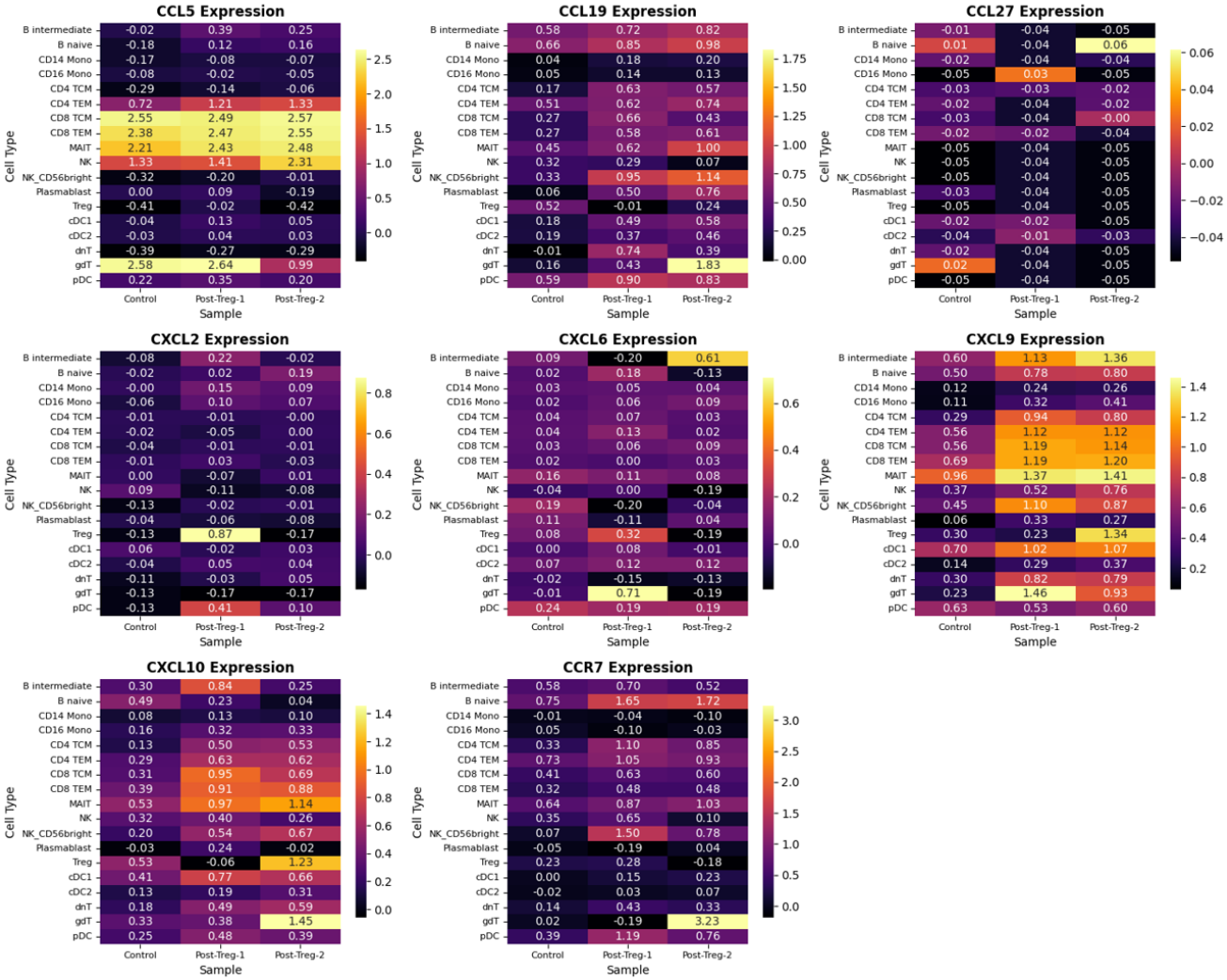


Figure A5.4 Chemokine and chemokine receptor expression across immune cell types in Control vs Post-Treg.

Heatmaps display the average expression levels of selected chemokines (e.g., CCL5, CCL19, CCL27, CXCL2, CXCL6, CXCL9, CXCL10) and the chemokine receptor CCR7 across annotated immune cell populations in Control, and Post-Treg-1-2 biopsy samples. Rows represent individual immune cell types, while columns show the experimental conditions. Colour intensity reflects the mean gene expression level (non-scaled, directly averaged from transcript counts) within each population.

Immune cell neighbourhood analysis in Control vs Post-Treg.

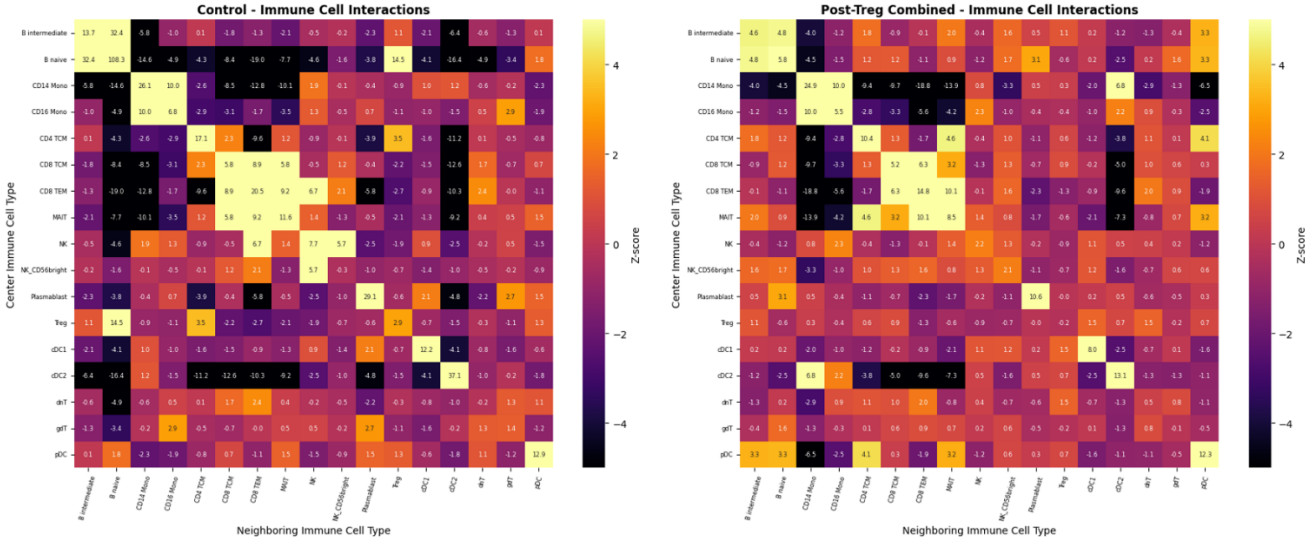


Figure A5.5 Neighbourhood enrichment analysis of immune cell interactions in Control vs Post-Treg.

Heatmaps illustrate the spatial co-localisation frequencies between annotated immune cell types in Control (left) and Post-Treg (right) samples. Each cell in the matrix reflects the degree of enrichment (Z-score) for the spatial proximity between a central immune cell type (rows) and its neighbouring immune cell type (columns).
Higher Z-scores (yellow) indicate stronger-than-expected co-localisation, while lower Z-scores (purple/black) represent spatial avoidance or under-representation.